Informed Non-Negative Matrix Factorization for Source Apportionment

Robert Chreiky

Numéro d'ordre : *2017.26*

THÈSE

Présentée et soutenue publiquement le *19 décembre 2017* **par :**

ROBERT CHREIKY

En vue de l'obtention du doctorat délivré par :

l'Université du Littoral Côte d'Opale (ULCO) et l'Université du Balamand (UOB)

Cotutelle internationale

Informed Non-Negative Matrix Factorization for Source Apportionment

sous la direction de

GILLES ROUSSEL	Professeur d'Université	ULCO
ANTOINE ABCHE	Professeur d'Université	Univ. Balamand
GILLES DELMAIRE	Maître de conférences	ULCO

JURY

STÉPHANE CANU	Professeur à l'INSA de Rouen	Rapporteur
CHAOUKI DIAB	Professeur à l'ISSAE-CNAM Liban	Rapporteur
NANCY BERTIN	Chargée de Recherche CNRS	Examinatrice
DOMINIQUE COURCOT	Professeur à l'ULCO	Examinateur
ELIE KARAM	Professeur à l'Université de Balamand	Examinateur
NAZIH MOUBAYED	Professeur à l'Université Libanaise de Beyrouth	Examinateur
MATTHIEU PUIGT	Maître de conférences à l'ULCO	Invité

École doctorale : *Sciences pour l'ingénieur*

Spécialité : *Automatique, Génie informatique, Traitement du Signal et des Images*

Unité de Recherche : *Laboratoire d'Informatique, Signal, Image de la Côte d'Opale (EA 4491)*

Acknowledgements

First, I would like to thank both my supervisors at the University of Littoral and the University of Balamand, Gilles Roussel and Antoine Abche, for giving me the opportunity and the privilege of being part of their team and for being there for me at all times and helping me to overcome the obstacles during the past years and for always pushing me to put more efforts either in good or bad moments of this thesis. Thank you both for your support and commitment. Thank you Gilles Roussel for all your help that you provide me during all my visits to Calais to make things easier for me and to make my stay as comfortable as possible. Also, thank you Antoine Abche for the help you provide me during the last few years and for being available for me at anytime i knock on your door.

I would like also to sincerely thank my supervisor, Gilles Delmaire. I was pleased and honored working with you during the past few years. I really admire you expertise and your dedication to the work. Thank you Gilles Delmaire for always being there for me during the whole time of the thesis despite all the other tasks you have. Thank you Gilles for doing the maximum in order to ensure the progress of the work and for working hard with me to reach the goals and to overcome all the obstacles that we face during the time of the thesis. None of this was possible without your contributions, you help and your advice. I will always remember the good times that I spent in LISIC, the skype sessions and the happiness each time our publications were accepted.

A special thanks for Mr. Mattieu Puigt for his help specifically for his bibliographic knowledge, his culture in source separation and his multiple proposals which gave us a great push in the work.

I would also like to thank the members of the jury, who made this work possible, by accepting to do me the honor of examining this work. Thank you to Mr. Stephane Canu, professor at Insa de Rouen, and Mr. Chaouki Diab, professor at ISSAE-CNAM for having accepted to be the reporters of this manuscript. Their remarks and suggestions during the reading of my thesis allowed me to make improvements. Thank you also for Mrs. Nancy Bertin, CNRS researcher, Mr. Nazih Moubayed, professor at the Lebanese university and Mr. Dominique Courcot, professor at the univerity of Littoral Côte D'Opale for having accepted to be the jury of my thesis.

I really appreciate the support of all the members of the Signal and Image processing lab. I thank all my colleagues for the friendly atmosphere in which I have worked during those years. I will really miss the time that I spent in the beautiful city of Calais. I would like also to thank my great parents for their encouragement and support during the years of the thesis.

Last and not least, I can not finish these lines without thinking about the most important people in my life and to whom I owe this achievement, my beautiful family: My dear wife Eliane and my two lovely daughters Maria and Christine who were born during my work on the thesis. I dedicate this work to my wife for her unconditional love, support, years of sacrifice. Throughout the last years, she has encouraged me and she was always successful in comforting me during the difficult moments. Your support was perfect and with you by my side, my dream has become true and I know that you are really proud of me. Thank you for all what you did. I hope that this success will be the beginning of a good chapter in our life.

Contents

Glossary **xi**

Table of Acronyms **xiii**

1 General Introduction **1**

1.1 General Framework 1

1.2 Objective 2

1.3 Thesis outline 2

1.4 General Conclusion 4

2 State of the Art **5**

2.1 Introduction 5

2.2 General Sensor Models 5

2.3 General Linear Mixture Models 9

2.4 Brief Overview of Factorization Methods 13

2.5 Conclusion 19

3 Non-negative Matrix Factorization **21**

3.1 Introduction 21

3.2 Classic NMF Problem 22

3.3 Exact NMF and Non Negative Rank 22

3.4 KKT conditions for the NMF problem 23

3.5 Uniqueness of the NMF solution 25

3.6 Review of the different families of algorithms 27

3.7 Weighted Non Negative Matrix Factorization (WNMF) 38

3.8 Applications 39

3.9 Conclusion 40

4 Robust NMF methods **43**

4.1 Introduction 43

4.2 Outliers 43

4.3 Robust Statistics and Robustness Properties 45

4.4 Sparseness Based NMF 49

4.5 NMF based on modified cost functions 51

4.6 Conclusion 62

5 Existing Informed NMF methods with set values and sum-to 1 variables. **63**

5.1 Introduction 63

5.2 Sum-to -1 variables in NMF problems 63

5.3 Set Values in the Profile Matrix 68

5.4 NMF with set values and sum-to-1 variables 74

5.5 Conclusion 78

6 New Informed NMF methods **79**

6.1 Introduction 79

6.2 Parametrization of the profile matrix 79

6.3 Informed Split Gradient NMF methods 81

6.4 Solving the different Problems 84

6.5 Summary of the different algorithms 88

6.6 Initialization issues 89

6.7 Validation on a toy simulation example 90

6.8 Medium scale experimentation 96

6.9 Real Data Case 103

6.10 Conclusion 106

7 General Conclusion **109**

7.1 Outline of the thesis chapters 109

7.2 Perspectives and Future Work 110

A Karush-Kuhn-Tucker conditions for weighted Frobenius NMF with set values **113**

B Update rules for Weighted $\alpha\beta$-NMF with set entries. **115**

C Operating conditions for the medium scale experimentation **117**

C.1 Profile matrix 117

C.2 Prior information 117

C.3 Initial Profile matrix. 117

D Operating conditions for the real data case and results **121**

D.1 Initial Profile matrix. 121

D.2 Prior information 121

D.3 Presentation of the profile estimation 121

Bibliography **145**

List of Figures

2.1 Characteristics of Linear and non Linear Sensors. 6

2.2 Equipment used for sampling. 8

2.3 Different Approaches of estimation for pollution sources. 20

3.1 Different cases of Uniqueness for Non-negative Matrix Factorization. 26

3.2 Majorization Minimization Algorithm. 29

3.3 Gradient Descent Algorithm. 31

4.1 Regression problem with the presence of Outliers. 45

4.2 Geometric point of view for chemical data corrupted with outliers. 46

4.3 The Huber Cost Function 53

4.4 Different areas as a function of α β. 57

5.1 Geometric point of view for Hyperspectral data. 64

5.2 Geometric point of view for chemical data. 65

6.1 Geometric plot of an informed source profile. 80

6.2 Performance of the various NMF methods as a function of the input *SNR*. 92

6.3 *MER* versus *SNR* for 5 outliers. 93

6.4 The performance of the NMF approaches as a function of the number of outliers. . . 94

6.5 Effect of different cutoff strategies on the performance. 95

6.6 *MER* of the various NMF Methods as a function of the input *SNR* : No Outlier . . . 97

6.7 *MER* of the various NMF Methods as a function of the input *SNR* : 2 Outliers 97

6.8 MERs of the various NMF Methods as a function of the input *SNR* : 5 Outliers . . . 98

6.9 Performance of the NMF methods as a function of the number outliers. The Performance Criterion: *MER* (in *dB*). 98

6.10 MER versus input *SNR*. The case without outliers 100
6.11 MER versus input *SNR*. The case with 5 outliers 101
6.12 MER versus input *SNR*. The case with 10 outliers 101
6.13 MER versus input *SNR*. The case with 20 outliers 102
6.14 Device used for sampling. 104

D.1 Estimation of the metal rich source profile. 123
D.2 Estimation of the Primary biogenic source. 124
D.3 Estimation of the Sea traffic source profile. 125
D.4 Estimation of the Road traffic source profile. 126
D.5 Estimation of the biomass source profile. 127
D.6 Estimation of the secondary sulfate source profile. 128
D.7 Estimation of the secondary nitrate source profile. 129
D.8 Estimation of the crustal dust source profile. 130
D.9 Estimation of the Aged sea source profile. 131
D.10 Estimation of the sea source profile. 132

List of Tables

4.1 Several popular M-estimator cost functions 48

4.2 Properties of α-zoom. 56

4.3 Weighting effect on the αβ-divergence. 56

5.1 Different methods with Normalization 78

6.1 Different methods with various shifts and weights 89

6.2 Exact profile matrix 90

6.3 Positions and values of the constraints used in the informed NMF methods. XX means no constraint. 91

6.4 Set Values used in the informed NMF methods. XX means no constraint. 95

6.5 Features of the different source profiles 99

6.6 Performance evaluation of αβ SG-CWNMF. 105

6.7 Performance evaluation of the Huber SG-CWNMF method. 105

C.1 Exact Source Profile 118

C.2 Matrix Ω 118

C.3 Matrix F_{init} 119

D.1 Matrix F_{init} 122

D.2 Matrix Ω 122

Glossary

Variables

General Notations

— u : scalar
— $\underline{u}$: column vector
— u_i : i-th component of vector $\underline{u}$
— $(G \cdot \underline{f})_i$: i-th component of vector $(G \cdot \underline{f})$
— U : matrice,
— $U_{.,i}$: i-th row vector extracted from the matrix,
— $U_{j,.}$: j-th column vector extracted from the matrix,
— $1_{i \times j}$: matrix $(i \times j)$ made with all 1 entries,
— $0_{i \times j}$: matrix $(i \times j)$ made with all 0 entries,
— I_j : $(j \times j)$ identity matrix,

Specific Notations

— n : sample number,
— m : number of chemical species,
— p : number of sources,
— X : $(n \times m)$ matrix of observed data,
— G : $(n \times p)$ contribution matrix,
— F : $(p \times m)$ profile matrix,
— Σ : $(n \times m)$ uncertainties matrix,
— Ω: $(p \times m)$ binary constraint mask applied on the matrix F,
— Φ : $(p \times m)$ matrix of set values in F,

Operators

Vector and matrix operators

— $\tilde{U}$: scaled (or normalized) matrix along the rows,
— $\hat{U}$: estimated matrix,
— $\underline{u}'$: centered version of the vector u,
— $\breve{\underline{u}}$: concatenated version of the vector $\underline{u}$,
— ^{T} : transposition operator,
— $\circ$: term by term matrix product,
— $/$: term by term matrix division,

— $\succeq$, $\preceq$: comparison operators, which apply to each element of a vector or matrix ($X \succeq 0$ means that all elements x_{ij} de X are positive or null),
— Tr : trace of a matrix,
— diag($\underline{u}$) : diagonal square matrix whose diagonal contains the elements of the vector $\underline{u}$,
— $\mathcal{L}(.)$: Langrangian,
— U^+ : projection of U on the non-negative orthant.

other operators

— $\nabla f(\underline{u})$: gradient of criterion f with respect to $\underline{u}$,
— $\mathcal{J}(.)$: scalar function to optimize
— $\mathcal{D}(.||.)$: divergence between two scalors, vectors or matrices,
— $\mathcal{D}_W(.||.)$: weighted divergence between two matrices,
— $\mathcal{D}_W^{\alpha,\beta}(.||.)$: weighted $\alpha\beta$ divergence between two vectors or two matrices,
— $\mathcal{H}_{x,w}^{\alpha,\beta}(.||.)$: majoring function of the weighted $\alpha\beta$ divergence between two vectors , $x = 1,2$

Sets

— $\mathbb{N}$: set of natural intergers,
— $\mathbf{R}$: set of reals,
— $\mathbf{R}_+$: set of positive reals,
— $\mathbf{R}_+^m$: set of vectors of size m with positive or null real components,
— $\mathbf{R}_+^{n\times m}$: set of matrices of size $(n \times m)$ with positive or null real components,

Table of Acronyms

— ALS : *Alternating Least Squares*,
— ANLS : *Alternating Non-negative Least Squares*,
— BSS: *Blind Source Separation*,
— CIM: *Correntropy Induced Metric*
— CWNMF : *Constrained Weighted Non-negative Matrix Factorization*
— HALS : *Hierarchical Alternating Least Squares*,
— ICA: *Independent Component Analysis*
— IRLS: *Iterative Reweighted Least Square*
— KKT (conditions) : *Karush-Kuhn-Tucker*,
— MER : *Mixing Error Ratio*,
— MM : *Majorization-Minimization*,
— N_x-CWNMF(-R) : *Normalized and Constrained Weighted Non-negative Matrix Factorization using (Residuals and) Normalization number* $x = 1, 2$,
— N_xB-CWNMF(-R) : *Normalized and then Bounded Constrained Weighted Non-negative Matrix Factorization using (Residuals and) Normalization number* $x = 1, 2$,
— NMF : *Non-negative Matrix Factorization* ,
— N_x-CWNMF(-R) : *Normalized Constrained Weighted Non-negative Matrix Factorization using (Residuals and) Normalization number* $x = 1, 2$,
— PCA : *Principal Component Analysis*,
— PMF : *Positive Matrix Factorization*,
— SCA : *Sparse Component Analysis* ,
— SIR : *Signal-to-Interference Ratio*,
— SNR : *Signal-to-Noise Ratio*,
— SG-CWNMF: *Split Gradient Constrained Weighted Non-negative Matrix Factorization*,
— SVD : *Singular Value Decomposition*,
— WNMF : *Weighted Non-negative Matrix Factorization*.

CHAPTER 1

General Introduction

1.1 General Framework

Air pollution is known to be one of the major contributors to climate change and therefore needs to be monitored and further understood. People can live without food and water for days but cannot survive without air for even a few moments. Population growth, industrialization, increased wealth and changing societal attitudes are among the significant changes that took place in the world. Needless to say, these changes in society and the economy may lead to an increase in air pollution. Moreover, it is important to analyze, model and understand the impacts of air pollution for the sustainable development of communities.

In several of their studies, the World Health Organization [168] stated that air suspended particles are an important factor of population health risk. Thus, inhaling air with particulate matter will cause irritation even to a minimum chronic organ. Another factor is that dust can be absorbed by plants or animals and can lead to its presence in the food chain. In addition, particles may sometimes contain even a small amount of toxic compounds which could affect negatively the human organs or cells.

As a consequence, it is helpful to study and to understand the mechanisms that generate this pollution to better fight its causes and reduce its impact. Thus, the identification of the particles from different origins that contribute to air pollution in dense urban areas would be very helpful to suggest potential actions that will reduce their emissions. The aim of this work is focused on this objective by integrating all information such as chemical measurements, expert knowledge in order to provide reliable results about the identification of sources of fine particulate matters.

In Europe, a set of instructions govern maximum concentrations for several pollutants. Thus, for particulate matter whose diameter is lower than $10\mu m$ (PM_{10}), the instruction $2008/50/CE$ defines the maximum concentration at $50\mu g.m^{-3}$ and tolerates 35 exceeding days. Europe constrains some regions such as Haut de France to limit their emissions due to numerous exceedings. Particularly, the Pas-de-Calais Detroit from Picardie Region to Belgium involves each day a huge maritime traffic.

Thus, ECUME project, funded by the french DREAL agency, was devoted to understand the reasons of these extreme situations. Professor Courcot (UCEIV lab, Dunkerque) and his team (F. Ledoux, C. Roche) has conducted the study. Their work consisted in conducting a data campaign over a long period and to collect data for further analysis, and understand the different features of sources. The numerical analysis was based on previous algorithms [96] developed in LISIC lab, which were relying on informed NMF with flexible set values and bounds.

Despite these satisfactory interpretations of the results, this thesis would like to answer the question whether dropping bounds constraints in NMF methods would be a good idea or not. It gives also the opportunity to develop new iterative methods which are consistent with the used constraints along iterations. Several outliers may be present in the collected data, so this work will also explore robust methods able to cope with outliers.

1.2 Objective

Starting from a matrix of concentrations associated with uncertainties, the objective of this thesis is to identify the different emitting sources with their relative contribution. A source is characterized by a matrix called the profile matrix which is stable over time. The profile matrix defines a set of proportions of emitted chemical species. Restoring the profiles of the different sources and their relative contributions is therefore the main stake of this thesis.

From a theoretical point of view, this problem is tackled in the frame of matrix factorization where the profile matrix and the contribution matrix are to be estimated. The noise on the collected data is of unknown distribution and may not assimilated to a Gaussian distribution. Moreover, the Signal to noise ratio (SNR) of the collected data is probably relatively small and the measurements are corrupted with outliers that may come from different physical origins. In addition to that, some knowledge is available on the profile matrix and or the contribution matrix

— The profile and the contribution matrices are non negative.
— The rows of the profile matrix sum to 1.
— Some entries of the profile matrix are known.

So the aim of this thesis is to solve a non-negative matrix factorization problem informed by the above knowledge and subject to outliers. The methods developed are dedicated to the identification of sources of pollution in the air.

1.3 Thesis outline

In addition to this general introduction, the thesis is organized into five regular chapters and a general conclusion. This thesis is decomposed into a state of the art on classical non-negative matrix factorization methods (chapter (3)), a chapter on robust NMF methods (Chapter (4)) and a chapter (5) which highlights Informed NMF methods with set values and sum-to 1 variables. Original contributions of this thesis are essentially concentrated in chapter (6) where new methods are developed.

1.3.1 State of the art

Chapter (2) reviews the complete chemical sensing problem, starting from the sensor model to the physical phenomenon under study. A special focus is performed on general mixtures models which essentially govern the overall source apportionment problem. Moreover, a matrix factorization point

of view together with an optimization framework is adopted. Usual Constraints associated with such an optimization problem are investigated with a special emphasis on non-negativity and sum-to-1 constraints.

In accordance with the definition of the source apportionment problem, the framework of this thesis is oriented towards non-negative matrix factorization methods since non-negativity of the factors is the central hypothesis of the problem.

1.3.2 Non Negative Matrix Factorization (NMF)

Chapter (3) provides an overview on classical NMF problems, by examining uniqueness conditions for exact NMF and KKT conditions for the approximate NMF problem. It also highlights several families of methods to solve this approximate problem. A special focus is also performed on weighted NMF problems which arise in chemical sensing where data are associated with uncertainties. The weight concept could be also adapted to the context of outliers which is further studied.

1.3.3 Robust NMF methods

Chapter (4) explores the impact of outliers present in the data for regression and NMF. Then, several robust regression methods and robust NMF are investigated, with a special care on modified cost functions.

1.3.4 Existing Informed NMF methods with set values and sum-to 1 variables

Chapter (5) is devoted to explore methods which involve set values row sum-to-1 variables. Each kind of information is investigated alone first, then both knowledge are incorporated by exploiting an informed NMF with set values and applying some specific normalization procedures.

1.3.5 New Informed NMF Methods

Chapter (6) first defines a parametrization consistent with row sum-to-1 profile and set values. This parametrization is used to develop new iterative algorithms which live at each iteration in the subspace of the parametrization. These new algorithms are developed together with a weighted Frobenius cost function and two weighted robust cost functions.

Validation are proposed along this chapter with two two simulation studies. Moreover, data from the ECUME project are exploited to extract estimated profiles which are compared with expert requirements.

1.4 General Conclusion

Finally, the General Conclusion (7) recalls the theoretical contributions discussed and investigated in this thesis and presents several perspectives of this work.

CHAPTER 2

State of the Art

2.1 Introduction

This chapter presents the various types of models encountered in the source separation field. A particular focus is on the family of linear models which are based on instantaneous mixture models. Then, the range of sensors used for measurements are discussed. Typically, the sensor model is provided with its technical description.

Then, the set of usual hypotheses associated to the mixtures models are reviewed. These hypotheses are combined with the general definition of the criterion by incorporating them either as soft or hard constraints. Once the whole model is obtained, the problem becomes a special matrix factorization problem which can be formulated as a non-negative optimization problem. Lastly, through a small description of the desired application, several tracks which will be further developed are presented.

2.2 General Sensor Models

This section is focused on sensors. Indeed, sensors play an important role in the quality of the separation process. Therefore, the input output characteristics of various kinds of sensors are introduced and the different available devices for air pollution are emphasized.

2.2.1 Sensor characteristics

The characteristic of a sensor is considered as its major feature. The sensor generally yields an electric output such as a voltage or a current corresponding to a physical quantity. Its characteristics provides the information to estimate the true physical value. Thus, the sensor's characteristic is usually represented by a voltage as a function of the true physical value. Typical characteristics of various sensors are illustrated in Figure (2.1). They are here divided into two categories: linear and non linear. The perfect linear sensor is represented by the red line whereas all the remaining curves represent non linear sensors. While the Green curve is associated with the concave type, the Magenta curve represents the convex type and the black curve denotes a sensor with saturation (hard thresholding) in which only part of the data can be retrieved. For example, the data between 1 and 8 can be recovered

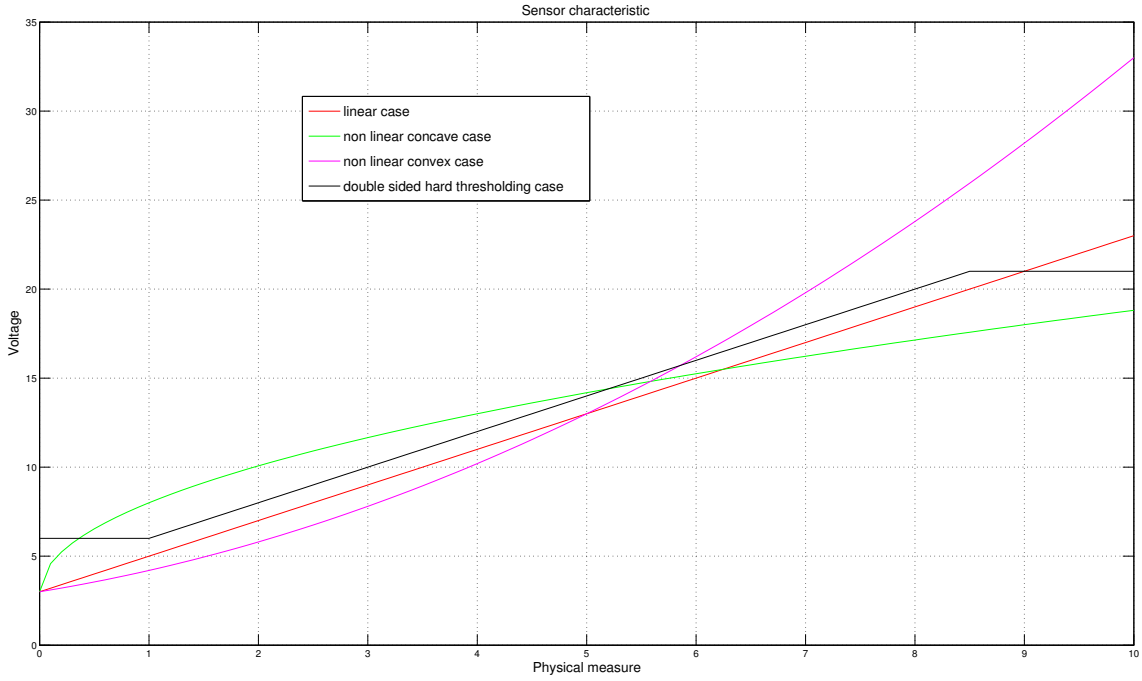

Figure 2.1 – Characteristics of Linear and non Linear Sensors.

because there is a linear correspondence between them. On the contrary, physical variables less than 1 and greater than 8 can not be retrieved.

Another possible issue related to sensor modelling is related to its time response. In this case, it may be modelled by a linear convolutive model. In the context of air pollution the observed phenomenon is very slowly varying, and consequently the time response of the sensor is generally not tricky.

2.2.2 Sensor devices for Air pollution

In this subsection, the emphasis is specifically on sensor devices for air pollution. Several types of sensors [133] exist according to their aim. First low cost and small size sensors for gas species are listed. Secondly, large size samplers which can deal simultaneously with several particulate matter species are highlighted.

2.2.2.1 Small size sensors

They are all dedicated to the measurement of a particular gas species only. Their measurements may be automated via their integration into electronic equipment.

1. Electro-catalytic sensors:
   They are small size sensors with a very affordable cost. One advantage is the simplicity of their operation. They just measure the amount of heat emitted by the combustion of the gas under study which comes into contact with a previously heated metal. However, they have several disadvantages, e.g., the measurements are not precise and are not stable. They need also to be calibrated regularly.

2. Semi Conductor sensors:
   They work almost as the previous sensors. An advantage is that the measurements are stable over time. The disadvantage is that they may be corrupted by certain gases and consequently, the sensors become unusable.

3. Infrared Sensors:
   They are based on a different concept which is the principle of selective absorption of the light i.e specific to a particular gas. They measure the amount of light absorbed for a given duration of time. This type is very reliable and is stable over time. The disadvantage is that they are not available for all gases and are of high cost.

4. Electrochemical sensors:
   These types of sensors are based on the principle of an electric cell with the gas to be measured as the reactive. The sensor yields an electrical potential related to the target gas concentration. Based on the reactive defined by the manufacturer, it is possible to have elements which react to a specific gas to be measured. These sensors are very reliable and are stable over time. However, they are of high cost.

2.2.2.2 Digital samplers

Contrary to sensors, digital samplers may be used to evaluate the particulate Matter (PM) mass into a specific air volume, enabling to compute a concentration.

It is designed to measure air suspended particulate matter concentration. Various classes of sizes exist, e.g., PM10 or PM2.5 and PM1 for particles whose diameter is lower than $10, 2.5, 1$ µm respectively. There are reference samplers, such as the german LECKEL SEQ 47/50 device, or the italian FAI Hydra Dual, which work on two channels, in order to measure simultaneously the concentration PM2.5 and PM10. The other reference sampler is the DA80 device from Digitel which is shown in Figure (2.2).

The principle of the DA80 device is to pump an air volume periodically in order to trap the particles present in the air on a filter. The sampler is equipped with a system able to control precisely the inlet flow. Besides, the available filtering system allows to keep on the filter the particles that correspond to PM2.5. Then, the filter is automatically stored and a new filter is installed. Afterwards, the concentration is determined in a lab, based on a particulate mass measure on the filter. The unit

Figure 2.2 – Equipment used for sampling.

is able to record various measurements including the concentration of the particulate matter, the time of collection of each sample, the pressure and the temperature. The measurements are collected every 24 hours and wind measurements are also available in the 60-minute period.

The chemical analysis performed in a lab does not detect particulate matter concentrations below a specific limit *LDD*. Thus, the true DA80 model corresponds to the model with a single hard thresholding (2.1) (for lower values) with a species depending cutoff parameter corresponding to the low detection limit (LDD_j). In this case, the measure will be assumed to be equal to $\frac{LDD_j}{2}$, and the relative uncertainty will be considered equal to 100%. The DA80 model will be approximated to be completely linear in conjunction with the assumption that the uncertainty is very large for these small values.

Besides to the above sampling devices, the Grimm and Dust monitor 1.108 is an optical sampling device which quantifies particulate matter according to different size bins. The sampling period could be adjusted to shorter values as the other devices, but it works differently since it provides a concentration for each size bin.

To conclude, the DA80 sampler has been used for different campaigns and it is considered in this thesis as a completely linear model.

2.3 General Linear Mixture Models

Various types of mixture models exist in the literature [32]. They may be classified according to the observation model that relates the observations to the different sources.

Here, the linear mixtures and their derivations are highlighted and non linear mixtures are excluded from this study. The interested reader may have a look at [36] where post non linear models and linear quadratic models are investigated.

As a result, different formulations of linear mixtures are developed below.

2.3.1 Linear Instantaneous Mixtures

Suppose that n observations resulting from p sources emitting activity at any time t are collected. The sources are mixed by a specific gain in each source sensor channel. The mixtures are observed by the different sensors. The observation $x_i(t)$ of sensor i at time t can be written as a linear combination of the different sources at the same instant t:

$$x_i(t) = \sum_{j=1}^{p} g_{ij} f_j(t) \quad \forall i = 1, \ldots, n, \tag{2.1}$$

where g_{ij} is the attenuation of the transmission channel from source j to sensor i, $\quad \forall i = 1, \ldots, n$, and $f_j(t)$ is the emission of source j at time t.

The integration of various sensors leads to the following matrix formulation:

$$\begin{pmatrix} x_1(t) \\ x_2(t) \\ \vdots \\ x_n(t) \end{pmatrix} = \begin{pmatrix} g_{11} & g_{12} & \cdots & g_{1p} \\ g_{21} & g_{22} & \cdots & g_{2p} \\ \vdots & \vdots & \ddots & \vdots \\ g_{n1} & g_{n2} & \cdots & g_{np} \end{pmatrix} \cdot \begin{pmatrix} f_1(t) \\ f_2(t) \\ \vdots \\ f_p(t) \end{pmatrix}, \tag{2.2}$$

or in a condensed form

$$\underline{x}(t) = G\underline{f}(t), \tag{2.3}$$

where

- G is the mixing matrix of size $n \times p$ and is supposed to be invariant over time or samples. This means that the mixing process is always the same over time.
- $\underline{x}(t) \triangleq [x_1(t), \ldots, x_n(t)]^T$ is the $n \times 1$ column vector accounting for the observations at time t.
- $\underline{f}(t) \triangleq [f_1(t), \ldots, f_p(t)]^T$ stands for the $p \times 1$ column vector gathering the different source signals at time t.

Considering m samples $\underline{x}_k = \underline{x}(k \cdot T_e)$, for $k = 1, \ldots, m$ and T_e is the sampling period, the expression (2.3) reads

$$\underline{x}_k = G\underline{f}_k, \tag{2.4}$$

where $\underline{f}_k = \underline{f}(k \cdot T_e)$.

Grouping m time samples together leads to an exact matrix product resulting from equation (2.4),

$$X = G \cdot F, \tag{2.5}$$

where $X \triangleq [\underline{x}_1, \ldots, \underline{x}_m]$ and $F \triangleq [\underline{f}_1, \ldots, \underline{f}_m]$ stand for the $n \times m$ measurement matrix and the $p \times m$ source matrix, respectively.

The formulation described in (2.5) is the usual convention adopted in Blind Signal Processing where the time is ordered by the rows. The symmetric point of view may be found in physics where the time is usually ordered by the columns. This leads to define a symmetric expression obtained from the previous one, e.g.,

$$X^T = F^T G^T. \tag{2.6}$$

In the following chapters, equation (2.5) is considered as the basis with an exchange in the definition of n and m.

Such linear mixture models may be applied in various fields such as:

— Telecommunication [35, 145]: multiple radio identification signals (RFID) are observed simultaneously by several sensors and each observation consists of an instantaneous linear combination of the various observed source signals.
— Biomedical [139, 92]: The model is implemented to process and to analyze the cardiac activity. The atrial and the ventricular activities are separated from the data that are collected by the electrodes placed on the surface of the skin. In similar studies, the instantaneous linear mixing model is applied to the electrocardiogram of pregnant women in order to separate the activity of the fetal heart from the activity of the mother's heart.
— Acoustics and signal processing audiophonic [163, 126]: The instantaneous linear model is not generally valid. There are few exceptions. It can be applied when multiple sources are sequentially recorded in the studio and are mixed by a sound engineer, using a mixer, with no added post-processing effect.
— Multispectral/ hyperspectral imaging: The same images of a geographical area are gathered at different wavelengths. Then, a data cube whose two axes indicate the spatial coordinates and the third provides the spectral information is generated. The observed spectral information in each voxel is perceived as an instantaneous linear mixture of the sources spectra [115, 110]. This concept can be also implemented in astrophysics and in remote sensing applications [79, 9]. Alternatively, for each wavelength, the collected images can be viewed as mixture snapshots of the source images.
— Chemistry [112, 113, 103]: The measurements of the optical fluorescence spectra and the Infrared Spectroscopy sampling are considered as instant linear mixing sources spectra. Similarly, in the environment, air pollution or water measurements may be treated as a linear instantaneous mixing problem, if the following conditions are fulfilled: First, the sources are not too far from the sensor compared with the distance traveled by the air during the sampling period of the data. Second, there is mainly no reaction between the species. Third, the sensors do not exhibit any non-linearity. In this work, these conditions are assumed to be checked.

2.3.2 Mixtures with attenuation and time delay

They are also called anechoic mixtures. They represent an extension of linear instantaneous mixtures where the time of arrival of the various signals to the sensors are subject to time delays due to the single-path propagation of the sources to the sensors. The observation $x_i(t)$ can be expressed as:

$$x_i(t) = \sum_{j=1}^{p} g_{ij} f_j(t - t_{ij}) \quad \forall i = 1, \ldots, n, \tag{2.7}$$

where g_{ij} and t_{ij} respectively correspond to the attenuation and the time delay due to the propagation from the source j to sensor i. As this model may be seen as a special case of convolutive mixtures, the matrix form will be only provided in the corresponding subsection.

The anechoic mixture model is mainly used in acoustics and it assumes that the environment is slightly reverberant. It is to be noted that this type of model is widely applied in source localization [87] and that some localization methods of multiple sources [11, 127] are directly inspired by the above model (Eq 2.7) . Furthermore, the approach [5] based on (Eq 2.7) has been proposed for image processing, where the shift is not temporal but spatial, i.e., each source is offset horizontally and vertically.

2.3.3 Convolutive mixtures

In most cases, the emissions from the sources to the sensors follow a multipath propagation that can be expressed as a sum of various mono-path propagation of the sources, i.e.,

$$x_i(k) \quad = \quad \sum_{j=1}^{p} \sum_{q=0}^{+\infty} g_{ijq} f_j(t - t_{ijq}) \tag{2.8}$$

where g_{ijq} and t_{ijq} are respectively the $(q+1)^{th}$ attenuation and the time delay due to the propagation from the source j to the sensor i. Thus, Eq. (2.8) can be written as a linear combination of the filtered version of the sources:

$$x_i(t) = \sum_{j=1}^{p} g_{ij}(t) * f_j(t) \tag{2.9}$$

where the symbol $*$ denotes the convolution operator and $g_{ij}(t)$ is the propagation from Source j to Sensor i. In practice, most of the blind source separation approaches consider that g_{ij} is a filter of finite impulse response of order Q, the maximum order of all the channels. By using the discrete

notations explained in section (2.3.1), the previous equations Eqs. (2.8, 2.9) can be written as follows:

$$x_i(k) = \sum_{j=1}^{p}\sum_{q=0}^{Q} g_{ij}(q) f_j(k-q) \quad \forall i = 1,\ldots,n, \tag{2.10}$$

$$= \sum_{j=1}^{p} g_{ij}(k) * f_j(k) \quad \forall i = 1,\ldots,n, \tag{2.11}$$

where $g_{ij}(k)$ is the modeling of the impulse response of the filter representing the propagation channel from Source j to Sensor i subject to the conditions of Sample k. By letting G_k be the $n \times p$ matrix that consists of the various impulse responses $g_{ij}(k)$ at a sample time k, Eq. (2.8) can be written in a matrix form by swapping the order of the sums and by turning out G_k , i.e,

$$\underline{x}_k = \sum_{q=0}^{Q} G_k \underline{f}_{k-q} \tag{2.12}$$

where $\underline{f}_{k-q} \triangleq [f_1(k-q),\ldots,f_p(k-q)]^T$ and $\underline{x}_k \triangleq [x_1(k),\ldots,x_n(k)]^T$. Equation (2.12) can be formulated as a general matrix product [157, 130, 107] by stacking K samples measurements,

$$\begin{cases} \underline{x}_k &= G_0\underline{f}_k + \ldots + G_Q\underline{f}_{k-Q}, \\ \underline{x}_{k-1} &= G_0\underline{f}_{k-1} + \ldots + G_Q\underline{f}_{k-Q-1}, \\ \vdots & \\ \underline{x}_{k-K+1} &= G_0\underline{f}_{k-K+1} + \ldots + G_Q\underline{f}_{k-K-Q+1}. \end{cases} \tag{2.13}$$

Then, it is possible to define an augmented vector $\underline{\check{x}}_k$ (of size $(n \cdot K) \times 1$) made with the past measurements vectors $\underline{x}_{k-j}$,

$$\underline{\check{x}}_k \triangleq [\underline{x}_k^T, \underline{x}_{k-1}^T, \ldots, \underline{x}_{k-K+1}^T]^T \tag{2.14}$$

Similarly, the $p \cdot (K+Q) \times 1$ vector $\underline{\check{f}}_k$ may be defined as the concatenation of past vectors $\underline{f}_k$,

$$\check{f}_k \triangleq [\underline{f}_k^T, \underline{f}_{k-1}^T, \ldots, \underline{f}_{k-K-Q+1}^T]^T \tag{2.15}$$

Finally, the convolutive mixture may be written as a specific matrix factorization form,

$$\underline{\check{x}}_k = \check{G} \cdot \underline{\check{f}}_k \tag{2.16}$$

where the matrix $\check{G}$ is a specific sylvester matrix

$$\check{G} = \begin{pmatrix} G_0 & \cdots & G_Q & 0 & 0 & \cdots & 0 \\ 0 & G_0 & \cdots & G_Q & 0 & \cdots & 0 \\ 0 & \ddots & \ddots & \ddots & \ddots & \ddots & 0 \\ 0 & \cdots & 0 & G_0 & G_1 & \cdots & G_Q \end{pmatrix}. \tag{2.17}$$

It should be mentionned that several approaches are implemented in the frequency domain by applying a time frequency transformation to the observations [129]. The factorization model in Eq. (2.5) is then

used successively and independently for each considered frequency. Consequently, the given mixture is approximated by a linear instantaneous model with complex values. This problem is easier to deal with in comparison with Eq. (2.17). However, other difficulties appear and complicate the separation problem when the results are transformed back to the time domain.

Lastly, convolutive mixtures are usually applied in acoustic field [129, 157].

2.3.4 Conclusion

Different kind of linear mixtures encountered in the literature are presented in the above subsections. It is shown that the data matrix may be linked to a special matrix product. The estimation of one factor (or both factors) requires additional assumptions that are investigated in the following sections.

2.4 Brief Overview of Factorization Methods

In this section, the factorization methods related to the linear mixture model are introduced. All these approaches require extra information related to one of the factors. They can be mapped into five large classes dealing with:

— source orthogonality
— statistical independence
— sparse assumption
— the normalization of one factor
— the non-negativity of one or both factors.

2.4.1 Principal components analysis (PCA)

Principal Components Analysis (PCA) is a multivariate statistical method introduced by K. Pearson [128] and then developed by H. Hotelling in 1933 [68]. The principle of PCA relies on a dimension reduction of the whole data including a large number of features which are geometrically related, to form a subspace of principal components. In this section, the matrix optimization viewpoint which bridges both the geometrical and statistical point of views is adopted.

Some geometrical interpretations are usually stated. It consists in finding a subspace of dimension p that best fits the n centered data vectors ($\in \mathbf{R}^m$) in a least square sense. This subspace is shown to be defined by the p basis vectors which are gathered into the matrix U_p (of size $m \times p$). This search may be formulated as an optimization problem subject to the orthogonality constraint. Let's define X' as the centered data matrix X, then X' may be written as an approximate matrix factorization [161] subject to an orthogonality constraint, i.e.,

$$X' \approx X' \cdot U_p \cdot U_p^T \qquad \text{s.t.} \quad U_p^T \cdot U_p = I_p \tag{2.18}$$

Finding a solution to this problem amounts to perform a Truncated Singular Value Decomposition (TSVD) restricted to the p highest singular values.

From a statistical setting, PCA aims at finding the right subspace (with dimension p) that maximizes the spreading of the projected data. Vidal [161] showed that the best p column vectors from U_p maximize the Frobenius norm of the matrix $(X' \cdot U_p)$ which, in turn, reflects the data spreading into the subspace. These column vectors are obtained by computing the eigenvectors corresponding to the p greater eigenvalues of the covariance matrix $\Sigma_x \triangleq X' \cdot X'^T$.

As an extension, PCA could be also applied into the field of low rank approximation. Schuermans [149, 117] developed some weighted low rank approximations which may be viewed as weighted extensions of Eq. (2.18). Let us stress that Singh & al. proposed a unified view [152] which highlights the connection between general factorization models and related PCA approaches.

Besides, PCA is known to be sensitive to outliers, which comes from the least square formulation of the optimization criterion. In fact, this leads to the effect that a single abnormal point may corrupt completely the estimation. To overcome this inconvenient, robust extensions of PCA have been investigated in order to split the data matrix into a low rank matrix and a sparse one, such as projection pursuit approaches [18, 170].

To conclude, PCA and related methods cover a very wide and active research field which leads to the approximization of a particular approximate matrix factorization of the centered data matrix. However, PCA seems inappropriate to solve the application of this thesis for several reasons:

— The orthogonality of the factors does not make sense in the thesis's application,
— Principal components may be negative and it is not the case,
— In the presence of outliers, the outcome of PCA is affected by even few abnormal points.

As a consequence, other techniques should be reviewed.

2.4.2 Independent Component Analysis (ICA)

Independent Component Analysis is a classical approach to separate source signals from multiple mixtures of these sources. In the frame of linear mixture models, ICA amounts to find a separation matrix S which enables to recover the source signals Y in the observation signals X, i.e.,

$$Y = S \cdot X. \tag{2.19}$$

Ideally, S should be equal to the pseudo-inverse of matrix G. Practically, the source signals can be recovered to a scale factor and a permutation. This leads to express a special link between S and G

$$S \cdot G \simeq D \cdot P, \tag{2.20}$$

where D is a diagonal matrix which consists of the scale factors and P accounts for a permutation matrix.

The first methods were proposed by Jutten and Herault [74, 78]. Then, Comon generalized the concept of ICA [31]. He showed that, if the source signals are mutually independent and not Gaussian, it is possible to extract these signals up to a scale factor and a permutation matrix by minimizing the dependence measure between the estimated signals. Different independence measures were developed to perform the source separation, e.g.,

— the maximization of the non Gaussianity by using higher order statistics such as 4^{th} order cumulants or Kurtosis [73].
— the maximization of the neguentropy which accounts for a dissimilarity measure to a Gaussian distribution [72].
— the minimization of the mutual information
— the maximization of the likelihood of source signals assuming that they belong to a specific probability density family [6].
— The non negative Independent Component analysis based on the newton optimization [121].

Besides, some approaches were used with second order statistics in conjunction with extra temporal assumptions based on non stationarity [154, 131] or autocorrelation [158, 7] leading to some famous algorithms such as SOBI [7].

By taking into account the application in question, the independence between factors appears to be unrealistic. Thus, it won't be discussed in this document.

2.4.3 Sparse Component Analysis(SCA)

Sparsity is an assumption which receives a growing interest in the community since the last decade. A signal is said to be sparse if it is often zero while its variance is not. Usually, the signal needs to be transformed into another domain to become sparse. While a few authors consider the separation problem as a penalized sparse inverse problem [12], most approaches [134]

— perform a joint sparse transformation (Discrete Cosinus Transform (DCT), Short-Time Fourier Transform (STFT), wavelets) of the observations,
— estimate the mixing parameters, i.e., the matrix G,
— carry out the estimation of the matrix F as an inverse problem.

The corresponding approaches can be classified according to their source sparseness assumption:

1. Many methods assume the sources to be W-disjoint orthogonal [77], i.e., in each time-frequency point, at most one source is active. The estimation of the sources is reduced to a clustering problem [174].

2. Some approaches [1, 37, 134, 138, 136, 108, 135] assume that the sources can overlap except in a few zones (or points in [138]) where one source is only active.

3. The remaining methods use a sparse assumption in between the above families. They assume the W-disjoint orthogonality with a single-source activity confidence measure to enhance the estimation of the mixing matrix [3].

Besides these historical techniques, other SCA techniques relax the sparsity assumption by assuming that several, say k, sources are always active (with k strictly lower than the number of observations) and by clustering the intersection of the hyperplanes which can be estimated in these zones [64, 115, 13]. Other authors assume that one source is silent in some zones and estimate the corresponding demixing column in these zones [140]. It is to be noted that the SCA techniques were also extended to other applications such as audio source localization in [11, 127].

Interestingly, SCA was recently revisited by extending sparse NMF techniques to audio signals [50]. Another trend consists of looking for a specific co-sparse operator which promotes sparsity [116].

However, in the context of the thesis's application, sparsity-based methods seem not be appropriate since none of both factors should be considered as sparse. For example, the loadings—i.e., the entries of G—may not be considered as sparse signals. In particular, temporal areas where a subset of sources are active, can not be easily identified. Similarly, the above sparse assumption is not satisfied for F and determining a sparsifying transformation well-suited for the considered application is tricky. As a consequence, this assumption will not be further explored in the following chapters.

2.4.4 Non-negativity based methods

Historically, ICA or PCA based methods suffer from poor interpretability of their results. In several applications, negative components contradict the physical meaning. As an example, a grayscale image or physical quantity have non negative values. As a consequence, non-negativity based methods received a growing attention in the last decades.

Essentially, Non-negativity based methods aim at finding matrix factors that satisfies the linear mixture model (2.5) in the least square sense. The minimization of the Frobenius norm of the modelling error enables the optimization of both factors. However, this problem remains ill-posed because it may provide non unique solutions, especially with respect to the scale matrix and the permutation matrix. Another issue is due to multiple local minima, which generally require several initializations.

The first studies, denoted Positive Matrix Factorization (PMF), appeared in 1994-1997 with Paatero's work [125, 2, 124] and consist in solving the problem in a least square sense around an operating point by linearizing the criterion. Their methods [125] were able to deal with uncertainties provided by the users which help stabilizing the solution with respect to noise. However, their methods present some drawbacks:

— The increase of the input matrix's size leads to an increase in the model's time consumption.
— It does not allow any control on the initialization and the stopping criteria.

Despite these inconvenients, many environmental studies have been successfully conducted using PMF.

Non-negative Matrix Factorization (NMF) became popular in 1999 with Lee and Seung's work [95, 94], who developed some multiplicative update rules. However, these methods does not allow to ensure the convergence toward a global minimum [147]. To enforce some properties of the solutions, many NMF methods may be expressed into the general following formulation,

$$\min_{G,F\succeq 0} \mathcal{J}(X,GF) = \min_{G,F\succeq 0} \mathcal{D}(X||GF) + \lambda_G \mathfrak{R}_G(G) + \lambda_F \mathfrak{R}_F(F), \tag{2.21}$$

where

— $\mathcal{D}$ stands for a general norm or more generally a divergence between the data matrix X and its estimation. The most classical function is the Frobenius norm which is an extension of the Euclidian distance intended for vectors to matrices.

— $\mathfrak{R}$ accounts for a penalty term to enforce a desired property in one factor.

Thus, according to the problem under consideration, many properties are able to be incorporated,

— different forms of relaxed orthogonality may be encountered [175, 176]

— sparsity based factor such as l_1 norm of one factor. The method is called Non-Negative Sparse Coding [69].

— The spreading of one matrix factor by minimizing a determinant based function [146, 147].

— Sum-to-one of one factor may be also desired but it will be developed in the next subsection.

Once the criterion is defined, NMF may be solved in different ways according to different tracks. The methods can be categorized into different classes. They include:

— the class of multiplicative updates and the very large references therein,

— the class of Alternated Non-negative Least Square (ANLS),

— the class of projected gradient based methods [101],

— the class of Alternative Direction Method of Multipliers (ADMM) [155].

All these families of algorithms will be reviewed in details in the next chapter.

2.4.5 Sum-to-one based methods

Although sum-to-one may be viewed as one special desired property of NMF, it is addressed in this subsection mainly because it is usually used in the framework of the hyperspectral unmixing under the name of full additivity. However, another viewpoint exists and is often overlooked. Thus, both views are presented while trying to bridge the gap between them.

Sum-to-one of the columns of F or rows of G: This property may be outlined by the following equation, i.e.,

$$G_{n\times p} \cdot 1_{p\times p} = 1_{n\times p} \tag{2.22}$$

where $1_{n\times p}$ is the matrix of 1 and of size $n \times p$. This equality states that the p entries in G sum to 1. By transposing Eq (2.5), the above property is exactly similar to the sum-to-one of the columns of matrix F (or rows of matrix F^T). This property is often encountered in hyperspectral unmixing where the reflectance data are assumed to be a linear combination of p endmembers weighted by their corresponding fractional abundances. In this case, abundances at one pixel may be viewed as a particular row of G, which, as a consequence, sum to 1. The approximated matrix factorization

Eq (2.5) and Eq (2.22) can be expressed as

$$\min \mathcal{D}(X||G\cdot F), \quad \text{subject to} \quad G_{n\times p}\cdot 1_{p\times 1} = 1_{n\times 1} \tag{2.23}$$

The above equation is optimized by splitting the search on G into n independent sub problems i.e.

$$\min \mathcal{D}(\underline{x}_i^T||\underline{g}_i^T\cdot F) \quad \text{subject to} \quad \underline{g}_i^T 1_{p\times 1} = 1_{1\times 1} \quad \forall i \in \{1\dots n\} \tag{2.24}$$

As a consequence, the first methods to solve Eq (2.24) rely on a vectorial point of view based on a linear least square [150]. Then, Heinz proposed to incorporate the sum-to-one information into a Sum-to-one Constrained Least Square (SCLS) solution [65].

Most authors propose a geometric interpretation (A survey is available in [38]) which views the data as belonging to a convex hull spanned by the endmembers.

However, the separability property of the problem into subproblems doesn't hold true for the second case that is investigated below.

Sum-to-one of the rows of F or columns of G: In the second case, the sum-to-one property is applied on the rows of F or the columns of G. Depending on which factor it is applied, the sum concerns n or m entries. It differs from the previous case where it was applied to the p entries. It is described by Eq. (2.25),

$$F_{p\times m}\cdot 1_{m\times m} = 1_{p\times m} \tag{2.25}$$

Thus, the row sum-to-one matrix $\tilde{F}$ may be computed from any unconstrained version of F such that,

$$\tilde{F} = \frac{F}{F\cdot 1_{m\times m}}, \tag{2.26}$$

where the quotient refers to Hadamard division. Similarly, the expression of $\tilde{G}$ can be defined as,

$$\tilde{G} = G\circ(1_{n\times m}\cdot F^T), \tag{2.27}$$

where the operator $\circ$ represents the entrywise multiplication of the matrices. The implementation of this transformation to (F,G) doesn't change the product $G\cdot F$, i.e.,

$$\tilde{G}\cdot\tilde{F} = G\cdot F \tag{2.28}$$

If the case of exact factorization is considered, i.e.,

$$X = G\cdot F, \tag{2.29}$$

The multiplication of Eq (2.29) by $1_{m\times m}$ and the combination of the result with (2.25), yield:

$$X_{n\times m}\cdot 1_{m\times m} = G_{n\times p}\cdot F_{p\times m}\cdot 1_{m\times m} = G_{n\times p}\cdot 1_{p\times m} \tag{2.30}$$

In other words, the sum of each row of G is equal to the sum of each row of X. This property is very

close to the property (2.22) which stands for the full additivity condition encountered for example in Hyperspectral Unmixing. In this last case, the relation is often treated as an exact constraint. However, in practice here, the exact equation (2.29) is not reached due to the presence of noise, outliers or modelling errors. Then, the deduced relation (2.30) becomes only an approximate relation which comes from the approximate version of Eq (2.29) , i.e.,

$$G_{n\times p}\cdot 1_{p\times m} \approx X_{n\times m}\cdot 1_{m\times m}. \tag{2.31}$$

To the best knowledge of the authors, constraints introduced in (2.31) are not considered in the literature except Lantéry [91] who considers them as exact relationships.

As a consequence, the new factorization problem may be addressed only with the hard constraint (2.25) and by dropping the approximate one,

$$X \approx G\cdot F, \quad \text{subject to} \quad F_{p\times m}\cdot 1_{m\times m} = 1_{p\times m} \tag{2.32}$$

This formulation corresponds in fact to the point of view adopted in this practical application. In contrast with the case of Hyperspectral Unmixing, the problem can not be divided into n sub-problems due to the constraint under consideration. This point leads to completely different procedures to solve the problem.

Besides, these assumptions are usually coupled with the non-negativity assumption [23].

2.5 Conclusion

In this chapter, an overview of the classical mixture models was provided and a brief review of different hypotheses which may be coupled with the previous models were presented. The main properties include: independence, sparsity and orthogonality. Besides, non-negativity and sum-to-one assumptions can be accounted also for frequent information. All these models in conjunction with the extra hypotheses can be cast in the frame of approximate matrix factorization which can be tackled by solving a dedicated optimization problem.

The desired application under consideration in this thesis, air pollution source apportionment, is also highlighted. The sensor device dedicated here for particulate matter measurement could be considered as an instantaneous linear one so that source apportionment may be viewed as a whole linear unmixing problem. Figure (2.3) provides an overview of methods used for source apportionment according to the available information. Knowing that the factors are all non-negative, NMF appears as a nice solution to be investigated. However, the indeterminacies of the blind NMF method which will be highlighted in the next chapter limit its scope. It seems interesting to develop in this thesis informed methods (2.3) which lie in between blind ones and regression methods. But first, the next chapter will be devoted to explore the features of blind NMF methods.

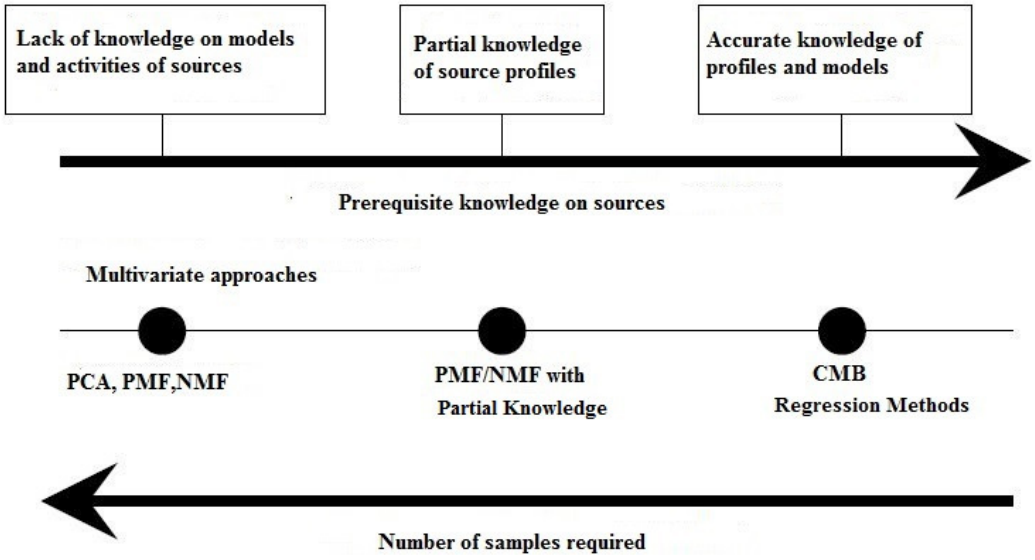

Figure 2.3 – Different Approaches of estimation for pollution sources.

CHAPTER 3

Non-negative Matrix Factorization

3.1 Introduction

In this chapter the basic concepts of Non-negative Matrix Factorization, as well as the families of algorithms allowing to solve them, are presented. This chapter is considered to be a bibliographical emphasizing the important characteristics of the given practical problem addressed in this thesis.

Given a data matrix that consists of concentrations of various chemical species collected at a sampling rate of 12 hours. These data are modelled as an instantaneous linear mixture of pollutant sources, which can be expressed into a mathematical form: given a data matrix X of size $n \times m$ with $x_{ij} \succeq 0$, NMF aims to find two non-negative matrices G of size $n \times p$ and F of size $p \times m$ such that their product is approximately equal to the data matrix X, i.e,

$$X \approx G \cdot F. \tag{3.1}$$

In the application considered in this thesis, matrices X, G and F represent the following:

1. X is the collected data matrix where x_{ij} is the chemical concentration of the species j in the sample i and expressed in ng/m^3. Each row of X contains the concentrations of the different chemical species at the same sample time.

2. G is the contribution matrix where each element g_{ik} represents the contribution in ng/m^3 of Source k for Sample i.

3. F is the profile matrix where each element f_{kj} reflects the relative proportion in ng/ng of chemical Species j for Source k. It represents the quantity of emitted mass by Species j per unit mass emitted by Source k. As a result, each row of F sums to 1. In this chapter, this last information is not taken into account.

In this chapter, the optimization problem is is addressed which leads to necessary conditions required for the solution. Then, different classes of algorithms associated with the classical NMF problem and its weighted counterpart as well are reviewed. Based mainly on Limem's thesis [96], this chapter yet presents an overview of new trends with up-to-date references.

3.2 Classic NMF Problem

In this section, the standard formulation of the NMF technique based on the Frobenius distance is presented. This distance, usually devoted to vectors, is an extension to matrices of the Euclidian norm. Non-Negative Matrix Factorization (NMF) is a multivariable data analysis approach which is intended to approximate physically significant components and/or features that characterize a particular application from the collected non-negative data. In other words, NMF is an approach that is mainly appropriate for the decomposition of non-negative data. The nonexistence of negative values is a very important characteristic of several applications in which many physical quantities (such as intensities, concentrations, frequencies, counts and probabilities) are collected.

The Frobenius based NMF problem is defined as the minimization of the Frobenius similarity criterion (Eq 3.2)

$$\min_{G,F\succeq 0} \mathcal{J}(G,F) = \min_{G,F\succeq 0} \sum_{i=1}^{n}\sum_{j=1}^{m}((x_{ij}-(GF)_{ij}))^2 = \min_{G,F\succeq 0} ||X-G\cdot F||_{\mathcal{F}}^2 \tag{3.2}$$

where $||.||_{\mathcal{F}}$ denotes the Frobenius norm of a matrix and $\mathcal{J}(.,.)$ accounts for the appropriate cost function. The factors must satisfy both conditions $G(\in \mathbf{R}^{n\times p}) \succeq 0$ and $F(\in \mathbf{R}^{p\times m}) \succeq 0$, i.e all the entries of both matrices are non negative. This decomposition (3.2) is obtained for the case of p sources, i.e. a maximum rank equal to p. This criterion is not convex with respect to both matrices G and F.

3.3 Exact NMF and Non Negative Rank

This section begins with the definition of the exact NMF of rank r:

The Exact NMF of rank r consists of finding a pair of matrices $(G \in \mathbf{R}_+^{n\times r}, F \in \mathbf{R}_+^{r\times m})$ such that $X = G\cdot F$. Thus, the answer for exact rank r NMF may be yes or no depending on the existence of such matrices.

Also, it can be expressed as the solution of the problem defined in Eq (3.2) with a minimum equal to 0, i.e

$$||X-G\cdot F||_{\mathcal{F}}^2 = 0 \tag{3.3}$$

The non-negative rank r, denoted $\text{rank}_+(X)$, can be defined as the minimum number r such that $X = G\cdot F$ where $G \in \mathbf{R}_+^{n\times r}$, and $F \in \mathbf{R}_+^{r\times m}$. Also, it implies that it is the minimum number of non-negative rank-one factors that is required to exactly reconstruct the data matrix X [57].

The non-negative rank may be bounded according to Eq (3.4),

$$rank(X) \leqslant rank_+(X) \leqslant min(m,n) \tag{3.4}$$

While the left inequality is trivial, the second is based on two basic non-negative factorizations

$X = I_m \cdot X$ and $X = X \cdot I_n$.

The left bound may be reached in special cases. Given rank(X) is equal to 1, X may be factorized by a non-negative product of rank 1 , $\underline{g} \cdot \underline{f}$. The factorization can be achieved for rank(X) $= 2$. The following lemma may be found in [66]:

Proposition 3.3.1. *Let $X \in \mathbb{R}_+^{n \times m}$ where rank(X)=2, then rank$^+(X) = 2$.*

The proof may be found in [66] by using some geometric arguments.

As a conclusion, when rank(X)$= 1, 2$, or $\min(n, m)$, it is always possible to perform an exact non-negative matrix factorization with the same non-negative rank. For matrices with different ranks, the determination of the non-negative rank is very difficult, but it may help in selecting the right number of components p in the NMF problem. Indeed, Vavavis [160] has proved the $\mathcal{NP}$ hardness of exact non-negative matrix factorization. As a result, all approximated algorithms are expected to provide a solution in a non polynomial time.

3.4 KKT conditions for the NMF problem

First, it is useful to stress some basic aspects in optimization theory.

3.4.1 Preliminaries

Let f be a continuously differentiable function defined over a space $\Omega \subset \mathbb{R}^n$ toward $\mathbb{R}$ and a point $\underline{x}^*$. If $\underline{x}^*$ is a local minimum of the function $f(x)$, then for all vector $\underline{x}$ in the neighbourhood of $\underline{x}^*$,

$$f(\underline{x}) \succeq f(\underline{x}^*) \tag{3.5}$$

The following lemma is derived from the Taylor expansion of the function f to the first order around $\underline{x}^*$ in conjunction with Equation (3.5).

Proposition 3.4.1. *If $\underline{x}^*$ is a local minimum of the function $f(\underline{x})$, then for all feasible direction $\underline{d}$ in the neighbourhood of $\underline{x}^*$, $\nabla f(\underline{x}^*)\underline{d} \geq 0$.*

Proposition (3.4.1) means that all possible directions will increase the function f around $\underline{x}^*$. Two cases may be highlighted,

1. If the corresponding point $\underline{x}^*$ is inside the domain Ω leading that all directions are acceptable, Proposition (3.4.1) can be now written as,

$$\nabla f(\underline{x}^*) = \underline{0} \tag{3.6}$$

2. If it is on the boundary defined by Ω, then the gradient $\nabla f(\underline{x}^*)$ is only different from the zero vector and only. Proposition (3.4.1) is valid.

Now, consider the optimization problem with equality and inequality constraints defined by

$$\min_{\underline{x}\in D} f(\underline{x}) \quad \text{s.t} \quad h_i(\underline{x}) = 0 \quad \forall i \in \{1,\ldots,c_E\}, \quad g_j(\underline{x}) \preceq 0 \quad \forall j \in \{1,\ldots,c_I\} \tag{3.7}$$

where

1. $h_i(\underline{x}) = 0$ is the i^{th} equality constraint for $i \in \{1,\ldots,c_E\}$
2. $g_j(\underline{x}) \preceq 0$ is the j^{th} inequality constraint for $j \in \{1,\ldots,c_I\}$
3. The two gradients $\nabla g_j(\underline{x}^*)$ and $\nabla h_i(\underline{x}^*)$ are independent.

Therefore, unique constants λ_i and μ_j exist such that,

$$\nabla f(\underline{x}^*) + \sum_{i=1}^{c_E} \lambda_i \nabla h_i(\underline{x}^*) + \sum_{j=1}^{c_I} \mu_j \nabla g_j(\underline{x}^*) = \underline{0}, \tag{3.8}$$

$$\mu_j \geq 0, \qquad \forall j = 1,\ldots,c_I, \tag{3.9}$$

$$\mu_j g_j(\underline{x}^*) = 0, \qquad \forall j = 1,\ldots,c_I. \tag{3.10}$$

it could be mentioned that,

1. The above conditions are generally obtained by writing a Lagrangian function that combines the objective and the constraints.
2. The KKT conditions are only necessary conditions for a local minimum.
3. These conditions are sufficient in the case of a convex function $f(x)$.

3.4.2 First order conditions for the classic NMF problem

The Lagrangian function related to Problem (3.2) can be defined as:

$$\mathcal{L}(G,F,\Gamma,\Lambda) = \frac{1}{2}||X - G\cdot F||_{\mathcal{F}}^2 - \Lambda \circ G - \Gamma \circ F, \tag{3.11}$$

where Γ (respectively Λ) is the Lagrange multipliers matrix with the same dimensions as F (respectively G) and are associated with the non-negativity constraints. The necessary conditions for a local minimum states that if (G F) is a local minimum, there exists non negative matrices (Γ, Λ) such that:

$$F \succeq 0, \qquad G \succeq 0, \tag{3.12}$$

$$\nabla \mathcal{L}_F(.) = 0, \qquad \nabla \mathcal{L}_G(.) = 0, \tag{3.13}$$

$$\Gamma \circ F = 0, \qquad \Lambda \circ G = 0. \tag{3.14}$$

By calculating the gradient of the Lagrangian function, (3.13) can be reformulated as:

$$G^T \cdot (G \cdot F - X) - \Gamma = 0, \qquad (G \cdot F - X) \cdot F^T - \Lambda = 0 \tag{3.15}$$

By using the non-negativity property for both matrices Γ and Λ and by replacing (3.15) into Eqs (3.13,3.14), the KKT conditions for the NMF problem are obtained:

$$F \succeq 0, \qquad G \succeq 0, \tag{3.16}$$
$$G^T \cdot (G \cdot F - X) \succeq 0, \qquad (G \cdot F - X) \cdot F^T \succeq 0, \tag{3.17}$$
$$F \circ \left(G^T \cdot (G \cdot F - X)\right) = 0, \qquad G \circ \left((G \cdot F - X)) \cdot F^T\right) = 0. \tag{3.18}$$

These conditions are the basis of the future problems defined in this thesis. They are usually called Karush-Kuhn Tucker (KKT) conditions. The third condition (3.18) which is called the complementary slackness condition expresses that if the factors are not lying on the border, both gradients of Problem (3.2) are required to be zero. However, it should be stressed again that the KKT conditions are only the necessary conditions for a local minimum.

3.5 Uniqueness of the NMF solution

This section is devoted to the question of uniqueness of the NMF solution.

Considering that a stationary solution (G, F) is available and an invertible matrix S of dimensions $p \times p$ exists; any solution of the form ($\breve{G} = G \cdot S$, $\breve{F} = S^{-1} \cdot F$) is equivalent since the same product $G \cdot F$ is produced. The stationarity condition for ($\breve{G}$, $\breve{F}$) is given by,

$$S^{-1} \cdot F \succeq 0, \qquad G \cdot S \succeq 0, \tag{3.19}$$
$$S^T \cdot G^T \cdot (G \cdot F - X) \succeq 0, \qquad (G \cdot F - X) \cdot F^T \cdot (S^{-1})^T \succeq 0, \tag{3.20}$$
$$(S^{-1} \cdot F) \circ \left(S^T \cdot G^T \cdot (G \cdot F - X)\right) = 0, \qquad (G \cdot S) \circ \left((G \cdot F - X)) \cdot F^T \cdot (S^{-1})^T\right) = 0. \tag{3.21}$$

These conditions can be easily verified if S is a permutation matrix making the new point a stationary one. However, the new point is nothing else than the permutation of the original point. In the general case, it is difficult to establish necessary and sufficient conditions for a unique solution. As a result, only sufficient conditions of uniqueness are explored in the literature. Besides, the uniqueness of the solution is often tackled in the frame of the exact factorization which differs from the framework of this thesis.

A geometric interpretation in $\mathbb{R}_+^m$ of the sufficient conditions is usually proposed for the uniqueness investigation. Most popular results come from [21], [40].

Definition 3.5.1. *The simplicial cone generated by a finite number of independent vectors* $(f_1, f_2, \ldots, f_p) \in \mathbb{R}_+^m$ *is the set* $C_F = \{\underline{x} | \underline{x} = \sum_{j=1}^{p} g_j \underline{f}_j, \quad g_j > 0\}$.

Let $\mathcal{X}$ be the convex set surrounding the row vectors of the matrix X. According to Chen [21],

Proposition 3.5.1. *The decomposition of X into a product $G \cdot F$ is unique if and only if the simplicial cone $\mathcal{C}_F$ such that $\mathcal{X} \subset \mathcal{C}_F$ is unique.*

This lemma does not provide a mean to check this condition. Moussaoui [112] proposed some sufficient conditions which ensure the uniqueness, e.g.,

Proposition 3.5.2. *The NMF factorization $X = G \cdot F$ is unique if the following two conditions are fulfilled*

1. The existence of a monomial [1] submatrix of F with a size of $p \times p$.
2. The existence of a monomial submatrix of G with a size of $p \times p$.

These two conditions [54, 56] are often viewed as the separability of X, (e.g., each column of G appears as a column of X) and the separability of X^T, (e.g., each row of F appears as a row of X). One of these conditions can be considered as the pure pixel assumption, usually encountered in Hyperspectral Unmixing.

Figure 3.1 depicts the conditions of the proposition 3.5.2 (left side) and of Donoho and Stodden (right side) [40] for the simplified case $p = 3$. By defining first $I(F) \triangleq Im(F) \cap \mathbf{R}_+^m$, the case of exact factorization can be interpreted for the condition on F as $I(F) = \mathcal{C}_F$ and for the condition on G, as p row vectors of X constitute the edges of the cone $I(F)$. For the Donoho's case, the conditions are less restrictive and make possible to guarantee the uniqueness of the solution if $p-1$ rows of X are located on each of the p facets of the cone $I(F)$. Thus, $p \cdot (p-1)$ rows of X belonging to the facets are sufficient to guarantee the uniqueness of the solution. These conditions are less restrictive than those provided by Chen [112].

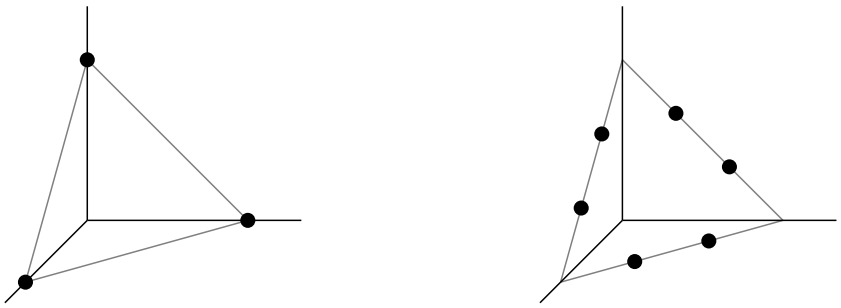

Proposition 3.5.2 Conditions de Donoho-Stodden [40]

Figure 3.1 – Different cases of Uniqueness for Non-negative Matrix Factorization.

However, these practical conditions are only sufficient conditions and are still very difficult to use. The supposed context corresponds to the context of the exact NMF factorization. In the framework of approximate factorization, the solutions should be verified to remain stationary points. In conclusion, the issue of the uniqueness of the solution still remains an open problem. Another alternative approach to limit the multiple solutions is to provide additional constraints to the initial NMF problem.

1. A monomial matrix is a permutation of a diagonal matrix with positive diagonal elements

3.6 Review of the different families of algorithms

The objective of this section is to review the different families of methods to solve the problem defined in Eq (3.2).

Several methods developed below can be used in order to estimate the unknown parameters but, before developing them, their common iterative nature may be stressed, which enables to move progressively toward the limit point.

3.6.1 Multiplicative Method

Multiplicative methods stand for iterates which are multiplied by an entry wise factor at each iteration. Multiplicative methods can be obtained from heuristic approaches, or from Majorization Minimization (MM) approaches.

3.6.1.1 Heuristic Approach

The Multiplicative methods usually tackle the Problem in Eq. (3.2) by first reformulating the cost function using the concept of matrix trace [2] , i.e.,

$$\mathcal{J}(G,F) = \mathrm{Tr}\left((X - G\cdot F)^T (X - G\cdot F)\right). \tag{3.22}$$

By developing the above expression, the cost function $\mathcal{J}(G,F)$ may be split into three terms, i.e.,

$$\begin{aligned}
\mathcal{J}(G,F) &= \mathrm{Tr}(X^T\cdot X) - \mathrm{Tr}(F^T\cdot G^T\cdot X) - \mathrm{Tr}(X^T\cdot G\cdot F) + \mathrm{Tr}(F^T\cdot G^T\cdot G\cdot F), && (3.23)\\
&= \mathrm{Tr}(X^T\cdot X) - 2\mathrm{Tr}(X^T\cdot G\cdot F) + \mathrm{Tr}(F^T\cdot G^T\cdot G\cdot F), && (3.24)\\
&= \mathcal{J}_1 - \mathcal{J}_2 + \mathcal{J}_3. && (3.25)
\end{aligned}$$

The calculation of the gradient of each function is performed here with respect to matrix F using theoretical results about matrix differentiation available in [130]. Similarly, the differentiation with respect to G may be obtained using some analogy results. Since the function $\mathcal{J}_1$ is independent of F, only $\mathcal{J}_2$ and $\mathcal{J}_3$ are to be differentiated.

The differentiation of $\mathcal{J}_2$ can be written as,

$$\partial\mathcal{J}_2 = 2(Tr(X^T\partial(G\cdot F))) = 2(Tr(X^T\cdot G\cdot\partial F)) \tag{3.26}$$

By using the property $\partial\mathcal{J}_2 = \mathrm{Tr}((\frac{\partial\mathcal{J}_2}{\partial F})^T\partial F)$, it follows that

$$\frac{\partial\mathcal{J}_2}{\partial F} = 2G^T\cdot X. \tag{3.27}$$

2. The trace of a matrix is the sum of its diagonal entries

Similarly, the differentiation of $\mathcal{J}_3$ is derived,

$$\partial \mathcal{J}_3 = \partial(Tr((G\cdot F)^T(G\cdot F)) = Tr(\partial((G\cdot F))^T + Tr((G\cdot F)^T\partial(G\cdot F)) \tag{3.28}$$

i.e.,

$$\frac{\partial \mathcal{J}_3}{\partial F} = 2G^T\cdot(G\cdot F) \tag{3.29}$$

Based on Eqs (3.27,3.29), the differentiation of $\mathcal{J}$ may be expressed as

$$\frac{\partial \mathcal{J}}{\partial F} = 2G^T\cdot(G\cdot F - X) \tag{3.30}$$

It is possible to write $\frac{\partial \mathcal{J}}{\partial F}$ as a difference of the terms $\nabla_F^+\mathcal{J}(G,F)$ and $\nabla_F^-\mathcal{J}(G,F)$, defined hereafter,

$$\nabla_F^+\mathcal{J}(G,F) = 2G^T\cdot(G\cdot F), \tag{3.31}$$

$$\nabla_F^-\mathcal{J}(G,F) = 2G^T\cdot X. \tag{3.32}$$

The update rules of G and F using the heuristic approach are derived from the previous gradient definition.

$$F \leftarrow F\circ\frac{\nabla_F^-\mathcal{J}(G,F)}{\nabla_F^+\mathcal{J}(G,F)}, \qquad G \leftarrow G\circ\frac{\nabla_G^-\mathcal{J}(G,F)}{\nabla_G^+\mathcal{J}(G,F)}. \tag{3.33}$$

Based on Eq (3.31, 3.32), the update rules for NMF with Frobenius cost function are

$$F \leftarrow F\circ\frac{(G^T\cdot X)}{(G^T\cdot G\cdot F)}, \qquad G \leftarrow G\circ\frac{(X\cdot F^T)}{(G\cdot F\cdot F^T)}. \tag{3.34}$$

These update rules ensure the non negativity of the elements of the two matrices G and F. According to [94], these rules will surely decrease the objective function of the classical NMF. Except in special cases where one entry is zero, the goal is to find limit matrices from Eq (3.34) whose fractions (next to G and F) are evolving with each iteration toward matrices whose elements are all 1. This will ensure the gradient to be cancelled as well as the KKT conditions (3.16,3.17,3.18) to be fulfilled.

3.6.1.2 Majorization Minimization Approach

One of the widely used technique is the Majorization-Minimization (MM) technique, which is reviewed by Hunter [71]. The MM approach is based on a two-steps approach (3.2) whose principle consists of:

1. The first step is to define an auxiliary function which majorizes the cost function $\mathcal{J}(G,F)$ at the current operating point.
2. The second step is to perform the minimization of the auxiliary function and repeat the process with the new operating point.

By looking at the structure of Eq (3.2), it is possible to split the problem into independent sub prob-

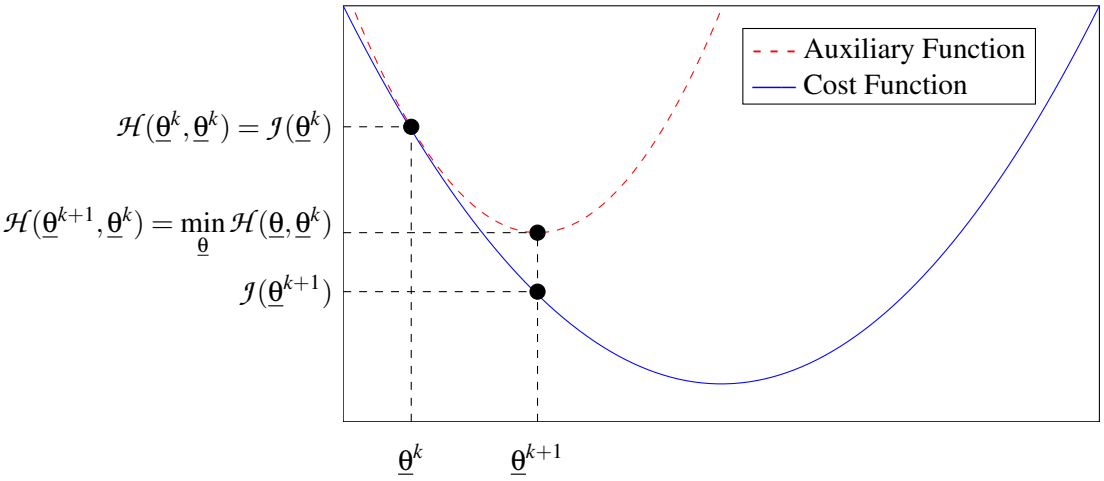

Figure 3.2 – Majorization Minimization Algorithm.

lems where the alternate search is limited to one column of F or one row of G.

Definition 3.6.1. *Let the two vectors $\underline{\theta}$ and $\underline{\theta}^k$, be respectively the vectors of the unknown and the unknown at iteration k*[3]*. A function $\mathcal{H}(\underline{\theta}, \underline{\theta}^k)$ is known as an auxiliary function of $\mathcal{J}(\underline{\theta})$ at the point $\underline{\theta}^k$ if and only if:*

$$\mathcal{H}(\underline{\theta}^k, \underline{\theta}^k) = \mathcal{J}(\underline{\theta}^k), \tag{3.35}$$

$$\mathcal{H}(\underline{\theta}, \underline{\theta}^k) \geq \mathcal{J}(\underline{\theta}). \tag{3.36}$$

The auxiliary function is a function which majorizes the cost function and is tangent to $(\underline{\theta} = \underline{\theta}^k)$. It is then possible to find a minimizer $\underline{\theta}^{k+1}$ which decreases the original cost function owing to relations (3.37),

$$\begin{array}{lll} \mathcal{J}(\underline{\theta}^{k+1}) & \leq \mathcal{H}(\underline{\theta}^{k+1}, \underline{\theta}^k) & \leq \mathcal{H}(\underline{\theta}^k, \underline{\theta}^k) \quad = \mathcal{J}(\underline{\theta}^k), \\ & (1) & (2) \qquad\quad (3) \end{array} \tag{3.37}$$

The difficult step of Majorization-Minimization approaches lies in designing an auxiliary function that is simpler to minimize than the original function. This step is performed either according to Jensen's inequality i.e., the case of convex functions $\mathcal{J}$ or with quadratic approximations [71]. In the classical NMF, the function $\mathcal{J}(G,F)$ can be reduced to its vectorial formulation and then may be rewritten according to the second order Taylor expansion of the vector $\underline{\theta}$, i.e.,

$$\mathcal{J}(\underline{\theta}) = \mathcal{J}(\underline{\theta}^k) + \nabla\mathcal{J}(\underline{\theta}^k)(\underline{\theta} - \underline{\theta}^k) + \frac{1}{2}(\underline{\theta} - \underline{\theta}^k)^T G^T \cdot G(\underline{\theta} - \underline{\theta}^k), \tag{3.38}$$

The second order majoring function takes the general form [66]

$$\mathcal{H}(\underline{\theta}, \underline{\theta}^k) = \mathcal{J}(\underline{\theta}^k) + \nabla\mathcal{J}(\underline{\theta}^k)(\underline{\theta} - \underline{\theta}^k) + \frac{1}{2}(\underline{\theta} - \underline{\theta}^k)^T \cdot A(\underline{\theta}^k) \cdot (\underline{\theta} - \underline{\theta}^k), \tag{3.39}$$

3. These vectors represent here one row of G or one column of F.

Given the special matrix $A(\underline{\theta}^k)$ proposed by Lee and Seung [94] which satisfies Eq (3.35),

$$A(\underline{\theta}^k) \triangleq \text{diag}(\frac{G^T \cdot G \cdot \underline{\theta}^k}{\underline{\theta}^k}). \tag{3.40}$$

The cancellation of the gradient of $\mathcal{H}(\underline{\theta}, \underline{\theta}^k)$ leads to,

$$\underline{\theta}^{k+1} = \underline{\theta}^k - A(\underline{\theta}^k)^{-1} \cdot \nabla \mathcal{J}(\underline{\theta}^k) = \underline{\theta}^k + \text{diag}(\frac{\underline{\theta}^k}{G^T \cdot G \cdot \underline{\theta}^k}) \cdot G^T(\underline{x} - G \cdot \underline{\theta}^k). \tag{3.41}$$

i.e,

$$\underline{\theta}^{k+1} = \underline{\theta}^k + \underline{\theta}^k \circ \frac{G^T(\underline{x} - G \cdot \underline{\theta}^k)}{G^T \cdot G \cdot \underline{\theta}^k}. \tag{3.42}$$

These equations may be collected for all columns of the matrix F (resp. all rows of G) to provide the final update rules,

$$F \leftarrow F \circ \frac{(G^T X)}{(G^T G F)}, \qquad\qquad G \leftarrow G \circ \frac{(X F^T)}{(G F F^T)}. \tag{3.43}$$

Using the Majorization-Minimization technique for the classical NMF problem, the derived update rules are the same as those obtained with the heuristic method, i.e., the update rules which are provided in Eq (3.34).

These multiplicative algorithms are shown to decrease strictly the cost function if none of the terms contain a zero entry [4] and if each entry of the gradient remains different from 0. In addition, these algorithms are known to be slowly converging towards a limit point.

3.6.2 Projected Gradient Approaches

The principle of projected gradient approaches relies on classical gradient techniques. Thus,the basic concepts are first introduced.

3.6.2.1 Basic concepts

Gradient methods constitute reference methods for solving a differentiable optimization problem. They usually start from a current vector, which moves towards a decrease of the criterion. This direction may result from several choices. The most popular choice is the opposite of the gradient of the function to minimize at the operating point.

Definition 3.6.2. *$\underline{d}^k$ is a descent direction if, starting from a current vector $\underline{\theta}^k$, the following property is fulfilled,*

$$\nabla \mathcal{J}(\underline{\theta}^k)^T \cdot \underline{d}^k < 0. \tag{3.44}$$

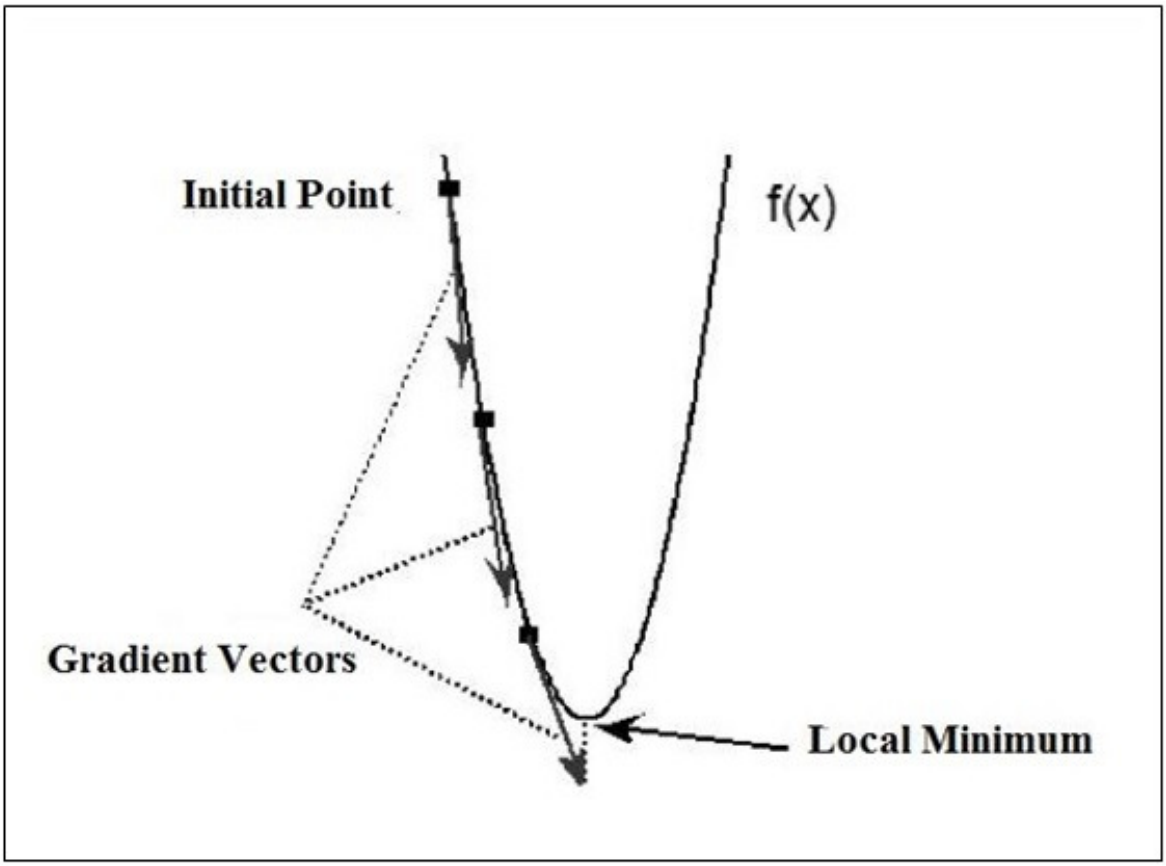

Figure 3.3 – Gradient Descent Algorithm.

In this case, every vector of the form

$$\underline{\theta}^{k+1} = \underline{\theta}^{k} + \alpha^{k}\underline{d}^{k}, \tag{3.45}$$

where $\alpha^{k} > 0$, leads to the decrease of the function $\mathcal{J}(.)$ and stands for the iterate of a gradient like method. The Gradient algorithm is illustrated in Figure (3.3). Differences between its variants essentially lie in the choice of various descent directions $\underline{d}^{k}$, as well as the stepsize α^{k}. Among the classical ones, $\underline{d}^{k} = -\nabla\mathcal{J}(\underline{\theta}^{k})$ is the most popular.

3.6.2.2 Projected gradients methods

There is a huge number of methods in this field and each method has its own specificity. Thus, the common features of these methods are only presented.

Projected Gradient methods update successively G and F. For each matrix, it follows a gradient like technique which project the iterate onto the non negative orthant, i.e.,

$$G^{k+1} = [G^{k} - \eta_{G} \cdot D_{G}^{k}]^{+}, \qquad F^{k+1} = [F^{k} - \eta_{F} \cdot D_{F}^{k}]^{+}, \tag{3.46}$$

where $+$ stands for $[X]^+ = \max(\varepsilon, X)$ while D_G^k et D_F^k are the descent directions. The Step sizes η_G et η_F are for for matrices and may take different forms. Accordingly , several Projected Gradients methods are available in the literature:

1. The Oblique Projection [111] [76]: this type of method, known as the oblique projection of Landweber, is a projected gradient following the general scheme (3.46) in which the descent direction is the opposite of a distorted gradient.
2. Split Gradient Methods [91]: It stands for a gradient scheme where the descent direction is the opposite of the current gradient. Assuming the gradient under the form $-(\nabla \mathcal{J}(F^k)) = P - Q$, a fix point strategy enables, from the third KKT condition, to write the update rule for one factor as
$$F^{k+1} = F^k + \eta_F \circ \frac{F^k}{Q^k} \circ \left[-\nabla \mathcal{J}(F^k)\right] \tag{3.47}$$
where η_F is a matrix of scale factor. Such an update could be used in the frame of NMF, where a shift needs to be designed in order to ensure non-negativity.
3. Lin's Projected Gradients [102] [29]: Another popular method is the projected gradient of Lin in which the descent direction corresponds exactly to the opposite of the gradient. Lin developped two variants: the first variant updates the two factors successively while the other updates them simultaneously. Besides, Lin has introduced an update of the scalar step size which follows the modified Armijo rule, detailed in [102]. However, Lin explained that this kind of direct updating procedure does not provide a gain in the computation of the cost function because it will lose its quadratic characteristic when the two matrices are optimized simultaneously.
4. Method of potential directions [29][22][118]: This method is based on the subspace techniques by defining potential directions in a subspace. When using the Non-negative Matrix Factorization, they are applied directly to the columns of the matrix F or the rows of the matrix G separately. In contrast with other methods, they combine 3 potential directions defined by Nemirovsky [118]: the current gradient, the move from the starting point, and a filtered version of the P latest gradients. The expression of the step size may be found in [29, Ch.5].
5. Method of Interior Points [109]: This method is usually found in quadratic optimization. It is not widely used in the context of the Non-negative Matrix Factorization. The method may be classified into the family of gradient based methods because the step size is searched to check non-negativity, thus avoiding the usual projection step. The update rules are expressed as,
$$G \leftarrow G^k - \eta_G \frac{G^k}{(G^k F^k \cdot (F^k)^T)} \circ [(X - G^k \cdot F^k) \cdot (F^k)^T], \tag{3.48}$$
$$F \leftarrow F^k - \eta_F \frac{F^k}{(G^k)^T \cdot G^k \cdot F^k} \circ [(G^k)^T \cdot (X - G^k \cdot F^k)]. \tag{3.49}$$
It should be mentioned that if both step sizes are equal to 1, it leads to the previous multiplicative update rules (3.43). In this method, the scalar stepsize is searched at each iteration, to minimize $\mathcal{J}(G^k, F^k + \eta D_F^k)$ satisfying the non-negativity of the factor.
6. Proximal methods (Nesterov,...) The search for an optimal step size is often a critical step in every Gradient Descent scheme. In 1983, Nesterov proposed to replace this step by an inner iterative gradient descent. In the case of NMF, this inner loop [60] consists of the minimization

of the proximal [4] function of $\mathcal{J}(G,.)$ at an operating point Y^k, obtained from a filtered version of F^k. It finally amounts to a simple gradient scheme with a constant scalar stepsize around the filtered version Y^k of F^k. Recently, some extended versions of Nesterov NMF were developed in the field of blind mobile sensors calibrations [44].

As a summary, a general principle from Lin [102] can be highlighted: the low cost per iteration often comes at the price of a high number of iterations while a fast convergence is usually attained with a high cost per iteration.

3.6.3 Exact Block coordinate methods

In the previous methods, an exact computation of the factor was not required at each outer iteration. This was the case of multiplicative updates or projected gradient based methods. In this section, some methods which solve each sub-problem in an exact way are presented. Kim and Park recently proposed an unified view of this class of problems under the name of exact block coordinate [85] which is able to perform several non negative least square procedures. The latter approach relies on the assumption that the unknown parameter space may be split into separable closed convex sets. This method allows to view the minimization separately on each subset successively. It involves Alternating Non-negative Least Squares methods as well as Hierarchical Alternating Least Square .

3.6.3.1 Alternating Non-negative Least Squares (ANLS) Methods

These methods corresponds to dividing the space of the search into two blocs i.e,

$$G^{k+1} = \arg\min_{G \succeq 0} ||X - G \cdot F^k||_{\mathcal{F}}^2 \tag{3.50}$$

$$F^{k+1} = \arg\min_{F \succeq 0} ||X - G^k \cdot F||_{\mathcal{F}}^2 \tag{3.51}$$

Each subproblem can be divided into m independent sub problems of type Non negative least square (NNLS) [20], each focuses on the search of one column of F (resp. one row of G), which can be outlined as

$$\min_{\underline{f} \succeq 0} \left\| \underline{x} - G \cdot \underline{f} \right\|_2^2, \tag{3.52}$$

where $\underline{x}$ et $\underline{f}$ stands for one column of X and F respectively.

A class of methods for solving such problems are active set methods, which consist in iteratively separating the indexes into two classes. The first class contains the zero entries (saturated entries) and the second containing the indexes of positive components. As soon as the index partitioning is known, the solution becomes a classical least square solution with a close form expression. Then, different partitions of indexes were explored to converge to the right solution. This algorithm was originally developed by Lawson and Hanson [93] and was further integrated into Matlab as the *lsqnonneg* function. A fast version of this algorithm were developed by Bro and De Jong [16] by computing only once

4. The proximal function is the extension of the concept of projection onto a convex set [30].

some common matrices. Recently, Kim and Park have applied this strategy to NMF on a modified cost function involving a sparseness penalty function [84] [83] and have extended it to the framework with a block pivoting strategy [82].

3.6.3.2 HALS methods

These methods come from a partitioning into $2p$ blocks coordinates. The initial problem (3.2) may be reformulated as the minimization of p subproblems,

$$\arg \min_{G_{.,L} \succeq 0, F_{L,.} \succeq 0} \mathcal{J}(G_{.,L}, F_{L,.}) = \arg \min_{G_{.,L} \succeq 0, F_{L,.} \succeq 0} \|R(-L) - G_{.,L} \cdot F_{L,.}\|_{\mathcal{F}}^2 \qquad \forall L \in \{1 \dots p\}, \tag{3.53}$$

where $R(-L)$ is the residual matrix built as the difference between the data matrix and the approximate product without the L^{th} source, i.e., $R(-L) = X - \sum_{l=1 \neq L}^{p} G_{.,l} \cdot F_{l,.}$. The new matrices $G_{.,L}$ and $F_{L,.}$ are special column and row matrices of G and F, according to $G \triangleq [G_{.,1}^T; \dots; G_{.,p}^T]^T$ and $F \triangleq [F_{1,.}; \dots; F_{p,.}]$.

Each of this problem may be solved exactly by searching for a single entry of the matrix F and extending it to the complete row of F [5], i.e.,

$$F_{L,.}^* = \left[\frac{G_{.,L}^T \cdot R(-L)}{G_{.,L}^T \cdot G_{.,L}} \right]_+, \quad \forall L \in \{1, \dots, p\}. \tag{3.54}$$

The above expression may be similarly extended to G, i.e.,

$$F_{L,.} = \left[\frac{G_{.,L}^T \cdot R(-L)}{G_{.,L}^T \cdot G_{.,L}} \right]_+, \quad G_{.,L} = \left[\frac{R(-L) \cdot F_{L,.}^T}{F_{L,.} \cdot F_{L,.}^T} \right]_+, \quad \forall L \in \{1, \dots, p\}. \tag{3.55}$$

Ho discovered the algorithm at the same period [66] which was called Rank-1 Residu Iteration (RRI). Fast implementations of these methods have been proposed to decrease the number of flops per iteration. One challenging aspect consists in the choice of the order of updating these $2\,p$ blocks. Consequently, two versions are widely used,

$$G_{.,1} \to F_{1,.} \to G_{.,2} \to F_{2,.} \dots \to G_{.,p} \to F_{p,.} \tag{3.56}$$

$$G_{.,1} \to G_{.,2} \dots \to G_{.,p} \to F_{1,.} \to F_{2,.} \dots \to F_{p,.} \tag{3.57}$$

Gillis and Glineur [55] have proposed to modify this classical order by repeating the process on G several times. Extended versions of theses algorithms can be found in [28] and in [86] for orthogonal NMF.

5. It should be mentioned that HALS update a row of F whereas usual ANLS basically update a column of F

3.6.4 Alternative Direction Method of Multipliers

The Alternating Direction Method of Multipliers (ADMM) is a very popular method which gained lot of attention during the past years due to the huge demand from some applications such as large-scale and data-distributed machine learning [123], compressed sensing [172], image restoration [59] and video process and matrix completion [58]. ADMM is considered to be a simple computational technique based on the augmented Lagrangian method [52] [156]. The principle of ADMM is based on the concept of variable partitioning which enables to split the function to minimize into several independent terms. Variable splitting is often presented in two blocks, i.e.,

$$\min f(\underline{x}) + g(\underline{y}) \qquad \text{s. t. } A\underline{x} + B\underline{y} = \underline{c} \tag{3.58}$$

where A, B and $\underline{c}$ are matrices or vectors of appropriate size.

The augmented Lagrangian function of (3.58) is defined as

$$\mathcal{L}_{\mathcal{A}}(\underline{x}, \underline{y}, \underline{\lambda}) = f(\underline{x}) + g(\underline{y}) + \underline{\lambda}^T (A\underline{x} + B\underline{y} - \underline{c}) + \frac{\gamma}{2} ||A\underline{x} + B\underline{y} - \underline{c}||_2^2 \tag{3.59}$$

where $\underline{\lambda}$ and γ are Lagrangian parameters. The classical ADMM algorithm is an extension of the augmented Lagrangian mulipliers methods which performs a minimization with respect to $\underline{x}$, $\underline{y}$, $\underline{\lambda}$ sequentially, i.e,

$$\underline{x}^{k+1} \leftarrow \arg\min \mathcal{L}_{\mathcal{A}}(\underline{x}, \underline{y}^k, \underline{\lambda}^k) \tag{3.60}$$

$$\underline{y}^{k+1} \leftarrow \arg\min \mathcal{L}_{\mathcal{A}}(\underline{x}^{k+1}, \underline{y}, \underline{\lambda}^k) \tag{3.61}$$

$$\underline{\lambda}^{k+1} \leftarrow \underline{\lambda}^k + \delta.\gamma.(A\underline{x}^{k+1} + B\underline{y}^{k+1} - \underline{c}) \tag{3.62}$$

where δ is a step length.

ADMM has recently been extended to solve NMF problems by introducing some auxiliary matrices G^+ and F^+ of appropriate size constrained to be positive [173] [15], i.e the NMF problem may be expressed as,

$$\min_{G,F,G^+,F^+} \mathcal{J}(G,F) \qquad \text{s.t. } X = G \cdot F, G = G^+, F = F^+, G^+ \succeq 0, F^+ \succeq 0 \tag{3.63}$$

The augmented Langrangian function of Eq (3.63) may be similarly written

$$\mathcal{L}(X,G,F,G_+,F_+,\Gamma_G,\Gamma_F) = ||X - G\cdot F||_{\mathcal{F}}^2 + < \Gamma_G, G - G^+ > + < \Gamma_F, F - F^+ > \tag{3.64}$$

$$+ \frac{\gamma_G}{2} ||G - G^+||_{\mathcal{F}}^2 + \frac{\gamma_F}{2} ||F - F^+||_{\mathcal{F}}^2 \tag{3.65}$$

where $< .,. >$ accounts for scalar product of the vectorial form of each matrix argument and Γ_G, Γ_F, γ_G, γ_F are Lagrangian parameters.

The ADMM method for (3.63) is derived by successively minimizing the augmented Lagrangian function with respect to the variables G,F,G_+,F_+,Γ_G,Γ_F, one at a time while assigning the remaining variables to their latest values. All these steps may be written in closed form expressions, which are

available in [178], i.e. allowing to get simple schemes.

However, there is no real guarantee that such methods converge to a stationary point [171] owing to the partitioning into more than 2 blocks and the required strict convexity of the function to minimize. Some extensions of this small introduction were proposed in the field of matrix completion [171]. More recently, Févotte proposed to deal with some special cost functions denoted β-divergences and proposed some ADMM formulations in a similar way [156]. Nowadays, the use of ADMM in NMF remains an unconventional track as it is still an open field.

3.6.5 Bayesian Approach for NMF

The NMF problem may be formulated in a statistical setting by using an additive random i.i.d. [6] noise to the receptor model, which may be formulated into a matrix form, i.e.,

$$X = G \cdot F + E, \tag{3.66}$$

where E is the matrix of individual noise. The most classical framework is the Gaussian model,

$$P(X|G \cdot F) = (\frac{1}{\sqrt{2\pi.\sigma}})^{nm} exp^{-\frac{||X-G \cdot F||_F^2}{2\sigma^2}} \tag{3.67}$$

This probability is called likelihood of the data and its maximum is equivalent to the classical NMF problem (3.2). Several variants of the last model involve modelling the data variance as an individual Gamma prior [148] or to break the Gaussian model into a Poisson distribution [164].

The Bayesian approach consists in defining some prior distribution on the factors which incorporate some prior knowledge. Usually, matrices F and G are considered to be independent variables [122] [113] [148]. The main challenge is to design appropriate prior information on both G and F by defining a prior distribution $p(G)$ and $p(F)$. In order to ensure the non-negativity of the factors, it is necessary to choose probability densities with positive supports. Several choices for these factors include the rectified Gaussian [148] [46], gamma priors [164] or Student-t Distributions [90]. By using the Bayes' theorem, the joint posterior distribution of the unknown factors is given by

$$p(F,G|X) = \frac{p(X|F,G) \times p(F) \times p(G)}{p(X)} \tag{3.68}$$

where $p(X|G,F)$ is the likelihood of the observations and $p(X)$ is the probability density of the observations. It should be noted that assuming the two matrices G and F are independent, the joint distribution reduces to a simple product $p(G,F) = p(G)p(F)$, and $p(X)$ appears as a normalization term. Eq (3.68) may be written as,

$$p(F,G|X) \propto p(X|F,G) \times p(F) \times p(G) \tag{3.69}$$

and MAP estimation is usually performed by taking the maximum of Eq (3.69) or its logarithm. The

6. i.i.d. stands for independent and identically distributed

two matrices G and F can be calculated from Eq (3.69) and by using several Bayesian estimators [141] which essentially perform approximate computations except in the case of special conjugate distributions. Thus, the posterior law allows the estimation of the two matrices either by the joint law or by the marginalization of the latter. The property of independence between the two estimated matrices G and F makes it possible to express the joint law as a posteriori $p(G,F|X)$ with the help of the marginals laws a priori. In fact, it is almost impossible to calculate the expression $p(G,F|X)$. thus, all the Bayesian algorithms use Markov Chain Monte Carlo (MCMC) in order to generate samples that are distributed according to posterior marginal laws.

The markov chain is a sequence of random variables such that the next value of the sequence is depending only on the previous value. Consider $\Theta(t)$ to be a state at iteration t. The next state $\Theta(t+1)$ is only depending on the current state $\Theta(t)$. Two major algorithms, the Metropolitan Hasting Algorithm and the Gibbs Sampling can be implemented to compute the next set of values that will form the Markov chain from which the elements of the matrices G and F are estimated. Having initialized the algorithm, the Metropolitan Hasting [62] [114] can be summarized as follows:

1. Generate a random variable (candidate variable) by sampling from a proposal distribution that depends only on the previous state.

2. Check if the generated candidate variable satisfies a defined condition. If it is satisfied, the generated variable will be the new state. Otherwise, the previous value will be assigned. This procedure will be repeated for a large number of iterations.

As for the Gibbs Sampling algorithm [53, 19], it is illustrated as follows:

Suppose $\theta_1,\theta_2 \sim p(\theta_1,\theta_2)$ and it can be sampled from $p(\theta_1|\theta_2)$ and $p(\theta_2|\theta_1)$. Beginning with an initial value θ_1^0,θ_2^0, the Gibbs sampler is given by:

1. Sample $\theta_1^j \sim p(\theta_1|\theta_2^{(j-1)})$ and then

2. Sample $\theta_2^j \sim p(\theta_2|\theta_1^{(j)})$

Taking into account that,

$$p(\theta_2|\theta_1) = \frac{p(\theta_1,\theta_2)}{p(\theta_1)} \tag{3.70}$$

$$p(\theta_1|\theta_2) = \frac{p(\theta_1,\theta_2)}{p(\theta_2)} \tag{3.71}$$

Where $p(\theta_2|\theta_1)$ and $p(\theta_1|\theta_2)$ are the conditional distribution, $p(\theta_1)$ and $p(\theta_2)$ are the marginal distribution and $p(\theta_1,\theta_2)$ is the joint distribution.
Gibbs sampling differs from the Metropolitan Hasting in the sense that it accepts all the generated candidate points and it requires that the conditional distribution of each variable to be known.

Note that the Gibbs Sampling algorithm appears to be simpler in the context of NMF. However, it is sometimes difficult to apply due to the conditional marginal distribution to compute.

As a summary, the Bayesian NMF is still difficult to apply in some specific NMF contexts where many constraints need to be incorporated or when the database is very large leading to very intensive computations.

3.7 Weighted Non Negative Matrix Factorization (WNMF)

3.7.1 Introduction

The classical NMF problem (3.2) considers the errors resulting from all the collected data to be identical. However, sometimes, data are of a heterogeneous nature. That is, they result from an acquisition process which exhibits different degrees of confidence. This will result mostly from either the conditions under which the measurements have been collected or from the different nature of the various sensors. It could be also even due to the loss of the data. Thus, the most reliable information should be very well considered. This information is encoded with the weight concept, which is defined to be high for a reliable element and low for the inverse situation. It is also defined as the confidence into the corresponding data x_{ij},

$$W_{ij} \triangleq \frac{1}{\sigma_{ij}^2} \tag{3.72}$$

where σ_{ij} accounts for the individual uncertainty of x_{ij}.

The new NMF problem becomes now the extension of problem (3.2), renamed as the Weighted NMF problem [61, 66]. Thus, Eq (3.22) can be extended to introduce the weight matrix W and it reads

$$\mathcal{J}(G,F) = \sum_{i=1}^{n}\sum_{j=1}^{m} W_{ij}(x_{ij} - (GF_{ij})^2 = Tr((X - G.F)^T.((X - G.F) \circ W)) \tag{3.73}$$

The weighted NMF problem can be defined as

$$\min_{G,F\succeq 0} \mathcal{J}(G,F) = \min_{G,F\succeq 0} Tr((X - G.F)^T.((X - G.F) \circ W)) \tag{3.74}$$

Although the extension of the original equation is straightforward, the solution of the WNMF problem is much more complex Therefore, it is necessary to use iterative algorithms to converge to local minima.

3.7.2 Outline of the main algorithms

While Srebo & al tackled a close problem by forgetting the non-negativity constraints [117], Guillamet & al [61] have investigated the weighted NMF problem in the field of image classification. The work of Ho [66] unified this problem by developing extended expressions. Therefore, the work of Ho, which is also reported in [96] is introduced hereafter.

KKT conditions may be obtained by differentiating $\mathcal{J}(G,F)$ with respect to each of the factor.

KKT conditions of the weighted case are expressed as

$$\begin{array}{ll} F \succeq 0, & G \succeq 0, \\ G^T \cdot (W \circ (G \cdot F - X)) \succeq 0, & (W \circ (G \cdot F - X)) \cdot F^T \succeq 0, \\ F \circ \left(G^T \cdot (W \circ (G \cdot F - X))\right) = 0, & G \circ \left((W \circ (G \cdot F - X)) \cdot F^T\right) = 0. \end{array} \tag{3.75}$$

The update rules of the weighted NMF problem may be obtained either by the heuristic method from the differentiation of $\mathcal{J}(G,F)$ or by using the Majorization Minimization strategy. They all lead to the same expressions which are:

$$F \leftarrow F \circ \frac{G^T \cdot (X \circ W)}{G^T \cdot (W \circ (G \cdot F))}, \qquad G \leftarrow G \circ \frac{(W \circ X) \cdot F^T}{(W \circ (G \cdot F)) \cdot F^T}. \tag{3.76}$$

Some important aspects should be highlighted, i.e,

1. The Non-negativity is naturally achieved in multiplicative expressions.
2. The weighted Euclidean cost function is never increasing for the proposed update.
3. A limit point is reached if the third KKT condition is verified.
4. In the case where $W = 1_{n \times m}$, the update rules correspond to the original classical NMF as shown in Eq (3.34).

Moreover, Ho [66] proposed an extension of HALS method to the weighted case. In contrast to multiplicative methods, it solves exactly the subproblem related to one factor at each iteration.

As a summary, depending on the context, some methods are favored to others. Moreover, the weight concept is extensively encountered in the field of blind calibration with missing entries [41, 42].

3.8 Applications

The Non-negative matrix factorization (NMF) has received a growing attention since the last decades. The assumption of non-negativity which is the basis of NMF can be applied in a wide range of natural signals, such as amplitude spectra, pixel intensities, and occurrence counts. The NMF and its variants have found their ways in applications in various fields:

1. Environmental Science and chemometrics in which concentrations are investigated. It may range from indoor [120] or outdoor air pollution [67], to river pollution [106] and soil pollution [182]. Individual sources of pollution are searched for so that one factor is the source by species factor while the other stands for the samples by sources factor. The important aspect is that each data is usually equipped with an individual uncertainty, which leads to weighted NMF methods.
2. Image Processing applications: Image data processing where relevant components of images are to be extracted. The emphasis lies mainly in face recognition [153] and image classification problems [177] such as the handwritten digit recognition.

3. Biomedical applications: microarray data analysis where the non-negative data correspond to gene expression levels is one such application. Also, the NMF was successfully applied for cancer classification, EEG signal separation and classification, the investigation of protein fold recognition [OP06] and medical imaging modalities such as Magnetic Resonance Imaging (NMR), Positron Emission Tomography (PET) or fluorescence spectroscopy.

4. Data Mining: applications are associated with Text mining [165], language modeling, and document clustering. The NMF is implemented to extract topics or semantic features from the collections of documents. For example, X may be a n by m word by document matrix. A set of features are derived from the documents. The factorization of X is performed into a word by feature matrix and a feature by document matrix.

5. Sound recognition and classification: acoustic features are extracted from sound recordings yielding for example instrument-specific patterns and solving the acoustic source separation problem.

6. Speech recognition (Speech denoising and Speaker separation): It is another application in which NMF and its extensions are applied with success. In audio processing, the basic role of NMF is to find a locally optimal factorization of a short-time magnitude spectrogram i.e., decompose into two components where the first component consists of the spectra of the events occurring in the signal and the second component reflects their time-varying gains. Earlier works on speech processing include the separation quality and the implementation of the NMF technique as a preprocessing step for conventional speech recognition procedures. Others researchers have implemented the NMF algorithm as a data-based features' extractor.
7. Recommender Systems: In a recommender system, there is a set of users who are voting about a set of items (for example movies). This provides a possibly incomplete matrix of votes similar to the data matrix X. The previous linear mixture model with the Non-negativity is used to define latent features associated for example with the movie genre. As a result, the NMF may be used to recover the latent features [89, 34].
8. Blind Sensor Calibration may be formulated as a weighted NMF problem with missing entries. According to the model of the sensor taken into account, it may lead to different formulations of the structured NMF problem [41, 42].

3.9 Conclusion

In this chapter, the objective was to introduce the basics of Non-negative Matrix Factorization. First, NMF has been addressed as an optimization problem using the Frobenius norm. The concept of non negative rank has been defined and sufficient conditions for the uniqueness of the solution of exact NMF –which is closely related to non negative rank– are reviewed. In the case of approximate NMF, necessary conditions for a local minimum, denoted KKT conditions, are provided.

Moreover, several approaches to solve the classical problem are reviewed. Among the classical

approaches, the multiplicative updates, the Alternated Non negative Least Square and the projected Gradient Approaches were presented. Some promising NMF methods, such as ADMM, Block coordinate or Bayesian NMF are also briefly revised.

Besides, the weighted NMF problem has been introduced and interesting solutions have been provided. The concept of weight appears to be attractive in the field of chemical sensing, where the data are provided with an associated uncertainty. In the next chapter, the data which are typically corrupted with abnormal data are discussed. Consequently, weight updating schemes could be an interesting track to be pursued with the weighted NMF problem.

CHAPTER 4

Robust NMF methods

4.1 Introduction

The previous chapter was devoted to an overview of Matrix factorization methods and constraints encountered in the literature. The objective of this chapter is to discuss robustness issues.

Data may be tainted with atypical measures which may cause classical algorithms to fail. Such an issue is often addressed in the field of robustness where the challenge is to design new algorithms whose results account for these data. It is mainly developed for regression and it has been rarely investigated in the field of matrix factorization. From a practical viewpoint, only studies of robustness performance are available in the literature references. Moreover, chemical data are often collected with a significant proportion of abnormal data. As a result, the scope of this chapter is to define the features of the expected outlying data and consequently, to review the different available schemes to solve such a problem. That is, low rank plus sparse decomposition approach and NMF based on modified cost functions are presented and discussed.

4.2 Outliers

In the previous chapters, the discussion was about the regular data obtained from the generating process which are governed by Eq (3.2). However and in most cases, the collected data could be somehow corrupted [143] i.e., it is very common that some of the observations are different from the majority and they are identified as outliers. Hawkins proposed a definition of outliers [63]

Definition 4.2.1. *An outlier is an observation which deviates so much from the other observations so as to arouse suspicions that it was generated by a different mechanism.*

This definition may be applied to scalar or vectors. In the case under consideration, the data matrix X is split into n row vectors $\underline{x}_i \in \mathbb{R}^m$, where n is the number of data. Mathematically the proportion of contaminated data, ε, is introduced and the problem can be viewed as a mixture of two distributions, the regular distribution $\mathcal{T}_n$ and the abnormal distribution $\mathcal{T}_a$, i.e.,

$$\underline{x}_i \sim \quad \mathcal{T} = (1-\varepsilon)\,\mathcal{T}_n + \varepsilon\,\mathcal{T}_a \tag{4.1}$$

The scalar ε is usually a small quantity and is often assumed to be known. In addition, the regular distribution is often considered as a centered narrow Gaussian distribution while the abnormal one is

a wide normal distribution.

Another point of view is associated with the statistical multivariate Tukey model [159] i.e.,

$$\underline{x}_i = (I - B) \cdot \underline{y}_i + B \cdot \underline{o}_i \tag{4.2}$$

where $\underline{y}_i$ (resp $\underline{o}_i$) stands for the regular vector data at time i (resp. abnormal data). B is a diagonal matrix defined by $B \triangleq diag(B_1, \ldots, B_m)$ and $B_1, \ldots, B_m$ are random Bernouilli variables with $p(B_i) = \varepsilon_i$. The special case in which $\underline{y}_i$ and B $\underline{o}_{i,}$ are independent is often considered. A special case in which $p(B_1 = B_2 \ldots = B_m) = 1$ accounts for full dependence of a vector and it leads to a vector which is either completely abnormal or completely regular. Such an outlier is called structural outlier or row outlier.

Another interesting case is the completely independent model in which $B_1 = B_2 \ldots = B_m$ are completely independent. This assumption is related to the entrywise outlier case. The assumption $\varepsilon_i = \varepsilon \quad \forall i \in \{1, \ldots, m\}$ leads to a probability of the vector $\underline{x}_i$ to be clean $p(\underline{x}_i) = (1 - \varepsilon)^p$ which may rapidly decrease with the value of p and the latter will be abnormal for large m and even for small ε.

Another case is the case of grouped outliers [169] in which a sparsity level is required for each vector and consequently, a maximum number of outlying components in each vector may be found.

In chemical sensing, outliers can occur for several reasons such as recording errors, transmission errors or an unexpected contamination prior to chemical analysis. They could also occur due to some exceptional conditions which account for accidental releases. However, outliers should constitute a small proportion of the whole data and consequently the regular model remains essentially valid.

It is very critical to know in advance the location of outliers because they will give a clear insight on any change in the production process or in the experimental situation. Moreover, their detection in a prior procedure is a difficult task. As a consequence, the estimation and the detection of outliers are usually performed in an embedded way.

In the regression context, methods based on l_2 norms are often implemented to identify outliers. However, such methods can be very sensitive to outliers in a way that the fitted model is attracted by them and, as a consequence, the deviating observations, a phenemenon referred to as the masking effect can not be distinguished on one hand. On the other hand, some of the data can be labelled as outliers whereas they are not since methods try to fit all data including outliers. This effect is called swamping effect. In the least square regression, outliers are defined as the data points with the highest residual error associated with the fitted model. Usual Regression methods attempt then to fit all the collected points in the same way. Figure (4.1) shows an example of a performed regression in [49]. The regression line corresponds to expected regular points and the two dashed lines represent the upper and lower boundaries of the average spreading of the data. Usually, outliers are expected to be outside this bounded area. However, the points with the highest residuals are not the true outliers in this example. They are just points which are far away from the regression and they do not correspond well to the majority of points.

In the NMF context, the problem is much more harder since neither the profile matrix nor the contribution are known. Figure (4.2) presents the situation encountered in air pollution where data

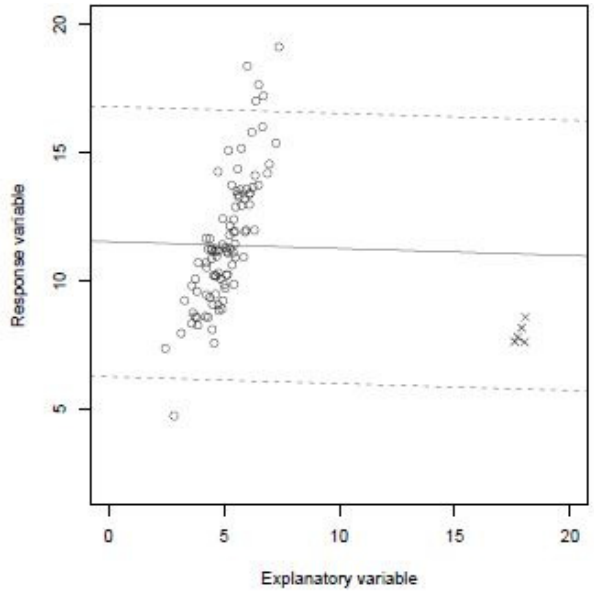

Figure 4.1 – Regression problem with the presence of Outliers.

vectors are spanned by three source profiles. Profiles appear as vertices of the simplicial cone. Regular points are assigned a blue color whereas the red color accounts for the outlying data. Since a geometric interpretation of NMF may consist in identifying those points which are vertices, the red points could appear as source profiles depending whether it is labelled as a regular point or not. Moreover, an outlier may also lie inside the simplicial cone, so that it will be impossible to detect.

In conclusion, it is very hard to detect the presence of outliers and the difficulty varies according to the dimensionality, i.e., it is much easier to identify the points that are far from the main data in one dimension and it becomes more difficult as the dimensionality increases because outliers could be in any direction and are not concentrated along a particular direction. In the NMF context, the lack of knowledge of both factors may lead to consider a special point either as a source profile or as an irregular point and consequently, results are possibly inconsistent.

4.3 Robust Statistics and Robustness Properties

Robust statistics is a wide area of research. It has gained a lot of attention and importance during the past years. Nowadays, many researchers are working on introducing the concept of robustness into the classical methods and are trying to develop new useful robustness theories. Thus, it is becoming necessary to always take into account this concept in any statistical data analysis [48]. Due to various deviations (the presence of outliers) of the processed data, the basic and usual assumptions such as normality and independence, may be not satisfied. Thus, the statistical estimators will not give the expected results and consequently, they emphasize the need to develop new estimators to deal with such deviations.

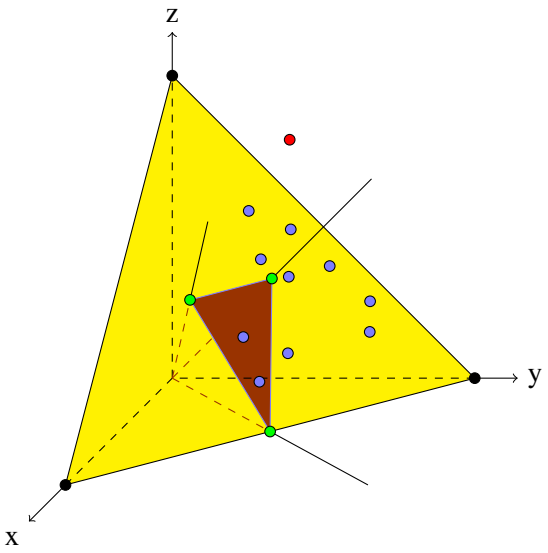

Figure 4.2 – Geometric point of view for chemical data corrupted with outliers.

Robust statistics is related with to the concept of stability of statistical procedures. It is defined by an approximate parametric model and at the same time deals with the presence of deviations based on ideal assumptions. If outliers exist, the estimated parameters can be far from the real values.
The classical methods such as the least square try as much as possible to fit the processed data points by minimizing the sum of the squared residuals in order to estimate the desired parameters. However, they make almost impossible to detect the presence of outliers because all the data points have the same weight and large deviations are spread over the residuals.

Robust statistics is a very good approach to cope with outliers by finding a fit that is similar to the case in which outliers do not exist. Then, the outliers can be easily defined due to their large residuals. Robust statistics must reduce the effect of the outliers and ensure good results. It is necessary not to ignore the outliers but to investigate and interpret them. Furthermore, robust estimators will resist the presence of outliers and provide a good estimation of the data.

4.3.1 Robustness indexes

The focus in this subsection is on some of the indexes currently used in Robust Statistics [49] to evaluate the stability of algorithms.

— The main idea behind the robustness is that if there is a contamination in the collected data, the robust estimator will not be affected. One way to assess the performance of the estimator under such circumstances is by varying one collected data point. Let's assume that one single component of the data matrix is replaced by an outlier with a varying gap z. The goal is to measure the difference between the estimation obtained with the corrupted data and the clean regular data over the ratio of contaminated data ε. This fraction should be evaluated when ε goes toward zero with respect to the variable z. This ratio is defined as the Empirical Influence

Function (EIF), i.e.,

$$EIF(z,T,\mathcal{T}_n) = \lim_{\varepsilon \to 0} \frac{T\left((1-\varepsilon)\,\mathcal{T}_n + \varepsilon\,\delta_z\right) - T\left(\mathcal{T}_n\right)}{\varepsilon}, \tag{4.3}$$

where $T(.)$ is the estimator under evaluation defined with either the contaminated density $(1-\varepsilon)\,\mathcal{T}_n + \varepsilon\,\delta_z$ or the regular one $\mathcal{T}_n$. The variable δ_z is the probability density which puts all the mass at z.

When using a non robust estimator, even a single outlier will affect the estimator and the EIF in this case is usually unbounded. When a robust regression estimator is applied, the EIF is bounded and its shape will give a good idea on how the estimator behaves with respect to the outliers. The shape of the EIF should be as smooth as possible in order to get stable results with respect to the number of outliers.

— The breakdown point relies on the definition of maxbias curve. Intuitively, the breakdown point reflects the proportion of contaminated data that an estimator could support before crashing. The maxbias accounts for the worse gap with the regular estimation with respect to the proportion of abnormal data. The curve is obtained as

$$maxbias(r,T,\mathcal{T}_n) = \sup_{\mathcal{T} \in V_\varepsilon(\mathcal{T}_n)} ||T(\mathcal{T}) - T(\mathcal{T}_n)|| \tag{4.4}$$

where r stands for the number of abnormal data among n data and ε is the ratio of contaminated data. $V_\varepsilon(\mathcal{T}_n)$ is the neighborhood of the regular distribution related to ε according to Eq (4.1). Usually, r out of n observations are corrupted. So, the breakdown point is the minimum ratio where the maxbias curve goes to infinity, i.e.,

$$\varepsilon_n^*(T,\mathcal{T}_n) = \min_r \left(\frac{r}{n}, \quad s.t. \quad maxbias(r,T,\mathcal{T}_n) = \infty\right) \tag{4.5}$$

It is defined for an estimator as the point on the x-axis where the bias curve goes towards infinity. This point gives the percentage of the data that can be considered as outliers before the estimator starts to provide bad results (for a non robust estimator, the percentage is zero whereas it can be up to 50 for a robust estimator). In conclusion, the goal is to design a robust estimator with a high breakdown point.

— Another measure is the statistical efficiency. It is often measured by a l_2 norm of the original data. However, robust estimators do not yield the best statistical efficiency, since robust estimators are trying to minimize a different measure of fit. A modest increase in the statistical efficiency is highly desirable.

To conclude, these features are interesting to compute. However, an analytic expression of these features is quite impossible to provide. As a consequence, extensive computations are required to estimate these quantities.

4.3.2 Robust estimators for regression

In regression methods, the data assumes a linear model to be fit (i.e., similar to Eq (3.1)) and the components $\underline{g}_{i,:}$ are known, i.e.,

$$x_{ij} = \underline{g}_{i,:}^T \cdot \underline{f}_j + r_{ij} \quad \forall i \in \{1,\ldots,n\} \tag{4.6}$$

Based on Eq (4.6), a scalar residual may be defined as $r_{ij} = x_{ij} - \underline{g}_{i,:}^T \cdot \underline{f}_j$. The M-estimator is defined as the minimization of a general cost function $\rho(r_{i,j})$ defined in terms of the residuals. The regression problem is defined as,

$$\hat{\underline{f}}_j = \underset{\underline{f}_j}{\operatorname{argmin}} \sum_{i=1}^{i=n} \rho\left(\frac{r_{i,j}}{\hat{\sigma}_{i,j}}\right) \quad \forall \quad j \in \{1,\ldots,m\} \tag{4.7}$$

where $\hat{\sigma}_{i,j}$ is a robust measure of scale, which can be computed or adapted according to the number of iterations. Special functions $\rho(.)$ include quadratic l_2 norms and l_1 norms as the popular choices. The condition of being insensitive to outliers requires that $\rho(.)$ increases less than r^2 for large residuals r. The efficiency condition imposing the solution to behave as a least square solution in the case without outlier requires a quadratic behavior for $\rho(.)$ for small residuals.

By differentiating Eq (4.7) with respect to the unknown variables $\underline{f}_j$, the set of M- estimating equations are obtained:

$$\sum_{i=1}^{i=n} \psi\left(\frac{r_{i,j}}{\hat{\sigma}_{i,j}}\right) \underline{g}_{i,:} = \underline{0} \quad \forall j \in \{1,\ldots,m\} \tag{4.8}$$

where $\psi \triangleq \rho'$. For the quadratic case, $\psi(r) = r$ yields the popular normal equations. Assuming $W(r) = \frac{\psi(r)}{r}$, Eq. (4.8) may be interpreted as weighted normal equations, i.e.,

$$\sum_{i=1}^{i=n} w_{ij} \left(x_{ij} - \underline{g}_{i,:}^T \cdot \underline{f}_j\right) \underline{g}_{i,:} = \underline{0} \quad \forall j \in \{1,\ldots,m\} \tag{4.9}$$

where the weights are defined as $w_{ij} \triangleq \frac{\psi(r_{ij})}{r_{ij}}$. Typical measures of fit are provided in Table (4.1), with a restriction to those functions $\rho(.)$ which are unbounded at infinity. Some authors [49] argue

Table 4.1 – Several popular M-estimator cost functions

Type	$\rho(r)$	$\psi(r)$	$w(r)$
l_2	$\frac{r^2}{2}$	r	1
l_1	$\lvert r\rvert$	$sign(r)$	$\frac{1}{\lvert r\rvert}$
$l_1 - l_2$	$2(\sqrt{1+\frac{r^2}{2}} - 1)$	$\frac{r}{\sqrt{1+\frac{r^2}{2}}}$	$\frac{1}{\sqrt{1+\frac{r^2}{2}}}$
Huber $\begin{cases} \text{if } \lvert r\rvert < c \\ \text{if } \lvert r\rvert > c \end{cases}$	$\begin{cases} \frac{r^2}{2} \\ c(\lvert r\rvert - \frac{c}{2}) \end{cases}$	$\begin{cases} r \\ c \cdot sign(r) \end{cases}$	$\begin{cases} 1 \\ \frac{1}{\lvert r\rvert} \end{cases}$
Fair	$c^2\left(\frac{\lvert r\rvert}{c} - log(1+\frac{\lvert r\rvert}{c})\right)$	$\frac{\lvert r\rvert}{1+\frac{\lvert r\rvert}{c}}$	$\frac{1}{1+\frac{\lvert r\rvert}{c}}$

that bounded $\rho(.)$ functions are recommended in order to cope with uncertainties present in $\underline{g}_{i,:}$, e.g., correntropy [104], Welsh [179] and Tukey [179] cost functions. However, all these cost functions have some drawbacks with respect to the requirements to cope with outliers [179].

The computation of the outcome of an M-estimator is a difficult task because an iterative procedure is required. Usually, this step is performed by an Iterative Re-Weighted Least Square procedure (IRWLS) which alternately updates the scale and the unknown vector. A correct initialization is expected in order to compute an approximate weight. When $\rho(.)$ is bounded, the function $\psi(.)$ tends to zero at infinity. Thus, the latter property impliespossible multiple solutions which yield crucial initialization step.

This section has given simply an overview of robustness concepts implemented for regression. Unlike regression approaches in which one matrix is completely known, these concepts are addressed in the next section in the framework of NMF approaches which are a much harder task because neither G nor F are known.

4.4 Sparseness Based NMF

4.4.1 Sparseness and low rank concepts

First, the definition of the ℓ_p norm for a vector is recalled as,

$$||\underline{r}||_p = \left(\sum_{i=1}^{n} |r_i|^p \right)^{\frac{1}{p}}. \tag{4.10}$$

This definition includes the ℓ_2 norm which is obtained with $p = 2$ and the ℓ_1 norm with $p = 1$. Matrix norms can be considered as an extension of vector norms. Whereas matrix norms may be defined as norms induced by vectors, the emphasis is on component wise matrix norms, such as the L_p norm

$$||A||_p = ||vec(A)||_p = \left(\sum_{i=1}^{n} \sum_{j=1}^{m} |a_{ij}|^p \right)^{\frac{1}{p}}. \tag{4.11}$$

This definition includes the Frobenius norm with $p = 2$, and the L_1 norm with $p = 1$ as special cases. Compared to the Frobenius norm, L_1 norms have moderate influence on large residuals and it is often used as a penalty term with respect to a matrix factor. Thus, sparse features could be expected with L_1 penalties. Besides, robustness in the data is often addressed by using L_1 as a modified objective function.

Moreover, $L_{2,1}$ norms are often used by considering a matrix as a set of column vectors to which ℓ_2 norms are applied, e.g.,

$$||A||_{2,1} = \sum_{i=1}^{n} \sqrt{\sum_{j=1}^{m} |a_{ij}|^2}. \tag{4.12}$$

They could be extended to $L_{p,q}$ norms and are defined as

$$||A||_{p,q} = \left(\sum_{i=1}^{n} \left(\sum_{j=1}^{m} |a_{ij}|^p \right)^{\frac{q}{p}} \right)^{\frac{1}{q}}. \tag{4.13}$$

$L_{2,1}$ norms have been implemented as modified cost functions in a robust subspace factorization problem [39] or in a robust NMF problem [88].

Besides, the definition of the nuclear norms are based on the Singular Value Decomposition of a matrix $A = U \cdot \Sigma \cdot V^T$, where Σ is a diagonal matrix that is defined as $\Sigma = \text{diag}(\sigma_1, \ldots, \sigma_r)$

$$||A||_* = \sum_{i=1}^{min(n,m)} \sigma_i(A). \tag{4.14}$$

In fact, the nuclear norm is often viewed as a convex relaxation of the number of non zero eigenvalues (i.e., the rank). Consequently, it is extensively used as a surrogate function of the rank. The next section illustrates these aspects.

4.4.2 Related Problems

The Matrix sparseness is a property which is often desired in order to obtain meaningful results. The matrix viewed as a collection of signals is mapped to a transformed domain where the signal tends to concentrate the information on few entries. The concept was first implemented in robust PCA technique in which the data matrix X is splitted into a low rank matrix L and a sparse matrix S that contains the outlying components [75], e.g.,

$$X = L + S \tag{4.15}$$

In such case, the matrix S conveys the few outliers that are present in the data. Except in special cases, no prior knowledge about the locations of the non zero entries are available. This decomposition is applied to similar problems such as Robust Principal Components Analysis (RPCA) [17], Robust Matrix Completion [43, 171], and Robust Low Rank Minimization [167]. Usually, factors are obtained by a relaxed convex optimization problem, called the Principal Components Poursuit, i.e.,

$$\hat{L}, \hat{S} = \underset{L,S}{\text{argmin}} \, ||L||_* + \mu ||S||_1 \quad \text{s.t.} \quad L + S = X \tag{4.16}$$

The problem may be perfectly solved under incoherence conditions [75], in conjunction with an analytic expression of the hyper parameter μ.

4.4.3 Sparse NMF

The Robust sparse NMF is based on the decomposition of the data matrix into low rank plus sparse matrices as defined in Eq (4.15). Furthermore, it assumes that the low rank matrix can be factorized

into non-negative factors, i.e.,

$$X = G \cdot F + S \tag{4.17}$$

Subsequently, G and F are forced to be non-negative. In order to favor a sparse decomposition of one factor, Shen [151] proposes an l_1 surrogate as the sparsity function. The problem can be formulated as

$$\underset{G,F\geq 0}{\operatorname{argmin}} ||X - G \cdot F - S||^2 + \lambda \sum_{j=1}^{m} ||S_{.,j}||_1^2 \tag{4.18}$$

Similarly, Zhang [180] proposes to solve a similar criterion in which the penalty term accounts for a complete ℓ_1 surrogate that acts on the complete matrix S, e.g.,

$$\underset{G,F\geq 0}{\operatorname{argmin}} ||X - G \cdot F - S||^2 + \lambda ||S||_1 \tag{4.19}$$

The resolution of such a problem involves in its main loop a soft thresholding step which may force S to be completely 0 if the residual is low. Rapin [137] suggests the use of a hard thresholding approach, whose behavior is close to a ℓ_0 penalty. Moreover, Févotte and Dobigeon [47] applied such concepts in the field of non-linear Hyperspectral unmixing, where the non linearity is viewed as a deviation from the linear model's assumption. In this case, the sparse matrix S includes the potential outliers and is required to be sparse by using a $\ell_{2,1}$ norm. In fact $\ell_{2,1}$ norm favors the sparsity of the energy of each column vector of S so that the whole criterion reads

$$\underset{G,F\geq 0}{\operatorname{argmin}} \mathcal{D}(X - G \cdot F - S) + \lambda ||S||_{2,1} \tag{4.20}$$

Besides, Woo and Park proposed a ℓ_1 control of the sparse matrix with the denseness of one matrix factor [169] which was devoted to the foreground/background video separation. Thus, the sparse matrix contains the moving objects.

As a conclusion, low rank plus sparse decomposition appears as a reliable way to deal with outliers.

4.5 NMF based on modified cost functions

4.5.1 Introduction

Some modified cost functions have been previously introduced for regression purposes. They may be viewed as an extension of the classical ℓ_2 norms. Most of them can be extended to the context of NMF by considering matrix norms. However, divergences which are a kind of extensions of norms, are usually used to measure a discrepancy. Some of the classical ones are then investigated.

4.5.2 Modified Cost functions

Several cost functions can be chosen to cope with outliers. Some functions can be found in Table (4.1). Some classical functions are first investigated, namely, $\alpha\beta$-divergences which are essentially discussed in [27], the correntropy cost function and the Huber cost function.

4.5.2.1 Huber function

The Huber dissimilarity measure belongs to the class of M-estimators. It is based on the derivable connection between ℓ_2 and ℓ_1 norms. It has been previously defined in Table (4.1).

$$\rho_{\text{huber}}(r) \triangleq \begin{cases} \frac{r^2}{2} \text{ if } |r| < c \\ c(|r| - \frac{c}{2}) \text{ if } |r| > c \end{cases} \tag{4.21}$$

Its role is to split the domain according to the value of the residual into the quadratic (ℓ_2) behavior and the linear behavior (ℓ_1) . The parameter c is defined as the cutoff parameter that allows to switch between the two domains. Figure (4.3) shows the behavior of the Huber cost function with a cutoff parameter that is equal to 1. The Huber cost function has several features which allows its classification as a robust cost function:

— It is convex but not strictly convex.
— It has a bounded influence function (ψ function provided in Table (4.1)).
— It has a stable minimum.
— It has a continuous first differentiation but it is not twice differentiable.
— It is hybrid between the quadratic (ℓ_2) and ℓ_1, e.g., it is quadratic for small residual values and linear for large residual values (i.e it acts as (ℓ_1) norm for large residuals and (ℓ_2) for small residuals).
— It has the outlier stability of (ℓ_1).

In the context of matrices, the Huber norm is usually defined as a component wise matrix norms (even though it should be used as a norm induced by vectors), e.g.,

$$||R||_{Huber} \triangleq ||vec(R)||_{Huber} = \sum_{i=1}^{n} \sum_{j=1}^{m} \rho_{\text{huber}}(r_{ij}). \tag{4.22}$$

By performing the minimization with iterative algorithms, the cutoff parameter should be estimated at each iteration. This cost function could be implemented as an interesting starting point to solve several NMF problems.

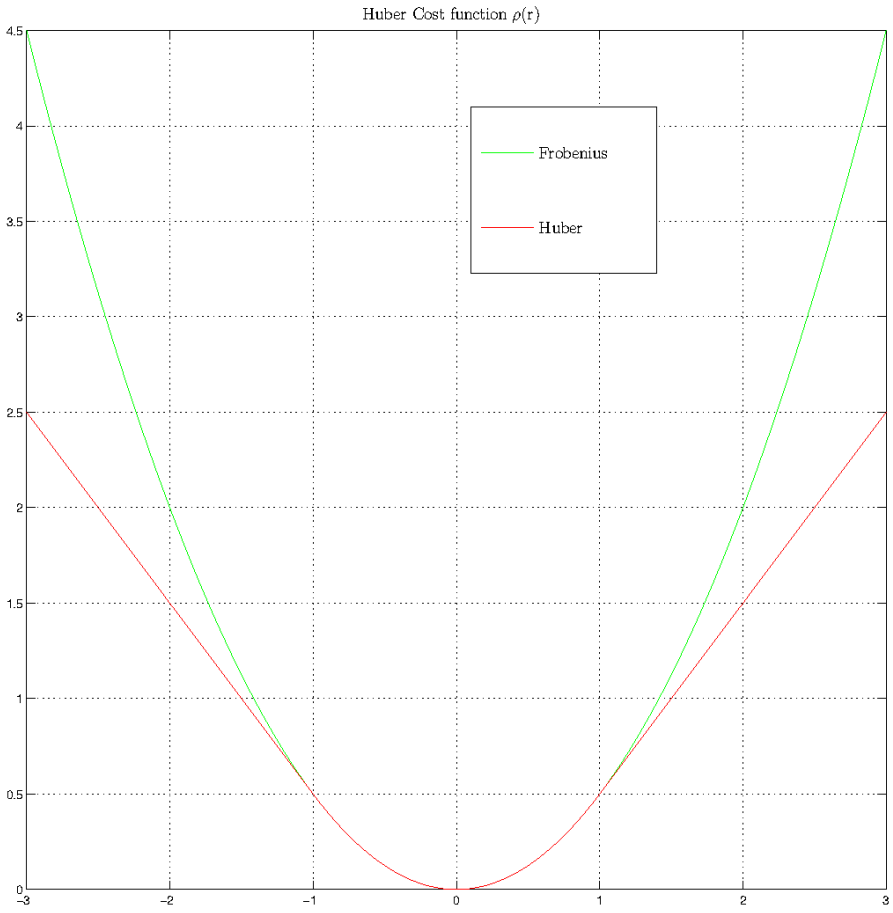

Figure 4.3 – The Huber Cost Function

4.5.2.2 Correntropy

In addition to the Huber loss, the concept of Correntropy is presented. Correntropy is a non linear local similarity measure between two variables defined as:

$$V(\underline{x},\underline{\hat{x}}) = \mathbb{E}\left(\mathcal{K}(\underline{x},\underline{\hat{x}})\right) \tag{4.23}$$

where $\mathbb{E}$ is for the expectation operator and $\mathcal{K}(.,.)$ is a kernel function which fulfills the shift invariance property of both input arguments. Practically, due to a finite number of samples $(\underline{x}_i,\underline{\hat{x}}_i)_{i=1}^n$, the sample estimation is often implemented e.g.,

$$V(\underline{x},\underline{\hat{x}}) = \frac{1}{n}\sum_{i=1}^{n}\mathcal{K}(\underline{x}_i,\underline{\hat{x}}_i) \tag{4.24}$$

Usually, parametric Gaussian kernels are used

$$\mathcal{K}(\underline{x},\underline{\hat{x}}) = \frac{1}{\sigma\sqrt{2\pi}}\,\mathcal{G}_\sigma\left(||\underline{x}-\underline{\hat{x}}||_2\right) \triangleq \frac{1}{\sigma\sqrt{2\pi}}\,e^{-\frac{||\underline{x}-\underline{\hat{x}}||_2^2}{2\sigma^2}} \tag{4.25}$$

The Correntropy should be approximated by a Taylor series expansion around $\underline{x} = \underline{\hat{x}}$, e.g.,

$$V(\underline{x},\underline{\hat{x}}) = \frac{1}{\sigma\sqrt{2\pi}}\sum_{k=0}^{\infty}\frac{(-1)^k}{2^k k!}\mathbb{E}\left(\frac{||\underline{r}||_2^{2k}}{\sigma^{2k}}\right) \tag{4.26}$$

The Correntropy involves even higher order moments of the residual error $\underline{r} \triangleq \underline{x}-\underline{\hat{x}}$. The Correntropy assesses how close two random variables are within a neighborhood tuned by the kernel bandwidth σ. This measure serves to decrease the influence of impulsive noises or outliers.

In Signal Processing and Machine Learning, the Maximum Correntropy Criterion (MCC) is often used to maximize the similarity between two variables. A dissimilarity measure may be designed by considering the negative correntropy [181], e.g.,

$$C(\underline{x},\underline{\hat{x}}) = \mathcal{K}(\underline{0},\underline{0}) - V(\underline{x},\underline{\hat{x}}) \tag{4.27}$$

It is also shown that a negative correntropy is belonging to the class of M-estimators as defined in the previous sections. Besides, some authors [105] [144] consider the Correntropy Induced Metric (CIM)– which is defined as the square root of the negative correntropy– as an equivalent dissimilarity measure,

$$CIM(\underline{x},\underline{\hat{x}}) = \sqrt{C(\underline{x},\underline{\hat{x}})} = \sqrt{\mathcal{K}(\underline{0},\underline{0}) - V(\underline{x},\underline{\hat{x}})} \tag{4.28}$$

CIM is a metric measure since it fulfills the basic properties of norms. According to the values of the residuals, three areas may be identified. CIM behaves as a ℓ_2 norm for small residuals while moderate residual values lead to a ℓ_1 behavior. When the residuals are very large (an outlier) compared to the kernel bandwidth σ, CIM is approaching the behavior of ℓ_0 norm, which highlights its robustness properties.

4.5.2.3 $\alpha\beta$-divergences

In this section, the information introduced in [27] and in [96] is mainly summarized. First, a divergence can be distinguished from a norm because the symmetry property is not satisfied. The $\alpha\beta$-divergence is developed to perform an asymmetric comparison of two matrices P and Q (exchanging the order of the comparison modifies the result) and is expressed as,

$$\mathcal{D}^{\alpha,\beta}(P||Q) = \sum_{i,j}\mathcal{D}^{\alpha,\beta}(p_{ij},q_{ij}) \tag{4.29}$$

where the individual scalar divergences are defined as

$$\mathcal{D}^{\alpha,\beta}(p_{ij},q_{ij}) = \begin{cases} \frac{-1}{\alpha\beta}(p_{ij}^{\alpha}q_{ij}^{\beta} - \frac{\alpha}{\alpha+\beta}p_{ij}^{\alpha+\beta} - \frac{\beta}{\alpha+\beta}q_{ij}^{\alpha+\beta}), & (\alpha,\beta,\alpha+\beta)\neq 0, \\ \frac{1}{\alpha^2}(p_{ij}^{\alpha}\ln\frac{p_{ij}^{\alpha}}{q_{ij}^{\alpha}} - p_{ij}^{\alpha} + q_{ij}^{\alpha}), & \alpha\neq 0,\beta=0, \\ \frac{1}{\alpha^2}(\ln\frac{q_{ij}^{\alpha}}{p_{ij}^{\alpha}} + (\frac{q_{ij}^{\alpha}}{p_{ij}^{\alpha}})^{-1} - 1), & \alpha=-\beta\neq 0, \\ \frac{1}{\beta^2}(q_{ij}^{\beta}\ln\frac{q_{ij}^{\beta}}{p_{ij}^{\beta}} - q_{ij}^{\beta} + p_{ij}^{\beta}), & \alpha=0,\beta\neq 0, \\ \frac{1}{2}(\ln p_{ij} - \ln q_{ij})^2, & \alpha,\beta=0. \end{cases} \tag{4.30}$$

The asymmetric behavior with respect to the value of the residual, implies that different schemes to address positive or negative outliers may be derived. This argument motivates the use of such a divergence. Cichoki's definition is adopted in this work [27]. Cichocki also showed that these individual measures are always positive. Two special cases may be distinguished:

1. The α-divergence, which may be encountered when $\alpha+\beta=1$.

2. The β-divergence, which accounts for $\beta=1$.

A scale property may be also shown between the data matrix X and the estimated data matrix $\hat{X}$,

$$\mathcal{D}^{\alpha,\beta}(\lambda X \parallel \lambda\hat{X}) = \lambda^{\alpha+\beta}\,\mathcal{D}^{\alpha,\beta}(X \parallel \hat{X}). \tag{4.31}$$

Another scale property may also be provided

$$\mathcal{D}^{\lambda\alpha,\lambda\beta}(X \parallel \hat{X}) = \frac{1}{\lambda^2}\,\mathcal{D}^{\alpha,\beta}(X^{\lambda} \parallel \hat{X}^{\lambda}). \tag{4.32}$$

The interesting value $\lambda = \frac{1}{\alpha+\beta}$ states that $\alpha\beta$-divergence reflects a general α-divergence, e.g.,

$$\mathcal{D}^{\frac{\alpha}{\alpha+\beta}}(X \parallel \hat{X}) = \mathcal{D}^{\frac{\alpha}{\alpha+\beta},\frac{\beta}{\alpha+\beta}}(X \parallel \hat{X}) = (\alpha+\beta)^2\,\mathcal{D}^{\alpha,\beta}(X^{\frac{1}{\alpha+\beta}} \parallel \hat{X}^{\frac{1}{\alpha+\beta}}). \tag{4.33}$$

The differentiation of the criterion with respect to the unknown vector $\underline{\theta}$ yields generalized normal Equations (4.9), e.g.

$$\frac{\partial\mathcal{D}^{\alpha,\beta}(X \parallel \hat{X})}{\partial\underline{\theta}} = -\sum_{i,j}\frac{\partial\hat{X}_{i,j}}{\partial\underline{\theta}}\underbrace{(\hat{X}_{ij})^{\alpha+\beta-1}}_{\text{weight}}\quad\underbrace{\ln_{1-\alpha}(X_{ij}/\hat{X}_{ij})}_{\alpha\text{-zoom}}, \tag{4.34}$$

where the function $\ln_{1-\alpha}(.)$ is defined as,

$$\ln_{1-\alpha}(z) \triangleq \begin{cases} \frac{z^{\alpha}-1}{\alpha}, & \text{if} \quad \alpha\neq 0, \\ \ln(z), & \text{if} \quad \alpha=0. \end{cases} \tag{4.35}$$

Two effects in Equation (4.34) are highlighted: an α zoom and a weighting effect. Table (4.2) explains the α zoom effect according to the ratio $\frac{X_{ij}}{\hat{X}_{ij}}$ and the values of the parameter α. When $\alpha>1$, the emphasis is set on larger values of the ratio $\frac{X_{ij}}{\hat{X}_{ij}}$ (large zoom), and the algorithm updates its estimation to a better fit. On the contrary, a small zoom implies that the algorithm can accept parameters with bad fit. The weighting effect ($\hat{X}_{ij}^{\alpha+\beta-1}$) is discussed according to $\hat{X}_{ij}$ and the values of $\alpha+\beta$ as illustrated

Table 4.2 – Properties of α-zoom.

α	$0 < \frac{X_{ij}}{\hat{X}_{ij}} < 1$	$\frac{X_{ij}}{\hat{X}_{ij}} > 1$
$\alpha > 1$	small zoom	large zoom
$\alpha < 1$	large zoom	small zoom

Table 4.3 – Weighting effect on the αβ-divergence.

$\alpha+\beta$	$0 < \hat{X}_{ij} < 1$	$\hat{X}_{ij} > 1$
$\alpha+\beta < 1$	large weighting	small weighting
$\alpha+\beta > 1$	small weighting	large weighting

in Table (4.3). A large weighting means a good confidence in the data and is forced the algorithm to find a better fit. On the other hand, a low weighting allows the algorithm to accept a bad fit. Thus, the combination of these two effects are leads to different scenarios and Figure (4.4) allustrates various areas as a function of α and β.

— Area 1 ($\alpha+\beta < 1$ and $\alpha < 1$): the algorithm allows outliers if $X_{ij} > \hat{X}_{ij}$ for large X_{ij}. The estimation has to fit well the low values of X_{ij} which are emphasized.

— Area 2 ($\alpha+\beta > 1$ and $\alpha < 1$): the algorithm allows outliers if $X_{ij} > \hat{X}_{ij}$ for small $\hat{X}_{ij}$. The estimation is required to fit large amplitudes of X_{ij} whose relevance is highlighted.

— Area 3 ($\alpha+\beta < 1$ and $\alpha > 1$): the algorithm allows outliers if $X_{ij} < \hat{X}_{ij}$ for large $\hat{X}_{ij}$. The estimation tries to fit low values whose importance is enhanced.

— Area 4 ($\alpha+\beta > 1$ and $\alpha > 1$): the algorithm allows outliers if $X_{ij} < \hat{X}_{ij}$ together with a moderate value of $\hat{X}_{ij}$. The estimation seeks to fit large values of X_{ij}.

As a summary and in the context of air pollution, it is preferably that the algorithm should fit large data and accept some misfit for low range data, i.e. $\alpha+\beta > 1$. Moreover, situations where $X_{ij} > \hat{X}_{ij}$ are favored regarding the opposite situations. Since a negative residual would not present a physical meaning for experts, the half space corresponding to $\alpha < 1$ will be selected.

Therefore, the area of interest is Area 2. These recommendations will be useful to select appropriate parameters during the tests.

4.5.3 Robust NMF Methods

In this section, some NMF methods based on the presented modified cost functions are investigated. That is, the Huber NMF, the Correntropy based NMF, and the αβ-divergences NMF are addressed even though other kinds of robust NMF can be reviewed. Actually, Kong developed a L_{21} robust NMF [88] and Ben-Hamza investigated a $L_1 L_2$ norm based NMF [8].

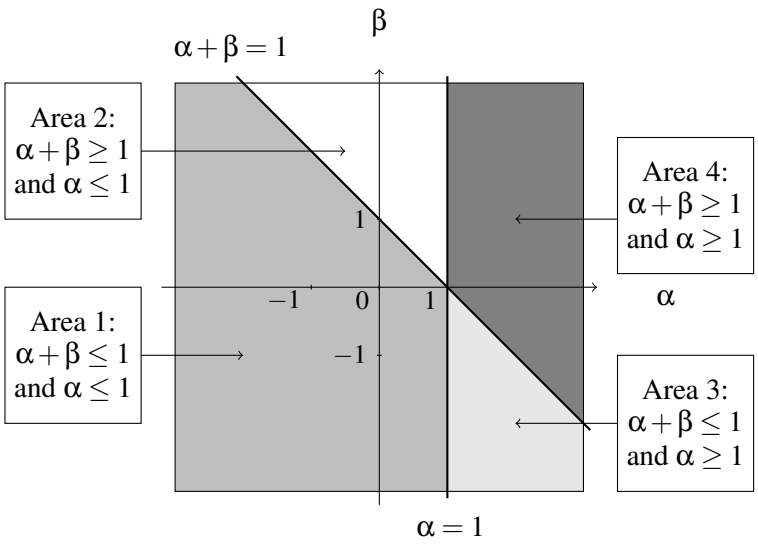

Figure 4.4 – Different areas as a function of α β.

4.5.3.1 Huber NMF

By taking into consideration Eq (4.21), the Huber NMF [45] is expressed as the following optimization problem,

$$\underset{G,F\succeq 0}{\operatorname{argmin}} \sum_{i=1}^{n}\sum_{j=1}^{m} \rho^{Huber}(r_{ij}), \tag{4.36}$$

where $\rho^{Huber}(.)$ is the Huber cost function. According to the values of the residuals, the previous criterion may be differentiated and it leads to the piecewise Frobenius NMF and L_1 NMF. It can be viewed also as a weighted NMF with a weight $w_{ij} = \frac{\rho'(r_{ij})}{r_{ij}}$ for each residual. Thus, a piecewise expression of the weight can be given as,

$$w_{ij} \triangleq \begin{cases} 1 & \text{if } |r_{ij}| < c, \\ \frac{c}{|r_{ij}|} & \text{otherwise.} \end{cases} \tag{4.37}$$

The update rules of both matrices G and F are obtained using the weighted NMF rules (3.76). Based on the work of Ding [39], the cutoff parameter c is usually chosen to be the median and it is usually expressed as,

$$c = median(|R_{ij}|) \tag{4.38}$$

However, it is suggested that this choice should be modified because half of the data would be labeled as outliers.

The Huber NMF algorithm may be summarized in Alg. (1) A crucial step in the implementation

Algorithm 1 Huber NMF description

Reading of X
Initialization of F, G and c
while the stopping rule is not fulfilled **do**
  Compute w_i according to Eq (4.37)
  Compute G according to Eq. (3.76)
  Update F according to Eq. (3.76))
  Update c according to Eq. (4.38)
end while

of this algorithm is the choice of parameter c, which delimits the two areas. Besides, this choice can be modified adaptively by computing at each iteration the percentage of outliers in the data. In the next section, NMF based on Correntropy Induced Metric (CIM) will be investigated.

4.5.4 Correntropy based NMF

In this section, existing Robust NMF functions that are based on the Correntropy Induced Metric (CIM) are presented. However, Du [45] proposed a slightly different concept of CIM that is introduced earlier.

The CIM-NMF criterion is defined as the square of the CIM measure in which matrix X is represented as $n.m$ scalar points, i.e.,

$$\underset{G,F\succeq 0}{\operatorname{argmin}} \sum_{i=1}^{N}\sum_{j=1}^{M}\left(1-\mathcal{G}_{\sigma}(X_{ij}-\sum_{k=1}^{p}G_{ik}F_{kj})\right) \tag{4.39}$$

where $\mathcal{G}_{\sigma}(.)$ is the gaussian distribution defined in Eq (4.25). Its solution is achieved by minimizing the above equation. Some authors proposed the introduction of an auxiliary matrix W with general entry w_{ij} and reformulate the problem as an augmented Lagrangian by using the half-quadratic theory [119], i.e.,

$$\underset{R,W}{\operatorname{argmin}} \sum_{i=1}^{n}\sum_{j=1}^{m}[\frac{1}{2}w_{ij}r_{ij}^{2}+\varphi(w_{ij})] \tag{4.40}$$

where w_{ij} is viewed as the weight associated with the corresponding data x_{ij}. The weight should be small for large errors and large for small errors. The term $\varphi(W_{ij})$ is the conjugate function of the negative Gaussian function $-\mathcal{G}_{\sigma}(r_{ij})$ [119, 14]. The weight w_{ij} can be calculated by differentiating each single member of Eq (4.39,4.40) with respect to r_{ij}, i.e.,

$$-\mathcal{G}'_{\sigma}(r_{ij}) = w_{ij}\, r_{ij}. \tag{4.41}$$

Eq. (4.41) is exactly the definition provided for the weight in Eq (4.9). It yields the following weight expression,

$$w_{ij} = \frac{1}{\sigma^{2}}\, e^{-\frac{r_{ij}^{2}}{2\sigma^{2}}}, \tag{4.42}$$

where σ^2 is defined as the average of the squared residual error, i.e.,

$$\sigma^2 = \frac{1}{2nm}\sum_{i=1}^{n}\sum_{j=1}^{m} r_{ij}^2 \tag{4.43}$$

Subsequently, the computations of G and F can be reduced to the weighted NMF with an adaptive choice of weights as provided in Eq. (4.42) [1]. Thus, the update rules are those provided in section Weighted NMF (3.76). The CIM-NMF algorithm is summarized in Alg. (refalg111111).

Algorithm 2 CIM-NMF Algorithm

Reading of X
Initialization of F, G and W
while the stopping rule is not fulfilled **do**
  Compute W according to Eq. (4.42)
  Compute G according to Eq. (3.76)
  Update F according to Eq. (3.76)
  Update σ^2 according to Eq. (4.43)
end while

Du [45] proposed an approach in which an entire row of the data matrix is considered as an outlier. It means that n residual vectors $\underline{r}_i \in \mathbf{R}^m$ are to be considered. They may be defined as

$$\underline{r}_i \triangleq \underline{x}_{i,\cdot}^T - F^T \cdot \underline{g}_{i,\cdot}^T \tag{4.44}$$

Consequently, the initial correntropy definition with n points is taken into account and all entries of a row are assigned the same weight. Therefore, the optimization problem (rCIM for row Correntropy Induced Metric) may be similarly reformulated as the minimization of the following objective function,

$$\underset{G,F\succeq 0,\underline{w}}{\operatorname{argmin}} \sum_{i=1}^{N} [w_i ||\underline{r}_i||^2 + \varphi(w_i)] \tag{4.45}$$

Using the same half quadratic process, the weight matrix can be written as,

$$w_i = exp(-\frac{||\underline{r}_i||^2}{2\sigma^2}) \tag{4.46}$$

A matrix weight W can be formed by defining $W = \underline{w} \cdot 1_{1\times m}$. The rCIM-NMF algorithm can be summarized as a weighted NMF defined in Alg. (3) with particular weights defined in Eq. (4.46). The scale factor σ^2 is defined as the half average of the square l_2 norm of residuals, i.e.,

$$\sigma^2 = \frac{1}{2n}\sum_{i=1}^{n} ||\underline{r}_i||^2 \tag{4.47}$$

To conclude, Correntropy allows the definition of several robust NMF, which are equivalent to particular weighted NMF. In the next section, the focus is on the divergence based NMF approaches.

1. This equivalence should also be proved directly by differentiating the cost function with respect to F and G. The same weight would appear in the equation.

Algorithm 3 rCIM-NMF Algorithm description

Reading of X
Initialization of F, G and Weight matrix w
while the stopping rule is not fulfilled **do**
  Compute w_i according to Eq 4.46, $W = \underline{w} \cdot 1_{1\times m}$
  Compute G according to Eq. (3.76)
  Update F according to Eq. (3.76))
  Update σ^2 according to Eq. (4.43)
end while

4.5.4.1 αβ-Divergence NMF

In this section, the αβ-divergence NMF problem is formulated as

$$\underset{G,F\succeq 0}{\operatorname{argmin}}\, \mathcal{D}_W^{\alpha,\beta}(X||G\cdot F) = \underset{G,F\succeq 0}{\operatorname{argmin}} \sum_{i,j} w_{ij}\, \mathcal{D}^{\alpha,\beta}(x_{ij}, \sum_{k=1}^{p} g_{ik} f_{kj}) \tag{4.48}$$

The proposed development is an alternative approach to solve Problem (4.48). However, it leads to the same update rules that are derived in [27]. The whole problem is divided into independent small problems and the investigation is made using a MM strategy. Due to property of separability of the criterion, it is possible to deal with one column data $\underline{x}$ and one column vector $\underline{f}$, e.g.,

$$\mathcal{D}_{\underline{w}}^{\alpha,\beta}(\underline{x}||G\cdot \underline{f}) = \sum_i w_i\, \mathcal{D}^{\alpha,\beta}\left(x_i||(G\cdot \underline{f})_i\right), \tag{4.49}$$

Eq (4.49) may be expressed as a function $h^{\alpha,\beta}(z)$,

$$\mathcal{D}_{\underline{w}}^{\alpha,\beta}(\underline{x}||G\Delta \underline{f}) = \sum_i w_i x_i^{\alpha+\beta} \cdot h^{\alpha,\beta}\left(\frac{\sum_j g_{ij} f_j}{x_i}\right), \tag{4.50}$$

where the function $h^{\alpha,\beta}(z)$ is defined as,

$$h^{\alpha,\beta}(z) \triangleq -\frac{1}{\alpha\beta}\left[z^{\beta} - \frac{\alpha}{\alpha+\beta} - \frac{\beta}{\alpha+\beta} z^{\alpha+\beta}\right] \quad \forall(\alpha,\beta,\alpha+\beta)\neq 0, \tag{4.51}$$

The function $h^{\alpha,\beta}(z)$ is shown to be convex for all $z>0$ in the domain described by $\beta \in [min(1,1-\alpha); max(1,1-\alpha)]$. In order to preserve this property, the parameters are restricted to this domain. Inspired by Limem's work ([96] chap 3 p85), a majoring function can be defined which depends on the starting point f_j^k,

$$\mathcal{H}_{1,w}^{\alpha,\beta}(f_j, f_j^k) = \sum_i w_i x_i^{\alpha+\beta} \sum_j \frac{g_{ij} f_j^k}{\sum_l g_{il} f_l^k} \cdot h^{\alpha,\beta}\left(\frac{f_j \sum_l g_{il} f_l^k}{x_i f_j^k}\right), \tag{4.52}$$

The cancellation of the differentiation of the majoring function $\mathcal{H}_{1,w}^{\alpha,\beta}$ leads to the simplified expression,

$$\left(\frac{f_j}{f_j^k}\right)^{\alpha} = \frac{\sum_i w_i g_{ij} \cdot x_i^{\alpha} \cdot (\sum_l g_{il} f_l^k)^{\beta-1}}{\sum_i w_i g_{ij} \cdot (\sum_l g_{il} f_l^k)^{\alpha+\beta-1}}. \tag{4.53}$$

The following expression may be extended to its vectorial form, i.e.,

$$\left(\frac{\underline{f}}{\underline{f}^k}\right)^{\alpha} = \frac{G^T\left[\underline{w} \circ \underline{x}^{\alpha} \circ (G\underline{f}^k)^{\beta-1}\right]}{G^T\left[\underline{w} \circ (G\underline{f}^k)^{\alpha+\beta-1}\right]}. \tag{4.54}$$

Expression (4.54) can be expressed in a matrix form, e.g.,

$$F^{k+1} \leftarrow F^k \circ M_F^{\alpha,\beta}, \tag{4.55}$$

where $M_F^{\alpha,\beta}$ is given by

$$M_F^{\alpha,\beta} = \left[\frac{G^T \cdot \left(W \circ X^{\alpha} \circ (G \cdot F)^{\beta-1}\right)}{G^T \cdot (W \circ (G \cdot F)^{\alpha+\beta-1})}\right]^{(\frac{1}{\alpha})}. \tag{4.56}$$

In order to avoid indeterminacies, the operator $+$ (defined as $x^+ = \max(x, \varepsilon)$) is added to each argument of the power function,

$$M_F^{\alpha,\beta} = \left[\frac{G^T \left(W \circ (X^+)^{\alpha} \circ ((G \cdot F)^+)^{\beta-1}\right)}{G^T \cdot \left(W \circ ((G \cdot F)^+)^{(\alpha+\beta-1)})\right)}\right]^{(\frac{1}{\alpha})}. \tag{4.57}$$

The new update rule of the contribution matrix may be also similarly obtained, i.e.,

$$G \leftarrow G \circ \left[\frac{\left(W \circ X^{\alpha} \circ (G \cdot F)^{\beta-1}\right) \cdot F^T}{(W \circ (G \cdot F)^{\alpha+\beta-1}) \cdot F^T}\right]^{(\frac{1}{\alpha})}. \tag{4.58}$$

These equations are shown to be valid in the domain where $\beta \in [min(1, 1-\alpha); max(1, 1-\alpha)]$. In practice, they could be used in a wider domain as soon as the x_{ij} and $\hat{x}_{ij}$ are not too far [27]. Furthermore, the KKT conditions should be fulfilled for the problem shown in Eq (4.48). The KKT conditions are provided in Limem 's work ([96] chap 3 p63) and reported hereafter,

$$\begin{array}{ll} F \succeq 0, & G \succeq 0, \\ \frac{1}{\alpha} G^T [W \circ (GF)^{\beta-1} \circ ((GF)^{\alpha} - X^{\alpha})] \succeq 0, & \frac{1}{\alpha} [W \circ (GF)^{\beta-1} \circ ((GF)^{\alpha} - X^{\alpha})] F^T \succeq 0, \\ F \circ \left(G^T [W \circ (GF)^{\beta-1} \circ ((GF)^{\alpha} - X^{\alpha})]\right) = 0, & G \circ \left([W \circ (GF)^{\beta-1} \circ ((GF)^{\alpha} - X^{\alpha})] F^T\right) = 0. \end{array} \tag{4.59}$$

It could be easily checked that the update rules are consistent with the above KKT conditions.

It is to be noted that some special choices of parameters α and β lead to bridge existing NMF methods, i.e., α-NMF, β-NMF. Moreover, these update rule are weighted versions of $\alpha\beta$-NMF. As a result and consistently with the previous robust methods based on Huber NMF or CIM-NMF, weights could

also be computed adaptively at each iteration. This formulation provides a more flexible framework to deal with outliers.

4.6 Conclusion

In this chapter, the concept of outliers was introduced and several kinds of outliers can be encountered. This problem has often been solved in robust regression and it served as an impetus to introduce current indexes applied in Robust Statistics. In the presence of outliers (deviations from a regular model), some authors proposed on one hand to split the data into a sparse matrix and a low rank matrix. This task is usually performed by an optimization framework which favors the sparsity of the sparse matrix and the low rank property of the other matrix. On the other hand, the framework of modified cost functions for an optimization purpose is extensively investigated. The context of M-estimators appears interesting such that many researchers have tried to extend this optimization framework to the case of NMF. In this chapter, the correntropy based NMF, the Huber NMF and the $\alpha\beta$-WNMF are reviewed and they can provide improved solutions. However, the incorporation of extra information reduces the solution domain. This kind of information is revisited in the next chapter.

CHAPTER 5

Existing Informed NMF methods with set values and sum-to 1 variables.

5.1 Introduction

The previous chapter highlighted the need for special cost functions to cope with irregular points in the data matrix. αβ-divergences were one of the various modified cost functions which are able to resist to this kind of abnormal points.

The purpose of this chapter is to investigate informed NMF with special constraints. The focus is on the sum-to-1 variables due to the definition of the profile matrix. Special structures of the factor are then studied as part of the NMF problem.

A second set of contraints which are reviewed are set values in one factor. The solutions which are essentially provided in Limem's work [96] are revisited.

Then, both previous constraints are addressed simultaneously by using special normalization of the previous updates obtained with set values. These methods are investigated and are able to be used in the field of pollution source apportionment.

5.2 Sum-to -1 variables in NMF problems

Sum-to-1 variables may be encountered in several fields and also in different ways which are described hereafter.

5.2.1 Sum-to-1 abundances in Hyperspectral Unmixing

The objective of Hyperspectral Unmixing is to recover from a data cube or a data matrix X the constituents spectra F (the endmembers) and their respective abundances contained in matrix G. Usually, the Linear Mixture Model (LMM) may be satisfied so that LMM can be written as [10]

$$X = G \cdot F, \tag{5.1}$$

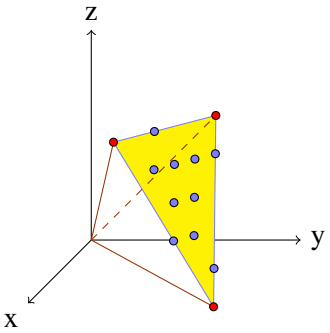

Figure 5.1 – Geometric point of view for Hyperspectral data.

where $X \in \mathbf{R}^{n \times m}$, n is the number of pixels and m the number of spectral bands. The abundance property (or full additivity) states that each row of G sums to 1, which may be expressed as

$$G \cdot 1_{p \times n} = 1_{n \times p} \tag{5.2}$$

X may be interpreted as n data points $\in \mathbf{R}^m$ which are generated from convex combinations of the endmembers contained in the rows of F. Since the p endmembers may be represented as belonging to $\mathbf{R}^m_+$, they may form vertices of a polytope. Due to the non-negative convex combination of these endmembers, n data points are lying inside a polytope delimited by the vertices formed with the rows of F. This interpretation is provided in Figure (5.1) in the case of $m = 3$ spectral bands. It may then be noticed that each row of G is lying in a $p-1$ unit simplex due to Eq (5.2).

The sum-to-1 constraint is often taken into account by considering that p variables are lying inside a $p-1$ simplex or by using ADMM [181]. Moreover, Eq. (5.2) may be usually split into individual constraints, which allows to solve several small problems [65].

5.2.2 Other sum-to-1 variables.

Another property encountered is a row sum-to-1 information associated with the second factor. Transposing Eq. (5.1) does not change the property. Sum-to-1 acts on the m entries of a row of F. Thus, it is completely different from the case of full additivity. This property is given as,

$$F_{p \times m} \cdot 1_{m \times m} = 1_{p \times m} \tag{5.3}$$

By using a geometrical viewpoint, the data matrix may be viewed as n row points lying in $\mathbf{R}^m_+$ which are non-negatively spanned by the p profiles. These profiles are belonging to a $m-1$ unit simplex according to Eq (5.3). The n data points are lying inside a convex hull spanned by these p profile vectors. So, the situation is quite different from the hyperspectral unmixing's case.

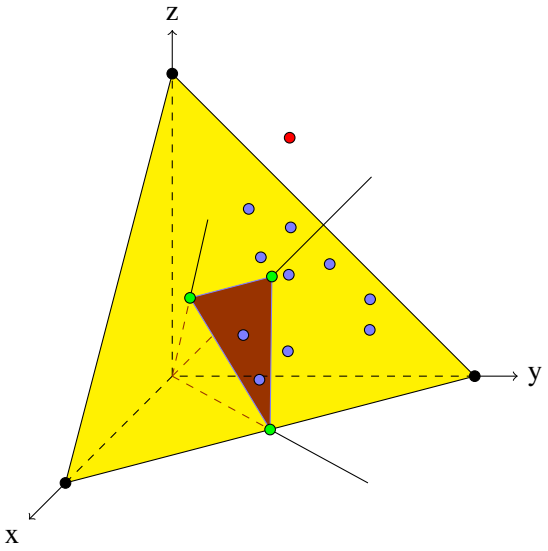

Figure 5.2 – Geometric point of view for chemical data.

5.2.3 Parametrization of the factors

The exact factorization of the data matrix $X = G \cdot F$ is assumed to be satisfied with the constraint of the sum-to-one of F. In this case, the sum of each data row could be evaluated

$$X_{n\times m} \cdot 1_{m\times m} = G_{n\times p} \cdot F_{p\times m} \cdot 1_{m\times m}, \tag{5.4}$$

$$= G_{n\times p} \cdot 1_{p\times m}, \tag{5.5}$$

This property states that the sum of each row of X is equal to the sum of each row of G when the exact factorization is assumed. When only approximate factorization is available, this property becomes an approximate relationship, i.e.,

$$G_{n\times p} \cdot 1_{p\times m} \approx X_{n\times m} \cdot 1_{m\times m}. \tag{5.6}$$

To authors best knowledge, such approximate constraints are not considered in the literature except by the authors from [91] who deal with both exact constraints.

Lantery [91] proposed to take into account such constraints by introducing auxiliary variables Z and T of appropriate dimensions which are only required to be non-negative and are respectively related to matrices F and G, [1]

$$F = \frac{Z}{Z \cdot 1_{m\times m}} \qquad \text{and} \qquad G = \frac{T \circ (X \cdot 1_{m\times p})}{T \cdot 1_{p\times p}}, \tag{5.7}$$

1. These definitions of the auxiliary variables corresponds to sum-to-1 variables along the rows whereas Lantery defined sum-to-1 variables along the columns. In order to perform the correpondence, the data matrix and the factors has to be transposed.

5.2.4 Solving the structured NMF problem

Lantery proposed to deal with such parametrization to solve the approximate NMF problem, e.g.,

$$\underset{G\succeq 0, F\succeq 0}{\operatorname{argmin}} \mathcal{J}(X, G\cdot F) \quad \text{s.t.} \begin{cases} F\cdot 1_{m\times m} = 1_{p\times m}, \\ G_{n\times p}\cdot 1_{p\times p} = X_{n\times m}\cdot 1_{m\times p}. \end{cases} \tag{5.8}$$

Using Eq. (5.7), Problem (5.8) could be formulated as an optimization problem with matrices Z and T, i.e.,

$$\{\hat{T},\hat{Z}\} = \underset{T\succeq 0, Z\succeq 0}{\operatorname{argmin}} \mathcal{J}\left(X, \frac{T\circ(X\cdot 1_{m\times p})}{T\cdot 1_{p\times p}}\cdot\frac{Z}{Z\cdot 1_{m\times m}}\right). \tag{5.9}$$

The Split Gradient Method (SGM) is an attractive approach [91] to solve the unconstrained Non-negative Matrix Factorization (NMF) problem as well as Problem (5.8). The SGM may be classified into Gradient based approaches. Eq (3.47) explains the descent scheme in the case of unconstrained NMF. Some relations with the multiplicative NMF are established by Lantery [91] in this case.

The purpose of this section is to develop the SGM technique for Problem (5.8). It needs to compute the gradient of the function $\mathcal{J}(X,.)$ with respect to each matrix factor. However, the focus is only on the rules for matrix F since the rules for G can be obtained similarly. Referring to Eq (5.7), the differentiation regarding Z_{ij} is taking into account the profile entries located in the same row due to Eq (5.8). So, the sum is acting on the column index j only, i.e.,

$$\frac{\partial \mathcal{J}}{\partial Z_{ik}} = \sum_{j=1}^{m}\frac{\partial \mathcal{J}}{\partial F_{ij}}\cdot\frac{\partial F_{ij}}{\partial Z_{ik}}. \tag{5.10}$$

The matrix differentiation with respect to Z_{ik} is derived from Eq (5.7)

$$\frac{\partial F_{ij}}{\partial Z_{ik}} = \frac{1}{\sum_l [Z]_{il}}\times(\delta_{jk} - [F]_{ij}) \tag{5.11}$$

where δ_{jk} is the kroneker delta function. It leads to drop the sum of the first term in the bracket, e.g.,

$$-\frac{\partial \mathcal{J}}{\partial Z_{ik}} = \frac{1}{\sum_l [Z]_{il}}\left((-\frac{\partial \mathcal{J}}{\partial F_{ik}}) - \sum_j [F]_{ij}(-\frac{\partial \mathcal{J}}{\partial F_{ij}})\right) \tag{5.12}$$

Starting from $-\frac{\partial \mathcal{J}}{\partial Z} = P - Q$,matrices P and Q may be chosen as

$$P = \left(-\frac{\partial \mathcal{J}}{\partial F}\right)_s \quad Q = \left(F\circ(-\frac{\partial \mathcal{J}}{\partial F})_s\right)\cdot 1_{m\times m} \tag{5.13}$$

where the subscript $_s$ stands for a shift applied to the partial differentiation $(-\frac{\partial \mathcal{J}}{\partial F})$. The SGM framework enables to conduct a gradient descent scheme on Z according to Eq (3.47),

$$Z^{k+1} = Z^k + \eta_F^k \circ Z^k \circ \left[\frac{\left(-\frac{\partial \mathcal{J}}{\partial F}\right)_s}{\left(F\circ(-\frac{\partial \mathcal{J}}{\partial F})_s\right)\cdot 1_{m\times m}} - 1_{p\times m}\right] \tag{5.14}$$

Using Eq (5.7) and by noticing that the flux along the rows is conservative –namely $Z^{k+1} \cdot 1_{m\times m} = Z^k \cdot 1_{m\times m}$– a simplified equation can be written as,

$$F^{k+1} = F^k + \eta_F^k \circ F^k \left[\frac{(\frac{-\partial \jmath}{\partial F^k})_s}{\left(F \circ (-\frac{\partial \jmath}{\partial F})_s\right) \cdot 1_{m\times m}} - 1_{p\times m} \right] \tag{5.15}$$

The same procedure could be applied to $\frac{G}{X \cdot 1_{m\times p}}$ since it is also a sum-to-1 variable, and it leads to a similar update rule with an extra scale factor, e.g.,

$$T^{k+1} = T^k + \eta_G^k \circ T^k \circ \left[\frac{(-\frac{\partial \jmath}{\partial G})_s}{\left(\frac{G}{X \cdot 1_{m\times p}} \circ (-\frac{\partial \jmath}{\partial G})_s\right) \cdot 1_{m\times m}} - 1_{p\times m} \right] \tag{5.16}$$

Then, the update rule for G should be derived by using the conservative property of the sum of T over iterations, e.g.,

$$G^{k+1} = G^k + \eta_G^k \circ G^k \left[\frac{(\frac{-\partial \jmath}{\partial G^k})_s}{\left(\frac{G}{X \cdot 1_{m\times p}} \circ (-\frac{\partial \jmath}{\partial G})_s\right) \cdot 1_{m\times m}} - 1_{n\times p} \right] \tag{5.17}$$

It could be noticed that a special form of $\eta_F^k = 1_{p\times m}$ leads to a multiplicative form of both update rules, e.g. for F,

$$F^{k+1} = F^k \frac{(\frac{-\partial \jmath}{\partial F^k})_s}{\left(F \circ (-\frac{\partial \jmath}{\partial F})_s\right) \cdot 1_{m\times m}} \tag{5.18}$$

Note also that the shift can be designed in several ways. Lantery proposed to use the following definition [91] in order to ensure the non-negativity,

$$\left(\frac{-\partial \jmath}{\partial F^k}\right)_s = \left(\frac{-\partial \jmath}{\partial F^k}\right) - \min_{i,j}\left(\frac{-\partial \jmath}{\partial F_{ij}^k}\right) 1_{p\times m}. \tag{5.19}$$

Finally, an example should be provided in order to illustrate the rules obtained in a simple case. Let's consider the Frobenius cost function, then the partial differentiation yields

$$\left(\frac{-\partial \jmath}{\partial F^k}\right)_s = G^T \cdot (X - G \cdot F) + \eta^k 1_{p\times m}. \tag{5.20}$$

where η^k is the shift scalar value at iteration k. In the case of a stepsize $\eta_F^k = 1_{p\times m}$, the update rule is

$$F^{k+1} = F^k \circ \frac{G^T \cdot (X - G^k \cdot F^k) + \eta^k 1_{p\times m}}{(F^k \circ (G^T \cdot (X - G^k \cdot F^k) + \eta^k 1_{p\times m})) \cdot 1_{m\times m}} \tag{5.21}$$

As a summary, the outline of the algorithm is provided in Algorithm (4)

Algorithm 4 SGM with sum-to-1 variables

Reading of X
Initialization of G and F
while the stopping rule is not fulfilled **do**
  Compute F with fixed G according to Eq. (5.15)
  Compute G with fixed F using Eq (5.17)
end while

5.3 Set Values in the Profile Matrix

5.3.1 Introduction

In several applications, the partial knowledge of variables is available. This knowledge is desired to be incorporated into algorithms. However, classical algorithms are providing a solution with a complete free variables. A projection onto the set of constraints may be performed either at the end of the iterations or at each iteration. The projection within iterations is illustrated in Alg. (5).

Algorithm 5 Projective NMF

while the stopping rule is not fulfilled **do**
  Update G with fixed F
  Update F with fixed G
  Project F onto the constraint subspace
end while

The projection of NMF within iterations onto the constraints is called here a projective NMF. So, a special parametrization which takes into account this knowledge is introduced. New algorithms for this parametrization are intended. The question to answer is whether this kind of algorithm would correspond to a simple projective NMF along the set of constraints.

5.3.2 Parametrization of the profile matrix

In several applications, the values of some entries of F may be provided by experts. The corresponding parameterization—proposed in [98] and outlined hereafter for the sake of clarity— takes into account this knowledge. Let Ω be a $p \times m$ binary matrix which informs the presence or the absence of constraints on each element F_{ij} of the matrix F, i.e.,

$$\Omega_{ij} \triangleq \begin{cases} 1 & \text{if } F_{ij} \text{ is known} \\ 0 & \text{otherwise} \end{cases} \tag{5.22}$$

Then the $p \times m$ binary matrix $\overline{\Omega}$ is defined as $\overline{\Omega} \triangleq 1_{p \times m} - \Omega$. Φ is the $p \times m$ sparse matrix of set values, i.e.,

$$\Phi \triangleq F \circ \Omega. \tag{5.23}$$

By construction, Φ_{ij}—the (i,j)-th element of Φ—is equal to zero when $\Omega_{ij}=0$. It can be easily proven that

$$\Phi \circ \Omega = \Phi, \qquad \Phi \circ \overline{\Omega} = 0. \tag{5.24}$$

From [98], ΔF is defined as the free part of the matrix profile under the form

$$\Delta F \triangleq F - \Phi \circ \Omega. \tag{5.25}$$

Following the general procedure in [98]—which combines Eqs. (5.25), (5.23), and (5.24)—the matrix F is obtained in the following form

$$F = \Omega \circ \Phi + \overline{\Omega} \circ \Delta F \tag{5.26}$$

Moreover, it may be noticed that this parametrization involves only non-negative matrices. As a result, F fulfills the following inequality,

$$F \succeq \Phi. \tag{5.27}$$

Matrix Φ is fixed and known in advance whereas ΔF accounts for the non-negative free matrix whose structure is imposed and which has to be found. Now, the parametrization (5.26) is used as a reference upon which it can be relied on.

5.3.3 New Informed Frobenius NMF versus naive projective Frobenius NMF.

In this section, we intend to develop dedicated methods for solving a NMF problem with constraints. The Frobenius case is highlighted here even if other dissimilarities may be used. The NMF problem under parametrization (5.26) may be reformulated as an optimization problem

$$\begin{aligned} \{G,F\} &= \arg\min_{G,F} \operatorname{Tr}\left((X-G\cdot F)^T((X-G\cdot F)\circ W)\right), \\ \text{s. t.} \qquad & G \succeq 0, \qquad F \succeq \Phi, \qquad F = \Omega \circ \Phi + \overline{\Omega} \circ \Delta F. \end{aligned} \tag{5.28}$$

The function $\mathcal{J}(.,.)$ is defined as $\mathcal{J}(.,.) \triangleq \operatorname{Tr}\left((X-G\cdot F)^T((X-G\cdot F)\circ W)\right)$. Problem (5.28) may be split into 2 coupled subproblems which alternatively set one unknown matrix, i.e.,

$$\begin{aligned} G^{k+1} &= \arg\min_{G\succeq 0} \operatorname{Tr}\left((X-G\cdot F^k)^T((X-G\cdot F^k)\circ W)\right), \\ F^{k+1} &= \arg\min_{F\succeq\Phi} \operatorname{Tr}\left((X-G^k\cdot F)^T((X-G^k\cdot F)\circ W)\right) \quad \text{s. t. } F = \Omega\circ\Phi + \overline{\Omega}\circ\Delta F. \end{aligned} \tag{5.29}$$

Let R be the residual matrix defined by $R \triangleq X - G\cdot(\Omega\circ\Phi)$. Appendix (A) derives the expression of the differentiation of $\mathcal{J}$ with respect to the free part of F, i.e.,

$$\frac{\partial \mathcal{J}}{\partial \triangle F} = 2\overline{\Omega} \circ \left(G^T \cdot ((G\cdot[\overline{\Omega}\circ\triangle F] - R)\circ W)\right). \tag{5.30}$$

The new method reported hereafter is introduced by using the 3^{rd} KKT condition which is available in Eq (A.14) [2]. It reads

$$\triangle F \circ \overline{\Omega} \circ \left(G^T \cdot (G \cdot [\overline{\Omega} \circ \triangle F]) \circ W)\right) = \triangle F \circ \overline{\Omega} \circ \left(G^T \cdot (R \circ W)\right) \tag{5.31}$$

By considering that $\triangle F = \triangle F^{k+1}$ or $\triangle F = \triangle F^k$, it could be easy to obtain the new update rules, i.e.,

$$\triangle F^{k+1} = \triangle F^k \circ \overline{\Omega} \circ \frac{G^T \cdot (R \circ W)}{G^T \cdot (G \cdot [\overline{\Omega} \circ \triangle F]) \circ W)} \tag{5.32}$$

Eq (5.32) should be seen as a projection operator on the free subspace. It behaves as a multiplicative scheme for the free entries. Note also that it considers equivalent data R instead of X in the classical scheme. As a consequence, R should be maintained non-negative along iterations. It is straightforward to check the 3^{rd} KKT condition by using these rules. In contrast, the 2^{nd} KKT condition is not ensured to be fulfilled since when $\triangle F_{ij} = 0$, the corresponding gradient entry may be negative. This problem is also reported in classical NMF in [66].

Another strategy may be used starting from Eq (5.31) and by moving $\triangle F \circ \overline{\Omega} \circ \left(G^T \cdot (G \cdot [\Omega \circ \Phi]) \circ W)\right)$ to the left side, e.g.,

$$\triangle F \circ \overline{\Omega} \circ \left(G^T \cdot (G \cdot [\Omega \circ \Phi + \overline{\Omega} \circ \triangle F]) \circ W)\right) = \triangle F \circ \overline{\Omega} \circ \left(G^T \cdot (X \circ W)\right). \tag{5.33}$$

The previous Equation yields

$$\triangle F^{k+1} = \triangle F^k \circ \overline{\Omega} \circ \frac{G^T \cdot (X \circ W)}{G^T \cdot (G \cdot [\Omega \circ \Phi + \overline{\Omega} \circ \triangle F]) \circ W)} \tag{5.34}$$

This method may be called naive method since it directly projects the unconstrained weighted rules onto the subspace of free entries. It also checks the 3^{rd} KKT condition. These two methods (5.32,5.34) may be also compared using the Split Gradient framework. The difference lies in a shift equal to $\overline{\Omega} \circ \left(G^T \cdot (G \cdot [\Omega \circ \Phi]) \circ W)\right)$ in the numerator and the denominator of the naive method. So the question which may be raised is: what is the difference between Eq. (5.32) and Eq. (5.34)? In fact, the difference comes from a numerical aspect. If Φ is considered to bear most of the information, namely each column $||\Phi_{:,i}||_1 >> ||\triangle F_{:,i}||_1$, then the numeric scheme (5.34) may be very slow due to a ratio of very large numbers. The number of iterations required becomes very huge. In the opposite case where $||\Phi_{:,i}||_1 << ||\triangle F_{:,i}||_1$, both schemes are performing equivalently since the residual matrix is close to X, i.e., $R \approx X$.

To conclude, it seems necessary to develop schemes which are not conventional Projective NMF. That is the purpose of the next section which focuses on the more general framework of $\alpha\beta$-divergences.

5.3.4 Informed $\alpha\beta$-divergence NMF

The problem to tackle here is the constrained NMF problem with a weighted $\alpha\beta$-divergence dissimilarity. This cost function is able to cope with a reasonable amount of outliers without beeing

2. The method is introduced in [96] by using a MM strategy. It leads exactly to the same expressions.

grossly affected. This part is a an outline from Limem 's work [96].

So, the first problem is formulated as

$$\begin{aligned} \{G,F\} &= \arg\min_{G,F} \mathcal{D}_W^{\alpha\beta}(X - G\cdot\Phi||G\cdot\triangle F) \\ \text{s. t.} \qquad & G\succeq 0, \qquad F\succeq\Phi, \qquad F=\Omega\circ\Phi+\overline{\Omega}\circ\triangle F. \end{aligned} \tag{5.35}$$

Problem (5.35) amounts to find an approximate solution to $X - G\Phi \approx G\triangle F$ in the $\alpha\beta$-divergence sense. Another viewpoint consist in trying to approximate X as $X \approx G\cdot(\Omega\circ\Phi)+G\cdot(\overline{\Omega}\circ\triangle F$, and it yields the second problem

$$\begin{aligned} \{G,F\} &= \arg\min_{G,F} \mathcal{D}_W^{\alpha\beta}(X||G\Phi + G\triangle F) \\ \text{s. t.} \qquad & G\succeq 0, \qquad F\succeq\Phi, \qquad F=\Omega\circ\Phi+\overline{\Omega}\circ\triangle F. \end{aligned} \tag{5.36}$$

Each problem is tackled in [96] using a MM strategy, by focusing on a column vector since each problem is separable into a set of vectorial subproblems.

The divergence of a column vector for Problems (5.35,5.36) is respectively expressed in the form,

$$\mathcal{D}_{\underline{w}}^{\alpha,\beta}(\underline{x}-G\cdot\underline{\varphi}||G\cdot\triangle\underline{f}) = \sum_i w_i\ \mathcal{D}^{\alpha,\beta}\left((\underline{x}-G\cdot\underline{\varphi})_i||(G\cdot\triangle\underline{f})_i\right), \tag{5.37}$$

and

$$\mathcal{D}_{\underline{w}}^{\alpha,\beta}(\underline{x}||G\cdot\underline{\varphi}+G\cdot\triangle\underline{f}) = \sum_i w_i\ \mathcal{D}^{\alpha,\beta}\left(x_i||(G\cdot\underline{\varphi})_i+(G\cdot\triangle\underline{f})_i\right). \tag{5.38}$$

Both equations can be expressed in terms of a single function $h^{\alpha,\beta}(z)$, defined as,

$$h^{\alpha,\beta}(z) = -\frac{1}{\alpha\beta}\left[z^{\beta}-\frac{\alpha}{\alpha+\beta}-\frac{\beta}{\alpha+\beta}z^{\alpha+\beta}\right] \quad \forall(\alpha,\beta,\alpha+\beta)\neq 0, \tag{5.39}$$

Let Γ be defined as the $p\times(p-l)$ orthonormal matrix of free parameters [96] linking the $p-l\times 1$ unknown vector $\underline{\theta}$ and the $p\times 1$ free column vector $\triangle\underline{f}$,

$$\triangle\underline{f} = \quad \Gamma\cdot\underline{\theta}, \tag{5.40}$$

and l is the number of set values in the current column vector. For the sake of clarity, let the matrix U (with general entry u_{ij}) be

$$U \triangleq G\cdot\Gamma. \tag{5.41}$$

and let λ be $\lambda \triangleq \alpha+\beta-1$. Using the previous scale property of the divergence (4.31), Eq. (5.37) and Eq. (5.38) become

$$\mathcal{D}_{\underline{w}}^{\alpha,\beta}(\underline{x}-G\cdot\underline{\varphi}||G\cdot\triangle\underline{f}) = \sum_i w_i\ (\underline{x}-G\cdot\underline{\varphi})_i^{\alpha+\beta}\ h^{\alpha,\beta}\left(\frac{\sum_j u_{ij}\theta_j}{(\underline{x}-G\cdot\underline{\varphi})_i}\right), \tag{5.42}$$

and

$$\mathcal{D}_{\underline{w}}^{\alpha,\beta}(\underline{x}||G\cdot\underline{\varphi}+G\cdot\triangle\underline{f})=\sum_i w_i\, x_i^{\alpha+\beta}\;\; h^{\alpha,\beta}\left(\frac{(G\cdot\underline{\varphi})_i+\sum_j u_{ij}\theta_j}{x_i}\right). \tag{5.43}$$

The function $h^{\alpha,\beta}(z)$ has the property of convexity for all $z>0$ in the domain of parameters described by $\beta\in[min(1,1-\alpha);max(1,1-\alpha)]$. This parameter domain is chosen so that the convexity property is preserved. Based on the convexity of $h^{\alpha,\beta}(z)$ and similarly to [96] (chap 3, p 83), two majoring functions may be deduced by applying twice the Jensen inequality ,

$$\mathcal{H}_{1,w}^{\alpha,\beta}(\theta_j,\theta_j^k)=\sum_i w_i\,(\underline{x}-G\underline{\varphi})_i^{\alpha+\beta}\sum_j\frac{u_{ij}\,\theta_j^k}{\sum_l u_{il}\,\theta_l^k}\cdot h^{\alpha,\beta}\left(\frac{\theta_j\sum_l u_{il}\,\theta_l^k}{(\underline{x}-G\underline{\varphi})_i\,\theta_j^k}\right), \tag{5.44}$$

and

$$\mathcal{H}_{2,w}^{\alpha,\beta}(\theta_j,\theta_j^k)=\sum_i w_i x_i^{\lambda}(\underline{x}-G\underline{\varphi})_i\sum_j\frac{u_{ij}\,\theta_j^k}{\sum_l u_{il}\,\theta_l^k}\cdot h^{\alpha,\beta}\left(\frac{\theta_j\sum_l u_{il}\,\theta_l^k}{(\underline{x}-G\underline{\varphi})_i\,\theta_j^k}\right). \tag{5.45}$$

Both majoring functions are the basis to design new update rules. Let us begin with the first majoring function.

5.3.4.1 First approach with residual

By cancelling the differentiation of the auxiliary function (5.44), the update rule of the j^{th} entry of the vector of the free parameters $\underline{\theta}$ is,

$$\left(\frac{\theta_j}{\theta_j^k}\right)^{\alpha}=\frac{\sum_i w_i u_{ij}\cdot\underline{r}_i^{\alpha}\cdot(\sum_l u_{il}\theta_l^k)^{\beta-1}}{\sum_i w_i u_{ij}\cdot(\sum_l u_{il}\theta_l^k)^{\lambda}}. \tag{5.46}$$

Therefore, the vector of free parameters may be expressed in the form,

$$\left(\frac{\underline{\theta}}{\underline{\theta}^k}\right)^{\alpha}=\frac{U^T\cdot\left[\underline{w}\circ\underline{r}^{\alpha}\circ(U\cdot\underline{\theta}^k)^{\beta-1}\right]}{U^T\cdot\left[\underline{w}\circ(U\cdot\underline{\theta}^k)^{\lambda}\right]}. \tag{5.47}$$

By combining Eq. (5.40) with the above relationship, the expression of one column of the matrix $\triangle F$ is derived:

$$\frac{\triangle\underline{f}^{k+1}}{\triangle\underline{f}^k}=\left[\frac{\Gamma\cdot U^T\cdot[\underline{w}\circ\underline{r}^{\alpha}\circ(U\cdot\underline{\theta}^k)^{\beta-1}]}{\Gamma\cdot U^T\cdot[\underline{w}\circ(U\cdot\underline{\theta}^k)^{\lambda}]}\right]^{\frac{1}{\alpha}}. \tag{5.48}$$

By replacing U according to Eq. (5.41), and by noticing that $\Gamma\cdot\Gamma^T=\mathrm{diag}(\overline{\underline{\omega}})=\mathrm{diag}(1_{p\times1}-\underline{\omega})$, the new update rule is derived:

$$\triangle\underline{f}^{k+1}\leftarrow\triangle\underline{f}^k\circ\overline{\underline{\omega}}\circ M_{\underline{f}^k}^{\alpha,\beta}, \tag{5.49}$$

where

$$M_{\underline{f}^k}^{\alpha,\beta}\triangleq\left(\frac{G^T\left[\underline{w}\circ\underline{r}^{\alpha}\circ(G\cdot\triangle\underline{f}^k)^{\beta-1}\right]}{G^T\left[\underline{w}\circ\underline{r}^{\alpha}\circ(G\cdot\triangle\underline{f}^k)^{\lambda}\right]}\right)^{\frac{1}{\alpha}}. \tag{5.50}$$

Eq. (5.49) may be extended to the matrix case by noticing that $\triangle \underline{f}$, $\underline{\omega}$ et $\underline{\varphi}$ are respectively vectors extracted from general matrices $\triangle F$, Ω et Φ. Then, the free matrix expression is (with $F^{k+1} = \Omega \circ \Phi + \overline{\Omega} \circ \triangle F^{k+1}$)

$$\triangle F^{k+1} = \triangle F^k \circ \overline{\Omega} \circ M_F^{\alpha,\beta}(G^k, F^k), \tag{5.51}$$

where $M_F^{\alpha,\beta}(G,F)$ accounts for

$$M_F^{\alpha,\beta}(G,F) = \left[\frac{G^T \cdot \left(W \circ R^{\alpha} \circ (G \cdot (F \circ \Omega))^{\beta-1} \right)}{G^T \cdot \left(W \circ (G \cdot (F \circ \Omega))^{\lambda} \right)} \right]^{(\frac{1}{\alpha})}, \tag{5.52}$$

and the residual matrix R is defined as $R \triangleq X - G \cdot \Phi$. The corresponding update rule for the contribution matrix remains unconstrained so that it follows the rule (4.58) which is recalled here

$$G \leftarrow G \circ \left[\frac{\left(W \circ X^{\alpha} \circ (G \cdot F)^{\beta-1} \right) F^T}{(W \circ (G \cdot F)^{\lambda}) F^T} \right]^{(\frac{1}{\alpha})}. \tag{5.53}$$

Equations (5.51,5.52,5.53) are the basis relationships of the Informed NMF method with residual based on weighted $\alpha\beta$-divergence.

5.3.4.2 Second approach without residual

Similarly, the update rules for the second approach may be obtained. Appendix (B) derives a complete proof of the update rules. The matrix form of the update rules for F are outlined hereafter

$$\triangle F^{k+1} = \triangle F^k \circ \overline{\Omega} \circ N_F^{\alpha,\beta}(G^k, F^k), \tag{5.54}$$

where $N_F^{\alpha,\beta}(G,F)$ is given by

$$N_F^{\alpha,\beta}(G,F) = \left[\frac{G^T \left(W \circ X^{\lambda} \circ R^{1-\beta} \circ (G \cdot (F \circ \Omega))^{\beta-1} \right)}{G^T (W \circ X^{\lambda} \circ R^{1-\alpha-\beta} \circ (G \cdot (F \circ \Omega))^{\lambda})} \right]^{(\frac{1}{\alpha})}. \tag{5.55}$$

In addition, the update rules for the contribution matrix remains the same as defined in Eq. (5.53). It should be stressed that $N_F^{\alpha,\beta}(G,F)$ in Eq. (5.55) and $M_F^{\alpha,\beta}(G,F)$ in Eq. (5.52) are the same if W is replaced in the latter expression by

$$W \triangleq W' \circ X^{\lambda} \circ R^{-\lambda}. \tag{5.56}$$

This means that the update rules for F may be viewed similar if the weights iteratively updated. [3]

The update rules of the second approach are based on Eqs (5.55,5.54) and Eq. (5.53) in the domain ($\beta \in [min(1, 1-\alpha); max(1, 1-\alpha)]$) [4]. The validity is only guaranteed within this convex domain. Outside this domain, some additional assumptions on the reconstructed data are needed to ensure the

3. However, the update rules for G would become different.
4. The same argument stands also for the first method.

local convexity property [27]. As we chose to set α and β so that they belong to Area 2 in Fig. (4.4), the convexity domain reduces the possible area to the intersection between Area 2 and the half-plane $\beta \leq 1$.

Besides, Limem [96] proved that the the KKT conditions are fulfilled for both methods [5].

5.3.5 Conclusion

In this section, solutions of NMF Problem with set values are presented and discussed. Different cost functions are investigated leading to different solutions. The special framework of $\alpha\beta$-divergences enables to propose 2 different NMF solutions depending on the way the dissimilarity is used. This framework enables to involve many other dissimilarities by an appropriate choice of parameters α and β. In addition, a weighted approach allows to consider various confidence in the measurements.

However, only one kind of constraints have been taken into account for the moment, either sum-to-1 constraints or set values. These one are conflicting since imposing one kind of constraints prevents to keep the other one. Now, we would like to cope with both kind of constraints in the next section.

5.4 NMF with set values and sum-to-1 variables

5.4.1 Introduction

The distinct implementation of the sum-to-1 constraints and the flexible set values in one factor has just been investigated. This has led to new update rules for F which are outlined in the previous sections. However, the simultaneous constraints are not dealt with. Subsequently, the proposed approach is to drop one constraint and apply an informed NMF scheme intended for the other kind of constraint, and then to perform a projection step on the remaining subspace corresponding to the other constraint. Thus, algorithms which are based on such a scheme are investigated in [102] where the

Algorithm 6 Projected Informed NMF scheme

while the stopping rule is not fulfilled **do**
  Compute F with fixed G
  Compute G with fixed F
  Project onto the subspace of dropped constraints
end while

emphasis is performed on both constraints in conjunction with projected Gradient. Note that,being multiplicative, the previous algorithms may generally be viewed as a special case of the gradient descent. As a consequence, a close connection with Lin's methods [102] may be established.

5. For a complete study of KKT conditions, please refer to [96]

5.4.2 Formulation of the different problems with both constraints

The general formulation of an approximate NMF solution under described constraints is

$$\underset{G,F}{\operatorname{argmin}}\, \mathcal{D}_W^{\alpha,\beta}\left(X||G\cdot F\right) \text{ s.c. } \begin{cases} F \succeq 0, G \succeq 0, \\ F \circ \Omega = \Phi, \\ F \cdot 1_{mm} = 1_{p\times m}. \end{cases} \tag{5.57}$$

Using the parametrization described in (5.26), Eq. (5.57) reduces to

$$\begin{aligned} &\min_{G,\Delta F}\ \mathcal{D}_W^{\alpha,\beta}\left(X||G\cdot(\Omega\circ\Phi)+G\cdot(\overline{\Omega}\circ\Delta F)\right) \\ &\qquad \text{s.t.} \begin{cases} \Delta F \succeq 0, G \succeq 0, \\ \Delta F \cdot 1_{mm} = 1_{p\times m} - \Phi\cdot 1_{mm}. \end{cases} \end{aligned} \tag{5.58}$$

An alternative inspired by variants found in previous sections may be investigated under the form

$$\begin{aligned} &\underset{G,\Delta F}{\operatorname{argmin}}\, \mathcal{D}_W^{\alpha,\beta}\left(X - G\cdot\Phi||G\cdot(\overline{\Omega}\circ\Delta F)\right) \\ &\qquad \text{s.t.} \begin{cases} \Delta F \succeq 0, G \succeq 0, \\ \Delta F \cdot 1_{mm} = 1_{p\times m} - \Phi\cdot 1_{mm}. \end{cases} \end{aligned} \tag{5.59}$$

Eq. (5.58,5.59) are the reference problems to be solved. The next section is dedicated to review what was done in Limem's work [96]. In the following sections, the definition which gathers the different masks is adopted, e.g.,

$$R_F^{\alpha,\beta} \triangleq \begin{cases} M_F^{\alpha,\beta} & \text{for the problem } (5.58), \\ N_F^{\alpha,\beta} & \text{for the problem } (5.59), \end{cases} \tag{5.60}$$

where $M_F^{\alpha,\beta}$ is defined according to Eq (5.52) while $N_F^{\alpha,\beta}$ relies on Eq (5.55).

5.4.3 NMF with set values and basic normalization

It is proposed to drop first the sum-to-1 constraint, perform an update which takes into account only the set values, and then to project the results onto the unit simplex. The unit simplex is defined as a component wise form

$$\sum_{j=1}^{m} f_{ij} = 1 \quad \forall = 1,.....,p, \tag{5.61}$$

or as its matrix form

$$F_{p\times m}\cdot 1_{m\times m} = 1_{p\times m} \tag{5.62}$$

To project onto the unit simplex [6], a normalization of the current estimate F may be performed. According to [91], it is possible to perform a normalization step (which may be viewed as an oblique

6. The projection onto the unit ball is usually defined by minimizing the Euclidian distance between the original point and its projection [33].

projection)

$$\tilde{F} = \frac{F}{F \cdot 1_{m\times m}}. \tag{5.63}$$

Eq. (5.63) is an ℓ_1 row normalization whereas a scaling along the columns of G may be performed, i.e.,

$$\tilde{G} = G \circ [1_{n\times m} \cdot F^T]. \tag{5.64}$$

These two joint steps are called hereafter normalization 1. The product $\tilde{G}\cdot\tilde{F}$ may be evaluated, using its matrix form,

$$\tilde{G}\cdot\tilde{F} = \frac{F}{F \cdot 1_{m\times m}} \cdot \left(G \circ [1_{nm} \cdot F^T]\right), \tag{5.65}$$

or using its general entry,

$$(\tilde{G}\cdot\tilde{F})_{ij} = \sum_k \frac{G_{ik}}{\sum_l F_{kl}} \cdot F_{ki} \cdot \sum_l F_{kl} = \sum_k G_{ik} F_{ki} = (G\cdot F)_{ij}. \tag{5.66}$$

It turns out that $\tilde{G}\cdot\tilde{F} = G\cdot F$ and it means that the operating point is not changed after these steps. This ensures that the descent direction proposed in previous algorithms is kept unchanged, and consequently ensures a sufficient decrease of the cost function. However, set values are not preserved, but it is expected to reach a limit point which checks both constraints including set values. The corresponding algorithm may be outlined as shown below:

Algorithm 7 Structure of the NMF algorithm with normalization

while the stopping rule is not fulfilled **do**
  Compute F with fixed G using Eq (5.55)
  Compute G with fixed F according to Eq. (5.53)
  Normalization 1 of G and F
end while

The algorithm (7) could be outlined in a single step. To achieve this, the update rule for F is reformulated as

$$\tilde{F}^{k+1} = \frac{\Omega\circ\Phi + \tilde{F}^k \circ \overline{\Omega} \circ R_F^{\alpha,\beta}(\tilde{G}^k, \tilde{F}^k)}{\left[\Omega\circ\Phi + \tilde{F}^k \circ \overline{\Omega} \circ R_F^{\alpha,\beta}(\tilde{G}^k, \tilde{F}^k)\right] 1_{mm}}, \tag{5.67}$$

It is also recalled that $\tilde{}$ operator means sum-to-1 variable for F and rescaled variable for G. The contribution matrix $\tilde{G}^{k+1}$ is expressed in its compact form as

$$\tilde{G}^{k+1} = \tilde{G}^k \circ M_G^{\alpha,\beta}(\tilde{G}^k, \tilde{F}^k) \circ (1_{nm} \cdot [\Omega\circ\phi + \tilde{F}^k \circ \overline{\Omega} \circ R_F^{\alpha,\beta}(\tilde{G}^k, \tilde{F}^k)]^T) \tag{5.68}$$

where the expression of $M_G^{\alpha,\beta}(G,F)$ is defined in Eq. (4.58). The drawback of this method is in its unability to keep the set values at the end of each iteration. Now, an alternative solution is investigated.

5.4.4 Alternative solution with normalization of free entries.

Limem [96] proposed to directly take into account both constraints, set values and the sum-to-1 of the profile matrix F. A new parametrization may be defined as,

$$\tilde{F} = \Omega \circ \Phi + \frac{Z \circ \overline{\Omega}}{(Z \circ \overline{\Omega}) \cdot 1_{m \times m}} \circ (1_{p \times m} - \Phi \cdot 1_{m \times m}), \tag{5.69}$$

where,

— $\Omega \circ \Phi$ accounts for the set values.

— $(1_{p \times m} - \Phi \cdot 1_{m \times m})$ is the matrix that consists of the sum of each row of the free entries

— $\frac{\overline{\Omega} \circ Z}{(\overline{\Omega} \circ Z) \cdot 1_{m \times m}}$ represents the different proportions of the free components.

Starting with an unnormalized version of F satisfying Eq. (5.23), then Eq. (5.69) suggests a new way to normalize a current profile F, while preserving set values, i.e.,

$$\tilde{F} = \Omega \circ F + \frac{\overline{\Omega} \circ F}{(\overline{\Omega} \circ F) \cdot 1_{mm}} \circ (1_{p \times m} - \Phi \cdot 1_{mm}) \tag{5.70}$$

Eq. (5.70) is the reference equation for a new normalization, denamed as N_2 normalization. From Eq. (5.54), the new normalized free part $\Delta \tilde{F}^k$ can be written as,

$$\triangle \tilde{F}^{k+1} = \frac{\overline{\Omega} \circ R_F^{\alpha,\beta} \circ \triangle \tilde{F}^k}{\left[\overline{\Omega} \circ R_F^{\alpha,\beta} \circ \triangle \tilde{F}^k\right] \cdot 1_{m \times m}} \circ (1_{p \times m} - \Phi \cdot 1_{m \times m}). \tag{5.71}$$

Then, it results in a complete normalized profile matrix,

$$\tilde{F}^{k+1} = \Omega \circ \Phi + \frac{\overline{\Omega} \circ R_F^{\alpha,\beta} \circ \triangle \tilde{F}^k}{\left[\overline{\Omega} \circ R_F^{\alpha,\beta} \circ \triangle \tilde{F}^k\right] 1_{m \times m}} \circ (1_{p \times m} - \Phi \cdot 1_{m \times m}), \tag{5.72}$$

which yields an expression related to the normalized profile $\tilde{F}^k$ at iteration k,

$$\tilde{F}^{k+1} = \Omega \circ \Phi + \frac{\overline{\Omega} \circ \tilde{F}^k \circ R_F^{\alpha,\beta}}{\left[\overline{\Omega} \circ \tilde{F}^k \circ R_F^{\alpha,\beta}\right] 1_{m \times m}} \circ (1_{p \times m} - \Phi \cdot 1_{m \times m}). \tag{5.73}$$

It should be stressed that this solution does not preserve the operating point (without normalization) and it may change the descent direction when processing the normalization. The update rule for G is not constrained at all because no scaling is allowed for G, it remains the same as previously except that the mask is applied with $\tilde{F}^k$, i.e.,

$$G^{k+1} = G^k \circ M_G^{\alpha,\beta}(G^k, \tilde{F}^k), \tag{5.74}$$

Table 5.1 – Different methods with Normalization

Methods	Rules on F	Rules on G	Mask on F	Mask on G
αβ-N_1-CWNMF-R	Eq (5.67)	Eq (5.68)	$M_F^{\alpha,\beta}(\tilde{G}^k,\tilde{F}^k)$	$M_G^{\alpha,\beta}(\tilde{G}^k,\tilde{F}^k)$
αβ-N_1-CWNMF	Eq (5.67)	Eq (5.68)	$N_F^{\alpha,\beta}(\tilde{G}^k,\tilde{F}^k)$	$M_G^{\alpha,\beta}(\tilde{G}^k,\tilde{F}^k)$
αβ-N_2-CWNMF-R	Eq (5.73)	Eq (5.74)	$M_F^{\alpha,\beta}(G^k,\tilde{F}^k)$	$M_G^{\alpha,\beta}(G^k,\tilde{F}^k)$
αβ-N_2-CWNMF	Eq (5.73)	Eq (5.74)	$N_F^{\alpha,\beta}(G^k,\tilde{F}^k)$	$M_G^{\alpha,\beta}(G^k,\tilde{F}^k)$

5.4.5 Algorithm summary

Table (5.1) outlines the different algorithms and the corresponding acronyms used herafter. They are all expressed in the form $\alpha\beta - N - CWNMF(-R)$ for Normalized and Constrained Weighted αβ-NMF (with or without) residuals. Practically, the two normalizations used above are formulated as N_1 or N_2. It is stressed that a backward update of the mask is applied and is computed with the previous operating point G^k or $\tilde{G}^k$ and $\tilde{F}^k$ which is a slight modification of what has been proposed in [96]. As a summary, four methods can be used to solve the constrained NMF problem.

In addition, other informed methods should have been adapted to this context. However, they can not be mentioned as reference methods because they are not available in the litterature. First, a semi informed Lantéri method [91] could be imagined where only the update of F would be required to follow a sum-to-1 scheme. A projected version of Lanteri's method onto the set values is another approach. The projection corresponds then to the mapping of Lantéri's update onto the set values.

5.5 Conclusion

In this chapter, sum-to-1 variables are first investigated. It is mentioned that each profile row accounts for a sum-to-1 variable which is noticed as a different situation from abundances in hyperspectral unmixing. Then, Lantery' Split Gradient Method is reviewed with a specific parametrization.

In a second part, set values in NMF problems are discussed and dedicated methods in the framework of αβ-divergences are presented, which yields two different update rules depending on the way the dissimilarity is performed.

Then, both sum-to-1 and set values constraints are considered in the NMF problem. It is tackled by using the previous update rules followed by a inner projection onto the unit simplex, called normalization. This normalization is either performed on a complete row of F or performed only on the free remaining variables of one row. However, each solution has its own drawbacks and none of them is completely satisfactory.

As a result, in the next chapter, the core of this thesis is presented and new informed NMF methods are developed and are implemented in the interior domain of the whole constraints.

CHAPTER 6

New Informed NMF methods

6.1 Introduction

In this chapter, new Informed NMF-based methods to address the source apportionment problem are proposed and presented. They incorporate the sum-to-1 property and set values in the profile matrix F.

The theoretical aspect of this chapter is based on the conference articles that are written during this thesis [26, 25, 24]. The first part is devoted to present a new parametrization of the profile matrix F which serves as a basis to develop new algorithms.

In the second part, new algorithms are presented, with a special emphasis on specific cost functions. All these algorithms are based on Split Gradient Methods developed by Lanteri et al [91] together with the new parametrization. Three variants of these methods are proposed and each depends on the cost function under consideration. Thus, the weighted Frobenius, the weighted $\alpha\beta$-divergence and the weighted Huber cost function are considered in order to achieve the factorization process. In each case, the corresponding update rules are derived and the analytical expressions are introduced.

In the third part, experiments are conducted using respectively "a toy simulation", a medium scale simulation extracted from real data, and a real data case. The performance of each approach is investigated in order to evaluate the potential improvement over existing methods.

6.2 Parametrization of the profile matrix

In many applications, the values of some components of the profile matrix may be provided by experts. In addition, each row of the profile matrix sums to 1. So, the objective of this section is to provide a parametrization which takes into account the above knowledge i.e., both constraints.

The general parametrization of the profile with set values used in chapter (5) is first recalled

$$F = \Omega \circ \Phi + \overline{\Omega} \circ \Delta F. \tag{6.1}$$

It should be noted that each row of F sums to 1 implies that

$$(\overline{\Omega} \circ \Delta F) \cdot 1_{m\times m} = 1_{p\times m} - \Phi \cdot 1_{m\times m} \succeq 0 \tag{6.2}$$

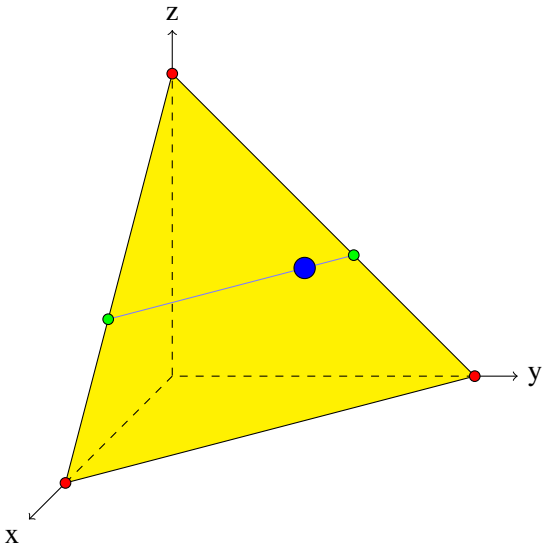

Figure 6.1 – Geometric plot of an informed source profile.

This means that $\overline{\Omega} \circ \Delta F$ may be viewed as a scaled sum-to-1 variable as in [91]. As a consequence, an unconstrained matrix Z [1] of the same size as the profile matrix F is defined, such that

$$F \circ \overline{\Omega} = \overline{\Omega} \circ \Delta F = \frac{\overline{\Omega} \circ Z}{(\overline{\Omega} \circ Z) \cdot 1_{m \times m}} \circ (1_{p \times m} - \Phi \cdot 1_{m \times m}). \tag{6.3}$$

Thus, the new parameterization is derived from Eq. (6.1) i.e.,

$$F = \Omega \circ \Phi + \frac{\overline{\Omega} \circ Z}{(\overline{\Omega} \circ Z) \cdot 1_{m \times m}} \circ (1_{p \times m} - \Phi \cdot 1_{m \times m}). \tag{6.4}$$

where $\overline{\Omega} \circ Z$ is required to be non-negative.

As an example, assume that F is a 1×3 profile matrix with $\Omega = [0,0,1]$ and $\Phi = [0,0,0.4]$. The expert knowledge then consists in the last entry of the source profile which is equal to 0.4.

The definition of Φ leads to

$$1_{1 \times 3} - \Phi \cdot 1_{3 \times 3} = [0.6, 0.6, 0.6]. \tag{6.5}$$

As a consequence, the parameterization based on Eq. (6.4) reads

$$F = \left[\frac{Z_{11} \cdot 0.6}{Z_{11} + Z_{12}}, \frac{Z_{12} \cdot 0.6}{Z_{11} + Z_{12}}, 0.4 \right]. \tag{6.6}$$

Figure (6.1) illustrates potential positions of the single source profile which may be on the green segment delimited by the two green extreme points. The blue point is an example of such profile. More generally, a source profile is defined as part of a polyhedron in $\mathbb{R}_+^m$.

1. Z is only required to be non-negative.

As for Eq. (6.4), a similar parameterization may be applied to G. In that case, the sum of each row of G should be equal to the sum of each row of X. Such a strategy was proposed in [91] for non-informed NMF. However, such parameterization is not applicable here because it is only valid in the framework of an exact factorization. Indeed, while the parameterization (6.4) is derived from the definition of the profile matrix, only an approximate row sum constraint may be applied to G. In addition, outliers may affect even more this relationship.

The parameterization (6.4) is the basis to develop the new informed methods. In the next section, the Split Gradient NMF is adapted to the context of this new parametrization and it will take into account several robust cost functions.

6.3 Informed Split Gradient NMF methods

6.3.1 Several problems to solve

The first problem to tackle is based on the Frobenius cost function in conjunction with the previous parametrization [26], e.g.,

$$\min \mathcal{J}(G,F) \triangleq \min_{G\succeq 0, F\succeq 0} \|X - G\cdot F\|^2_{\mathcal{F},W} \quad \text{s.t. } F \text{ satisfies Eq. (6.4)}, \tag{6.7}$$

The $\alpha\beta$-divergence cost function is a robust cost function which extends the previous one, so the new problem can be formulated as [25],

$$\min \mathcal{J}(G,F) \triangleq \min_{G\succeq 0, F\succeq 0} \mathcal{D}_W^{\alpha,\beta}(X||G\cdot F) \quad \text{s.t. } F \text{ satisfies Eq. (6.4)}, \tag{6.8}$$

Another cost function which is able to cope with outliers is the weighted Huber cost function

$$\min \mathcal{J}(G,F) \triangleq \min_{G\succeq 0, F\succeq 0} \mathcal{R}_{\sigma}^{Huber}(R) \quad \text{s.t. } F \text{ satisfies Eq. (6.4)}, \tag{6.9}$$

where R is defined as the residual matrix and the weighted Huber cost function is given by

$$\mathcal{R}_{\sigma}^{Huber}(R) \triangleq \sum_{i,j} \rho^{Huber}\left(\frac{r_{i,j}}{\sigma_{i,j}}\right). \tag{6.10}$$

All these problems are difficult to split into independent vectorial problems. Thus, a MM strategy may be difficult to apply and consequently, new tracks should be explored. That is, a SGM scheme based on partial differentiation of auxiliary variables is adopted in the following.

6.3.2 Computation of $\frac{\partial \mathcal{J}}{\partial Z}$

Since the parametrization is related to a matrix Z, a scheme which is related to Z is to be derived. To achieve this objective, the differentiation of $\mathcal{J}(.)$ with respect to its general term Z_{ik}, which is related to the i-th row of F only, is required. The differentiation is then expressed as a sum of partial

differentiations with respect to each general entry of F belonging to the same row, e.g.,

$$\frac{\partial \mathcal{J}}{\partial Z_{ik}} = \sum_{j=1}^{m} \frac{\partial \mathcal{J}}{\partial F_{ij}} \cdot \frac{\partial F_{ij}}{\partial Z_{ik}}. \tag{6.11}$$

The first step involves the differentiation of Eq. (6.4) to express $\frac{\partial F_{ij}}{\partial Z_{ik}}$, e.g.,

$$\frac{\partial F_{ij}}{\partial Z_{ik}} = (1 - \sum_{l=1}^{m} \Phi_{il}) \frac{\partial}{\partial Z_{ik}} \left(\frac{\overline{\Omega}_{ij} Z_{ij}}{\sum_{l=1}^{m} \overline{\Omega}_{il} Z_{il}} \right). \tag{6.12}$$

Noticing that $\frac{\partial}{\partial Z_{ik}} (\sum_{l=1}^{m} \overline{\Omega}_{il} Z_{il}) = \overline{\Omega}_{ik}$, Eq (6.12) can be written as:

$$\frac{\partial}{\partial Z_{ik}} \left(\frac{\overline{\Omega}_{ij} Z_{ij}}{\sum_{l=1}^{m} \overline{\Omega}_{il} Z_{il}} \right) = \frac{\overline{\Omega}_{ik} \delta_{jk}}{\sum_{l=1}^{m} \overline{\Omega}_{il} Z_{il}} + \overline{\Omega}_{ij} Z_{ij} \frac{\partial}{\partial Z_{ik}} \left(\frac{1}{\sum_{l=1}^{m} \overline{\Omega}_{il} Z_{il}} \right), \tag{6.13}$$

$$= \frac{\overline{\Omega}_{ik} \delta_{jk}}{\sum_{l=1}^{m} \overline{\Omega}_{il} Z_{il}} - \frac{\overline{\Omega}_{ij} Z_{ij}}{\left(\sum_{l=1}^{m} \overline{\Omega}_{il} Z_{il} \right)^2} \overline{\Omega}_{ik}, \tag{6.14}$$

where δ_{jk} is the Kronecker function and is equal to 1 when $j = k$. Eq. (6.12) is then expressed as:

$$\frac{\partial F_{ij}}{\partial Z_{ik}} = (1 - \sum_{l=1}^{m} \Phi_{il}) \frac{\overline{\Omega}_{ij}}{\sum_{l=1}^{m} \overline{\Omega}_{il} Z_{il}} \left[\delta_{jk} - \frac{\overline{\Omega}_{ik} Z_{ij}}{\sum_{l=1}^{m} \overline{\Omega}_{il} Z_{il}} \right]. \tag{6.15}$$

In the second step, $\mathcal{J}(.)$ is differentiated with respect to Z_{ik} using Eq. (6.11). The substitution of Eq. (6.15) into Eq. (6.11) leads to

$$\frac{\partial \mathcal{J}}{\partial Z_{ik}} = \frac{1 - \sum_l \Phi_{il}}{(\sum_{l=1}^{m} Z_{il} \overline{\Omega}_{il})} \left(\frac{\partial \mathcal{J}}{\partial F_{ik}} . \overline{\Omega}_{ik} - \frac{\overline{\Omega}_{ik}}{(\sum_{l=1}^{m} Z_{il} \overline{\Omega}_{il})} \sum_{j=1}^{m} (\frac{\partial \mathcal{J}}{\partial F_{ij}} . Z_{ij} . \overline{\Omega}_{ij}) \right), \tag{6.16}$$

which can be transformed into a matrix form by noticing that the sums in the above equation correspond to the right multiplication by $1_{m \times m}$.

$$\frac{\partial \mathcal{J}}{\partial Z} = \frac{1_{p \times m} - \Phi \cdot 1_{m \times m}}{(Z \circ \overline{\Omega}) \cdot 1_{m \times m}} \circ \left[\frac{\partial \mathcal{J}}{\partial F} \circ \overline{\Omega} - \overline{\Omega} \circ \left((\frac{\partial \mathcal{J}}{\partial F} \circ \frac{Z \circ \overline{\Omega}}{(Z \circ \overline{\Omega}) \cdot 1_{m \times m}}) \cdot 1_{m \times m} \right) \right]. \tag{6.17}$$

By noticing that for any matrices A and B,

$$(\frac{B}{A \cdot 1_{m \times m}}) \cdot 1_{m \times m} = \frac{(B \cdot 1_{m \times m})}{(A \cdot 1_{m \times m})} \tag{6.18}$$

and that

$$\frac{\overline{\Omega} \circ Z}{(\overline{\Omega} \circ Z) \cdot 1_{m \times m}} = \frac{\overline{\Omega} \circ F}{1_{p \times m} - \Phi \cdot 1_{m \times m}}, \tag{6.19}$$

the matrix form of Eq. (6.16) is

$$\frac{\partial \mathcal{J}}{\partial Z} = \frac{1_{p\times m} - \Phi \cdot 1_{m\times m}}{(Z \circ \overline{\Omega}) \cdot 1_{m\times m}} \circ \left[\frac{\partial \mathcal{J}}{\partial F} \circ \overline{\Omega} - \frac{\overline{\Omega}}{1_{p\times m} - \Phi \cdot 1_{m\times m}} \circ \left((\frac{\partial \mathcal{J}}{\partial F} \circ F \circ \overline{\Omega}) \cdot 1_{m\times m} \right) \right]. \tag{6.20}$$

Let $U \triangleq -\frac{\partial \mathcal{J}}{\partial F}$. The matrix $(-\frac{\partial \mathcal{J}}{\partial Z})$ may be written with respect to U as

$$(-\frac{\partial \mathcal{J}}{\partial Z}) = \overline{\Omega} \circ \left(U - \frac{(U \circ \overline{\Omega} \circ F) \cdot 1_{p\times m}}{1_{p\times m} - \Phi \cdot 1_{m\times m}} \right) \circ \left(\frac{1_{p\times m} - \Phi \cdot 1_{m\times m}}{(Z \circ \overline{\Omega}) \cdot 1_{m\times m}} \right). \tag{6.21}$$

The third KKT condition with respect to Z (which is a necessary condition to get a stationary point) is expressed as $Z \circ \frac{\partial \mathcal{J}}{\partial Z} = 0$. This expression may be written with respect to F by using the property (6.3), i.e.,

$$F \circ \overline{\Omega} \circ \frac{\partial \mathcal{J}}{\partial Z} = 0. \tag{6.22}$$

In the case of a stationary point ($F = F^k = F^{k+1}$), combining Eqs. (6.21) and (6.22) yields

$$\overline{\Omega} \circ F^k \circ U - \frac{(U \circ \overline{\Omega} \circ F^k) \cdot 1_{m\times m}}{1_{p\times m} - \Phi \cdot 1_{m\times m}} \circ F^{k+1} \circ \overline{\Omega} = 0. \tag{6.23}$$

Since $(F^{k+1} \circ \overline{\Omega})$ is the free part of F^{k+1}, it turns out that the free part of the profile matrix is given by

$$F^{k+1} \circ \overline{\Omega} = \overline{\Omega} \circ \frac{F^k \circ U}{[U \circ \overline{\Omega} \circ F^k] \cdot 1_{m\times m}} \circ (1_{p\times m} - \Phi \cdot 1_{m\times m}) \tag{6.24}$$

The update rule for F follows the general scheme

$$F^{k+1} = \Omega \circ \Phi + \overline{\Omega} \circ \frac{F^k \circ U}{[U \circ \overline{\Omega} \circ F^k] \cdot 1_{m\times m}} \circ (1_{p\times m} - \Phi \cdot 1_{m\times m}). \tag{6.25}$$

which is consistent with the previous parametrization (6.4).

6.3.3 Design of a shift

In this subsection, the proof that the third KKT condition is fulfilled with the new matrix U_s (instead of U) is provided. The new form for U_s is proposed and is available hereafter.

Theorem 1. *Every U_s of the form $U_s = U + S \cdot 1_{m\times m}$ fulfills the third KKT condition (6.23).*

Provided that U satisfies the condition (6.23), it amounts to check the necessary condition at convergence,

$$\overline{\Omega} \circ F^k \circ (S \cdot 1_{m\times m}) - \frac{((S \cdot 1_{m\times m}) \circ \overline{\Omega} \circ F^k) \cdot 1_{m\times m}}{1_{p\times m} - \Phi \cdot 1_{m\times m}} \circ F^{k+1} \circ \overline{\Omega} = 0. \tag{6.26}$$

By using the property

$$((S \cdot 1_{m\times m}) \circ B) \circ 1_{m\times m} = (S \cdot 1_{m\times m}) \circ (B \cdot 1_{m\times m}), \tag{6.27}$$

it turns out that

$$\overline{\Omega} \circ F^k \circ (S \cdot 1_{m\times m}) - \frac{(S \cdot 1_{m\times m}) \circ ((\overline{\Omega} \circ F^k) \cdot 1_{m\times m})}{1_{p\times m} - \Phi \cdot 1_{m\times m}} \circ F^{k+1} \circ \overline{\Omega} = 0. \tag{6.28}$$

Knowing that $(\overline{\Omega} \circ F^k) \cdot 1_{m\times m} = 1_{p\times m} - \Phi \cdot 1_{m\times m}$, it leads that the necessary condition to get a stationary points is

$$\overline{\Omega} \circ F^k \circ (S \cdot 1_{m\times m}) - (S \cdot 1_{m\times m}) \circ F^{k+1} \circ \overline{\Omega} = 0 \tag{6.29}$$

Given that F reachs a limit point ($F^k = F^{k+1}$), the necessary condition (6.29) is always fulfilled. This completes the proof.

Provided this result, the new update rule is defined as

$$F^{k+1} = \Omega \circ \Phi + \overline{\Omega} \circ \frac{F^k \circ U_s}{[U_s \circ \overline{\Omega} \circ F^k] \cdot 1_{m\times m}} \circ (1_{p\times m} - \Phi \cdot 1_{m\times m}). \tag{6.30}$$

At this point, some possible choices of matrix S[2] which ensures the non-negativity of U_s should be highlighted. To achieve this goal, assume a specific form of U i.e,

$$U = P - Q \tag{6.31}$$

P and Q could be always chosen such that they are non-negative. As a consequence, S should be chosen as $S \triangleq Q$ so that U_s is

$$U_s = P - Q + Q \cdot 1_{m\times m} \tag{6.32}$$

Since $\overline{\Omega} \circ \overline{\Omega} = \overline{\Omega}$, the replacement of U by $\overline{\Omega} \circ U$ could be proposed in Eq (6.25). Consequently, S could be chosen as $S \triangleq \overline{\Omega} \circ Q$. Thus, another possible expression of U_s can be defined, i.e.,

$$U_s = \overline{\Omega} \circ P - \overline{\Omega} \circ Q + (\overline{\Omega} \circ Q) \cdot 1_{m\times m}. \tag{6.33}$$

Note that the last equation may be numerically more attractive since the shift may be lower than in Eq (6.32). Thus, the ratio is far from 1 in Eq (6.30) (a situation which favors large changes in the update). The two options (6.32,6.33) are extensively used hereafter in solving the mentionned problems.

6.4 Solving the different Problems

This section summarizes the different update rules of the problems defined above. It is essentially based on the scheme (6.30) which is adapted to the context of each specific cost function.

2. Lantery proposed to choose U_s as $U_s \triangleq U - U_{min} 1_{m\times m}$.

6.4.1 Solution to Problem (6.7)

In the case of a weighted Frobenius cost function, the partial differentiation of $\mathcal{J}(.)$ with respect to F is available in Eq (3.75) by looking at the left part of the second equation. So, U is expressed as

$$U = G^T \left((X - G \cdot F) \circ W\right) \tag{6.34}$$

In this case, Q should be chosen equal to $Q = G^T \cdot (G \cdot F \circ W)$. As a consequence, U_s may be defined as

$$U_s = G^T \cdot \left((X - G \cdot F) \circ W\right) + \left[G^T \cdot \left((G \cdot F) \circ W\right)\right] 1_{m \times m}. \tag{6.35}$$

Another choice should be

$$U_s = \overline{\Omega} \circ \left(G^T \cdot \left((X - G \cdot F) \circ W\right)\right) + \left(\overline{\Omega} \circ \left[G^T \cdot \left((G \cdot F) \circ W\right)\right]\right) \cdot 1_{m \times m}. \tag{6.36}$$

These two options are combined with the mentioned update rules for F in Eq (6.30). In addition, these rules are completed by an unconstrained weighted Frobenius version of G available in Eq (3.76) and recalled hereafter,

$$G = G \circ \frac{(W \circ X) \cdot F^T}{(W \circ (G \cdot F)) \cdot F^T} \tag{6.37}$$

As a summary, the update rule of F satisfies (i) the non-negativity of F, (ii) sum-to-1 constraints and set values and (iii) the third KKT condition.

6.4.2 Solution to Problem (6.9)

In this section, another strategy suggests the use of a robust cost function between the components of Eq. (2.5). The weighted Huber cost function accounts for a weighted Frobenius norm for small residuals while providing weighted ℓ_1 penalization to large residuals.

The Huber cost function is an M-estimator [70] technique that can cope very well with the presence of outliers. It is a robust cost function designed to provide less residuals to large entries of R. It is based on ℓ_2 and ℓ_1 norms.

The update rules of the profile matrix F which are consistent with the KKT conditions are determined by differentiating $\mathcal{J}(.)$ in Eq. (6.9) with respect to F in both cases. For that purpose, the following weight matrices W_1 and W_2 are defined:

$$W_{1,ij} \triangleq \frac{1}{\sigma_{ij}^2}, \quad W_{2,ij} \triangleq \begin{cases} 1 & \text{if } \frac{(GF-X)_{ij}}{\sigma_{ij}} < c, \\ \frac{c \cdot \sigma_{ij}}{|GF-X|_{ij}} & \text{otherwise.} \end{cases} \tag{6.38}$$

The matrix W_2 should be seen as an adaptive re-weighting matrix and is depending on the small/large weigthed residuals. In the case of a single data point labelled as an outlier, the weight in W_2 is proportional to the inverse of the residual value and is less than 1. Since $W_2 = 1_{n \times m}$ for the ℓ_2 component of

the cost function, the differentiation of $\mathcal{J}(.)$ with respect to a single entry F_{rj} is given by,

$$\frac{\partial \mathcal{J}}{\partial F_{rj}} = G_{ir}(GF - X)_{ij} W_{1_{ij}}. \tag{6.39}$$

The differentiation of $\mathcal{J}(.)$ for the ℓ_1 component yields

$$\frac{\partial \mathcal{J}}{\partial F_{rj}} = \sum_{i=1}^{n} \frac{c}{\sigma_{ij}} \cdot G_{ir} \cdot \text{sign}((GF - X)_{ij}). \tag{6.40}$$

Then, using the definition of the sign function, an equivalent expression is derived, i.e.,

$$\frac{\partial \mathcal{J}}{\partial F_{rj}} = \sum_{i=1}^{n} \frac{c \cdot \sigma_{ij}}{\sigma_{ij}^2} \cdot G_{ir} \cdot \frac{(GF - X)_{ij}}{|GF - X|_{ij}}. \tag{6.41}$$

Lastly, Eq. (6.42) is derived from Eq. (6.38)

$$\frac{\partial \mathcal{J}}{\partial F_{rj}} = G_{ir}(GF - X)_{ij} W_{1_{ij}} W_{2_{ij}}. \tag{6.42}$$

Equations (6.39) and (6.42) yield a unified matrix expression, i.e.,

$$\frac{\partial \mathcal{J}}{\partial F} = G^T [W \circ (GF - X)], \tag{6.43}$$

where W accounts for the generalized weight matrix defined as

$$W \triangleq W_1 \circ W_2. \tag{6.44}$$

The differentiation of $\mathcal{J}(.)$ has a similar expression for both the quadratic and the linear components of the Huber function. The difference is in the reweighting process for large residuals, as explained with the definition of W_2. As a consequence, U follows the same expression as in Eq. (6.34) and possible shifted versions of U_s are described in Eq. (6.35,6.36).

6.4.2.1 Update rules for G

As stated earlier, the contribution matrix G is unconstrained. Once again, the weight W should be taken into account in the update rules. Due to the symmetry in the expression of the weighted Huber cost function, the differentiation with respect to G leads to a similar equation to Eq. (6.43) i.e,

$$\frac{\partial \mathcal{J}}{\partial G} = [W \circ (G \cdot F - X)] \cdot F \tag{6.45}$$

The Expression (6.45) is similar to the expression resulting from the differentiation of the quadratic loss function in [66], with a weight matrix which depends on the individual residual defined in Eq. (6.44). Thus, the expression of the update rules for G follows the same scheme in addressing Problem (6.7), as described in Eq. (6.37). It should be mentioned however that the update of the weight matrix should be made prior to the computation of F and G. This implies that the cutoff

parameter, which is an adpative parameter, should be carefully tuned.

6.4.2.2 Choice of the cutoff parameter

The cutoff parameter is an adaptive parameter depending on the residuals. It is usually selected as the median of the residuals [45]. In the framework of this thesis, it is related to weighted residuals. While it could also be chosen as the median—i.e., half of the data are labeled as outliers— this choice prevents to update the matrices in a sufficient way at each iteration and as a consequence, a different strategy should be proposed. At the beginning of the NMF algorithm, all the data should be processed in the quadratic region of the Huber function. Thus, c should go to the maximum value of the data. At the end of the algorithm , it is expected that c should tend to an intermediate value. This will lead to identify the outliers points. As a consequence, an heuristic choice of c could be proposed and is based on the quantile function with a probability value linearly depending on the current iteration number k, i.e.,

$$c = \text{quantile}(R^{\sigma}, 1 - \frac{k}{\text{Itermax}} * 0.1) \tag{6.46}$$

where R^{σ} is the residual matrix and its general entry $R^{\sigma}_{ij} \triangleq \frac{r_{ij}}{\sigma_{ij}}$, and Itermax is the maximum number of iterations. This choice implicitly states that a maximum of 10 percent of the data may be labeled as outliers data. This value of c was found to be a good trade-off in the preliminary tests. Different strategies are also proposed by setting some constant percentage of outliers over iterations such as 10 or 20 percent.

6.4.2.3 Huber Algorithm

The algorithm may be summarized as follows:

Algorithm 8 Weighted Huber Informed NMF description (Huber SG-CWNMF).

while the stopping rule is not fulfilled **do**
  Compute R and the weighted residuals R^{σ}
  Compute c according to Eq. (6.46)
  Update W according to Eqs. (6.38) and (6.44)
  Update F according to Eq. (6.30) with Eq. (6.35) or Eq. (6.36)
  Update G at fixed F according to Eq. (6.37)
end while

6.4.3 Solution to Problem (6.8)

The weighted $\alpha\beta$-divergence may be used as a robust cost function. Except the second kind of shift (6.33), it has been completely investigated in [25]. The partial differentiation of the criterion

with respect to F is expressed as

$$\frac{\partial \jmath}{\partial F} = \frac{1}{\alpha} G^T \cdot [W \circ (G \cdot F)^{\beta-1} \circ ((G \cdot F)^{\alpha} - X^{\alpha})] \tag{6.47}$$

By recalling that $U \triangleq -\frac{\partial \jmath}{\partial F}$ and by dropping the scalar factor in Eq. (6.47), U can be written as

$$U = G^T \cdot (W \circ (X^{\alpha} \circ (G \cdot F)^{\beta-1})) - G^T \cdot (W \circ (G \cdot F)^{\alpha+\beta-1}). \tag{6.48}$$

The non-negativity of F should be preserved and is automatically ensured when U is positive. An analytic shift equal to the sum of the negative part of $-\frac{\partial \jmath}{\partial F}$ provided in Eq. (6.47) is proposed. Thus, the shifted matrix U_s, consistent with the scheme in Eq (6.32) is given by

$$\begin{aligned} U_s =& G^T \cdot (W \circ (X^{\alpha} \circ (G \cdot F)^{\beta-1})) - G^T \cdot (W \circ (G \cdot F)^{\alpha+\beta-1}) \\ &+ [G^T \cdot (W \circ (G \cdot F)^{\alpha+\beta-1})] \cdot 1_{m \times m}. \end{aligned} \tag{6.49}$$

An alternative solution for U_s follows the scheme described in Eq. (6.33), and it yields

$$\begin{aligned} U_s =& \overline{\Omega} \circ \left[G^T \cdot (W \circ (X^{\alpha} \circ (G \cdot F)^{\beta-1})) \right] - \overline{\Omega} \circ \left[G^T \cdot (W \circ (G \cdot F)^{\alpha+\beta-1}) \right] \\ &+ \left(\overline{\Omega} \circ [G^T \cdot (W \circ (G \cdot F)^{\alpha+\beta-1})] \right) \cdot 1_{m \times m}. \end{aligned} \tag{6.50}$$

The update rules of the proposed $\alpha\beta$-divergence Split-Gradient Method for Constrained Weighted NMF ($\alpha\beta$-SG-CWNMF) consist of using U_s defined either in Eq. (6.49) or in Eq. (6.50) instead of U in Eq. (6.25). The update rules with both matrices U_s satisfy (i) the non-negativity of F, (ii) the sum-to-one constraints, and (iii) the third KKT condition.

G remains unconstrained in the considered Problem and the update rules should take into account the weight matrix W. Therefore, a Weighted $\alpha\beta$-NMF ($\alpha\beta$-WNMF) approach yields the following update rules for G:

$$G^{k+1} = G^k \circ \mathcal{N}_G^{\alpha,\beta}(G^k, F^k) \tag{6.51}$$

where,

$$\mathcal{N}_G^{\alpha,\beta} \triangleq \left[\frac{\left(W \circ \left(X^{\alpha} \circ (G \cdot F)^{\beta-1} \right) \right) \cdot F^T}{(W \circ (G \cdot F)^{\alpha+\beta-1}) \cdot F^T} \right]^{\left(\frac{1}{\alpha}\right)}. \tag{6.52}$$

Eqs. (6.30,6.51) and the choice of U_s described either in Eq. (6.49) or in Eq. (6.50) leads to the solution of Problem (6.8). Also, it addresses the first Problem (6.7) by selecting $\alpha = 1$ and $\beta = 1$.

6.5 Summary of the different algorithms

This section summarizes the different algorithms described before and the available options. Update rules and acronyms may be found in Table (6.1). The weight definition is based mainly on W_1 as expressed in Eq. (6.38). S1 or S2 refers to the choice of the shift defined in the references. While SG

Table 6.1 – Different methods with various shifts and weights

Methods	Rules on F	Rules on G	U_s	Weight W
SG-CWNMF-S1	Eq (6.30)	Eq (6.37)	Eq. (6.35)	$W = W_1$
SG-CWNMF-S2	Eq (6.30)	Eq (6.37)	Eq. (6.36)	$W = W_1$
αβ-SG-CWNMF-S1	Eq (6.30)	Eq (6.51)	Eq. (6.49)	$W = W_1.^{(\frac{\alpha+\beta}{2})}$
αβ-SG-CWNMF-S2	Eq (6.30)	Eq (6.51)	Eq. (6.50)	$W = W_1.^{(\frac{\alpha+\beta}{2})}$
Huber -SG-CWNMF-S1	Eq (6.30)	Eq (6.37)	Eq. (6.35)	$W = W_1 \circ W_2$
Huber -SG-CWNMF-S2	Eq (6.30)	Eq (6.37)	Eq. (6.36)	$W = W_1 \circ W_2$

means Split Gradient, CWNMF refers to Constrained Weighted NMF. The left part of the acronym indicates the special choice of the cost function such as Huber or αβ- divergence. These methods will be extensively evaluated by performing various experiments.

6.6 Initialization issues

In the total absence of prior knowledge, some authors suggest to perform some random initializations for both factors. However, this strategy implies several runs and does not fit with informed situations.

The prior knowledge is proposed on F as an approximate initial matrix. Then, the second factor is computed by using a weighted Frobenius criterion with constraints. Let $\underline{w}_i$, $\underline{x}_i$, and $\underline{g}_i$ be the i^{th} row of W, X, and G, respectively. The i^{th} row of the contribution matrix minimizes a weighted least-square cost function under some specific constraints, i.e.,

$$J(\underline{g}_i) = \left(\underline{x}_i^T - F^T \underline{g}_i^T\right)^T \cdot D_{w_i} \cdot \left(\underline{x}_i^T - F^T \underline{g}_i^T\right), \tag{6.53}$$

where $D_{w_i} = \text{diag}(\underline{w}_i)$. This function may be written under a quadratic form

$$J(\underline{g}_i) = \frac{1}{2}\underline{g}_i^T \cdot H \cdot \underline{g}_i^T + u' \cdot \underline{g}_i^T, \tag{6.54}$$

with $H = 2F \cdot D_{w_i} \cdot F^T$ and $u' = -2\underline{x}_i \cdot D_{w_i} \cdot F^T$. Initializing G consists in estimating $\underline{g}_i$ for each i

$$\min_{\underline{g}_i} J(\underline{g}_i) \quad \text{s.t.} \quad \underline{g}_i^T \succeq 0, \sum_i \underline{g}_i = \sum_i \underline{x}_i, \text{and } \underline{x}_i^T \succeq \Phi^T \cdot \underline{g}_i^T. \tag{6.55}$$

The three constraints state that (i) each entry of $\underline{g}_i$ is non-negative, (ii) the contributions must be normalized because the profiles are proportions, and (iii) the known part of the data has to be lower than the whole data. In practice, Eq. (6.55) is solved using the interior-point convex algorithm from Matlab.

6.7 Validation on a toy simulation example

6.7.1 Introduction of the toy simulation

The data is made with 50 samples and 7 species (Iron Fe, Calcium Ca^{2+}, Sulfate SO_4^{2-}, Zinc Zn, Magnesium Mg^{2+}, Aluminium Al and Chromium Cr) with a known uncertainty measure σ_{ij}— provided by a chemical expert— and associated with each data point x_{ij}. Thus, the matrix X has a size of 50×7 . Each collected data point x_{ij} is corrupted by a uniform noise ranging in the interval $[-\min(\lambda\sigma_{ij}; x_{ij}); \lambda\sigma_{ij}]$ while preserving the positivity of the collected data i.e x_{ij} is greater than 0. Note that λ is also related to an input Signal-to-Noise Ratio (*SNR*). The profile matrix—whose initialization is provided by chemical experts—consists of three (partially correlated) industrial profiles. The exact profile matrix is provided in Table (6.2).

	Fe	Ca^{2+}	SO_4^{2-}	Zn	Mg^{2+}	Al	Cr
Source 1	0.7	0.1	0.08	0.06	0.04	0.02	0
Source 2	0.3	0.4	0.005	0	0.2	0.075	0.02
Source 3	0.4	0.2	0.08	0	0.12	0.2	0

Table 6.2 – Exact profile matrix

The contribution matrix G is initialized as the solution of a weighted and constrained least-square cost function [132].

6.7.2 *MER* index for performance evaluation

Several performance indexes are available in the literature. However in this work, only the *MER* index (*MER* for *Mixing Error Ratio*) is considered [162]. It is obtained from each column of G. For each source, a scalar quantity MER_j expressed in dB may be obtained. For one exact vector $\underline{g}_j$ and its estimate $\underline{\hat{g}}_j$, it is possible to write $\underline{\hat{g}}_j$ under the form

$$\underline{\hat{g}}_j = \underline{\hat{g}}_j^{coll} + \underline{\hat{g}}_j^{orth}, \tag{6.56}$$

where $\underline{\hat{g}}^{coll}$ and $\underline{\hat{g}}^{orth}$ are respectively colinear and orthogonal to the exact vector $\underline{g}$. This decomposition allows to express the *MER* of source j, denoted as MER_j, defined as,

$$MER_j = 10 \log_{10} \frac{\| \underline{\hat{g}}_j^{coll} \|^2}{\| \underline{\hat{g}}_j^{orth} \|^2}. \tag{6.57}$$

Infinite values mean exact separation while 0 dB correspond to an angle equal to 45°. These values may be summed up into a vector which gathers the performance of each source. Generally, a global

	Fe	Ca^{2+}	SO_4^{2-}	Zn	Mg^{2+}	Al	Cr
Source 1	0.7	XX	XX	XX	XX	XX	0
Source 2	XX	0.4	0.005	0	XX	0.075	XX
Source 3	0.4	XX	XX	0	XX	XX	0

Table 6.3 – Positions and values of the constraints used in the informed NMF methods. *XX* means no constraint.

indicator is obtained by averaging each index over all sources, i.e.,

$$MER = \frac{1}{p}\sum_{j=1}^{p} MER_j. \tag{6.58}$$

This index will be extensively used along simulations.

6.7.3 First experiment with 9 constraints

This part is a summary of the simulation part provided in [26]. In this first experiment, outliers are not considered. 9 constraints (among 21 entries) are associated with the profile matrix as shown in Table (6.3). The letter (*XX*) indicates that there is no constraint at the corresponding location of the Profile matrix. If the value is set to zero, it indicates that the corresponding source does not emit that species.

The proposed SG-CWNMF method (which is based on the Frobenius norm) is evaluated by performing a comparison with four existing approaches, namely, the blind NMF [95], the WNMF [66], the SG-WNMF (a weighted version of [91] with the proposed shift of SG-CWNMF), and our informed Frobenius method CWNMF [98]. The performance criterion is the average Mixing Error Ratio (*MER*) [162] which is computed on the contribution matrix *G*. The respective algorithms used $5\,10^5$ iterations.

Figure (6.2) shows the performance (*MER*) of the various methods as a function of the input *SNR*. The proposed SG-CWNMF clearly outperforms all the other methods (around 2 dB in the noisiest scenarios). Additionally, in a noiseless case—not shown in Fig. 6.2—the SG-CWNMF method provides a *MER* at least 200 dB higher than those obtained from the other NMF-based methods. However, for low *SNR*, the gap with other methods is really small which limits in this case the interest for the new method.

6.7.4 Second experiment with 9 constraints

This section aims at highlighting the effect of several outliers on the overall performance of investigated methods. This subsection is essentially based on [24].

The process of data generation is a bit modified with respect to the previous experiment. The

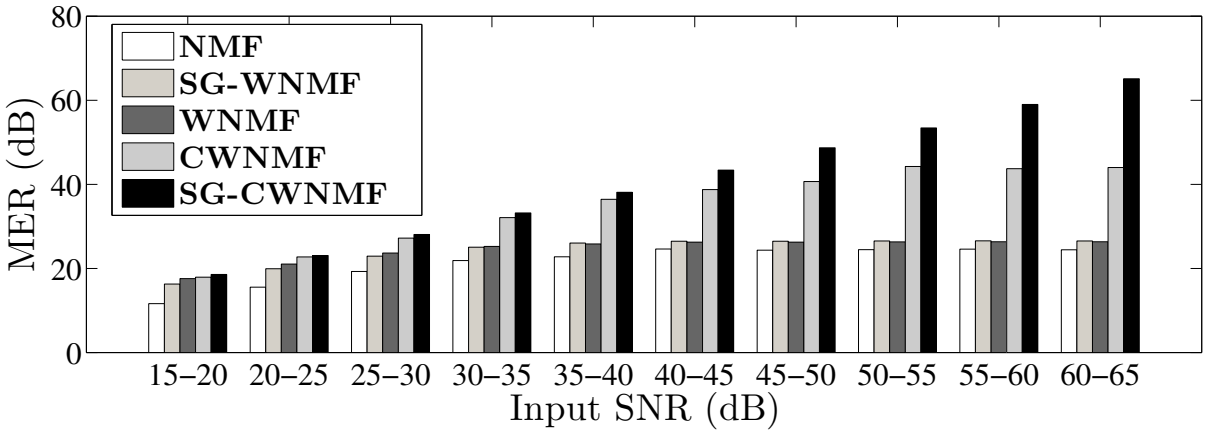

Figure 6.2 – Performance of the various NMF methods as a function of the input *SNR*.

collected samples are corrupted by outliers at random locations and are tuned by a gain which is always greater than one in order to simulate a pollutant contamination. Then, a uniform noise generated from the interval $[-\min(\lambda\sigma_{ij}; x_{ij}); \lambda\sigma_{ij}]$, identical to the previous case, simulates the acquisition process.

Moreover, the constraints recalled in Table (6.3) are the same as in the first experiment. Each method under study uses the same initialization. The performance of the Huber Split Gradient Constrained Weighted NMF (Huber SG-CWNMF) is quantitatively investigated with respect to state-of-the art methods. Its performance is compared with

— Blind-based separation approaches that are based on β-divergence, namely the original unweighted β-NMF [51], the weighted β-NMF [66] and the robust NMF (rNMF) [47] in which the data matrix is split into a low rank matrix satisfying Eq. (2.5) and a sparse matrix containing the outliers,
— Informed approaches based on the β-divergence, namely the β-CWNMF with the Residuals (β-CWNMF-R) and without the residuals (β-CWNMF) [97] with β is set to 0.8,
— a weighted version of the Split Gradient approach developped by Lantéri *et al.* [91], which involves a sum-to-1 parameterization (SG-WNMF),
— the newly proposed αβ-SG-CWNMF with $\alpha = \beta = 0.6$ [25].
— the Huber upper bound of the performance is computed using the Huber regression method by assigning F to its real value and by implementing the update rules (6.52) together with the iterative re-weighting process (6.38).

Figure (6.3) shows the performance of several methods over a wide range of input *SNR* in the case of 5 outliers. The *MER* of each method is averaged over the trials inside the same slice of *MER*.

It turns out that

— The proposed Huber-SG-CWNMF method outperforms all the based-NMF methods as illustrated in Figure (6.3), for various input *SNR* intervals in the presence of 5 outliers.
— The performance of the newly proposed informed NMF behaves very similarly to the bound in all slices of *SNR*.
— The rNMF method completely fails in all simulated experiments and as consequence, it is also

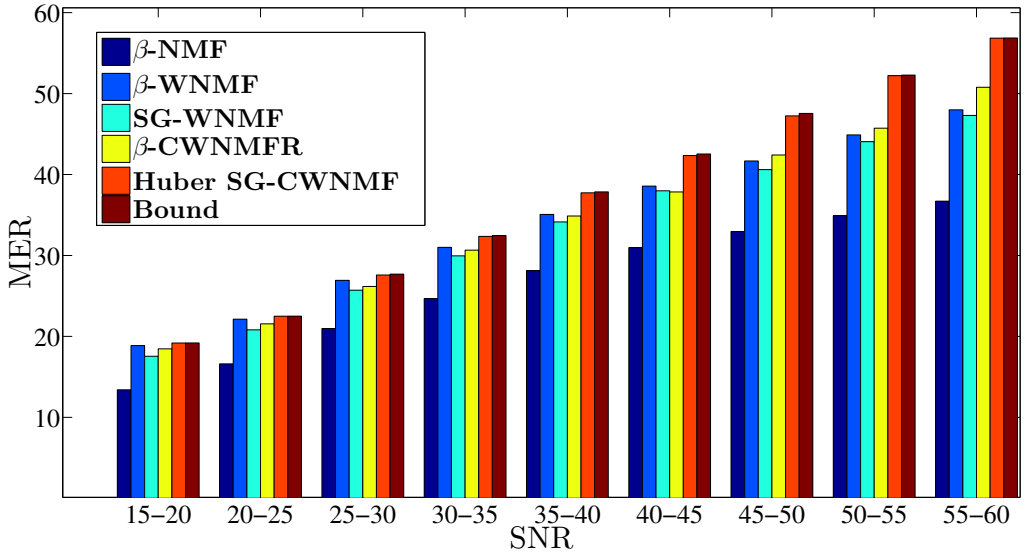

Figure 6.3 – *MER* versus *SNR* for 5 outliers.

not shown in Fig. (6.3). This is probably due to the fact that rNMF is not able to split the data matrix into an appropriate sparse and a low rank matrices. Indeed, the outliers are relatively small for high input *SNR* and medium-sized for low *SNR*. Such a situation is challenging for rNMF which performs well in the presence of larger outliers.

6.7.4.1 Effect of the number of outliers

A second experiment is performed in order to investigate the influence of the number of outliers on the performance of the various NMF-based methods. Figure (6.4) shows the computed *MER* as a function of the number of outliers for an input *SNR* of $40\,dB$ before introducing the outliers. It is to be noted that the achieved *SNR* after corrupting the collected data is shown between brackets in Figure (6.4). The number of outliers in this experiment varies from 0 to 5 and the *SNR* is affected by less than $10\,dB$. The results show that:

— For each method, the *MER* decreases with the number of outliers.

— Similar to the previous experiment, the proposed Huber SG-CWNMF method outperforms all the other approaches.

— The performance of the proposed Huber-SG-CWNMF is very close to the Bound for each case. Moreover, the Huber SG-CWNMF *MER* is roughly equal to the *SNR* even in the presence of outliers.

As a conclusion, the new method shows its relevance in the context of a few irregular data.

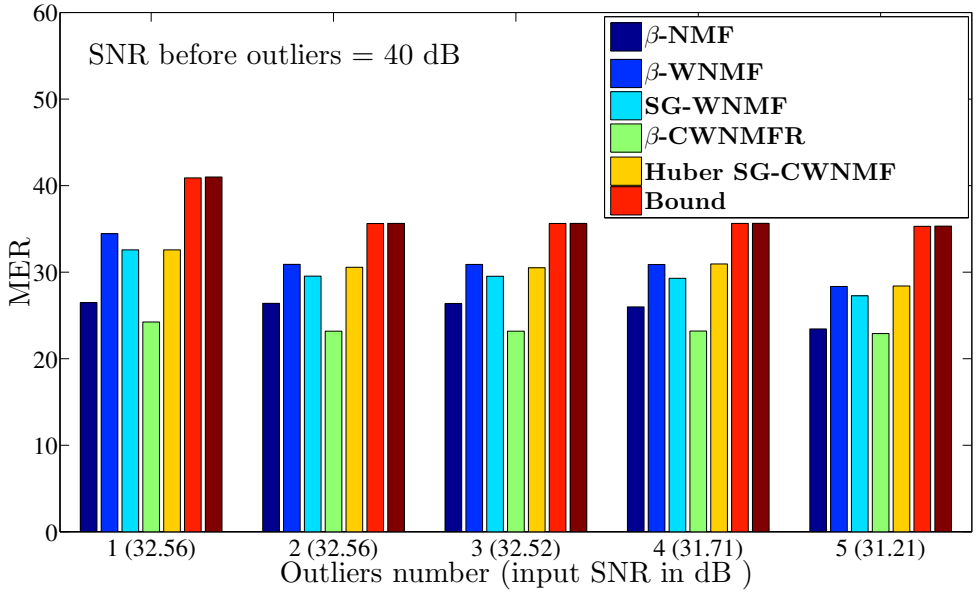

Figure 6.4 – The performance of the NMF approaches as a function of the number of outliers.

6.7.4.2 Effect of various cutoff parameters

As already discussed in subsection (6.4.2.2), the selection of the cutoff parameter might significantly affect the results of the new method. The question of constant cutoff or adaptive may be raised. Consequently, the quantitative evolution of the effect of various choices of the cutoff parameter on the Huber-SG-CWNMF approach is proposed.

Two constant cutoffs along iterations were investigated (20% and 50%) and two adaptive cutoffs with linear decrease of the quantile value along iterations are proposed (0 to 10% and 0 to 50% are outliers). This adaptive case suggests that an increasing number of data may be tagged as outliers along iterations thus switching to the ℓ_1 mode. At the end of the run, there is a possibly 10% or 50% respectively of the data which are viewed as outliers. Figure (6.5) summarizes the different performances. The legend specifies the percentage of data points considered in the ℓ_1 part of the Huber function at the beginning and at the end of the iterations. It appears that

— The first test of the proposed Huber-SG-CWNMF approach is conducted with an adaptive cutoff between 0 and 10%. This method outperforms all the others for all slices of input *SNR*.

— The second test of the proposed Huber-SG-CWNMF approach is conducted with a constant cutoff of 50%. The method has an acceptable performance for the range between $15\,dB$ to $35\,dB$ of input *SNR* but the performance is bad for the remaining intervals.

— The third test of the proposed Huber-SG-CWNMF approach is conducted with a constant cutoff of 20%. In this case, the method also is performing good and remains close to the performance of the first conducted test.

— The last test of the proposed Huber-SG-CWNMF approach is conducted with an adaptive cutoff between 0 and 50%. The performance of this method remains correct in each slice of *SNR*.

In conclusion, the best choice is achieved with the cutoff proposed in Eq. (6.46) as indicated in Figure (6.5). Moreover, the usual choice of the median proposed in the literature [45] is shown to be inappropriate.

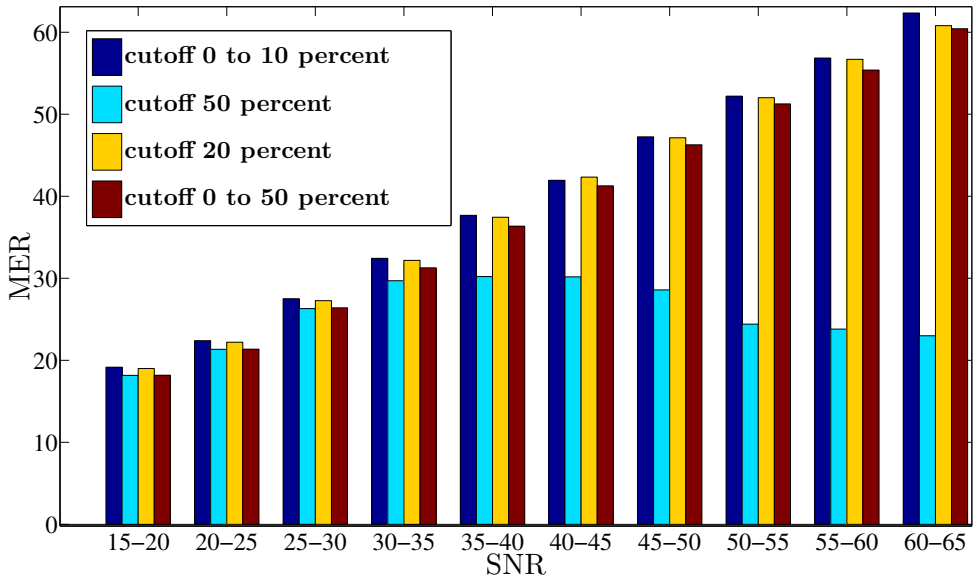

Figure 6.5 – Effect of different cutoff strategies on the performance.

6.7.5 Third experiment with 6 constraints

This subsection is essentially based on the results published in [25]. It focuses on the same example with only 6 set values. It should be stressed that 0 values have been dropped here. It is important to check if this change has an impact on the results. They are gathered in Table (6.4).

	Fe	Ca	SO_4	Zn	Mg	Al	Cr
Source 1	0.7	XX	XX	XX	0.04	XX	XX
Source 2	0.3	XX	XX	XX	XX	0.075	XX
Source 3	XX	0.2	XX	XX	0.12	XX	XX

Table 6.4 – Set Values used in the informed NMF methods. XX means no constraint.

In this section, the αβ SG-CWNMF approach is validated experimentally. The performance of the second newly proposed method is investigated by conducting several experiments with and without outliers.

The quantitative evaluation is performed with various NMF-based techniques. Four blind methods are implemented. Two of the algorithms are based on the β-divergence namely the β-NMF [51] and

the β-WNMF [66]. A value of 0.8 is selected for β for comparaison purposes. The two other blind approaches are based on the Frobenius cost function, i.e., the robust NMF (rNMF) [47] which places the outliers into a sparse matrix and the weighted version of the Split-Gradient NMF (SG-WNMF) that is proposed in [91]. Moreover, two state-of-the-art informed approaches are evaluated, i.e., the previous informed β-NMF method [97] denoted by β-CWNMF and β-CWNMF-R. The best achieved performance of the two methods in the experimental simulations is included i.e., the β-CWNMF-R. All these methods are compared with the new developed Split Gradient Constrained Weighted NMF (denoted αβ-SGCWNMF) in which α is set to 0.6 and β to 0.6. In addition, the performance of αβ-WNMF when F is set to the true profile matrix (the corresponding plot is denoted Bound" in the figure) is presented.

The performance of the proposed method as well as the various NMF based approaches as a function of the Signal to Noise Ratio (SNR) of the input and for a various number of outliers in the collected data is illustrated in Fig. (6.6), Fig. (6.7) and Fig. (6.8). While Fig. (6.6) shows the performance of the NMF methods where the number of outliers is 0, Fig. (6.7) and Fig. (6.8) display the performance when the number of outliers is 2 and 5, respectively. Each figure displays the MER in function of the SNR of the input. The SNR varies from 15 to $55dB$. The difference between the three figures is the number of outliers in the collected data. To generate each graph, 400 simulation experiments are performed for evaluation purposes and each experiment corresponds to a particular SNR. In these graphs, the Bound MER is roughly equal to the input SNR.

It is to be noted that the shown SNR stands for the SNR that is computed after placing the outliers. In the case of a large SNR, several small outliers coexist with very low noise. On the contrary, low SNR may be obtained by medium size outliers with large noise. It turns out in all the three graphs that the rNMF approach [47] is always failing as noticed earlier. The new proposed method αβ-SGCWNMF outperforms all the other approaches for every range of SNR. Moreover, it remains very close to the computed Bound with and without outliers and consequently, this will show its relevance.

In order to confirm this behaviour, another test is performed in which the input SNR is set to $40dB$ before introducing the outliers. Then, the influence of the number of outliers is shown. The multiplicative outlier factor is selected such that it enables the increase of the unnoisy entry data by 30 percent. Figure (6.9) shows the dependence of the accuracy of the various approaches in terms of MER versus the number of outliers. Once again, it is clear that all the methods provide a decreasing performance when the number of outliers increases. However, the proposed αβ-SGCWNMF outperforms all the other approaches and remains very close to the "Bound" obtained by the regression on G.

As a conclusion, αβ SG-CWNMF seems to bring a significant enhancement in the performance of the separation process without and with a few outliers.

6.8 Medium scale experimentation

In this section, our methods are investigated in a medium scale simulation drawn from real data campaign. These data consisted in evaluating concentrations of Air Suspended Particulate Matter over

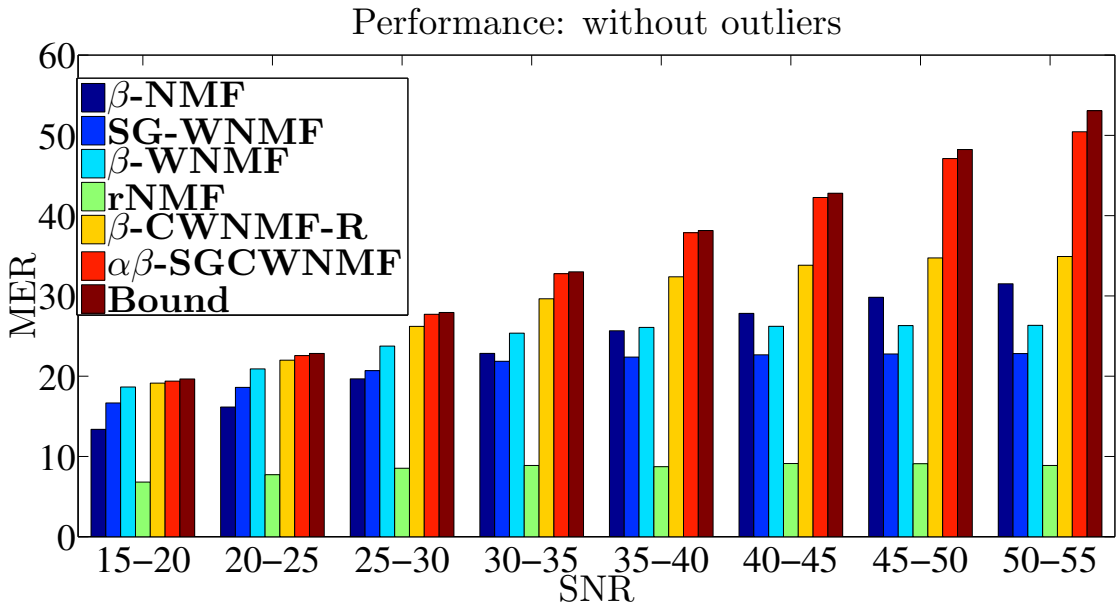

Figure 6.6 – *MER* of the various NMF Methods as a function of the input *SNR* : No Outlier

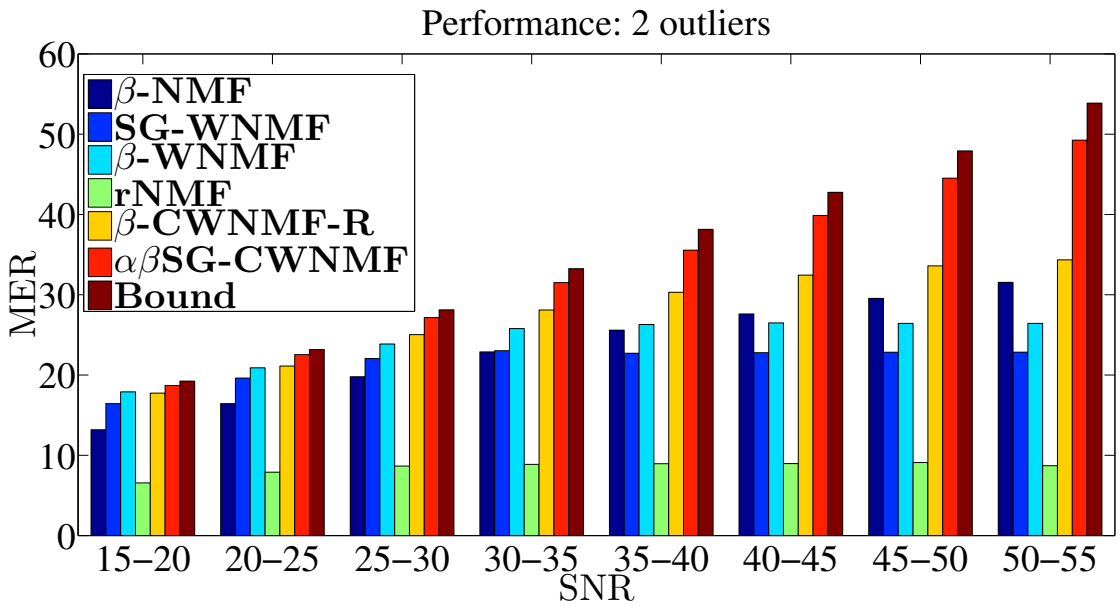

Figure 6.7 – *MER* of the various NMF Methods as a function of the input *SNR* : 2 Outliers

a long period. Sampling time was equal to 24 hours. Particles whose diameter was lower than 10μm were focused on. Species under study were divided into 16 metal tracers (Al, Cr, Fe, Mn, P, Sr, Ti, Zn, V, Ni, Co, Cu, Cd, Sb, La, Pb), 8 water soluble ionic species (Na^+, NH_4^+, K^+, Mg^{2+}, Ca^{2+}, Cl^-, NO_3^-, SO_4^{2-}), Carbon compounds either organic (OC) or elementary (EC), and Levoglucosan and Polyols.

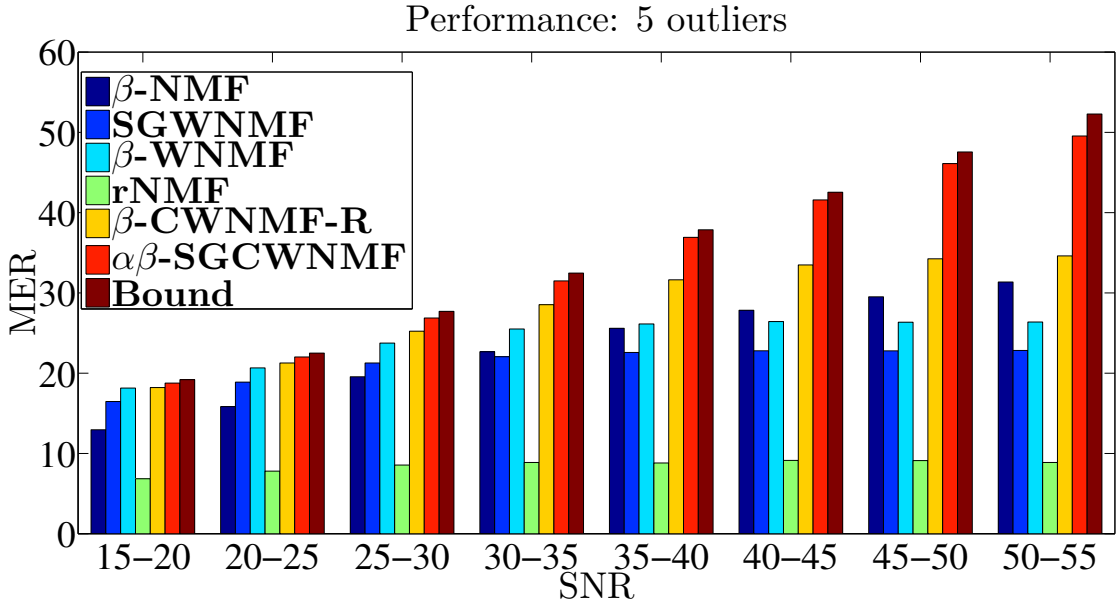

Figure 6.8 – MERs of the various NMF Methods as a function of the input *SNR* : 5 Outliers

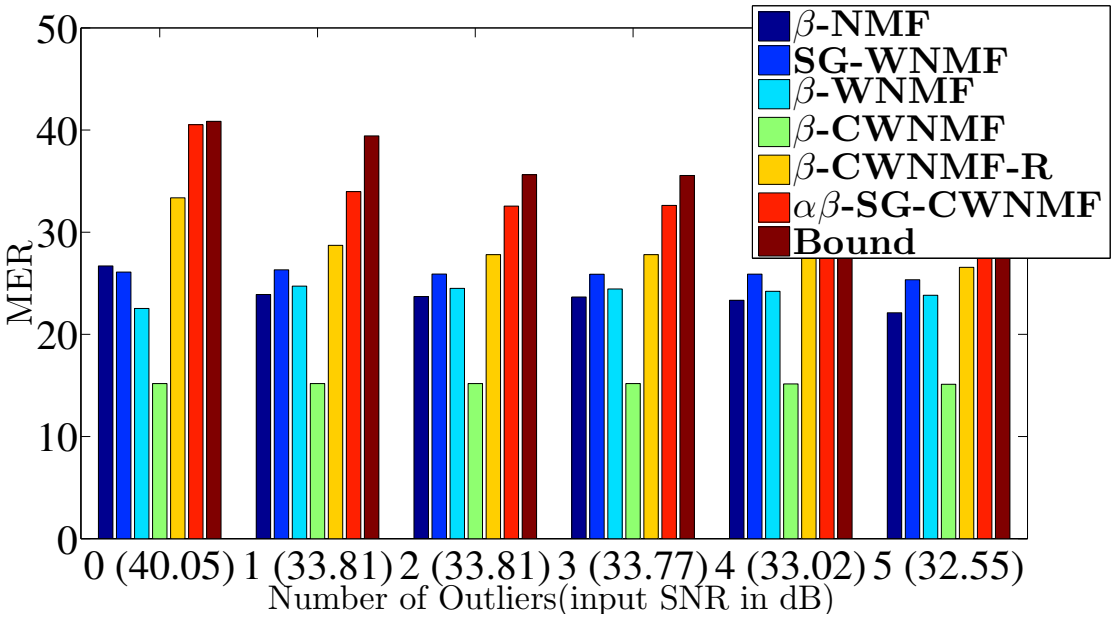

Figure 6.9 – Performance of the NMF methods as a function of the number outliers. The Performance Criterion: *MER* (in *dB*).

These data were extracted from ECUME Project [3] which consisted in evaluating the impact of Marine Traffic to the concentration over one city station and one rural station, both located on the coast of the English Channel. From the validated profile and contribution matrices obtained during the campaign, simulation data were built by taking into account the individual uncertainty provided

3. ECUME project was funded by the DREAL French agency from 2013 to the beginning of 2016.

Table 6.5 – Features of the different source profiles

Profiles	Type	Major species	References
Sea salts	Natural	Cl^-,Na^+,SO_4^{2-},Mg^{2+},K^+,Ca^{2+},Sr	[80]
Crustal dust	Natural	Al, Ca^{2+}, Fe, K^+, OC, Ti, NO_3^-, Na^+	[81]
Primary biogenic emission	Natural	OC, EC, Polyols, P	[166]
Aged sea salts	Anthropised	NO_3^-, Na^+, SO_4^{2-}, Mg^{2+},K^+, OC,Ca^{2+},Sr,Cl^-	[166]
Secondary nitrates	Anthropised	NO_3^-, OC, NH_4^+, EC, Ca^{2+},Fe, Zn, Cu	[166]
Secondary sulfates	Anthropised	SO_4^{2-}, NH_4^+, OC, Ca^{2+}, K^+, Fe, Pb, Zn	[81]
Biomass combustion	Anthropogenic	OC, EC, Levoglucosan, NO_3^-, K^+, Zn	[166]
Road traffic	Anthropogenic	EC, OC, NO_3^-, Cu, Sb, Zn, Fe	[166]
Sea traffic	Anthropogenic	OC, EC,V, Ni, Co, SO_4^{2-}, NH_4^+, NO_3^-	[166]
Rich metal source	Anthropogenic	Fe, Al, Cr, Pb, Zn, Mn	[166]

by the real campaign. So, the data matrix consists in a 280×28 matrix associated with individual uncertainties. The uncertainties are exactly those provided by the chemical analysis.

In addition, several cases with outliers were investigated. It is to be assumed that outliers come from an additional individual contamination which consist in multiplying the theoretical data entry by a scalar factor greater than 1. Then, a uniform noise which preserves non-negativity simulates the measurement process. Among the 280 samples, 5 10 and 20 outliers are considered. The *SNR* index drops then in the worst case by 1 dB if the set of outliers are taken into consideration.

6.8.1 Source profiles

In this study, 10 sources are highlighted. Among these sources, some of them are purely natural or purely anthropogenic but some of them became anthropised. Table (6.5) describes major species present in each source profile. Other species than those listed in the corresponding source profile may be assimilated as near 0 entries. It is to be noted that the real profile is perfectly known.Table (C.1) indicates the different source profiles. Also, it is to be noticed that the source profile is presented here as a per thousand profile matrix. It means that it sums to thousand instead of 1.

6.8.2 Equality constraints

Equality constraints or set values enable to inform the algorithm about some entries of the profile matrix. This knowledge is taken into account by specifying matrices Ω and Φ. These matrices are available in Appendix (C). It is to be stressed that the only used knowledge here is the absence of some compounds in some source profiles. As a result, matrix Φ reduces to $0_{10\times 28}$.

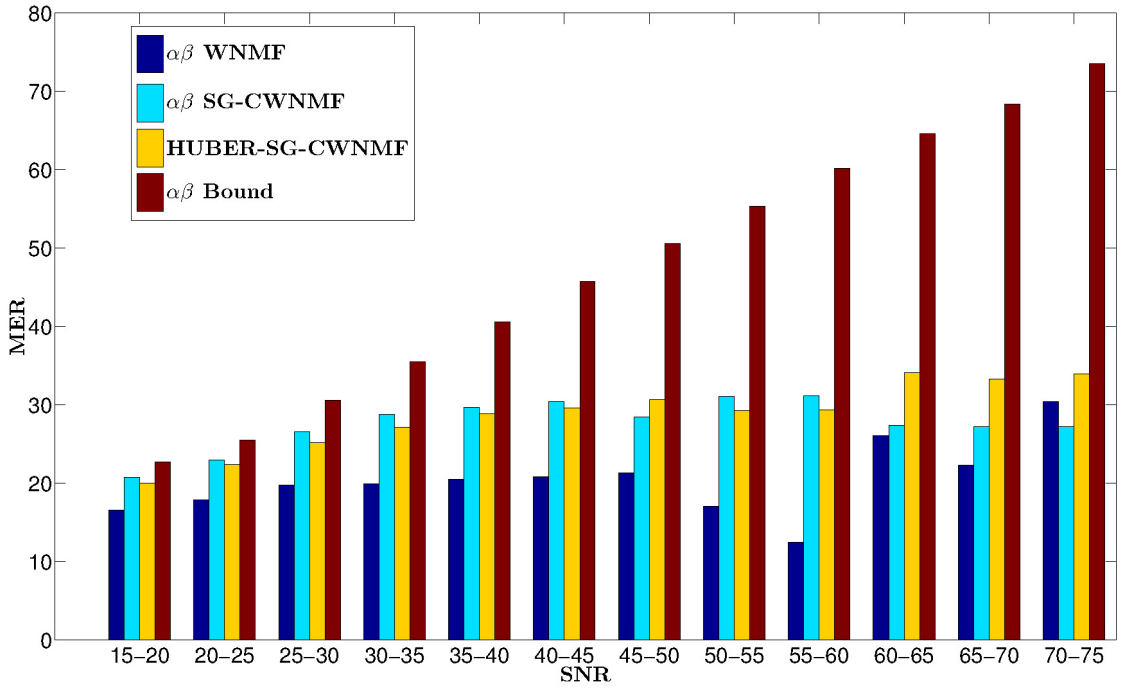

Figure 6.10 – MER versus input *SNR*. The case without outliers

6.8.3 Initialization

An approximate prior knowledge of F is used as a starting point for each informed NMF algorithm. Table (C.3) gathers the different entries used. Then, as described in the section (6.6), a quadratic estimation of the contribution matrix G is performed so that each method has the same initial factors.

6.8.4 Performance evaluation

In all the cases under study, the *MER* is represented as a function of the input *SNR*. In this study, intensive computations are made with 1 million iterations over a platform dedicated for parallel computing (`https://www-calculco.univ-littoral.fr/`). In our comparison, only 4 methods are selected; among them, 1 is uninformed, 1 accounts for the bound and 2 are our informed methods.

In our tests, the input *SNR* is ranging from 15 dB to 70 dB. The *MER* index is computed between the estimated contribution matrix and the exact contribution matrix G but it may also be computed for the comparison of the profile matrix F. Results are provided for *MER* into slices of 5 dB width. In our informed methods, the shift proposed hereafter is the second shift ($S2$), but this mention is dropped in the acronyms for clarity. Figure (6.10) shows the performance for the case without outliers while Figures (6.11,6.12,6.13) respectively describe the case of 5 outliers, 10 outliers and 20 outliers. It appears that rNMF [47] (not represented here) performs very poorly ($MER \approx 1dB$). Moreover, the bound is computed with an αβ-divergence cost function, and it is equivalent to semi NMF with an exact profile matrix. It turns out to be roughly equal to *SNR* in every case.

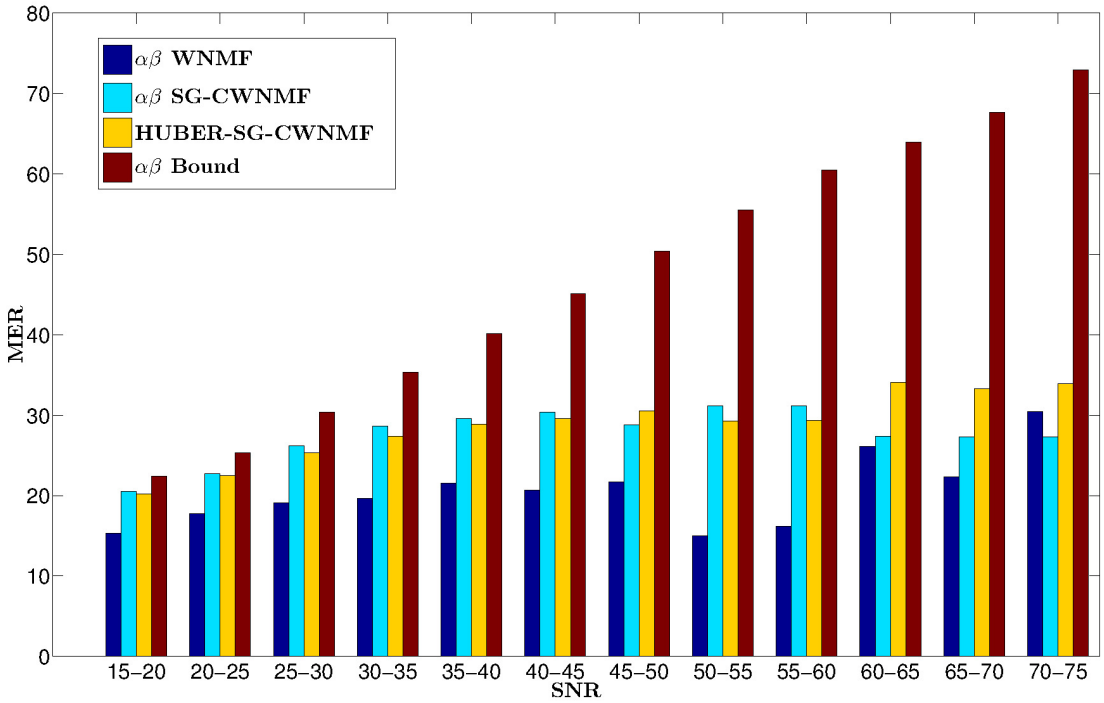

Figure 6.11 – MER versus input *SNR*. The case with 5 outliers

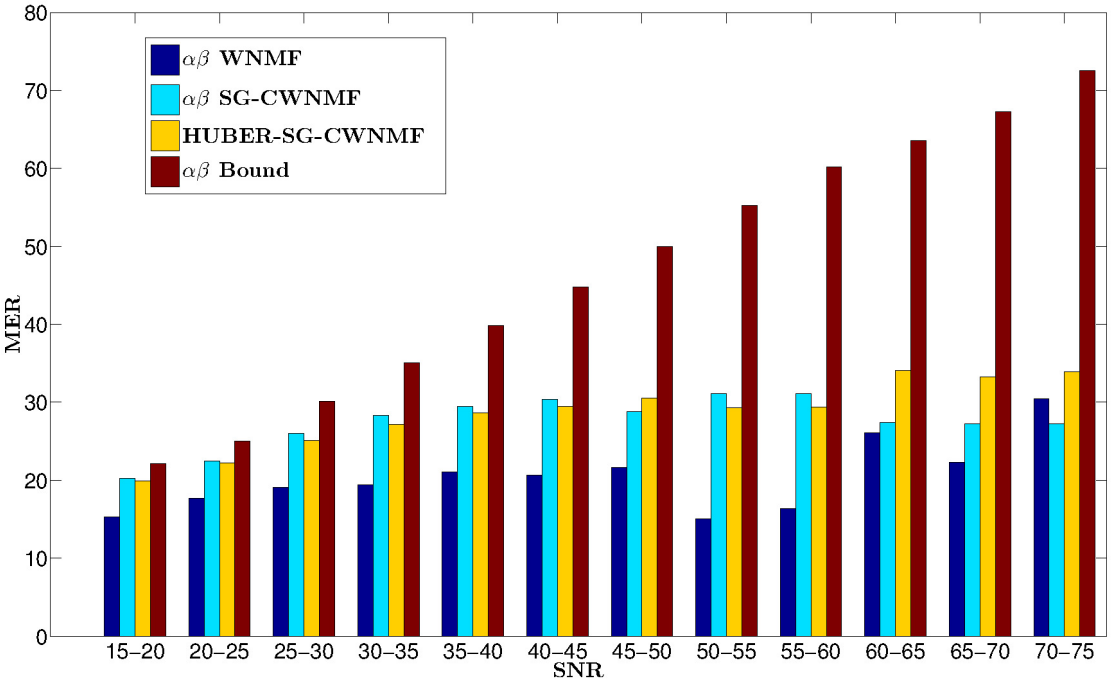

Figure 6.12 – MER versus input *SNR*. The case with 10 outliers

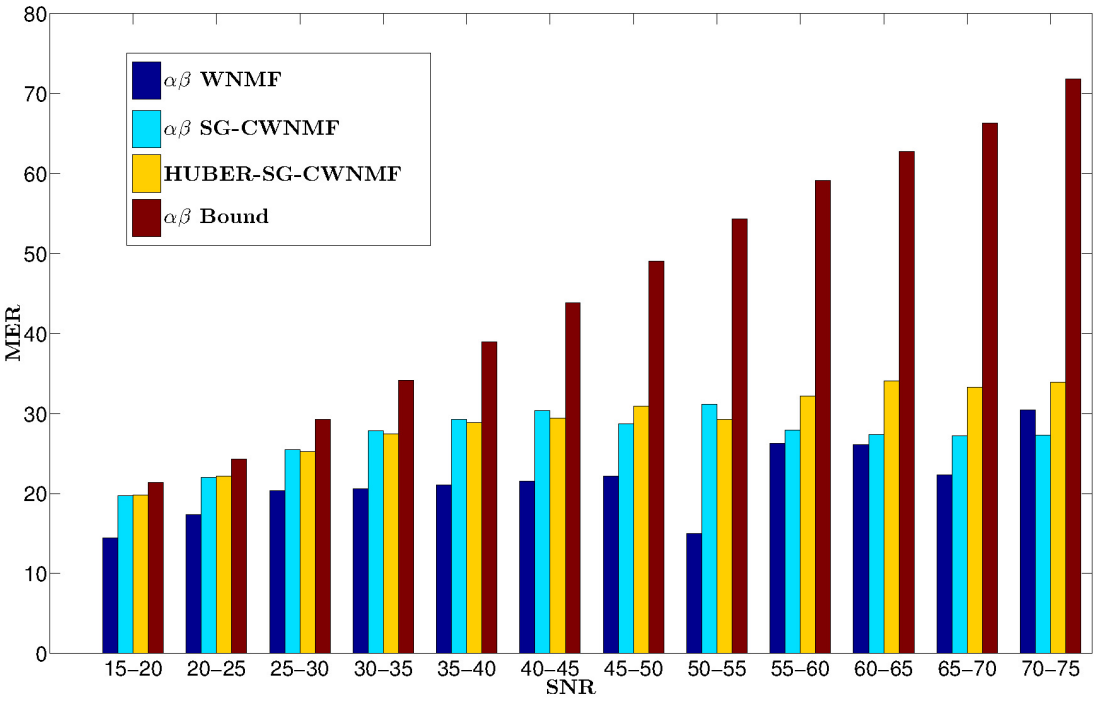

Figure 6.13 – MER versus input *SNR*. The case with 20 outliers

Besides, αβ-WNMF appears as the worst method except for a few slices ($70-75$ dB) in all cases. However, the number of outliers taken in account here does not affect the performance of the method, thus leading to its stability.

In addition to, 2 informed methods were experimented. First, αβ SG-CWNMF appears as a good method which behaves very similarly to the αβ Bound, but its performance decreases significantly for large *SNR*.

Second, Huber SG-CWNMF outperforms the other NMF methods for medium and large *SNR*, but is a bit less efficient for low *SNR*. Practically, it is to be noticed that several trials (among the list of low *SNR*) gave poor results for this method thus affecting the overall performance in this slice. These events cause the Huber method to drop by 1 dB in this slice regarding αβ SG-CWNMF. It seems that Huber SG-CWNMF seems more sensitive to the noise in low *SNR* than αβ-SG-CWNMF.

Finally, it seems that the overall effect of outliers seems limited here. However, the quality of the whole results is not completely satisfying. In light of the toy simulation, the performance of informed methods close to the αβ Bound is expected. From this point of view, this result seems a bit disappointing.

6.9 Real Data Case

The real data campaign has been conducted by Professor D. Courcot and F. Ledoux during C. Roche Phd thesis [4] [142], from the UCEIV laboratory (Université du Littoral Côte d'Opale). The first goal of this thesis was to provide ratios of trace species which are specific of some source profiles. Then, some flexible bound profiles and set profile entries were proposed. Using this knowledge, the challenge was to implement an informed NMF method–developed in [96]– in order to reconstruct the origin of Particulate Matter.

Contrary to [142], we would like here to drop the bound information and test whether the new methods are still competitive.

6.9.1 Context

A data campaign over a long period (16 months) in Le Cap Gris-Nez and over a shorter period in the port of Calais (3 months) enables to get 281 sample measurements collected with a DA80 sampler. Le Cap Gris-Nez is a rural site while Calais port is an urban site where a huge number of boats are docking. The DA80 device (6.14) is an equipment which is able to trap particulate matter on filters, which are stored and a posteriori analyzed by chemists. A special sieve enables to select only PM_{10} particulate matter, i.e., whose diameter is lower than $10\mu m$. The machine is also able to save wind conditions and time. The sampling period was chosen equal to 24 hours. Along this period, meteorological conditions concentration levels were highly varying. Thus, after analyzing the filters, several data files were available to address the pollution source apportionment problem.

6.9.2 Input Data

Appendix (D) provides operating conditions for the run performed. Based on expert knowledge provided by chemists and information described in table (6.5), it allows to specify matrix Ω which defines 55 set value locations (among 280 profile entries) provided in Table (D.2). In the same way as in (6.8), matrix Φ is equal to $0_{p\times m}$.

Moreover, the bound information provided in [142] is decided to be dropped, thus preventing to guide the run toward a consistent estimate with chemical expertise.

In addition to, an expert initial profile matrix is chosen and provided in Appendix (D).

6.9.3 Results evaluation

The results were obtained in the case of 10 identified sources and $1E6$ iterations for each method. Profiles under study were specified in Table (6.5). However, their estimation remains a difficult task

4. This thesis has been done in the frame of the ECUME project.

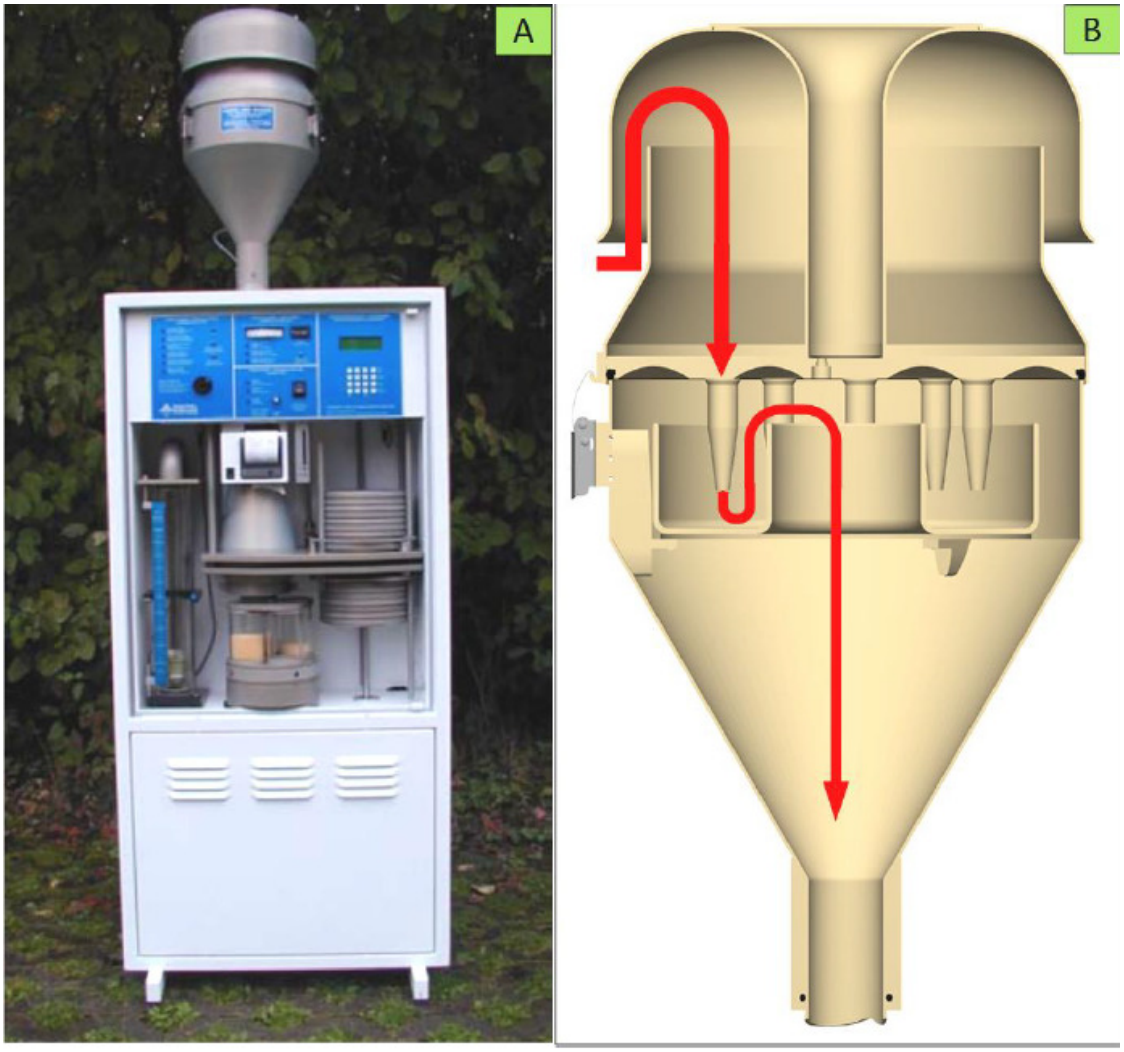

Figure 6.14 – Device used for sampling.

for several reasons listed hereafter

- Data are corrupted with an unknown number of outliers. Their origin may be of various kinds, such as the presence of a new source which affects the data at some sparse moments.
- an additional overall pollution which may not be assigned to a particular source.
- Some Source profiles may be geometrically close, only a few tracer species are able to distinguish them.
- Bounds (Except non-negativity) have been dropped in this study.

Even if a database with existing profiles is available at `http://source-apportionment.jrc.ec.europa.eu/Specieurope/sources.aspx`, the list of species under study are usually not the same leading to difficulties to build an appropriate profile matrix. So, it appears difficult to assess the quality of the results. It is decided to display the source profiles in a descending order of expected species. A correct source profile would be then displayed as decreasing proportions from the left to the right of each figure. On the contrary, a large proportion on the right of profile figure implies that the estimation has partly failed.

Table 6.6 – Performance evaluation of αβ SG-CWNMF.

Profiles	Max	Min	Comments
Crustal dust	SO_4^{2-}		SO_4^{2-} very close to the bound
Biomass combustion	NH_4^+		NH_4^+ very close to the bound
Road traffic	NO_3^-, OC	EC	very close to the bound
Sea traffic	EC	Fe	EC very close to the bound
Primary biogenic	Na^+, NO_3^-, SO_4^{2-}		P underestimated

Table 6.7 – Performance evaluation of the Huber SG-CWNMF method.

Profiles	Max	Min	Comments
Crustal dust	SO_4^{2-}	K^+	K^+ very close to the bound
Biomass combustion		Mg^{2+}	
Road traffic	NO_3^-, OC	EC	EC a bit low
Sea traffic	OC	Fe	OC very close to the bound
Primary biogenic	Na^+, SO_4^{2-}		P underestimated

The complete list of estimated profiles together with observations are provided in Appendix (D), only general results are discussed in this section. Roche's results [142] are denamed as αβ BN_2-CWNMF for αβ Bounded Constrained Weighted NMF in each profile figure of Appendix (D). In order to evaluate the consistency of the source profiles, the bounds provided in [142] are used to assess the consistency of our profiles together with Table (6.5). In [142], there were 67 bounds which were dropped here.

First, αβ WNMF presents 34 bounds inconsistencies over 67. In addition, species which are expected to be zero are not satisfied. Thus, this method turns out to fail completely. Second, αβ SG-CWNMF presents 10 entries outside of the bounds which are summarized in Table (6.6), 4 of which are very close to the proposed bound. So the method appears to be competitive with the one provided in [142].

Then, the last proposed method (Huber SG-CWNMF) appears to get 10 inconsistencies among 67 bounds. Among the 10 inconsistencies, 3 are very close to the proposed bound.

Moreover, our methods satisfy the major species described in Table (6.5). As a result, both informed methods (Huber SG-CWNMF, αβ SG-CWNMF) are behaving well with respect to the expected proportions in the overall profile matrix. To conclude, the new methods appear to outperform other state-of-the-art methods such as αβ WNMF or rNMF [47] and remains competitive with Bounded Weighted informed NMF [142] while dropping bounds information.

6.10 Conclusion

In this chapter, 3 informed non negative matrix factorization methods were developed, each of them were based on a specific cost function. The proposed methods naturally incorporate the expert knowledge such as set values (i.e., assign set values to some entries of the profile matrix) and the sum-to-one of each row of the profile matrix by taking into account a special parametrization. Contrary to chapter (5), the proposed updates remain always consistent with the constraints along iterations.

The first new proposed NMF approach is referred to as the Split Gradient Constrained Weighted NMF (SG-CWNMF) approach and update rules derive from the Split Gradient Framework. They can be viewed as multiplicative updates applied to the free component of the profile matrix. In that sense, SG-CWNMF approach is far more elegant than a previous method [99]—which sequentially tackles these constraints—and can be easily extended to a gradient-like technique, as in [91].

The second new informed proposed NMF method for the source apportionment problem is referred to as αβ Split Gradient Constrained Weighted NMF, i.e αβ SG-CWNMF. It is based on a weighted αβ-divergence cost function which is able to resist to outliers. Then, a general form of the update rules is derived heuristically by differentiating the weighted αβ divergence criterion with respect to the newly introduced matrix. By proposing a new analytic shift, new analytic update rules are proposed.

Finally, a third robust informed NMF method is proposed to address the source apportionment problem. This approach can be referred to as the Huber Split Gradient Constrained Weighted NMF (Huber SG-CWNMF). It is based on a weighted symmetric Huber cost function which adaptively switches between the weighted ℓ_2 and ℓ_1 norms according to the value of the computed residuals. A new shift enables to express analytical rules for the Huber case.

A validation has been performed in three different contexts. In the case of simulations, the MER index expressed in dB has been extensively used for the evaluation of the performance.

First, a toy simulation enables to validate each method in a noisy synthetic data case without outliers and then with outliers. The two robust methods (αβ SG- CWNMF, Huber SG- CWNMF) are shown in this case to outperform all the state-of-the-art methods. Moreover, our robust methods are very close to a bound computed with a robust regression method. In the case of αβ SG-CWNMF, the experiments were conducted on many couples of α β parameters and the focus afterwards is on the parameters which fit the situation. In addition, we tested different configurations of the cutoff parameter in Huber SG-CWNMF methods and an adaptive cutoff seems to work well in this context.

Second, a medium scale simulation inspired from real data has been conducted. It was built from the estimation of G and F obtained in [142]. Different situations with several outliers were explored in this case. It appeared that a large number of iterations was required in order to reach a limit point. It turns out that our robust informed methods were also outperforming αβ WNMF methods in each slice of input SNR and the MER index was expected to reach the input SNR as in the toy simulation but the MER was largely lower especially for large SNR.

Finally, a real data situation has been explored, by using data obtained in the work from Roche

[142] in the frame of the ECUME project. From the previous study, the number of iterations for all methods has been chosen equal to $1E6$. The validation process consisted in comparing the profile matrix with expected major species and bounds specification provided in [142]. It turns out also that $\alpha\beta$ WNMF was not able to provide a consistent estimation of the profile matrix. It appears also that our robust informed methods provide consistent results with the expected species and with the bounds. Moreover, it remains competitive with the method presented in [142] while dropping 67 bound constraints. As a consequence, our methods seem to be an interesting track for further real data analysis.

CHAPTER 7

General Conclusion

7.1 Outline of the thesis chapters

This thesis is divided into several parts. In the first part, sensors models are investigated as an important part of an acquisition process of a physical phenomenon. Besides, general mixtures models are reviewed with a special emphasis on linear mixture models which essentially govern air pollution problems. Then, a matrix factorization point of view is adopted to estimate factors present in the previous models. However, some additional information to the factorization are required to perform an estimation of factors. Typical properties encountered are independence, orthogonality, non-negativity and sum-to-1 of factors. In this thesis, the non-negativity together with row sum-to-1 properties are specifically highlighted.

In a second chapter, the concept of exact Non-negative Matrix Factorization (NMF) is first introduced which is closely related to the definition of Non-negative rank. Sufficient conditions for its uniqueness are formulated which connects to the concept of separability. Then, the problem of approximate factorization is expressed as an optimization problem whose local minima should satisfy KKT conditions. Solving such a NMF problem has attracted huge research interests over the last decades which gave rise to lots of algorithms. We reviewed here the most popular ones, among them, heuristic based NMF, multiplicative methods, gradient like NMF methods, ADMM and Bayesian methods.

In the chemical sensing community, data are associated with uncertainties which give rise to weighted NMF problems. Update rules for this problem are visited which may be viewed as an extension of classical NMF rules. From a general point of view, weights could play an important role in the case of abnormal data.

In the third chapter, the definition of outliers was introduced along with expected properties of robust algorithms. Robust statistics is usually addressed in the regression community in which M-estimators are widely used. As a consequence, robustness is often tackled in the NMF context either as a low rank plus sparse decomposition or by using modified cost functions which are belonging to the class of M-estimators. Several robust NMF methods are then investigated such as the Huber NMF, the Correntropy based NMF and the $\alpha\beta$-divergence NMF. Such a robust algorithm appears attractive but does not ensures alone to provide a realistic solution.

In order to limit the potential number of stationary points, the work then focuses on informed NMF with Sum-to-1 information and set values. This chapter reviews various existing solutions with inner specific normalizations which guarantee at convergence the satisfaction of the prior knowledge.

However, the current estimate at each iteration was not belonging to the subspace of the prior knowledge.

Then, in the last chapter, new informed NMF based methods are presented taking into consideration both sum-to-1 and set values at each iteration. Several weighted and robust cost functions were investigated and new update rules fulfilling the KKT conditions for each cost function were developed. Different versions of these solutions (Huber SG-CWNMF and $\alpha\beta$ SG-CWNMF) were presented according to the shift under consideration.

The experiments were conducted first on a small synthetic dataset in the presence of outliers. Extensive tests enable to show that both new methods outperform several state-of-the-art methods for a wide range of SNR with and without several outliers. The enhancement obtained is a few dB in low SNR while the gap for large SNR is much more significant.

A medium scale experimentation drawn for real dataset enables to build semi-synthetic data with and without outliers. Estimation of both factors appeared as a complex task provided that all methods have got difficulties to retrieve the factors. Our methods remain the best among state-of-the-art methods in every slice of SNR but the bound obtained through a regression method appears to be significantly better.

This medium scale simulation serves as a starting point for analyzing the real dataset obtained through ECUME project and performed in the area of Calais during a long period. The run have been evaluated with expected major species on one hand and bounds provided in [142] in the other hand. Our both robust methods seem to be consistent with these requirements and seem to be competitive with the one obtained in [142].

7.2 Perspectives and Future Work

However, even results along this thesis are promising results, real data situations call for further possible improvements provided along these tracks:

— One immediate perspective of this work would be to apply bound information in the iterative process of the new methods developed here. The development is straightforward and we could expect real improvements in the case of real data analysis.

— Then, new robust cost functions may be explored. In the case of α β-divergences, the parameters are selected so as to restore efficiently major species. Moreover, the value of the two parameters α and β are selected to respect the convexity of the cost function. As a result, the weighted α β-divergence is investigated in a limited domain in the NMF context. Thus, it could be envisaged to extend the Huber cost function by combining α β-divergence for small residuals and the ℓ_1 norm for high residuals. The cutoff parameter should be chosen at the inflection point of α β-divergence thus enabling to get extended convex cost functions for a wider domain of parameters α β.

— In the case of robust cost functions, Correntropy was discussed theoretically during this thesis. It was one of the cost function which goes to 1 when the residual goes to infinity. In this work, unbounded cost functions were tested while experiments were not conducted with such

bounded cost functions able to deal with outliers. Perhaps, it would be very interesting to develop new methods according to a weighted Correntropy together with flexible set values and row sum-to 1 profiles.

— The Bayesian context could be also one of the potential areas that could be further explored. However the usual Gaussian distribution of the noise should be dropped since outliers may be also modelled as a mixture of two probabilities densities thus making the problem more difficult. Moreover, chemical sensing data calls generally for individual uncertainties which does not fit with usual distributions. Besides, developing some prior probability densities which check the parametrization and then computing the posterior density becomes analytically impossible. The price for this kind of solution lies in the necessary intensive computations of multiple integrals which may be prohibitive. The benefit for this kind of approach may be to obtain several solutions which account for local minima of the posterior distribution. So, in the short term period, it is needed to first simplify the problem and to solve one discussed problem at a time.

— Lastly, some different kind of information in the profile matrix could be explored. Some knowledge may be modelled as known ratios of different entries of F which result in a different parametrization of the profile matrix. Since the parametrization could be flexible, this should be combined with the parametrization used along this thesis.

APPENDIX A

Karush-Kuhn-Tucker conditions for weighted Frobenius NMF with set values

---

First, the equivalent data as $R \triangleq X - G \cdot \Phi$ is defined. It will be used throughout this appendix. Solving Problem (5.28) leads to consider $\mathcal{J}(.)$, defined as,

$$\mathcal{J}(\triangle F) = Tr\left((R - G(\triangle F \circ \overline{\Omega}))'((R - G(\triangle F \circ \overline{\Omega})) \circ W)\right) = \mathcal{J}_1 - 2\mathcal{J}_2 + \mathcal{J}_3, \tag{A.1}$$

where

$$\left\{ \begin{array}{ll} \mathcal{J}_1 & = Tr(R'(R \circ W)) \\ \mathcal{J}_2 & = Tr\left((R \circ W)'G(\triangle F \circ \overline{\Omega})\right) \\ \mathcal{J}_3 & = Tr\left((\triangle F \circ \overline{\Omega})'G'((G(\triangle F \circ \overline{\Omega})) \circ W)\right) \end{array} \right. \tag{A.2}$$

Second, the following properties can be used

$$Tr(U^T(V \circ W)) = Tr((U \circ W)^T V). \tag{A.3}$$

and

$$Tr(V \circ W) = Tr(V^T W). \tag{A.4}$$

The differential of $\mathcal{J}_2$ may be formulated by relying on property (A.3),

$$\begin{aligned} \partial\mathcal{J}_2 &= \partial Tr\left((R \circ W)'G(\triangle F \circ \overline{\Omega})\right) = Tr\left((R \circ W)'\partial(G(\overline{\Omega} \circ \triangle F))\right) \\ &= Tr\left((R \circ W)'G \cdot \partial(\overline{\Omega} \circ \triangle F)\right) = Tr\left(((R \circ W)'G) \circ \overline{\Omega}')\partial\triangle F\right). \end{aligned} \tag{A.5}$$

The differentiation of $\mathcal{J}_2$ with respect to $\triangle F$ yields,

$$\frac{\partial\mathcal{J}_2}{\partial\triangle F} = \overline{\Omega} \circ (G'(R \circ W)). \tag{A.6}$$

In the same way, the differential of $\mathcal{J}_3$ gives

$$\begin{aligned} \partial\mathcal{J}_3 &= \partial Tr\left((\triangle F \circ \overline{\Omega})'G'[(G(\triangle F \circ \overline{\Omega}) \circ W]\right) \\ &= 2 \cdot Tr\left((W \circ G(\overline{\Omega} \circ \triangle F))'.G.(\overline{\Omega} \circ \partial\triangle F)\right). \end{aligned} \tag{A.7}$$

By using property (A.3), (A.7) may be expressed as,

$$\partial \mathcal{J}_3 = 2 \cdot Tr\left(\left(\left(W \circ G(\overline{\Omega} \triangle F)\right)'.G\right) \circ \overline{\Omega}'\right) \partial \triangle F\Big). \tag{A.8}$$

Similarly, the differentiation of $\mathcal{J}_3$ with respect to $\triangle F$ leads to

$$\frac{\partial \mathcal{J}_3}{\partial \triangle F} = 2[G'(W \circ (G(\overline{\Omega} \circ \triangle F)))] \circ \overline{\Omega}. \tag{A.9}$$

Using Eq. (A.6,A.9) enables to express the differentiation of the function $\mathcal{J}(.)$ as

$$\frac{\partial \mathcal{J}}{\partial \triangle F} = 2\overline{\Omega} \circ \left(G^T\left((G[\overline{\Omega} \circ \triangle F] - R) \circ W\right)\right). \tag{A.10}$$

The Lagrangian function is

$$\mathcal{L}(G,F) = \frac{1}{2}\mathcal{J}(\triangle F) - Tr(\Gamma_G \circ G) - Tr(\Gamma_F \circ \triangle F). \tag{A.11}$$

Cancelling the differentiation of the Lagrangien with respect to $\triangle F$ yields the following relationships,

$$\frac{\partial \mathcal{L}}{\partial \triangle F} = \overline{\Omega} \circ \left(G'\left((G[\overline{\Omega} \circ \triangle F] - R) \circ W\right)\right) - \Gamma_F = 0, \tag{A.12}$$

which provides the expression Γ_F. KKT conditions for solving Problem (5.28) are

$$\begin{array}{ll} \triangle F \succeq 0, & G \succeq 0, \\ \frac{\partial \mathcal{J}}{\partial \triangle F} \succeq 0, & \frac{\partial \mathcal{J}}{\partial G} \succeq 0, \\ \triangle F \circ \Gamma_F = 0, & G \circ \Gamma_G = 0. \end{array} \tag{A.13}$$

For a sake of clarity, let $F^* \triangleq \Omega \circ \Phi + \overline{\Omega} \circ \triangle F$. Replacing Eq (A.12) into Eq (A.13) and similarly for G, it is straightforward to get KKT conditions for the problem under consideration,e.g.,

$$\begin{array}{ll} \triangle F \succeq 0, & G \succeq 0, \\ \overline{\Omega} \circ \left(G^T\left((G \cdot (\overline{\Omega} \circ \triangle F) - R) \circ W\right)\right) \succeq 0, & (W \circ (G\widetilde{F} - X))F^* \succeq 0, \\ \triangle F \circ \overline{\Omega} \circ \left(G^T\left((G \cdot (\overline{\Omega} \circ \triangle F) - R) \circ W\right)\right) = 0, & G \circ \left((W \circ (GF^* - X))F^{*T}\right) = 0. \end{array} \tag{A.14}$$

APPENDIX B

Update rules for Weighted αβ-NMF with set entries.

This appendix is to provide a proof of the update rules for αβ-NMF with set values. For convenience, let λ be $\lambda \triangleq \alpha+\beta-1$.

Proposition B.0.1. *Update rules for the free part of the profile matrix are*

$$\triangle F^{k+1} \leftarrow \triangle F^{k} \circ \overline{\Omega} \circ N_F^{\alpha,\beta}(G^k, F^k), \tag{B.1}$$

where

$$N_F^{\alpha,\beta}(G,F) \triangleq \left[\frac{G^T\left(W \circ X^{\lambda} \circ R^{1-\beta} \circ (G\cdot(\triangle F))^{\beta-1}\right)}{G^T\left(W \circ X^{\lambda} \circ R^{-\lambda} \circ (G\cdot(\triangle F))^{\lambda}\right)} \right]^{(\frac{1}{\alpha})} \tag{B.2}$$

Proof. A column of the data is considered since the divergence may be split into independent partial divergences. Let k be the current iteration index. Expression (5.41) is incorporated with Eq. (5.40) provide

$$\mathcal{D}_{\underline{w}}^{\alpha,\beta}(\underline{x} \parallel G\underline{\varphi} + G\triangle\underline{f}) = \mathcal{D}_{\underline{w}}^{\alpha,\beta}(\underline{x} \parallel G\underline{\varphi} + U\underline{\theta}). \tag{B.3}$$

The weighted αβ-divergence between two corresponding column vectors is defined as

$$\mathcal{D}_{\underline{w}}^{\alpha,\beta}(\underline{x} \parallel G\underline{f}) = \sum_i w_i x_i^{\alpha+\beta} h^{\alpha,\beta}\left(\frac{(G\underline{\varphi})_i + \sum_j u_{ij}\theta_j}{x_i}\right) \tag{B.4}$$

where $\quad \forall(\alpha,\beta,\alpha+\beta) \neq 0,$

$$h^{\alpha,\beta}(z) \triangleq \frac{1}{\alpha\beta}\left[\frac{\alpha}{\alpha+\beta} + \frac{\beta}{\alpha+\beta} z^{\alpha+\beta} - z^{\beta}\right]. \tag{B.5}$$

Noticing that $h^{\alpha,\beta}(z)$ is convex for $z \geq 0$ and $\beta \in [\min(1,1-\alpha); \max(1,1-\alpha)]$ [27] and provided that $h^{\alpha,\beta}(1) = 0$, Jensen's inequality may be applied twice, e.g.,

$$h^{\alpha,\beta}\left(\frac{(G\underline{\varphi})_i + \sum_j u_{ij}\theta_j}{x_i}\right) \leq \frac{r_i}{x_i} h^{\alpha,\beta}\left(\frac{\sum_j u_{ij}\theta_j}{r_i}\right) \tag{B.6}$$

and

$$h^{\alpha,\beta}\left(\frac{\sum_j u_{ij}\theta_j}{r_i}\right) \leq \sum_j \frac{u_{ij}\theta_j^k}{\sum_l u_{il}\theta_l^k} h^{\alpha,\beta}\left(\frac{\theta_j \sum_l u_{il}\theta_l^k}{r_i \theta_j^k}\right), \tag{B.7}$$

where the superscript k is the current iteration number and θ_j is the j-th element of the free parameters vector $\underline{\theta}$ introduced in Eq. (5.40). Equation (B.4) with Expressions (B.6) and (B.7) yield the following auxiliary function:

$$\mathcal{H}_{2,w}^{\alpha,\beta}(\theta_j,\theta_j^k)=\sum_i w_i x_i^{\alpha+\beta-1} r_i \sum_j \frac{u_{ij}\theta_j^k}{\sum_l u_{il}\theta_l^k}\cdot h^{\alpha,\beta}\left(\frac{\theta_j \sum_l u_{il}\theta_l^k}{r_i \theta_j^k}\right). \tag{B.8}$$

The cancelation of its gradient $\frac{\partial \mathcal{H}_{2,w}^{\alpha,\beta}(\theta_j,\theta_j^k)}{\partial \theta_j}$ leads to the optimum, i.e.,

$$\left(\frac{\theta_j}{\theta_j^k}\right)^{\alpha}=\frac{\sum_i w_i u_{ij} r_i^{1-\beta} x_i^{\lambda}(\sum_l u_{il}\theta_l^k)^{\beta-1}}{\sum_i w_i u_{ij} x_i^{\lambda} r_i^{-\lambda}(\sum_l u_{il}\theta_l^k)^{\lambda}}, \tag{B.9}$$

which is expressed in its vector form as

$$\left(\frac{\underline{\theta}}{\underline{\theta}^k}\right)^{\alpha}=\frac{U^T[\underline{w}\circ\underline{x}^{\lambda}\circ\underline{r}^{1-\beta}\circ(U\underline{\theta}^k)^{\beta-1}]}{U^T[\underline{w}\circ\underline{x}^{\lambda}\circ\underline{r}^{-\lambda}\circ(U\underline{\theta}^k)^{\lambda}]}. \tag{B.10}$$

By combining Eq. (5.40) with the above relationship, the expression of one column of the matrix $\triangle F$ is derived :

$$\frac{\triangle \underline{f}^{k+1}}{\triangle \underline{f}^{k}}=\left[\frac{\Gamma U^T[\underline{w}\circ\underline{x}^{\lambda}\circ\underline{r}^{1-\beta}\circ(U\underline{\theta}^k)^{\beta-1}]}{\Gamma U^T[\underline{w}\circ\underline{x}^{\lambda}\circ\underline{r}^{-\lambda}\circ(U\underline{\theta}^k)^{\lambda}]}\right]^{\frac{1}{\alpha}}. \tag{B.11}$$

By replacing U according to Eq. (5.41), and by noticing that $\Gamma\Gamma^T=\mathrm{diag}(\overline{\underline{\omega}}^E)$, it results in the new update rule:

$$\triangle \underline{f}^{k+1}\leftarrow \triangle \underline{f}^{k}\circ\overline{\underline{\omega}}\circ N_{\underline{f}^k}, \tag{B.12}$$

where

$$N_{\underline{f}^k}\triangleq\left(\frac{G^T\left[\underline{w}\circ\underline{x}^{\lambda}\circ\underline{r}^{1-\beta}\circ(G\triangle\underline{f}^k)^{\beta-1}\right]}{G^T\left[\underline{w}\circ\underline{x}^{\lambda}\circ\underline{r}^{-\lambda}\circ(G\triangle\underline{f}^k)^{\lambda}\right]}\right)^{\frac{1}{\alpha}}. \tag{B.13}$$

Similarly to [100], the update rules can be derived by writing the matrix form of Eq. (B.13), and that completes the proof. □

APPENDIX C

Operating conditions for the medium scale experimentation

C.1 Profile matrix

Table (C.1) specifies the different entries of the true profile matrix for the medium scale experimentation.

C.2 Prior information

Prior information is provided through the specification of both Ω (C.2) and Φ. We choose to select only set values which specify the absence of some species in the profile matrix. As a consequence, Φ is equal to $\Phi = 0_{p \times m}$.

C.3 Initial Profile matrix.

The chemists are able to provide an initial profile matrix given in Table (C.3). It is to be noted that the same initial matrix is applied for informed and uninformed methods. The quantity $1,00E-11$ is chosen because uninformed methods are starting approximately with the same profile even if set values are applied to this entry.

Table C.1 – Exact Source Profile

Profiles	Al	Cr	Fe	Mn	P	Sr	Ti	Zn	V	Ni	Co	Cu	Cd	Sb
Sea	0,0019	0	0	0	0,00025	0,2034	0	0	0	0	0	0	0	0
Aged sea	0	7,2351E-05	0	0	0,5	0,4	1,877E-4	0	0	0	0,0001785	1,7941E-05	0	0
Crustal	119,13	8,589E-05	77,35	1,782	3,0680	0,7846	8,9121	1,868	0,3503	0	0,0276	0,0081	0	0
nitrates	4,00E-03	2E-05	3,5	0,11	0,0749	0	0	0,7742	0	0	7,0408E-04	0,1	6,486E-03	0,01975
sulfate	0	5E-05	0	0,02825	0,05313	0	0	0,1334	0	0	0,003287	8,00E-06	0	0
Biomass	0,001	0	2,554	0,05527	0	1,016E-05	0	0,1415	0	0	0	0	0	0,0385
Road traffic	0	0	39,0414	0,1404	2,659	0	0	10,908	0	0	1,00E-08	2,7712	0	0,8964
Sea traffic	0,001147	1,2012E-04	0,1002	0	0	0,0217	9,42E-05	0	7,4920	5,5348	0,1829	1,752E-04	1,315E-06	0
Biogenic	0	0	0	0	14,528	0,04308	8,941E-04	0	0	0	0	0	0	5,2E-04
Metal	64,430	33,332	780,16	33	0,7	2	0	0	0	10	0,15	1,5	1,55	0
Bis	La	Pb	Na^+	NH_4^+	K^+	Mg^{2+}	Ca^{2+}	Cl^-	NO_3^-	SO_4^{2-}	OC	EC	Levo.	Polyols
Sea	0	0	297,03	0	10,71	32,75	9,183	581,02	0	69,08	0	0	0	0
Aged sea	0	0,1	280	0	4	30	10	1,00E+02	395	150	30	0	0	0
Crustal	0,0594	0	1,8333E-04	4,36E-05	5	5	301,81	0	49,95	39,96	384,92	0	0	0
nitrates	7,178E-4	0,2075	0	216,26	3,2	0	0	1,21E-05	730,73	0	45	0	0	9,027E-11
sulfate	0	0,0729	0	260,83	4,43	0	0	8,66E-08	0	680,59	53,84	0	0	0
Biomass	0	0,1007	2,650	2,85E-12	12,26	0,001	11,67	25,48	35,16	56,84	692,10	91,14	69,78	1,477E-07
Road traffic	0,0121	3,353	0	5,14E-010	39,84	0	3,00E-08	3,40E-08	50,19	60,22	301,13	488,81	0	0
Sea traffic	0,0941	0	0	0,0626	0	0	0	0	75,17	300,69	500,76	109,87	0	0
Biogenic	0	0	5,023	0,0968	29,056	0	0	0,2975	0	20,094	854,02	0	0	76,83
Metal	0,2215	22,95	0	0	0	0	0	0	0	50,00	0	0	0	0

Table C.2 – Matrix Ω

Ω	Al	Cr	Fe	Mn	P	Sr	Ti	Zn	V	Ni	Co	Cu	Cd	Sb
Sea	0	1	1	1	0	0	1	1	1	1	1	1	1	1
Aged sea	1	0	1	1	0	0	0	1	1	1	0	0	1	1
Crustal	0	0	0	0	0	0	0	0	0	1	0	0	1	1
nitrates	0	0	0	0	0	1	1	0	1	1	0	0	0	0
sulfate	1	0	1	0	0	1	1	0	1	1	0	0	1	1
Biomass	0	1	0	0	1	0	1	0	1	1	1	1	1	0
Road traffic	1	1	0	0	0	1	1	0	1	1	0	0	1	0
Sea traffic	0	0	0	1	1	0	0	1	0	0	0	0	0	1
Biogenic	1	1	1	1	0	0	0	1	1	1	1	1	1	0
Metal	0	0	0	0	0	0	1	1	1	0	0	0	0	1
	La	Pb	Na^+	NH_4^+	K^+	Mg^{2+}	Ca^{2+}	Cl^-	NO_3^-	SO_4^{2-}	OC	EC	Levo.	Polyols
Sea	1	1	0	1	0	0	0	0	1	0	1	0	1	1
Aged sea	1	0	0	1	0	0	0	0	0	0	0	1	1	1
Crustal	0	0	0	0	0	0	0	1	0	0	0	1	1	1
nitrates	0	0	1	0	0	0	1	0	0	1	0	0	1	0
sulfate	1	0	1	0	0	0	1	0	1	0	0	0	1	1
Biomass	1	0	0	0	0	0	0	0	0	0	0	0	0	0
Road traffic	0	0	1	0	0	1	0	0	0	0	0	0	1	1
Sea traffic	0	0	1	0	1	0	1	0	0	0	0	0	1	1
Biogenic	1	1	0	0	0	0	1	0	0	0	0	1	1	0
Metal	0	0	1	0	1	0	1	1	1	0	1	1	1	1

Table C.3 – Matrix F_{init}

F_{init}	Al	Cr	Fe	Mn	P	Sr	Ti	Zn	V	Ni	Co	Cu	Cd	Sb
Sea	0,2	1,00E-11	1,00E-11	1,00E-11	0,01	0,8	1,00E-11	1,00E-11	1,00E-11	1,00E-11	1,00E-11	1,00E-11	1,00E-11	1,00E-11
Aged sea	1,00E-11	0,001	1,00E-11	1,00E-11	1	1	0,01	1,00E-11	1,00E-11	1,00E-11	0,01	0,01	1,00E-11	1,00E-11
Crustal	200	0,001	150	2	2	2	20	2	2	1,00E-11	0,001	0,0001	1,00E-11	1,00E-11
nitrates	1,00E-05	2,00E-006	8	1	0,4	1,00E-11	1,00E-11	4	1,00E-11	1,00E-11	0,001	0,5	0,01	0,2
sulfate	1,00E-11	1,00E-004	1,00E-11	1,00E-004	0,5	1,00E-11	1,00E-11	0,4	1,00E-11	1,00E-11	0,01	1,00E-004	1,00E-11	1,00E-11
Biomass	5	1,00E-11	10	2	9,43E-11	0,001	1,00E-11	1	1,00E-11	1,00E-11	1,00E-11	1,00E-11	1,00E-11	1,006E-10
Road traffic	1,00E-11	1,00E-11	50	1	1,00E+00	1,00E-11	1,00E-11	24	1,00E-11	1,00E-11	1,00E-011	4	1,00E-11	2
Sea traffic	0,01	1,00E-004	0,4	1,00E-11	1,00E-11	0,1	1,00E-004	1,00E-11	18	10	1	1,00E-003	1,00E-004	1,00E-11
Biogenic	1,00E-11	1,00E-11	1,00E-11	1,00E-11	5	7,96E-10	7,96E-10	1,00E-11	1,00E-11	1,00E-11	1,00E-11	1,00E-11	1,00E-11	7,96E-10
Metal	73	70	650	50	3	5	1,00E-11	1,00E-11	1,00E-11	30	1	3	4	1,00E-11
	La	Pb	Na^+	NH_4^+	K^+	Mg^{2+}	Ca^{2+}	Cl^-	NO_3^-	SO_4^{2-}	OC	EC	Levo.	Polyols
Sea	1,00E-11	1E-09	320	5E-05	10	38	11	550	1E-05	70	1E-05	1E-05	9,98E-11	9,98E-11
Aged sea	1,00E-11	0,01	250	1E-08	1	40	15	150	320DA80.eps	210	12	1,00E-011	9,99E-11	9,99E-11
Crustal	0,0001	1E-07	0,0001	0,0001	10	10	250	1,00E-011	30	30	290	1,00E-011	1,00E-10	1,00E-10
nitrates	0,2	0,5	1E-10	300	5	1,00E-011	1,00E-011	0,2	600	1,00E-011	80	1,00E-011	1,00E-10	1,00E-10
sulfate	1,00E-11	0,1	1,00E-008	305	10	1,00E-011	1,00E-011	1,00E-003	1,00E-011	584	100	1,00E-011	1,00E-10	1E-11
Biomass	1,00E-11	1	3	28	72	5	38	66	66	66	510	70	57	9,43E-11
Road traffic	1	9,99	1,00E-10	1,00E-008	57	0,00049	1,00E-006	1,00E-011	79,99	80	260	430	9,99E-11	9,99E-11
Sea traffic	0,5	1,00E-8	1E-11	1,00E-2	1E-11	1E-11	1,00E-11	1E-11	110	250	450	160	8,37E-11	8,37E-11
Biogenic	1,00E-11	7,96E-10	1	1	9	4	1,00E-11	7,96E-10	5	5	800	1E-11	7,96E-10	170
Metal	1	40	1,00E-11	1,00E-2	1,00E-11	1,00E-2	1,00E-11	0,005	0,001	70	0,00164	1,64E-10	1,64E-10	1,64E-10

APPENDIX D

Operating conditions for the real data case and results

D.1 Initial Profile matrix.

The chemists are able to provide an initial profile matrix given in Table (D.1). It is to be noted that the same initial matrix is applied for informed and uninformed methods. ε is a very small quantity to make the initialization very close to the case of informed methods where set values are zeros.

D.2 Prior information

Prior information is provided through the specification of both Ω (D.2) and Φ. The set value configuration is the same as those presented in [142]. As a consequence, Φ is equal to $\Phi = 0_{p\times m}$.

D.3 Presentation of the profile estimation

This section provides a complete list of estimated profiles. Figure (D.1) shows the different proportions of species present in the rich metal source. Our new methods are consistent with major species described in Table (6.5) while αβ WNMF provides some inconsistencies. There is a small overestimation of Phosphorus species in our αβ SG-CWNMF and Huber SG-CWNMF methods.

Figure (D.2) displays the profile of the primary biogenic source. αβ SG-CWNMF and Huber SG-CWNMF are satifying the requirement for major species but present some overestimation of species Na^{+}, $\mathrm{SO}_4^{2-}$and NO_3^{-}. On the contrary to Figure (D.1), there is a slight underestimation of Phosphorus species in our αβ SG-CWNMF and Huber SG-CWNMF methods. (D.3) displays the profile of the Sea Traffic source. αβ SG-CWNMF and Huber SG-CWNMF are satisfying the requirements for main species except for OC, $\mathrm{Fe}$for Huber SG-CWNMF and EC and $\mathrm{Fe}$for αβ SG-CWNMF. Figure (D.4) displays the profile of the Road Traffic source. αβ SG-CWNMF and Huber SG-CWNMF are satisfying the requirements for main species except for NO_3^{-}or EC and EC. Figure (D.5) displays the profile of the biomass source. αβ SG-CWNMF and Huber SG-CWNMF are consistent with the expected species except for NH_4^{+} for αβ SG-CWNMF and $\mathrm{Mg}^{2+}$for Huber SG-CWNMF. Figure (D.6) shows the profile of the secondary sulfate source. αβ SG-CWNMF and Huber SG-CWNMF are consistent

Table D.1 – Matrix F_{init}

F_{init}	Al	Cr	Fe	Mn	P	Sr	Ti	Zn	V	Ni	Co	Cu	Cd	Sb
Sea	0,19	ε	ε	ε	1,00	8,00	ε	ε	ε	ε	ε	ε	ε	ε
Aged sea	0,10	0,01	0,50	0,01	1,00	8,00	0,02	0,02	ε	ε	1,00	0,01	0,01	0,01
Crustal	266,67	0,14	150	2,00	ε	2,00	20	0,50	0,50	0,07	0,07	0,07	ε	0,01
nitrates	0,98	0,98	30	0,98	ε	0,98	0,98	20	ε	0,98	0,98	10	0,98	0,98
sulfate	1,00	1,00	30	1,00	ε	1,00	15,00	20	ε	1,00	1,00	1,00	1,00	1,00
Biomass	4,00	ε	9,00	1,00	ε	1,00	1,00	10	ε	ε	ε	1,00	ε	ε
Road traffic	20	1,00	50	5,00	ε	1,00	ε	50	5,00	10	5,00	50	5,00	50
Sea traffic	10	ε	10	ε	ε	ε	ε	5,00	55,00	55,00	30	ε	ε	ε
Biogenic	0,01	ε	0,01	ε	20	ε	ε	ε	ε	ε	ε	1,00	ε	ε
Metal	80	80	358	40	8	18,00	40	40	30	30	1,00	40	50	30
	La	Pb	Na^+	NH_4^+	K^+	Mg^{2+}	Ca^{2+}	Cl^-	NO_3^-	SO_4^{2-}	OC	EC	Levo.	Polyols
Sea	ε	ε	320,00	ε	10,00	40,00	10,00	540,08	ε	70,00	0,64	0,09	ε	ε
Aged Sea	ε	0,01	250,00	ε	10,00	25,00	10,00	200,00	275,30	210,00	8,00	1,00	ε	ε
Crustal	ε	0,14	10,00	3,00	100,00	70,14	210,00	7,00	20,00	35,07	90,00	12,62	ε	ε
nitrates	ε	0,98	ε	200,00	0,98	0,98	40,00	0,98	547,30	ε	100,00	40,00	ε	ε
sulfate	ε	20,00	ε	200,00	34,00	1,00	40,00	1,00	ε	554,00	60,00	16,00	ε	ε
Biomass	0,00	0,94	2,83	28,31	70,00	4,72	37,74	66,05	70,00	66,05	500,61	69,29	56,46	ε
Road traffic	ε	10,00	ε	10,00	10,00	ε	21,00	2,00	80,00	40,00	271,73	303,27	ε	ε
Sea traffic	15,00	10,00	ε	10,00	ε	ε	20,00	ε	10,00	30,00	580,00	160,00	ε	ε
Biogenic	ε	ε	1,00	1,00	5,00	4,00	1,00	ε	5,00	5,00	760,00	50,00	ε	146,98
Metal	1,00	80,00	ε	1,00	48,00	10,00	5,00	ε	ε	10,00	ε	ε	ε	ε

Table D.2 – Matrix Ω

Ω	Al	Cr	Fe	Mn	P	Sr	Ti	Zn	V	Ni	Co	Cu	Cd	Sb
Sea	0	1	0	1	0	0	1	1	1	1	1	1	1	1
Aged sea	0	0	0	0	0	0	0	0	1	1	0	0	0	0
Crustal	0	0	0	0	0	0	0	0	0	0	0	0	0	0
nitrates	0	0	0	0	0	0	0	0	1	0	0	0	0	0
sulfate	0	0	0	0	0	0	0	0	1	0	0	0	0	0
Biomass	0	1	0	0	0	0	0	0	1	1	0	0	0	0
Road traffic	0	0	0	0	0	0	0	0	0	0	0	0	0	0
Sea traffic	0	0	0	0	0	0	0	0	0	0	0	0	0	0
Biogenic	0	0	0	1	0	0	0	0	1	1	0	0	1	0
Metal	0	0	0	0	0	0	0	0	0	0	0	0	0	0
	La	Pb	Na^+	NH_4^+	K^+	Mg^{2+}	Ca^{2+}	Cl^-	NO_3^-	SO_4^{2-}	OC	EC	Levo.	Polyols
Sea	1	1	0	1	0	0	0	0	1	0	0	0	1	1
Aged sea	0	0	0	1	0	0	0	0	0	0	0	0	1	1
Crustal	0	0	0	0	0	0	0	0	0	0	0	0	1	1
nitrates	0	0	1	0	0	0	0	0	0	1	0	0	1	0
sulfate	0	0	1	0	0	0	0	0	1	0	0	0	1	0
Biomass	0	0	0	0	0	0	0	0	0	0	0	0	0	0
Road traffic	0	0	1	0	0	1	0	0	0	0	0	0	1	1
Sea Traffic	0	0	1	0	0	0	0	0	0	0	0	0	1	1
Biogenic	1	1	0	0	0	0	0	0	0	0	0	0	1	0
Metal	0	0	1	0	0	0	0	1	1	0	1	1	1	1

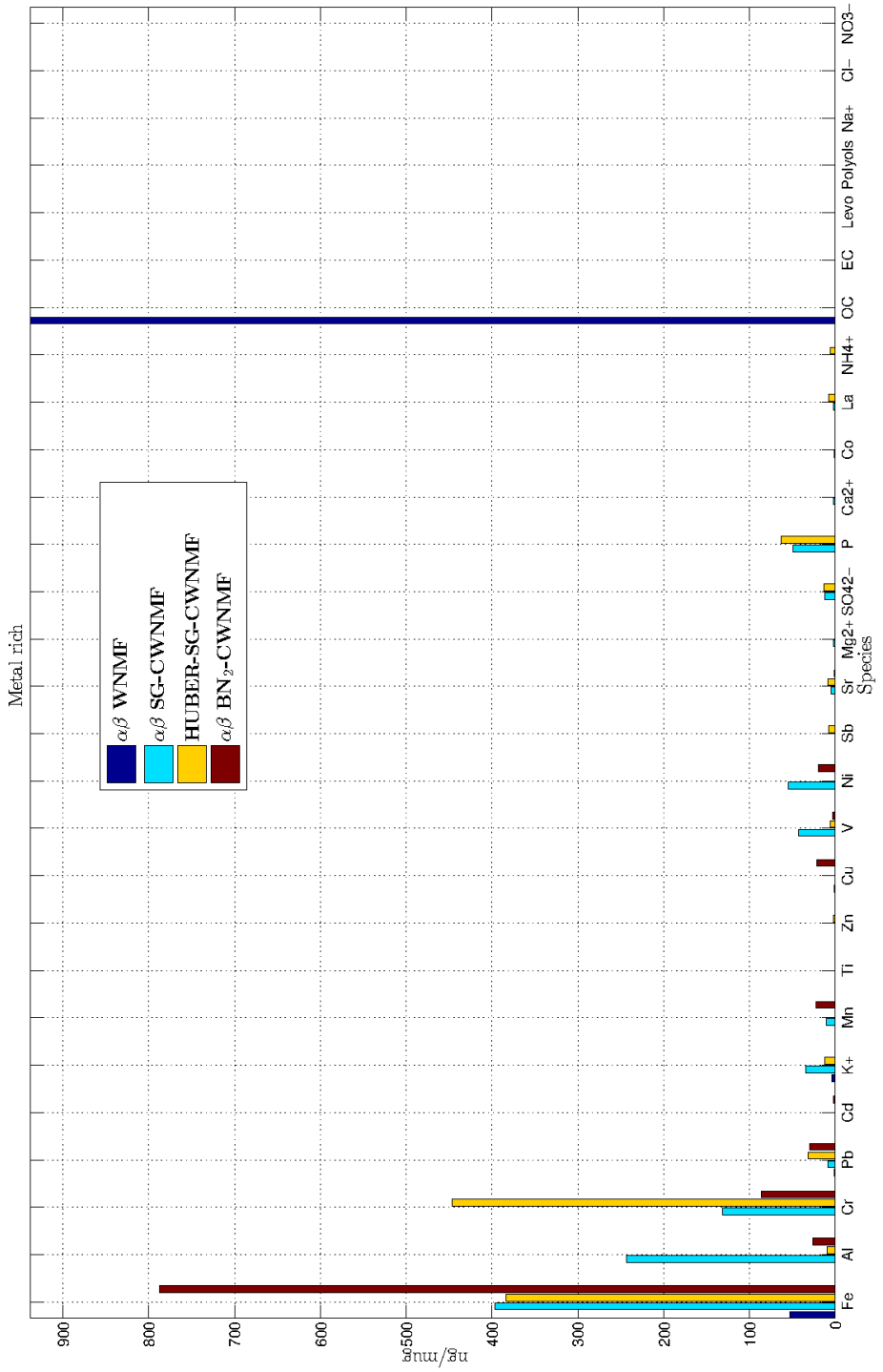

Figure D.1 – Estimation of the metal rich source profile.

with all the expected species. Figure (D.7) shows the profile of the secondary nitrate source. αβ SG-CWNMF and Huber SG-CWNMF are consistent with all the expected species. Figure (D.8)

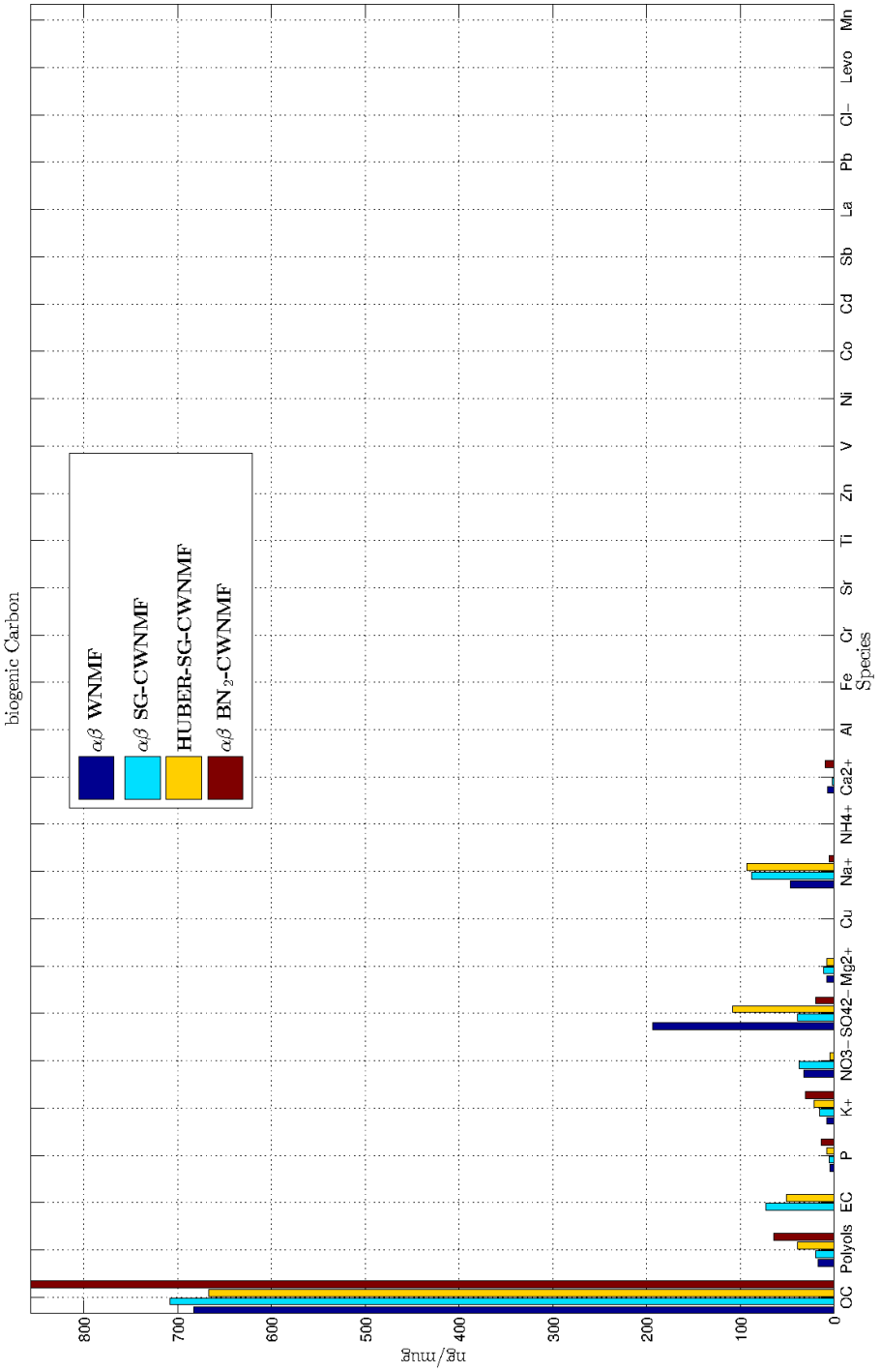

Figure D.2 – Estimation of the Primary biogenic source.

shows the profile of the crustal dust source. αβ SG-CWNMF and Huber SG-CWNMF are consistent with the main expected species except for $SO_4^{2-}$for both methods and $K^+$for Huber SG-CWNMF. Figure (D.9) shows the profile of the Aged sea source. αβ SG-CWNMF and Huber SG-CWNMF

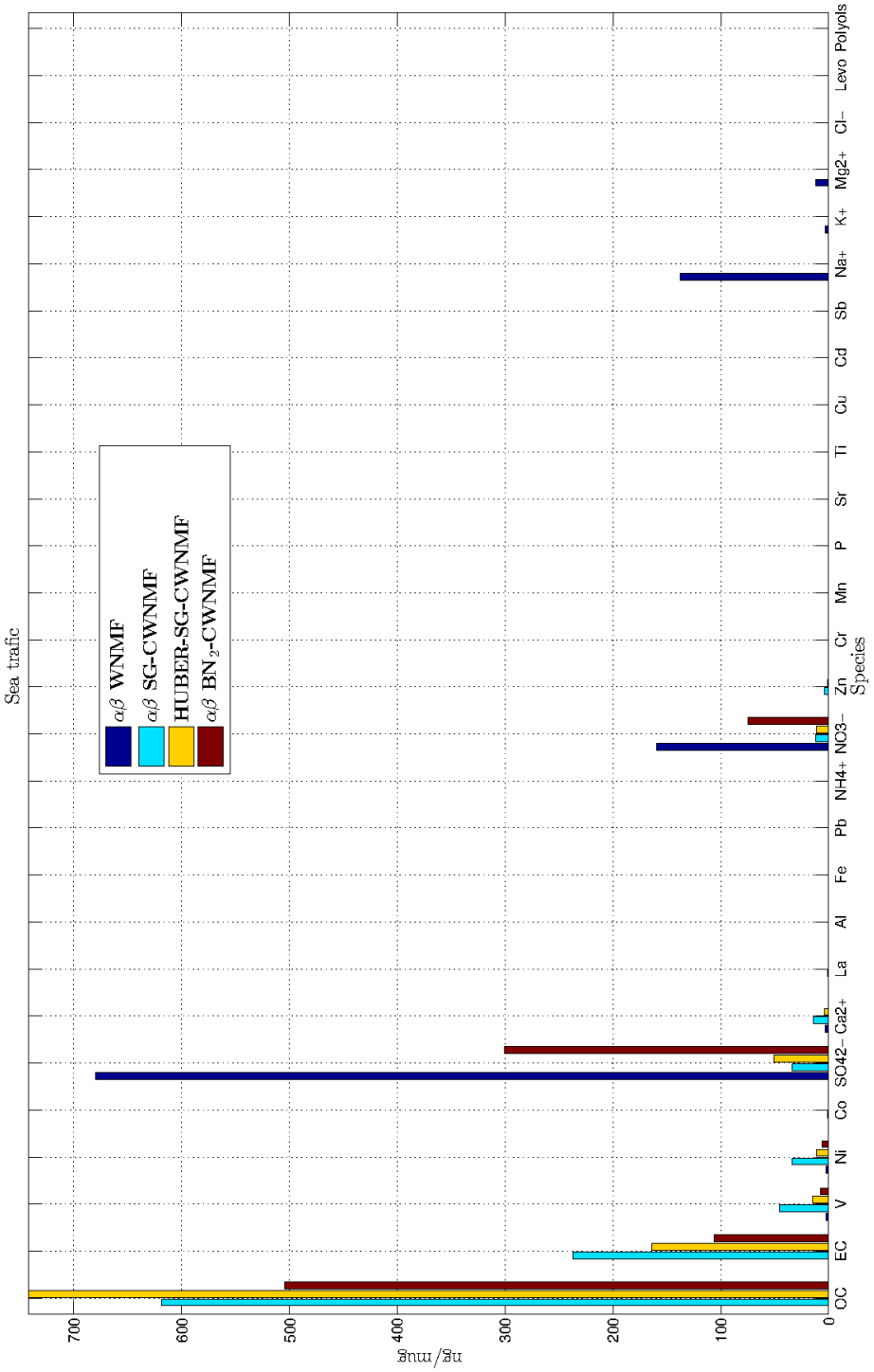

Figure D.3 – Estimation of the Sea traffic source profile.

are consistent with all the expected species. Figure (D.10) shows the profile of the sea source. αβ SG-CWNMF and Huber SG-CWNMF are consistent with all the expected species.

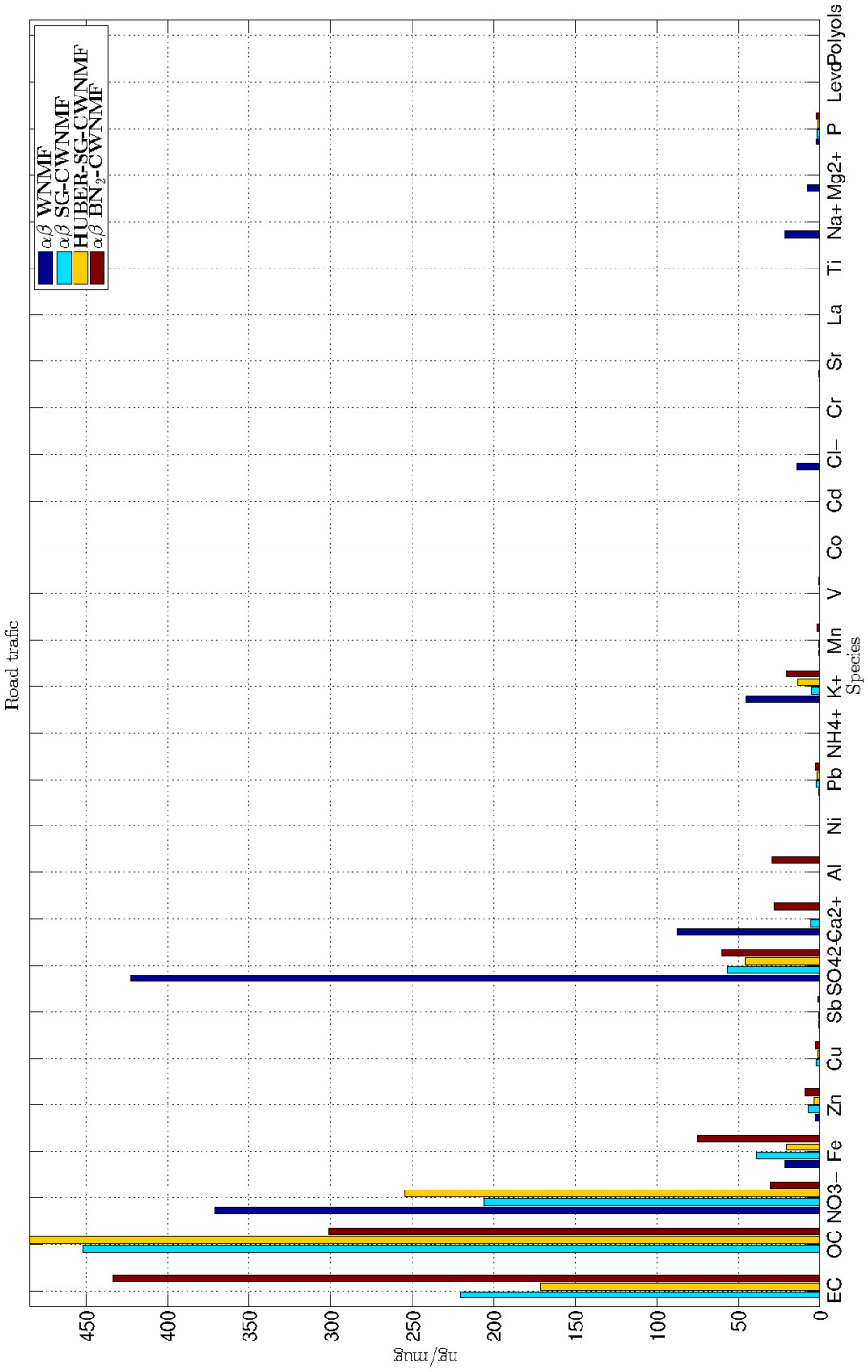

Figure D.4 – Estimation of the Road traffic source profile.

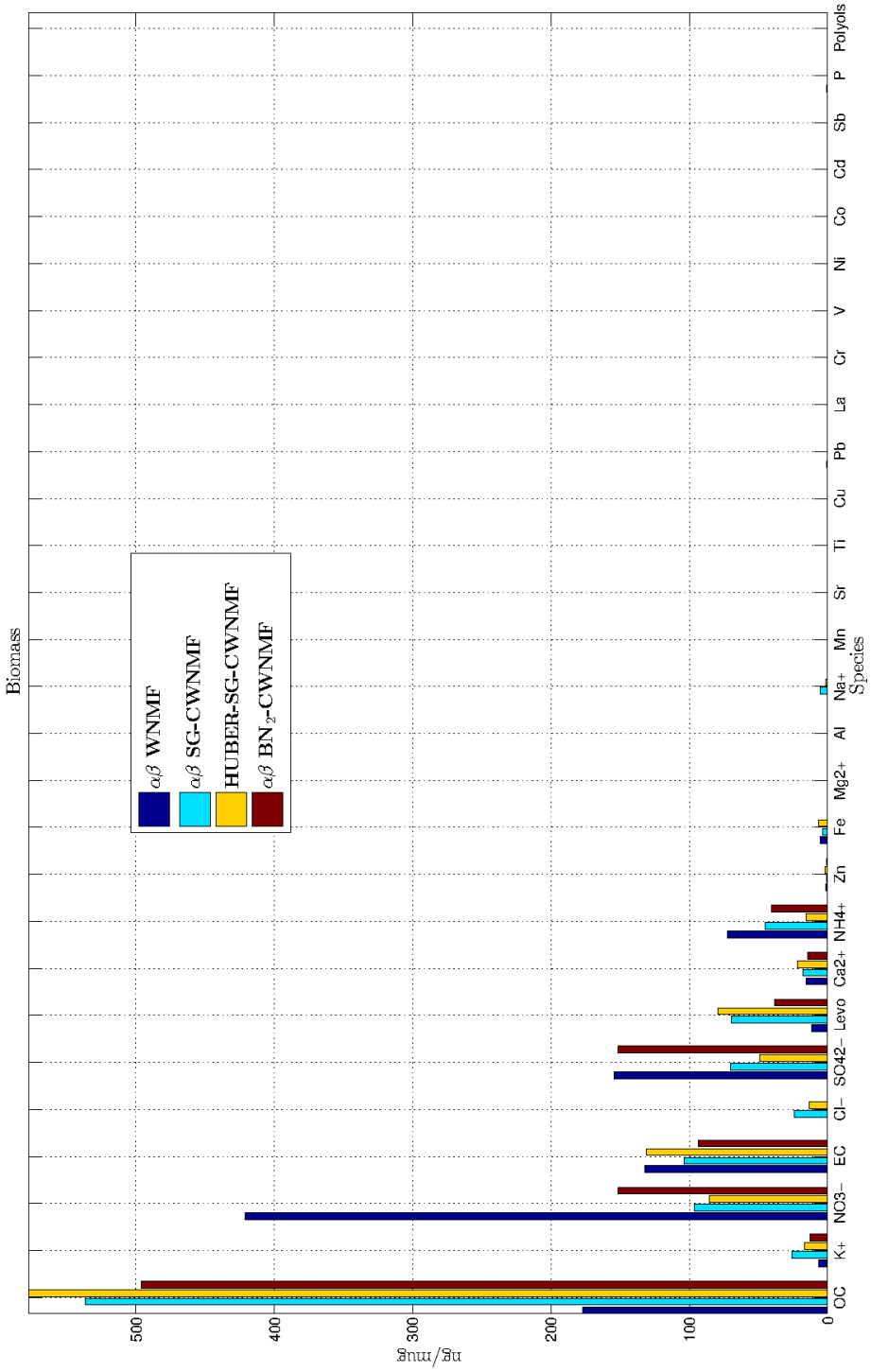

Figure D.5 – Estimation of the biomass source profile.

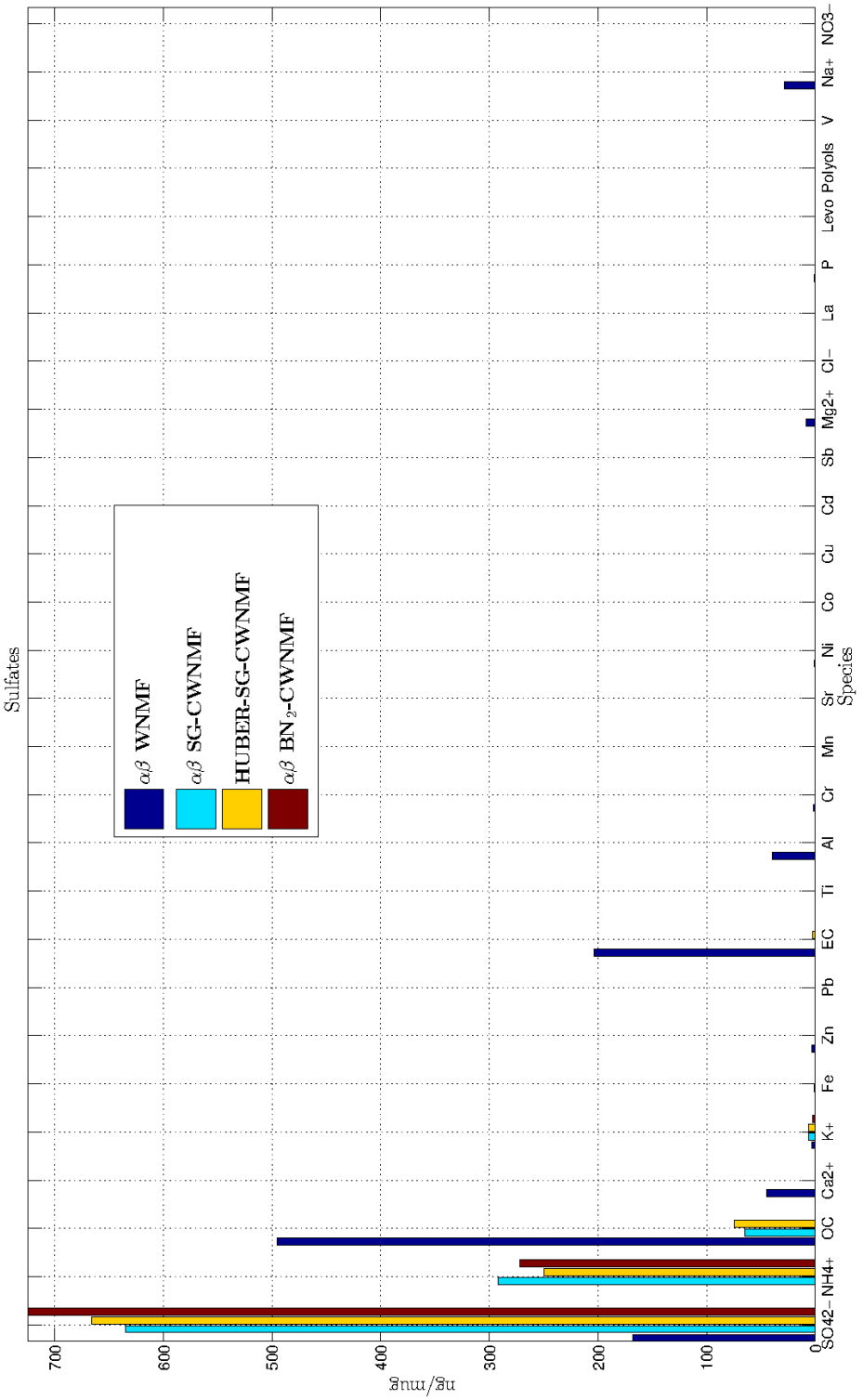

Figure D.6 – Estimation of the secondary sulfate source profile.

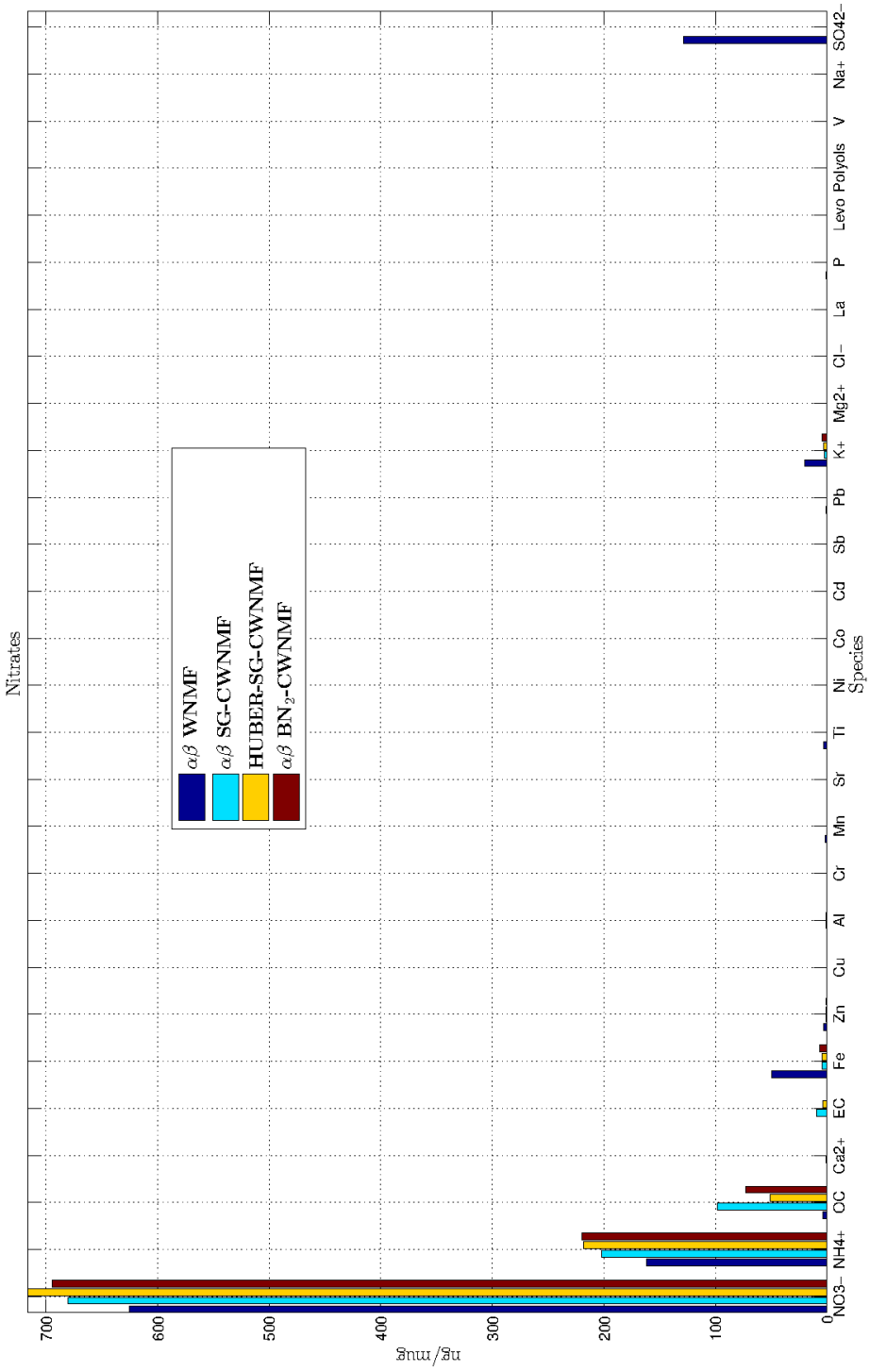

Figure D.7 – Estimation of the secondary nitrate source profile.

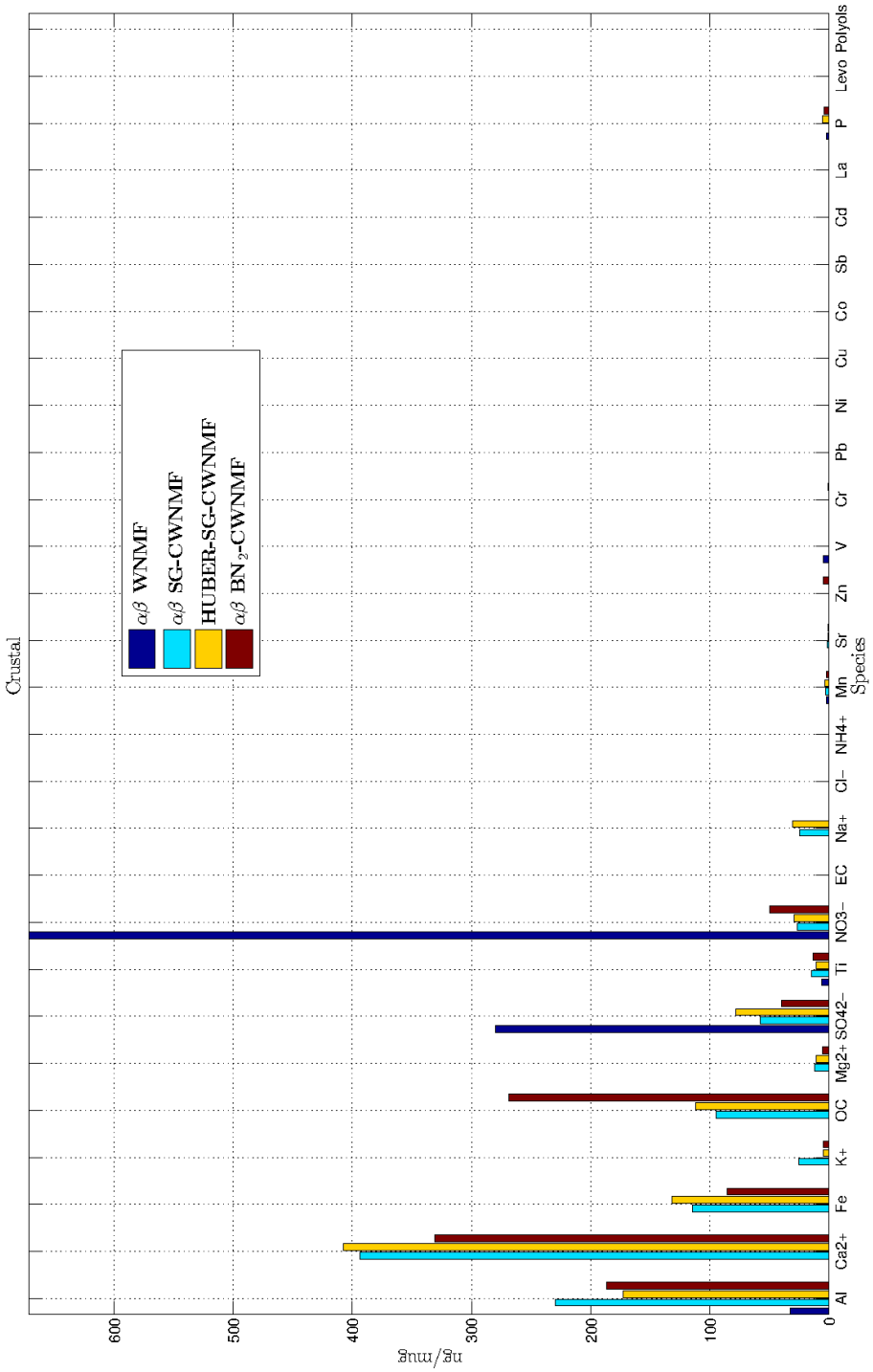

Figure D.8 – Estimation of the crustal dust source profile.

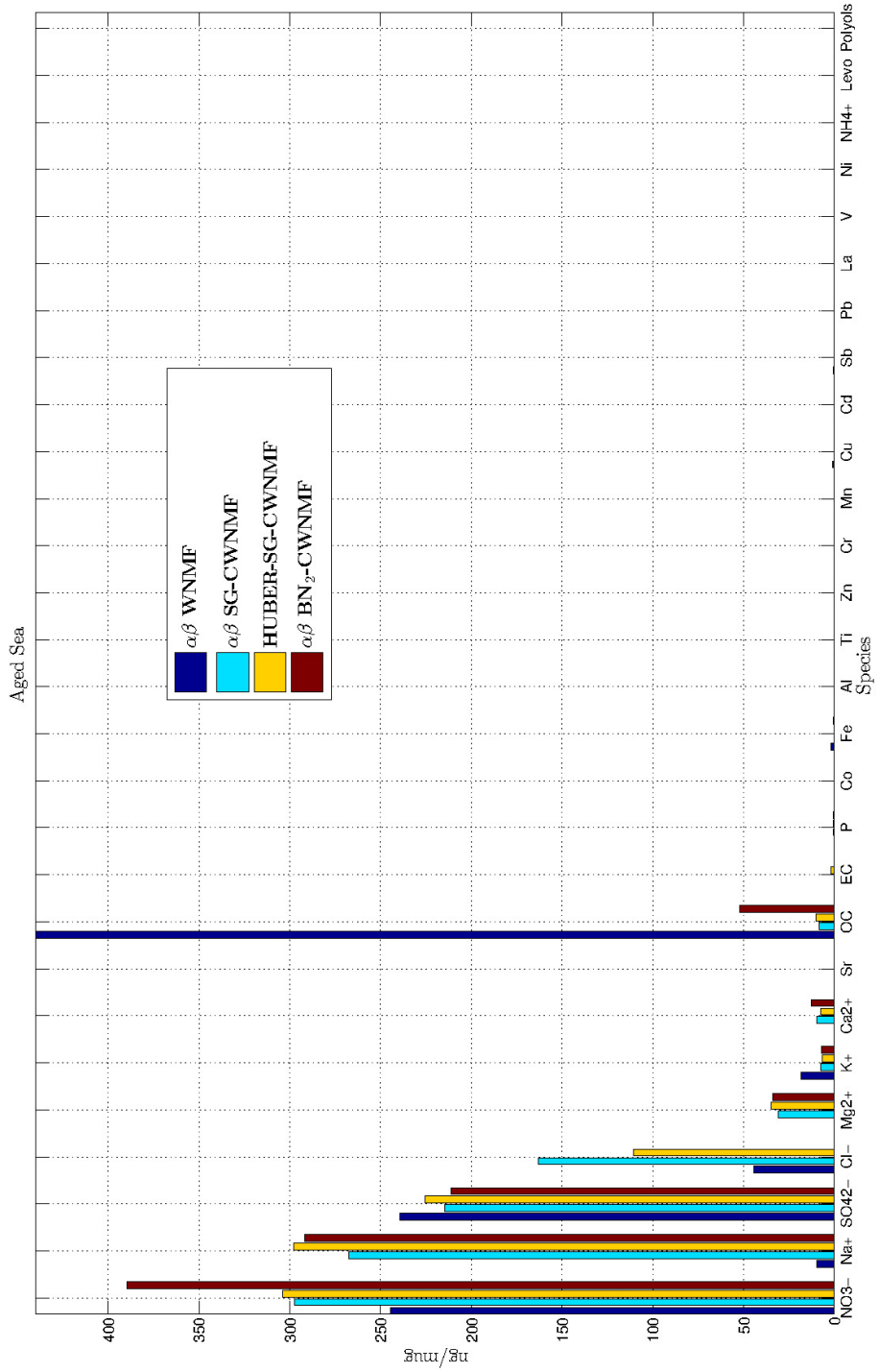

Figure D.9 – Estimation of the Aged sea source profile.

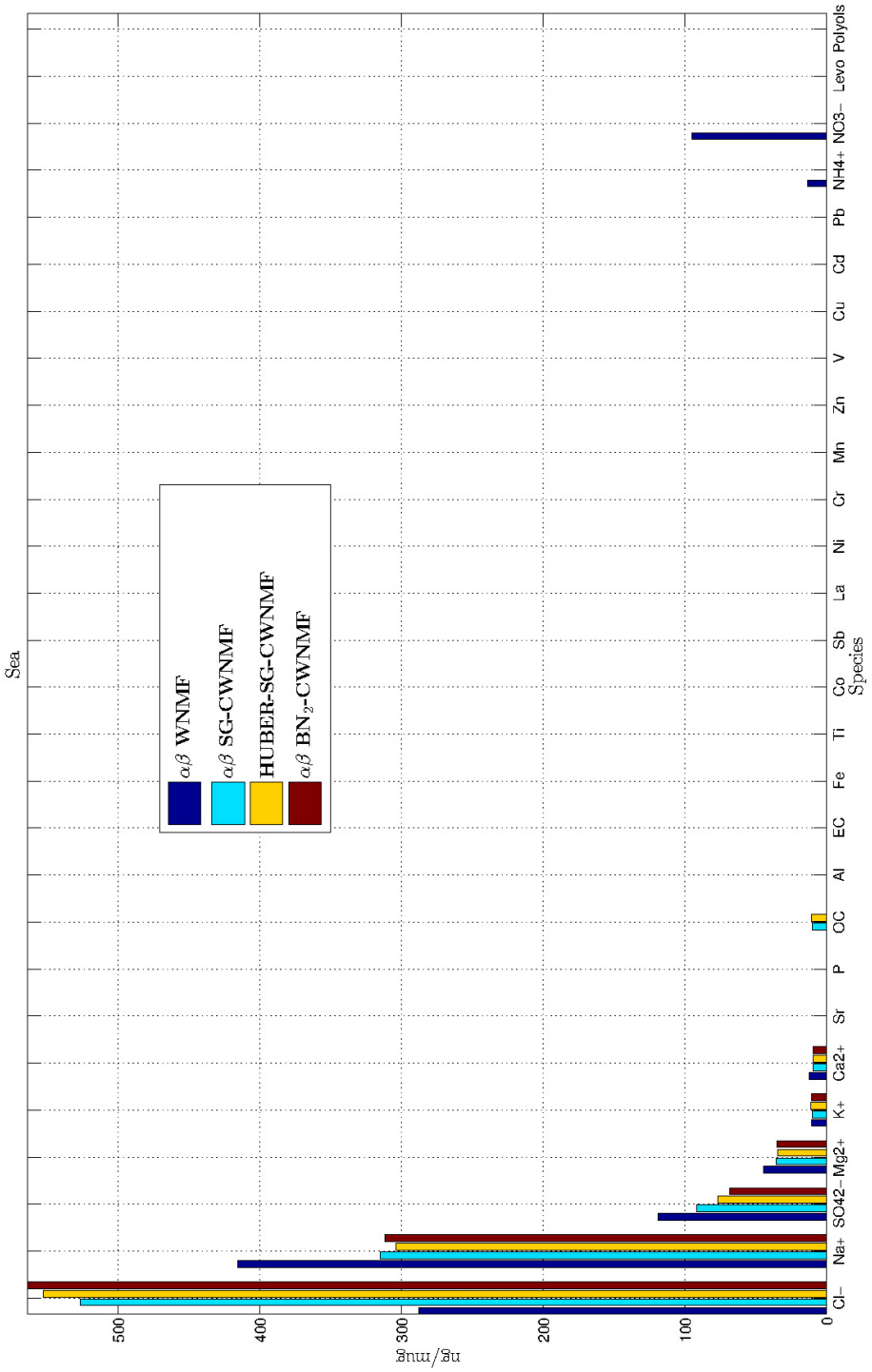

Figure D.10 – Estimation of the sea source profile.

Bibliography

[1] F. Abrard and Y. Deville. « A time-frequency blind signal separation method applicable to underdetermined mixtures of dependent sources ». In: *Signal Processing* 85.7 (July 2005), pp. 1389–1403.

[2] P. Anttila, P. Paatero, U. Tapper, and O. Järvinen. « Source identification of bulk wet deposition in Finland by positive matrix factorization ». In: *Atmospheric Environment* 29.14 (1995), pp. 1705–1718.

[3] S. Arberet, R. Gribonval, and F. Bimbot. « A Robust Method to Count and Locate Audio Sources in a Multichannel Underdetermined Mixture ». In: *IEEE Transactions on Signal Processing* 58.1 (Jan. 2010), pp. 121 –133.

[4] Roland Badeau, Nancy Bertin, and Emmanuel Vincent. « Stability Analysis of Multiplicative Update Algorithms and Application to Nonnegative Matrix Factorization ». In: *IEEE Transactions on Neural Networks* 21.12 (Dec. 2010), pp. 1869–1881.

[5] E. Be'ery and A. Yeredor. « Blind Separation of Reflections With Relative Spatial Shifts ». In: *Proceedings of the 2006 IEEE International Conference on Acoustics, Sound and Signal Processing (ICASSP 2006)*. Vol. 5. Toulouse, France, May 2006, pp. 625–628.

[6] A. J. Bell and T. J. Sejnowski. « An information-maximisation approach to blind separation and blind deconvolution ». In: *Neural Computation* 7 (1995), pp. 1129–1159.

[7] A. Belouchrani, K. Abed-Meraim, J.-F. Cardoso, and E. Moulines. « A blind source separation technique using second-order statistics ». In: *IEEE Transactions on Signal Processing* 45.2 (Feb. 1997), pp. 434–444.

[8] A. Ben Hamza and D. J. Brady. « Reconstruction of Reflectance Spectra Using Robust Nonnegative Matrix Factorization ». In: *IEEE Trans. on Signal Processing* 54.9 (2006), pp. 3637–3642.

[9] O. Berné, C. Joblin, Y. Deville, J. D. Smith, M. Rapaccioli, J. P. Bernard, J. Thomas, W. Reach, and A. Abergel. « Analysis of the emission of very small dust particles from Spitzer spectro-imagery data using Blind Signal Separation methods ». In: *Astronomy & Astrophysics* 469.2 (July 2007), pp. 575–586.

[10] J. M. Bioucas-Dias, A. Plaza, N. Dobigeon, M. Parente, Q. Du, P. Gader, and J. Chanussot. « Hyperspectral unmixing overview: Geometrical, statistical, and sparse regression-based approaches, » in: *IEEE J. on Sel. Topics Appl. Earth Observations Remote Sensing* 5 (2 2012), pp. 354–379.

[11] C. Blandin, A. Ozerov, and E. Vincent. « Multi-source TDOA estimation in reverberant audio using angular spectra and clustering ». In: *Signal Processing* 92 (2012), pp. 1950–1960.

[12] J. Bobin, J.-L. Starck, M.J. Fadili, and Y. Moudden. « Sparsity, Morphological Diversity and Blind Source Separation ». In: *IEEE Transactions on Image Processing* 16.11 (2007), pp. 2662–2674.

[13] A. Boulais, Y. Deville, and O. Berné. « A Blind Identification and Source Separation Method Based on Subspace Intersections for Hyperspectral Astrophysical Data ». In: *In Proc. Latent Variable Analysis and Signal Separation*. Ed. by P. Tichavský, M. Babaie-Zadeh, O.J.J. Michel, and N. Thirion-Moreau. Springer International Publishing, 2017, pp. 367–380.

[14] S. Boyd and L. Vandenberghe. *Convex optimization*. 2nd. Cambridge University Press, 2009.

[15] S. Boyd, N. Parikh, E. Chu, B. Peleato, and J. Eckstein. « Distributed optimization and statistical learning via the alternating direction method of multipliers ». In: *Foundations and Trends in Machine Learning,* vol. 3.

[16] R. Bro and S. De Jong. « A fast non-negativity-constrained least squares algorithm ». In: *Journal of Chemometrics* 11 (1997), pp. 393–401.

[17] Emmanuel J. Candès, Xiaodong Li, Yi Ma, and John Wright. « Robust Principal Component Analysis? » In: *J. ACM* 58.3 (June 2011), 11:1–11:37.

[18] E. J. Candès, X. Li, Y. Ma, and J. Wright. « Robust Principal Component Analysis ». In: *Journal of ACM* 58.1 (2009), pp. 1–37.

[19] G. Casella and E. I. George. « "Explaining the Gibbs sampler," » in: *Amer. Stat.,* 46 (1992), pp. 167–174.

[20] D. Chen and R.J. Plemmons. « Nonnegativity constraints in numerical analysis. » In: *The Birth of Numerical Analysis*. September 2009, pp. 109–140.

[21] J. C. Chen. « Non-negative rank factorization of non-negative matrices ». In: *Linear Algebra and its Applications* 62 (1984), pp. 207–217.

[22] E. Chouzenoux. « Recherche de pas par Majoration-Minoration. Application à la résolution de problèmes inverses. » Thèse de doctorat. Ecole Centrale de Nantes, 2010.

[23] E. Chouzenoux, S. Moussaoui, M. Legendre, and J. Idier. « Algorithme primal-dual de points interieurs pour l'estimation pénalisée des cartes d'abondances en imagerie hyperspectrale ». In: *Traitement du Signal* (Apr. 2013).

[24] R. Chreiky, G. Delmaire, M. Puigt, G. Roussel, and A. Abche. « Informed split gradient Non-negative Matrix Factorization using Huber cost function for source apportionment ». In: *Proc. of IEEE ISSPIT*. 2016.

[25] R. Chreiky, G. Delmaire, C. Dorffer, M. Puigt, G. Roussel, and A. Abche. « Robust Informed Split Gradient NMF Using Alpha Beta-Divergence for Source Apportionment ». In: *Proc. of MLSP*. 2016.

[26] R. Chreiky, G. Delmaire, M. Puigt, G. Roussel, and A. Abche. « Split Gradient Method for Informed Non-negative Matrix Factorization ». In: *Proc. of LVA-ICA*. 2015, pp. 376–383.

[27] A. Cichocki, S. Cruces, and S. Amari. « Generalized Alpha-Beta divergences and their application to robust nonnegative matrix factorization ». In: *Entropy* 13 (2011), pp. 134–170.

[28] A. Cichocki, A. H. Phan, and C. Caiafa. « Flexible HALS algorithms for sparse non-negative matrix/tensor factorization ». In: *Proceedings of 2008 IEEE International Workshop on Machine Learning for Signal Processing*. 2008, pp. 73–78.

[29] A. Cichocki, R. Zdunek, A. H. Phan, and S. Amari. *Nonnegative Matrix and Tensor Factorizations - Applications to Exploratory Multi-way Data Analysis and Blind Source Separation*. Wiley, 2009.

[30] P. L. Combettes and J.-C. Pesquet. « Proximal splitting methods in signal processing ». In: *Fixed-Point Algorithms for Inverse Problems in Science and Engineering*. New York: Springer Verlag, 2011, p. 185.

[31] P. Comon. « Independent component analysis, a new concept? » In: *Signal Processing* 36.3 (Apr. 1994), pp. 287–314.

[32] P. Comon and C. Jutten. *Handbook of blind source separation. Independent component analysis and applications*. Academic Press, 2010.

[33] Laurent Condat. « Fast Projection onto the Simplex and the l1 Ball ». In: *Mathematical Programming, Series A* 158.1 (July 2016), pp. 575–585.

[34] J. Delporte. « Factorisation Matricielle, application à la recommandation personnalisée de préférences. » Phd thesis. Université de Rouen, 2014.

[35] Y. Deville, J. Damour, and N. Charkani. « Multi-tag radio-frequency identification systems based on new blind source separation neural networks ». In: *Neurocomputing* 49 (2002), pp. 369–388.

[36] Y. Deville and L.T. Duarte. « An Overview of Blind Source Separation Methods for Linear-Quadratic and Post-nonlinear Mixtures ». In: *Lecture Notes in Computer Science book series (LNCS, volume 9237)*. Liberec, Czech republic, 2015.

[37] Y. Deville and M. Puigt. « Temporal and time-frequency correlation-based blind source separation methods. Part I: linear instantaneous mixtures ». In: *Signal Processing* 87.3 (Mar. 2007), pp. 374–407.

[38] J. M. Bioucas Dias. « Alternating direction method of multipliers for non-negative matrix factorization with the beta-divergence ». In: *Proc. of LVA-ICA*. Feb. 2017.

[39] C. Ding, D. Zhou, X. He, and H. Zha. « R1-pca:rotational invariant l1-norm principal component analysis for robust space factorization ». In: *in ICML, 2006*. 2006, pp. 281–288.

[40] D. Donoho and V. Stodden. « When Does Non-Negative Matrix Factorization Give a Correct Decomposition into Parts? » In: *Advances in Neural Information Processing Systems 16*. Ed. by Sebastian Thrun, Lawrence Saul, and Bernhard Schölkopf. Cambridge, MA: MIT Press, 2003, None.

[41] C. Dorffer, M. Puigt, G. Delmaire, and G. Roussel. « Blind Calibration of Mobile Sensors Using Informed Nonnegative Matrix Factorization ». English. In: *Proc. of LVA-ICA*. Vol. 9237. LNCS. 2015, pp. 497–505.

[42] C. Dorffer, M. Puigt, G. Delmaire, and G. Roussel. « Blind mobile sensor calibration using a nonnegative matrix factorization with a relaxed rendezvous model ». In: *Proc. of ICASSP*. Mar. 2016.

[43] C. Dorffer, M. Puigt, G. Delmaire, and G. Roussel. « Fast nonnegative matrix factorization and completion using Nesterov iterations ». In: *Proc. of LVA/ICA*. Vol. LNCS 10179. Feb. 2017, pp. 26–35.

[44] Clément Dorffer, Matthieu Puigt, Gilles Delmaire, and Gilles Roussel. « Fast Nonnegative Matrix Factorization and Completion Using Nesterov Iterations ». In: *13th International Conference on Latent Variable Analysis and Signal Separation (LVA/ICA 2017)*. Vol. 10169. LNCS. Grenoble, France, Feb. 2017, pp. 26–35.

[45] L. Du, X. Li, and Y.-D. Shen. « Robust Non-negative matrix factorization via half-Quadratic minimization ». In: *Proc. of ICDM*. Springer, 2012, pp. 201–210.

[46] Leonardo Tomazeli Duarte, Christian Jutten, and Saïd Moussaoui. « Bayesian source separation of linear and linear-quadratic mixtures using truncated priors ». In: *Journal of Signal Processing Systems* 65.3 (2011), pp. 311–323.

[47] C. Févotte and N. Dobigeon. « Nonlinear hyperspectral unmixing with robust nonnegative matrix factorization ». In: *IEEE Trans. Image Processing* 24.12 (Dec. 2015), pp. 4810–4819.

[48] P. Filzmoser and Rousseeuw P.J. *Robust Statistics*. 2nd. Encyclopedia of Life Support Systems, UNESCO and EOLSS, www.eolss.org, Oxford (2002)., 2002.

[49] P. Filzmoser, S. Serneels, R. Maronna, and P.J. Van Espen. *Robust multivariate methods in Chemometrics*. 2nd. In B. Walczak, R.T. Ferre, and S. Brown, editors, Comprehensive Chemometrics, 2009.

[50] X. Fu, W.-K. Ma, K. Huang, and N.D. Sidiropoulos. « Blind Separation of Quasistationary Sources: Exploiting Convex Geometry in Covariance Domain ». In: *IEEE Trans. on Signal Processing* 63.9 (May 2015), pp. 2306–2320.

[51] C. Févotte and J. Idier. « Algorithms for non-negative matrix factorization with the beta-divergence ». In: *Neural computation* 23.9 (Sept. 2011), pp. 2421–2456.

[52] D Gabay and B Mercier. « A dual algorithm for the solution of nonlinear variational problems via finite element approximation ». In: *Computers and Mathematics with applications*. Vol. 2(1). 1976.

[53] S. Geman and D. Geman. « "Stochastic relaxation, Gibbs distributions and the Bayesian restoration of images," » in: *IEEE Trans. Pattern Anal. Mach. Intell.,* 6.6 (1984), pp. 721–744.

[54] N. Gillis. « Sparse and Unique Nonnegative Matrix Factorization Through Data Preprocessing ». In: *Journal of Machine Learning Research* 13 (Nov. 2012), pp. 3349–3386.

[55] N. Gillis and F. Glineur. « Accelerated Multiplicative Updates and Hierarchical ALS Algorithms for Nonnegative Matrix Factorization ». In: *Neural Computation* 24.4 (2012), pp. 1085–1105.

[56] N. Gillis and S.A. Vavasis. « Fast and Robust Recursive Algorithms for Separable Nonnegative Matrix Factorization ». In: *IEEE Trans. on Pattern Analysis and Machine Ilntelligence* 36.4 (2014), pp. 698–714.

[57] Nicolas Gillis. « Nonnegative Matrix Factorization Complexity, Algorithms and Applications ». Ph.D. Thesis. Université catholique de Louvain, 2011.

[58] Donald Goldfarb, Shiqian Ma, and Katya Scheinberg. « Fast alternating linearization methods for minimizing the sum of two convex functions ». In: *Math. Program.* 141.1-2 (2013), pp. 349–382.

[59] T. Goldstein and S. Osher. « The split bregman method for l1-regularized problems. » In: *SIAM J. Imaging Sci.,* vol. 2(2).

[60] N. Guan, D. Tao, Z. Luo, and B. Yuan. « NeNMF: An Optimal Gradient Method for Nonnegative Matrix Factorization ». In: *IEEE Trans. Sig. Proc.* 60.6 (June 2012), pp. 2882–2898.

[61] D. Guillamet, J. Vitria, and B. Schiele. « Introducing a weighted non-negative matrix factorization for image classification ». In: *Pattern Recognition Letters* 24.14 (2003), pp. 2447–2454.

[62] W. K. Hastings. « "Monte Carlo sampling methods using Markov chains and their applications," » in: *Biometrika,* 57.1 (1992), pp. 97–109.

[63] D. M. Hawkins. *Identification of outliers*. Monographs on applied probability and statistics. London [u.a.]: Chapman and Hall, 1980.

[64] Z. He, A. Cichocki, Y. Li, S. Xie, and S. Sanei. « K-hyperline Clustering Learning for Sparse Component Analysis ». In: *Signal Processing* 89 (2009), pp. 1011–1022.

[65] D. C. Heinz and C. Chang. « Fully constrained least squares linear mixture analysis for material quantification in hyperspectral imagery ». In: *IEEE Trans. on Geoscience and Remote Sensing* 39 (2001), pp. 529–545.

[66] N.-D. Ho. « Non negative matrix factorizations algorithms and applications ». Ph.D. Thesis. Université Catholique de Louvain, 2008.

[67] P. K Hopke. « Review of receptor modeling methods for source apportionment ». In: *Journal of the Air & Waste Management Association* 66.3 (2016), pp. 237–259.

[68] H. Hoteling. « Analysis of a complex of statistical variables into principal components ». In: *Journal of Educational Psychology* 24.7 (1933), pp. 498–520.

[69] P. O. Hoyer. « Non-negative matrix factorization with sparseness constraint ». In: *Journal of Machine Learning Research* 5 (November 2004), pp. 1457–1469.

[70] P. J. Huber and E. M. Ronchetti. *Robust Statistics*. second. Wiley, 2009.

[71] D. R. Hunter and K. Lange. « A tutorial on MM algorithms ». In: *Amer. Statist* (2004), pp. 30–37.

[72] A. Hyvärinen. « Fast and Robust Fixed-Point Algorithms for Independent Component Analysis ». In: *IEEE Transactions on Neural Networks* 10.3 (May 1999), pp. 626–634.

[73] A. Hyvärinen and E. Oja. « A Fast Fixed-Point Algorithm for Independent Component Analysis ». In: *Neural Computation* 9.7 (Oct. 1997), pp. 1483–1492.

[74] J. Hérault, C. Jutten, and B. Ans. « Détection de grandeurs primitives dans un message composite par une architecture de calcul neuromimétique en apprentissage non-supervisé ». French. In: *Actes du* $10^{ème}$ *colloque GRESTI*. Nice, France, May 1985, pp. 1017–1022.

[75] Candes E. J. and Recht B. (2009). « Exact matrix completion via convex optimization ». In: *Found. Comput. Math.* 9.6 (Dec. 2009), pp. 717–772.

[76] B. Johansson, T. Elfving, V. Kozlov, Y. Censor, P.-E. Forssén, and G. Granlund. « The Application of an Oblique-Projected Landweber Method to a Model of Supervised Learning ». In: *Mathematical and Computer Modelling* 43 (Apr. 2006), pp. 892–909.

[77] A. Jourjine, S. Rickard, and O Yilmaz. « Blind separation of disjoint orthogonal signals: Demixing n sources from 2 mixtures ». In: (June 2000), pp. 2985–2988.

[78] C. Jutten and J. Hérault. « Blind separation of sources, Part 1: an adaptive algorithm based on neuromimetic architecture ». In: *Signal Processing* 24 (1991), pp. 1–10.

[79] M. S. Karoui, Y. Deville, S. Hosseini, and A. Ouamri. « Blind spatial unmixing of multispectral images: New methods combining sparse component analysis, clustering and non-negativity constraints ». In: *Pattern Recognition* 45 (12 2012), pp. 4263–4278.

[80] A. Kfoury. « Origin and physicochemical behaviour of atmospheric *PM*2.5 in cities located in the littoral area of the Nord-Pas-de-Calais region, France ». Phd Thesis. Université du Littoral Côte d'Opale, 2013.

[81] Adib Kfoury, Frédéric Ledoux, Cloé Roche, Gilles Delmaire, Gilles Roussel, and Dominique Courcot. « PM2.5 source apportionment in a French urban coastal site under steelworks emission influences using constrained non-negative matrix factorization receptor model ». In: *Journal of Environmental Sciences* 40.Supplement C (2016). Changing Complexity of Air Pollution, pp. 114 –128.

[82] H. Kim and H. Park. « Fast nonnegative matrix factorization: An active-set-like method and comparisons ». In: *SIAM Journal on Scientific Computing* 33.6 (2011), pp. 3261–3281.

[83] H. Kim and H. Park. « Nonnegative Matrix Factorization Based on Alternating Nonnegativity Constrained Least Squares and Active Set Method ». In: *SIAM Journal on Matrix Analysis and Applications* 30.2 (2008), pp. 713–730.

[84] H. Kim and H. Park. « Sparse Non-negative Matrix Factorizations via Alternating Non-negativity-constrained Least Squares for Microarray Data Analysis ». In: *Bioinformatics* 23.12 (June 2007), pp. 1495–1502.

[85] J. Kim, Y. He, and H. Park. « Algorithms for nonnegative matrix and tensor factorizations: A unified view based on block coordinate descent framework ». In: *Journal of Global Optimization* 28.2 (Feb. 2014), pp. 285–319.

[86] Keigo Kimura, Yuzuru Tanaka, and Mineichi Kudo. « A Fast Hierarchical Alternating Least Squares Algorithm for Orthogonal Nonnegative Matrix Factorization ». In: *Proceedings of the Sixth Asian Conference on Machine Learning*. Ed. by Dinh Phung and Hang Li. Vol. 39. Proceedings of Machine Learning Research. Nha Trang City, Vietnam: PMLR, Nov. 2015, pp. 129–141.

[87] C. H. Knapp and G. C. Carter. « The generalized correlation method for estimation of time delay ». In: *IEEE Transactions on Acoustics, Speech, and Signal Processing* 24.4 (Aug. 1976).

[88] D. Kong, C. Ding, and H. Huang. « Robust Non-negative matrix factorization using L_{21}-norm ». In: *Proc. of CIKM*. 2011, pp. 673–682.

[89] Y. Koren, R. Bell, and C. Volinsky. « Matrix Factorization Techniques for Recommender Systems ». In: *Computer* 42.8 (Aug. 2009), pp. 30–37.

[90] B. Lakshminarayanan, G. Bouchard, and C. Archambeau. « Robust Bayesian Matrix Factorisation ». In: *Proceedings of the Fourteenth International Conference on Artificial Intelligence and Statistics*. Ed. by Geoffrey Gordon, David Dunson, and Miroslav Dudík. Vol. 15. Proceedings of Machine Learning Research. Fort Lauderdale, FL, USA: PMLR, Apr. 2011, pp. 425–433.

[91] H. Lantéri, C. Theys, C. Richard, and C. Févotte. « Split Gradient Method for Nonnegative Matrix Factorization ». In: *Proc. of EUSIPCO Conference*. Aalborg, Denmark, 2010.

[92] L. De Lathauwer, B. De Moor, and J. Vandewalle. « Fetal electrocardiogram extraction by blind source subspace separation ». In: *IEEE Transactions on Biomedical Engineering* 47.5 (May 2000), pp. 567–572.

[93] C. L. Lawson and R. J. Hanson. *Solving least squares problems*. 3rd ed. Englewood Cliffs: Prentice-Hall, 1974, 1995, pp. 1–337.

[94] D. D. Lee and H. S. Seung. « Algorithms for Non-negative Matrix Factorization ». In: *Neural Information Processing Systems (NIPS)*. MIT Press, 2001, pp. 556–562.

[95] D. D. Lee and H. S. Seung. « Learning the parts of objects by non negative matrix factorization ». In: *Nature* 401.6755 (1999), pp. 788–791.

[96] A. Limem. « Méthodes informées de factorisation matricielles non-négatives. Application à l'identification de sources de particules industrielles. » Ph.D. Thesis. Université du Littoral Côte d'Opale, Calais, France, 2014.

[97] A. Limem, M. Puigt, G. Delmaire, G. Roussel, and D. Courcot. « Bound constrained weighted NMF for industrial source apportionment ». In: *Proc. of MLSP*. Reims, France, 2014.

[98] A. Limem, G. Delmaire, M. Puigt, G. Roussel, and D. Courcot. « Non-negative matrix factorization under equality constraints—a study of industrial source identification ». In: *Applied Numerical Mathematics* 85 (Nov. 2014), pp. 1–15.

[99] A. Limem, G. Delmaire, M. Puigt, G. Roussel, and D. Courcot. « Non-negative Matrix Factorization under equality constraints—a study of industrial source identification ». In: *Applied Numerical Mathematics* 85 (2014), pp. 1–15.

[100] A. Limem, G. Delmaire, M. Puigt, G. Roussel, and D. Courcot. « Non-negative matrix factorization using weighted beta divergence and equality constraints for industrial source apportionment ». In: *Proc. of MLSP*. Southampton, UK, 2013.

[101] C.-J. Lin. « On the Convergence of Multiplicative Update Algorithms for Nonnegative Matrix Factorization ». In: *Neural Networks, IEEE Transactions on* 18.6 (Nov. 2007), pp. 1589–1596.

[102] C.-J. Lin. « Projected Gradients Methods for Non-Negative Matrix Factorization ». In: *Neural Computation* 19 (2007), pp. 2756–2779.

[103] J. W. Lingwall and W. F. Christensen. « Pollution source apportionment using a priori information and positive matrix factorization ». In: *Chemometrics and Intelligent Laboratory Systems* 87.2 (2007), pp. 281–294.

[104] Weifeng Liu, Puskal P. Pokharel, and José C. Príncipe. « Correntropy: Properties and Applications in Non-Gaussian Signal Processing ». In: *IEEE Trans. Signal Processing* 55.11 (2007), pp. 5286–5298.

[105] Weifeng Liu, Puskal P. Pokharel, and Jose C. Principe. « Correntropy: Properties and Applications in Non-Gaussian Signal Processing. » In: *IEEE Trans. Signal Processing* 55.11 (2007), pp. 5286–5298.

[106] X.-J. Luo, S.-J. Chen, B.-X. Mai, G.-Y. Sheng, J.-M. Fu, and E. Y. Zeng. « Distribution, source apportionment, and transport of PAHs in sediments from the Pearl River Delta and the northern South China Sea ». In: *Archives of Environmental Contamination and Toxicology* 55.1 (2008), pp. 11–20.

[107] A. Mansour. « A mutually referenced blind multiuser separation of convolutive mixture algorithm ». In: *Signal Processing* 81.11 (2001), pp. 2253–2266.

[108] I. Meganem, Y. Deville, and M. Puigt. « Blind separation methods based on correlation for sparse possibly-correlated images ». In: *Proceedings of the 2010 IEEE International Conference on Acoustics, Speech, and Signal Processing (ICASSP 2010)*. Dallas, Texas, USA, Mar. 2010, pp. 1334–1337.

[109] M. Merritt and Y. Zhang. « An Interior-Point Gradient Method for Large-Scale Totally Nonnegative Least Squares Problems. » In: *J. Optimization Theory and Applications* 126.1 (2005), pp. 191–202.

[110] L. Miao and H. Qi. « Endmember Extraction From Highly Mixed Data Using Minimum Volume Constrained Nonnegative Matrix Factorization ». In: *IEEE Trans. Geoscience and Remote Sensing* 45.3 (2007), pp. 765–777.

[111] N. Mohammadiha and A. Leijon. « Nonnegative matrix factorization using projected gradient algorithms with sparseness constraints ». In: *2009 IEEE International Symposium on Signal Processing and Information Technology (ISSPIT)*. New York, USA, 2009, pp. 418–423.

[112] S. Moussaoui. « Séparation de sources non-négatives. Application au traitement des signaux de spectroscopie ». Thèse de doctorat. Université Henri Poincaré, Nancy 1, 2005.

[113] S. Moussaoui, D. Brie, A. Mohammad-Djafari, and C. Carteret. « Separation of Non-Negative Mixture of Non-Negative Sources Using a Bayesian Approach and MCMC Sampling ». In: *Signal Processing, IEEE Transactions on* 54.11 (2006), pp. 4133–4145.

[114] M. Rosenbluth N. Metropolis A. Rosenbluth. « A. Taller, and E. Taller, [17] C. L. Lawson and R. J. Hanson,"Equation of state calculation by fast computing machines," » in: *J. Chem.Phy.,* 21 (1953), pp. 1087–1092.

[115] F. M. Naeini, H. Mohimani, M. Babaie-Zadeh, and C. Jutten. « Estimating the mixing matrix in sparse component analysis (SCA) based on partial k-dimensional subspace clustering ». In: *Neurocomputing (Elsevier)* 71 (June 2008), pp. 2330–2343.

[116] S. Nam, M. E. Davies, M. Elad, and R. Gribonval. « The Cosparse Analysis Model and Algorithms ». In: *Applied and Computational Harmonic Analysis* 34.1 (2013), pp. 30–56.

[117] Nathan Srebro Nati and Tommi Jaakkola. « Weighted Low-Rank Approximations ». In: *20th International Conference on Machine Learning*. Washingtown, DC, USA: AAAI Press, 2003, pp. 720–727.

[118] A. Nemirovski. « Orth-method for smooth convex optimization. » In: *Izvestia AN SSSR, Transl.: Eng. Cybern. Soviet J. Comput. Syst. Sci.* 2 (1982), pp. 937–947.

[119] M. Nikolova and M. Ng. « Analysis of half-quadratic minimization methods for signal and image recovery ». In: *SIAM Journal on Scientific computing* 27.3 (200), pp. 937–966.

[120] R. Ouaret, A. Ionescu, O. Ramalho, and Y. Candau. « Indoor air pollutant sources using Blind Source Separation Methods ». In: *Proc. of ESANN*. 2017.

[121] W. S. B. Ouedraogo, A. Souloumiac, and C. Jutten. « Non-negative Independent Component Analysis Algorithm Based on 2D Givens Rotations and a Newton Optimization ». In: *Proc. of 9th International Conference on Latent Variable Analysis and Signal Separation (LVA/ICA)*. Vol. 6365. Saint Malo, France: Springer, Sept. 2010, pp. 522–529.

[122] Wendyam Ouedraogo. « Methode geometrique de separation de sources non-negatives : applications a l'imagerie dynamique TEP et a la spectrometrie de masse ». Ph.D. Thesis. Universite De Grenoble, 2013.

[123] Hua Ouyang, Niao He, Long Q. Tran, and Alexander Gray. « Stochastic Alternating Direction Method of Multipliers ». In: *Proceedings of the 30 th International Conference on Ma- chine Learning, Atlanta, Georgia, USA, 2013. (JMLR:W and CP)*. Vol. 28.

[124] P. Paatero. « Least squares formulation of robust non-negative factor analysis ». In: *Chemometrics and Intelligent Laboratory Systems* 37.1 (1997), pp. 23–35.

[125] P. Paatero and U. Tapper. « Positive matrix factorization: a non negative factor model with optimal utilization of error estimates of data values ». In: *Environmetrics* 5.2 (1994), pp. 111–126.

[126] M. Parvaix. « Séparation de sources audio informée par tatouage pour mélanges linéaires instantanés stationnaires ». Thèse de doctorat. Institut National Polytechnique de Grenoble, 2010.

[127] D. Pavlidi, A. Griffin, M. Puigt, and A. Mouchtaris. « Real-time multiple sound source localization and counting using a circular microphone array ». In: *IEEE Transactions on Audio, Speech, and Language Processing* 21.10 (Oct. 2013), pp. 2193–2206.

[128] K. Pearson. « On Lines and Planes of Closest Fit to Systems of Points in Space ». In: *Philosophical Magazine* 2.6 (1901), pp. 559–572.

[129] M. S. Pedersen, J. Larsen, U. Kjems, and L. C. Parra. « A Survey of Convolutive Blind Source Separation Methods ». In: *Springer Handbook of Speech*. Springer Press, Sept. 2007.

[130] K. B. Petersen and M. S. Pedersen. *The Matrix Cookbook*. Technical University of Denmark, 2012.

[131] D.-T. Pham and J.F. Cardoso. « Blind separation of instantaneous mixtures of nonstationary sources ». In: *IEEE Transactions on Signal Processing* 49.9 (Sept. 2001), pp. 1837–1848.

[132] M. Plouvin, A. Limem, M. Puigt, G. Delmaire, G. Roussel, and D. Courcot. « Enhanced NMF initialization using a physical model for pollution source apportionment ». In: *Proc. of the 22nd European Symposium on Artificial Neural Networks, Computational Intelligence and Machine Learning*. Bruges, Belgique, Apr. 2014, pp. 261–266.

[133] A. Poberznick. *Développement d'un boîtier de mesure de la qualité de l'air pour le crowdsensing*. RAPPORT DE STAGE. 2015.

[134] M. Puigt. « Méthodes de séparation aveugle de sources fondées sur des transformées temps-fréquence. Application à des signaux de parole ». Thèse de doctorat. Université de Toulouse, 2007.

[135] M. Puigt, A. Griffin, and A. Mouchtaris. « Nonlinear blind mixture identification using local source sparsity and functional data clustering ». In: *Proceedings of the 7th IEEE Sensor Array and Multichannel Signal Processing (SAM 2012)*. Hoboken, NJ, USA, June 2012, pp. 489–492.

[136] M. Puigt, A. Griffin, and A. Mouchtaris. « Post-nonlinear speech mixture identification using single-source temporal zones & curve clustering ». In: *Proc. of the 19th European Signal Processing Conference (EUSIPCO 2011)*. Barcelona, Spain, 2011, pp. 1844–1848.

[137] J. Rapin, J. Bobin, A. Larue, and J. L. Starck. « Sparse and Non-Negative BSS for Noisy Data ». In: *IEEE Trans. on Signal Processing* 61.22 (2013), pp. 5620–5632.

[138] V. G. Reju, S. N. Koh, and I. Y. Soon. « An algorithm for mixing matrix estimation in instantaneous blind source separation ». In: *Signal Processing* 89.9 (2009), pp. 1762–1773.

[139] J. J. Rieta, F. Castells, C. Sánchez, V. Zarzoso, and J. Millet. « Atrial activity extraction for atrial fibrillation analysis using blind source separation ». In: *IEEE Transactions on Biomedical Engineering* 51.7 (2004), pp. 1176–1186.

[140] B. Rivet. « Blind non-stationnary sources separation by sparsity in a linear instantaneous mixture ». In: *Proceedings of the 8th International Conference on Independent Component Analysis and Blind Source Separation (ICA 2009)*. Ed. by Springer-Verlag. Vol. LNCS 5441. Paraty, RJ, Brazil, Mar. 2009, pp. 314–321.

[141] C. Robert. « The Bayesian Choice, 2nd ed. » In: *New York: Springer-Verlag,* (2001).

[142] C. Roche. « Etude des concentrations et de la composition des PM_{10} sur le littoral du Nord de la France- Evaluation des contributions maritimes de l'espace Manche- Mer du Nord. » Ph.D. Thesis. Université du Littoral Côte d'Opale, Dunkerque, France, 2016.

[143] P. J. Rousseeuw, M. Debruyne, S. Engelen, and M. Hubert. « Robustness and Outlier Detection in Chemometrics ». In: *Critical Reviews in Analytical Chemistry* 36.3-4 (2006), pp. 221–242.

[144] Ignacio Santamaría, Puskal P. Pokharel, and José C. Príncipe. « Generalized correlation function: definition, properties and application to blind equalization ». In: *IEEE Transactions on Signal Processing* 54.6 (June 2006), 2187–2196.

[145] H. Saylani, S. Hosseini, Y. Deville, and M. Habibi. « A multi-tag radio-frequency identification system using new blind source separation methods based on spectral decorrelation / Système d'identification radio-fréquence multi-badge utilisant de nouvelles méthodes de séparation aveugle de sources à décorrélation spectrale ». In: *Physical and Chemical News* 35 (May 2007), pp. 31–42.

[146] R. Schachtner, G. Pöppel, and E. W. Lang. « Towards unique solutions of non-negative matrix factorization problems by a determinant criterion ». In: *Digital Signal Processing* 21 (2011), pp. 528–534.

[147] R. Schachtner, G. Pöppel, A.-M. Tomé, and E. W. Lang. « Minimum Determinant Constraint for Non-negative Matrix Factorization ». In: *Independent Component Analysis and Signal Separation*. Vol. LNCS 5441. 2009, pp. 106–113.

[148] Mikkel Schmidt. « Linearly constrained bayesian matrix factorization for blind source separation ». In: *Advances in neural information processing systems*. 2009, pp. 1624–1632.

[149] M. Schuermans. « Weighted Low Rank Approximation: Algorithms and applications ». Phd Thesis. Faculty of Engineering, K.U.Leuven (Leuven, Belgium), 2006.

[150] J. J. Settlle and N. A. Drake. « Linear mixing and the estimation of ground cover proportions ». In: *International Journal of Remote Sensing* 14 (1993), pp. 1159–1177.

[151] B. Shen, L. Si, R. Ji, and B. Liu. « Robust Nonnegative Matrix Factorization via L_1 Norm Regularization ». In: *arXiv preprint arXiv:1204.2311* (2012).

[152] A. P. Singh and G. J. Gordon. « A Unified View of Matrix Factorization Models ». In: *European Conference on Machine Learning and Knowledge Discovery in Databases (ECML/PKDD)*. ECML/PKDD-2008. 2008.

[153] D. Soukup and I. Bajla. « Robust Object Recognition under Partial Occlusions Using NMF ». In: *Computational Intelligence and Neuroscience* (2008).

[154] A. Souloumiac. « Blind source detection and separation using second-order non-stationarity ». In: *Proceedings of the IEEE 1995 International Conference on Acoustics, Speech, and Signal Processing (ICASSP 1995)*. Vol. 3. Detroit, Michigan, USA, May 1995, pp. 1912–1915.

[155] D. L. Sun and C. Févotte. « Blind Hyperspectral Unmixing ». In: *Proc. of ICASSP*. May 2014.

[156] Dennis L. Sun and Cedric Fevotte. « Alternating direction method of multipliers for non-negative matrix factorization with the beta-divergence ». In: *Acoustics, Speech and Signal Processing (ICASSP), 2014 IEEE International Conference*. Florence, Italy, 2014.

[157] J. Thomas, Y. Deville, and S. Hosseini. « Time-domain fast fixed-point algorithms for convolutive ICA ». In: *IEEE Signal Processing Letters* 13.4 (Apr. 2006), pp. 228–231.

[158] L. Tong, R. W. Liu, V. C. Soon, and Y. F. Huang. « Indeterminacy and identifiability of blind identification ». In: *IEEE Transactions on Circuits and Systems* 38.5 (May 1991), pp. 499–509.

[159] John W. Tukey. « The Future of Data Analysis ». In: *Ann. Math. Statist.* 33.1 (Mar. 1962), pp. 1–67.

[160] S.A. Vavasis. « On the Complexity of Nonnegative Matrix Factorization ». In: *SIAM J. on Optimization* 20.3 (2009), pp. 1364–1377.

[161] R. Vidal, Y. Ma, and S. Sastry. *Generalized Principal Component Analysis (GPCA)*. Dec. 2005.

[162] E. Vincent, S. Araki, and P. Bofill. « The 2008 Signal Separation Evaluation Campaign: A community-based approach to large-scale evaluation ». In: *Proc. of ICA*. Paraty, Brazil, 2009, pp. 734–741.

[163] E. Vincent, H. Sawada, P. Bofill, S. Makino, and J.P. Rosca. « First stereo audio source separation evaluation campaign: data, algorithms and results ». In: *Proc. of Int. Conf. on Independent Component Analysis and Signal Separation (ICA)*. 2007, pp. 552–559.

[164] Tuomas Virtanen, A Taylan Cemgil, and Simon Godsill. « Bayesian extensions to non-negative matrix factorisation for audio signal modelling ». In: *Acoustics, Speech and Signal Processing, 2008. ICASSP 2008. IEEE International Conference on*. IEEE. 2008, pp. 1825–1828.

[165] N. Langville V. Pauca W. Berry M. Browne and J. Plemmons. « Algorithms and applications for approximate nonnegative matrix factorization ». In: *Computational Statistics and Data Analysis* 52.1 (September 2007), pp. 155–173.

[166] A. Waked, O. Favez, L. Y. Alleman, C. Piot, J.-E. Petit, T. Delaunay, E. Verlinden, B. Golly, J.-L. Besombes, J.-L. Jaffrezo, and E. Leoz-Garziandia. « Source apportionment of PM_{10} in a north-western Europe regional urban background site (Lens, France) using positive matrix factorization and including primary biogenic emissions ». In: *Atmospheric Chemistry and Physics* 14.7 (2014), pp. 3325–3346.

[167] Siming Wei and Zhouchen Lin. « Analysis and Improvement of Low Rank Representation for Subspace segmentation ». In: *CoRR* abs/1107.1561 (2011).

[168] WHO. *Air quality guidelines for Europe, 2nd edition*. WHO regional publications. European series 91. WHO Regional Office for Europe, 2000.

[169] Hyenkyun Woo and Haesun Park. « Robust Asymmetric Nonnegative Matrix Factorization ». In: November (2014).

[170] J. Wright. « Robust principal component analysis: Exact recovery of corrupted low-rank matrices via convex optimization ». In: *Advances in Neural Information Processing Systems 22*. 2009.

[171] Yangyang Xu, Wotao Yin, Zaiwen Wen, and Yin Zhang. « An alternating direction algorithm for matrix completion with non-negative factors ». In: *Frontiers of Mathematics in China* 7.2 (2012), pp. 365–384.

[172] J Yang and Y Zhang. « Alternating direction algorithms for l1-problems in compressive sensing. » In: *SIAM J. on Scientific Computing,* vol. 33(1).

[173] Zaiwen Wen Yangyang Xu Wotao Yin and Yin Zhang. « "An alternating direction algorithm for matrix completion with nonnegative factors," » in: *Frontiers of Mathematics in China,* vol. 7.

[174] Ö. Yilmaz and S. Rickard. « Blind separation of speech mixtures via time-frequency masking ». In: *IEEE TSP* 52.7 (2004), pp. 1830–1847.

[175] J. Yoo and S. Choi. « Nonnegative Matrix Factorization with Orthogonality Constraints ». In: *Journal of computing science and engineering* 4.2 (June 2010), pp. 97–109.

[176] Z. Yuan and E. Oja. « Projective nonnegative matrix factorization for image compression and feature extraction ». In: *In Proc. of Scandinavian Conference on Image Analysis*. 2005, pp. 333–342.

[177] R. Zdunek, A. H. Phan, and A. Cichocki. « Image Classification with Nonnegative Matrix Factorization based on Spectral Projected Gradient ». In: *Artificial Neural Networks: Methods and Applications in Bio-/Neuroinformatics*. Vol. 4. Springer, 2015, pp. 31–50.

[178] Y. Zhang. *An alternating direction algorithm for Non-negative Matrix Factorization*. Tech. rep. Houston, USA: Rice Research Technical Report, 2010.

[179] Zhengyou Zhang. « Parameter estimation techniques: a tutorial with application to conic fitting. » In: *Image Vision Comput.* 15.1 (Mar. 1997), pp. 59–76.

[180] Zheng M. Zhang L. Chen Z. and He X. « Robust non-negative matrix factorization, » in: *Fron. Electr. Electron. Eng.China,* 6 (2 2011), pp. 192–200.

[181] Fei Zhu, Abderrahim Halimi, Paul Honeine, Badong Chen, and Nanning Zheng. « Correntropy Maximization via ADMM - Application to Robust Hyperspectral Unmixing ». In: *IEEE Transactions on Geoscience and Remote Sensing* 55.9 (Sept. 2017), pp. 1–12.

[182] Q. Zuo, Y.H. Duan, Y. Yang, X.J. Wang, and S. Tao. « Source apportionment of polycyclic aromatic hydrocarbons in surface soil in Tianjin, China ». In: *Environmental Pollution* 147.2 (2007), pp. 303–310.

Abstract — Source apportionment for air pollution may be formulated as a NMF problem by decomposing the data matrix X into a matrix product of two factors G and F, respectively the contribution matrix and the profile matrix. Usually, chemical data are corrupted with a significant proportion of abnormal data. Despite the interest for the community for NMF methods, they suffer from a lack of robustness to a few abnormal data and to initial conditions and they generally provide multiple minima. To this end, this thesis is oriented on one hand towards robust NMF methods and on the other hand on informed NMF by using some specific prior knowledge. Two types of knowledge are introduced on the profile matrix F. The first assumption is the exact knowledge on some of flexible components of matrix F and the second hypothesis is the sum-to-1 constraint on each row of the matrix F. A parametrization able to deal with both information is developed and update rules are proposed in the space of constraints at each iteration. These formulations have been applied to two kind of robust cost functions, namely, the weighted Huber cost function and the weighted $\alpha\beta$ divergence. The target application–namely, identify the sources of particulate matter in the air in the coastal area of northern France– shows the relevance of the proposed methods. In the numerous experiments conducted on both synthetic and real data, the effect and the relevance of the different information is highlighted to make the factorization results more reliable.

Keywords : Informed Non-negative matrix factorization, Robustness, Air pollution.

Résumé — Le démélange de sources pour la pollution de l'air peut être formulé comme un problème de NMF en décomposant la matrice d'observation X en le produit de deux matrices non négatives G et F, repectivement la matrice de contributions et de profils. Généralement, les données chimiques sont entâchées d'une part de données aberrantes. En dépit de l'intérêt de la communauté pour les méthodes de NMF, elles souffrent d'un manque de robustesse à un faible nombre de données aberrantes et aux conditions initiales et elles fournissent habituellement de multiples minima. En conséquence, cette thèse est orientée d'une part vers les méthodes de NMF robustes et d'autre part vers les NMF informées qui utilisent une connaissance experte particulière. Deux types de connaissances sont introduites dans la matrice de profil F. La première hypothèse est la connaissance exacte de certaines composantes de la matrice F tandis que la deuxième information utilise la propriété de somme-à-1 de chaque ligne de la matrice F. Une paramétrisation qui tient compte de ces deux informations est développée et des règles de mise à jour dans le sous-espace des contraintes sont proposées. L'application cible qui consiste à identifier les sources de particules dans l'air dans la région côtière du nord de la France montre la pertinence des méthodes proposées. Dans la série d'expériences menées sur des données synthétiques et réelles, l'effet et la pertinence des différentes informations sont mises en évidence et rendent les résultats de factorisation plus fiables.

Mots-clés: Factorisation matricielle non-négative Informée, Robustesse, Pollution de l'air.